LEABHARLANN CHOLÁISTE NA TRÍONÓIDE, BAILE ÁTHA CLIATH | TRINITY COLLEGE LIBRARY DUBLIN
Ollscoil Átha Cliath | The University of Dublin

Terms and Conditions of Use of Digitised Theses from Trinity College Library Dublin

Copyright statement

All material supplied by Trinity College Library is protected by copyright (under the Copyright and Related Rights Act, 2000 as amended) and other relevant Intellectual Property Rights. By accessing and using a Digitised Thesis from Trinity College Library you acknowledge that all Intellectual Property Rights in any Works supplied are the sole and exclusive property of the copyright and/or other IPR holder. Specific copyright holders may not be explicitly identified. Use of materials from other sources within a thesis should not be construed as a claim over them.

A non-exclusive, non-transferable licence is hereby granted to those using or reproducing, in whole or in part, the material for valid purposes, providing the copyright owners are acknowledged using the normal conventions. Where specific permission to use material is required, this is identified and such permission must be sought from the copyright holder or agency cited.

Liability statement

By using a Digitised Thesis, I accept that Trinity College Dublin bears no legal responsibility for the accuracy, legality or comprehensiveness of materials contained within the thesis, and that Trinity College Dublin accepts no liability for indirect, consequential, or incidental, damages or losses arising from use of the thesis for whatever reason. Information located in a thesis may be subject to specific use constraints, details of which may not be explicitly described. It is the responsibility of potential and actual users to be aware of such constraints and to abide by them. By making use of material from a digitised thesis, you accept these copyright and disclaimer provisions. Where it is brought to the attention of Trinity College Library that there may be a breach of copyright or other restraint, it is the policy to withdraw or take down access to a thesis while the issue is being resolved.

Access Agreement

By using a Digitised Thesis from Trinity College Library you are bound by the following Terms & Conditions. Please read them carefully.

I have read and I understand the following statement: All material supplied via a Digitised Thesis from Trinity College Library is protected by copyright and other intellectual property rights, and duplication or sale of all or part of any of a thesis is not permitted, except that material may be duplicated by you for your research use or for educational purposes in electronic or print form providing the copyright owners are acknowledged using the normal conventions. You must obtain permission for any other use. Electronic or print copies may not be offered, whether for sale or otherwise to anyone. This copy has been supplied on the understanding that it is copyright material and that no quotation from the thesis may be published without proper acknowledgement.

Identification and Characterisation of Serotonin Transporter Interacting Proteins

A dissertation submitted to Trinity College Dublin for the degree of

Doctor of Philosophy

by

Heidi Kaastrup Müller

School of Biochemistry and Immunology, Trinity College Dublin

July 2006

TRINITY COLLEGE
25 SEP 2008
LIBRARY DUBLIN
THESIS
8582

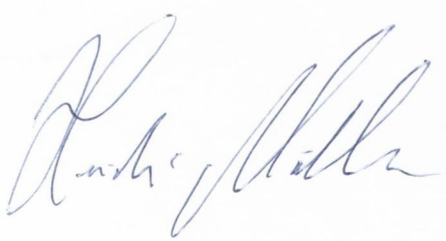
DECLARATION

This thesis has not been submitted as an exercise for a degree at any other university. Except where stated, the work described therein was carried out by me alone.

I give permission for the Library to lend or copy this thesis upon request.

19/8-08

Signed:



Declaration

I certify that none of the work in this thesis has been submitted for any degree or diploma at this or any other University and that all of the work described in this thesis is entirely my own work.



Acknowledgements

I would like to express my gratitude and thanks to my supervisor Dr. Jana Haase, for her constant support and enthusiasm and for putting up with my strict rules for lab behaviour.

I wish to thank Prof. Clive Williams for inviting me to work in his lab at Trinity College.

I am grateful to Ove Wiborg for his constant interest in my work.

Many thanks go to Anja Fjorback, for her hard work and for keeping me company on the green island – although mainly in the pub!

I also wish to thank Francesca Magnani for valuable guidance and continuous encouragement.

Many thanks go to Joanna, Sandra and Jonathan. I hope I'll get to see more of you guys – keep the boss busy, please!

Thanks to Bill and Yvonne for being great friends from day one.

Thanks to the Gethin McBean group, especially Andrew and Therese for providing a friendly atmosphere in the lab. And thanks to Billy O'Connor and members of his group.

And finally, I wish to thank Erik for doing the right thing - coming with me to Dublin.

Summary

The serotonin transporter (SERT) is an integral plasma membrane protein that mediates the high-affinity re-uptake of the neurotransmitter serotonin from the synaptic space. SERT is of particular clinical and pharmacological interest as it has been implicated in a variety of neuropsychiatric disorders as well as several dysfunctions in the periphery. It is the primary target for a number of widely prescribed antidepressants and is also the site of action for drugs of abuse. By regulating the concentration of serotonin in extracellular fluids SERT plays a key role in modulating serotonergic neurotransmission. The control of SERT activity via intrinsic and trafficking mediated events is therefore central to the spatial and temporal regulation of synaptic serotonin levels. SERT and related transporters are thought to be regulated through association with a number of signalling and structural proteins.

In this study, the yeast two-hybrid approach was used in the search for proteins interacting with the N- and C-terminal domains of SERT. A number of putative SERT interacting partners were isolated in a total of five yeast two-hybrid screens. The third member of the NY-ESO-1 gene family, ESO3, was isolated using the N-terminal domain of SERT. The function of ESO3 is unknown but confocal microscopy revealed localization of ESO3 to the endoplasmic reticulum (ER). Co-expression of ESO3 with SERT in mammalian cells resulted in sequestering of SERT in the ER causing a reduction in 5-HT uptake and cell surface expression of the transporter. A deletion mutant of ESO3 was unable to affect SERT function but rather resulted in an increase in SERT mediated 5-HT uptake activity. Application of siRNAs targeting endogenous ESO3 in HEK-293 cells transiently expressing SERT resulted in an increase in 5HT uptake. Furthermore, ESO3 appeared to affect SERT function via a mechanism distinct from PKC-mediated SERT down-regulation.

The secretory carrier membrane protein 2 (SCAMP2) also interacts with the N-terminal domain of SERT. SERT was found to form a complex with SCAMP2 as demonstrated by co-immunoprecipitation from a heterologous expression system and from rat brain homogenate. Co-expression of SERT and SCAMP2 resulted in a subcellular redistribution of SERT with a decrease in cell surface SERT and a concomitant reduction in 5-HT uptake activity. In neurons, confocal microscopy revealed co-localization of endogenous SERT with SCAMP2 in structures also containing the lipid raft marker flotillin-1 and the SNARE protein syntaxin 1A. In contrast, SERT/SCAMP2-positive structures were clearly segregated from the transferrin receptor, a marker of the general endocytic recycling pathway. A single amino acid mutation, cysteine-201 to alanine, within the conserved cytoplasmic E peptide of SCAMP2, abolished SCAMP2-mediated down-regulation of SERT, although this mutation had no effect on the physical interaction between SERT and SCAMP2.

In summary, this study demonstrates the identification of three proteins interacting directly with SERT in a regulatory manner and thus, provides new insight into the subcellular pathways that control transporter function.

DECLARATION *i*

ACKNOWLEDGEMENTS *ii*

SUMMARY *iii*

TABLE OF CONTENTS *iv*

INDEX OF FIGURES *viii*

INDEX OF TABLES *xi*

ABBREVIATIONS *xii*

1. INTRODUCTION **1**

1.1 THE SEROTONERGIC SYSTEM 1
1.1.1 Serotonin *1*
1.1.2 Serotonergic pathways *1*
1.1.3 The synthesis, storage, and metabolism of 5-HT *2*
1.1.4 Serotonin receptors *3*
1.1.5 Serotonin and Depression *4*
1.2 THE SEROTONIN TRANSPORTER 7
1.2.1 Molecular cloning of Na^+/Cl^- dependent neurotransmitter transporters *7*
1.2.2 Cloning and expression of the serotonin transporter *8*
1.2.3 The serotonin transporter gene *9*
1.2.4 Transporter topology and structural analysis *11*
1.2.5 Transport mechanism of the serotonin transporter *14*
1.2.6 Genetic regulation of the serotonin transporter *16*
1.3 TRAFFICKING AND REGULATION OF THE SEROTONIN TRANSPORTER 18
1.3.1 Membrane trafficking *18*
1.3.2 Serotonin transporter trafficking *21*
1.3.3 Regulation of the serotonin transporter by protein kinases *24*
1.3.4 Regulation of the serotonin transporter by interacting proteins *28*
1.4 AIM OF STUDY 31

2. MATERIALS AND METHODS **32**

2.1 MATERIALS 32
2.1.1 Plasmids *32*
2.1.2 Escherichia coli and Saccharomyces cerevisiae strains *32*
2.1.3 Enzymes *33*
2.1.4 Antibodies *33*
2.1.5 Other Materials *33*
2.2 METHODS 36
2.2.1 E. coli media recipes *36*
2.2.2 Antibiotics *37*
2.2.3 Saccharomyces cerevisiae media recipes *38*
2.2.4 Growth and maintenance of E. coli and Saccharomyces cerevisiae *40*

2.2.5 Preparation of competent E. coli cells 40
2.2.6 Transformation of competent E. coli cells 41
2.2.7 Preparation of plasmid DNA from E. coli 41
2.2.8 DNA enzymatic manipulations 42
2.2.9 Agarose electrophoresis 43
2.2.10 Purification of DNA fragments from agarose gels 43
2.2.11 Purification of RNA from mammalian cells 44
2.2.12 Reverse Transcriptase Polymerase chain reaction (RT-PCR) 44
2.2.13 Polymerase chain reactions (PCR) 45
2.2.14 Site directed mutagenesis 46
2.2.15 DNA sequencing 47
2.2.16 Preparation of yeast competent cells 47
2.2.17 Transformation of yeast competent cells 48
2.2.18 Isolation of DNA from yeast 48
2.2.19 Yeast Two-Hybrid Screening 49
2.2.20 Mating assay – verification of two-hybrid clones 50
2.2.21 Colony-lift filter assay 51
2.2.22 Liquid β-galactosidase assay 51
2.2.23 Preparation of yeast crude extract for Western blotting 52
2.2.24 Maintenance and storage of mammalian cells 52
2.2.25 Transient transfection of mammalian cells 53
2.2.26 Preparation of cell lysates 54
2.2.27 Preparation of rat brain extract 54
2.2.28 Markwell protein assay 54
2.2.29 SDS-polyacrylamide gel electrophoresis (SDS-PAGE) 55
2.2.30 Western Blotting 55
2.2.31 GST Pull-down assay 56
2.2.32 Co-immunoprecipitaion 57
2.2.33 5-HT uptake assay (on transiently transfected cells) 57
2.2.34 Cell surface biotinylation 58
2.2.35 Sucrose Gradient Fractionation 59
2.2.36 Confocal Microscopy 59
2.2.37 siRNA interference 60

3. IDENTIFICATION OF POTENTIAL SEROTONIN TRANSPORTER BINDING PROTEINS **61**

3.1 INTRODUCTION 61
3.1.1 The Yeast Two-Hybrid system 61
3.1.2 Aim of study 63
3.2 RESULTS 65
3.2.1 Analysis of clones identified using the yeast two-hybrid system 65
3.2.1.1 Yeast two-hybrid screening 65
3.2.1.2 Sequence analysis of selected clones isolated in the yeast two-hybrid screens 67
3.2.1.3 Verification of protein interactions by yeast mating 69
3.2.1.4 Selection of clones for further analysis 72
3.2.2 Further evaluation of Mint3 and ESO3 in yeast 74
3.2.2.1 Liquid β-galactosidase assays on Mint3 and ESO3 74
3.2.2.2 Liquid growth assays on Mint3 and ESO3 74
3.2.3 Analysis of known transporter interacting proteins for binding to SERT 75

3.2.3.1 PICK1 and Hic-5 75
3.2.3.2 Yeast Two-Hybrid analysis of PICK1 and Hic-5 76
3.2.3.3 GST-pulldown assays on PICK1 and Hic-5 77
3.3 DISCUSSION 78

4. FUNCTIONAL INTERACTION BETWEEN ESO3 AND 83
THE SEROTONIN TRANSPORTER 83

4.1 INTRODUCTION 83
4.2 RESULTS 84
4.2.1 Endogenous expression of ESO3 and SERT in different cell lines 84
4.2.2 PCR cloning of human and rat ESO3 84
4.2.3 Characterisation of an antibody raised against the C-terminal of ESO3 85
4.2.3.1 Prediction of antigenic peptide 85
4.2.3.2 Western blot analysis of ESO3 polyclonal antibody 86
4.2.4 Direct interaction between ESO3 and SERT 87
4.2.4.1 GST pull-down assays 87
4.2.4.2 Co-immunoprecipitaion 88
4.2.5 Mapping of binding domains in ESO3 and SERT 89
4.2.6 Effect of ESO3 on SERT function 89
4.2.6.1 5-HT transport assay 89
4.2.6.2 Cell surface biotinylation 90
4.2.6.3 Confocal microscopy 91
4.2.7 Effect of PKC activation on ESO3-mediated SERT down-regulation 91
4.2.8 Suppression of endogenous ESO3 by siRNA 92
4.2.8.1 Optimisation of semi-quantitative RT-PCR 92
4.2.8.2 Optimisation of siRNA transfection 93
4.2.8.3 Suppression of endogenous ESO3 expression in HEK-293 cells increases 5-HT uptake 94
4.3 DISCUSSION 95

5. SUBCELLULAR REDISTRIBUTION OF THE 102
SEROTONIN TRANSPORTER BY SECRETORY 102
CARRIER MEMBRANE PROTEIN 2 102

5.1 INTRODUCTION 102
5.2 RESULTS 104
5.2.1 Cloning of human SCAMP2 104
5.2.2 SCAMP2 interacts directly with SERT 104
5.2.2.1 GST pull-down assay 104
5.2.2.2 Co-immunoprecipitation 105
5.2.3 Overexpression of SCAMP2 causes a reduction in 5-HT uptake resulting from a cellular redistribution of SERT 105
5.2.3.1 5-HT transport assay 105
5.2.3.2 Cell surface biotinylation 106
5.2.4 SERT and SCAMP2 co-localize in HEK-293 cells 106
5.2.5 Endogenous SERT co-localizes with SCAMP2 in RN46A cells 107

5.2.6 Similarly to SERT, SCAMP2 is present in lipid rafts *108*
5.2.7 The presence of SCAMP2 prevents PKC-mediated down-regulation of SERT in HEK-293 cells *108*
5.2.8 Cysteine-201 within the highly conserved E peptide of SCAMP2 is critical for the cellular redistribution of SERT *109*
5.3 DISCUSSION 110

6. CONCLUDING REMARKS 117

REFERENCES 122

APPENDIX A 140
APPENDIX B 141
APPENDIX C 142
APPENDIX D 143
APPENDIX E 144
APPENDIX F 145
APPENDIX G 149
APPENDIX H 155

Index of Figures

Chapter 1

1.1 Biosynthesis of 5-HT 2

1.2 Schematic representation of the serotonergic synapse 3

1.3 Two-dimensional representation of the serotonin transporter 11

1.4 $LeuT_{Aa}$ structure 11

1.5 Schematic representation of the secretory pathway 18

Chapter 3

3.1 Principle of the yeast two-hybrid system 62

3.2 SERT bait constructs generated in pGBKT7 65

3.3 Illustration of yeast mating by replica plating 69

3.4 Illustration of Mint3 73

3.5 Illustration of ESO3 73

3.6 Verification of ESO3 and Mint3 protein expression 74

3.7 Liquid β-galactosidase assay on Mint3 74

3.8 Liquid β-galactosidase assay on ESO3 (clone no. 790) 74

3.9 Liquid growth assay on Mint3 75

3.10 Liquid growth assay on ESO3 (clone no. 790) 75

3.11 PICK1 binds to the C-terminal domain of SERT 77

3.12 Hic-5 binds to the C-terminal domain of SERT 77

3.13 Increased concentration of detergent eliminates non-specific binding between Hic-5 and GST 77

Chapter 4

4.1 Endogenous expression of ESO3 in various cell lines 84

4.2 Endogenous expression of SERT in various cell lines 84

4.3 Secondary structure prediction of human ESO3 85

4.4 Prediction of antigenic peptide 85

4.5 Evaluation of ESO3 anti-sera 86

4.6 Anti-ESO3 does not recognize rat ESO3 86

4.7 Coomassie staining of GST-fusion proteins 87
4.8 ESO3 interacts with the N-terminal domain of SERT 88
4.9 ESO3 binds specifically to the long N-terminal domain of SERT 88
4.10 ESO3 interacts with the N-terminal domain of DAT 88
4.11 The full-length SERT interacts with ESO3 in HEK-293 cells 88
4.12 Protein sequence comparison of human, rat, and mouse ESO3 89
4.13 Mapping of ESO3 region responsible for interaction with SERT 89
4.14 Mapping of SERT binding domain involved in the interaction with ESO3 89
4.15 SERT uptake activity is reduced by ESO3 in a dose-dependent manner 90
4.16 Western blot of whole cell lysates from co-transfected HEK-293 cells 90
4.17 Overexpression of ESO3 down-regulates SERT uptake activity 90
4.18 ESO3 overexpression downregulates SERT uptake activity by decreasing the cell-surface levels of the transporter 90
4.19 Overexpression of ESO3 changes SERT subcellular localization 91
4.20 ESO3 accumulates in the ER 91
4.21 Down-regulation of SERT by ESO3 and PKC is mediated by distinct mechanisms 92
4.22 Determination of the optimal concentration of ESO3 primers 92
4.23 Determination of the optimal concentration of GAPDH primers 92
4.24 Determination of the linear range of ESO3 amplification 93
4.25 Determination of the linear range of GAPDH amplification 93
4.26 Determination of the linear range of amplification for ESO3 and GAPDH 93
4.27 Control for competition between primer pairs 93
4.28 Comparison of three different reagents for siRNA transfection 94
4.29 Optimised conditions for GAPDH siRNA transfection 94
4.30 Comparison of the effect of three siRNAs on ESO3 mRNA levels 94
4.31 Time course effect of siRNA sequence B on ESO3 mRNA levels 94
4.32 Western blot of whole cell lysates from siRNA transfected HEK-293 cells 95
4.33 5-HT uptake is increased by suppression of ESO3 95
4.34 Western blots of whole cell lysates from siRNA transfected HEK-293 cells 95

Chapter 5

5.1 Endogenous expressions of SCAMP2 and SCAMP3 but not SCAMP1 in HEK-293 cells 104

5.2 SCAMP2 interacts with the N-terminal domain of SERT and DAT 104

5.3 SCAMP2 co-immunoprecipitates with the full-length SERT in transfected HEK-293 cells 105

5.4 SERT interacts with SCAMP2 in rat brain 105

5.5 5-HT uptake is reduced by SCAMP2 in a dose-dependent manner 105

5.6 Western blot of whole cell lysates from co-transfected HEK-293 cells 105

5.7 Overexpression of SCAMP2 decreases SERT uptake activity 105

5.8 Overexpression of SCAMP2 decreases SERT cell surface expression 106

5.9 SERT co-localizes with SCAMP2 in HEK-293 cells 107

5.10 Co-localization of endogenous SERT with SCAMP2 in immortalised neurons 107

5.11 SCAMP2 associates with lipid rafts in rat brain tissue 108

5.12 SCAMP2 prevents PKC-mediated SERT down-regulation 109

5.13 Mutations of C201 or W202 do not affect the binding of SCAMP2 to SERT 109

5.14 The SCAMP2 mutant C201A has no affect on SERT uptake activity 109

5.15 Western blots of whole cell lysates from co-transfected HEK-293 cells 110

5.16 The C201A mutant is unable to down-regulate SERT cell surface expression 110

Chapter 6

6.1 Possible mechanism for ESO3-mediated SERT regulation 119

6.2 SCAMP2-mediated subcellular redistribution of SERT 120

Index of Tables

Chapter 2

2.1 List of Antibodies 33

Chapter 3

3.1 Calculation of mating efficiency and number of clones screened 66

3.2 Number of clones isolated in the yeast two-hybrid screens 67

3.3 Identity of selected clones 72

3.4 Re-testing of selected clones 72

Abbreviations

ATP	Adenosine triphosphate
BSA	Bovine serum albumin
BLAST	Basic Local Alignment Search Tool
CFU	Colony forming units
CMC	Critical-micelle-concentration
CNS	Central nervous system
ConA	Concanavalin A
COP	Coat protein
CSF	Cerebrospinal fluid
CTBP	Cterminal binding protein
DA	Dopamine
DAT	Dopamine transporter
DMEM	Dulbecco's Modified Eagle's Medium
DMSO	Dimethylsulphoxide
DNA-BD	DNA binding domain
DTT	Dithiothreitol
EDTA	Ethylenediaminetetraacetic acid
EGF	Epidermal growth factor
EH	EPs15 homology
EL	Extracellular loop
ER	Endoplasmic reticulum
FCS	Foetal calf serum
FRET	Fluorescence resonance energy transfer
GABA	γ-aminobutyric acid
GAPDH	Glyceraldehyde-3-phosphate dehydrogenase
GAT	GABA transporter
GLUT	Glucose transporter
GTP	Guanine triphosphate
GLYT	Glycine transporter
GST	Glutathione-S-transferase
HEK	Human embryonic kidney

5-HIAA	5-hydroxyindoleacetic acid
5-HT	5-hydroxytryptamine (Serotonin)
5HTTLPR	5-HT transporter gene-linked polymorphic region
IFN	Interferon
IPTG	Isopropyl-1-thio-β-D-galactopyranoside
LC	Light chain
MAO	Monoamine oxidase
MAP	Microtubule-associated protein
MAPK	Mitogen-activated protein kinase
MDMA	3,4-methylenedioxy-methamphetamine
NCBI	National Center for Biotechnology
NE	Norepinephrine
NET	Norepinephrine transporter
NPF	Asp-Pro-Phe
OD	Optical density
ONPG	o-Nitrophenyl β-D-galactopyranoside
PAGE	Polyacrylamide gel electrophoresis
PBS	Phosphate buffered saline
PCR	Polymerase chain reaction
PDZ	Postsynaptic density protein-95, postsynaptic discs large, and zona occludens-1
PGDS	Prostaglandin D synthase
PICK1	Protein interacting with C-kinase 1
$PI(4,5)P_2$	Phosphatidylinositol 4,5-biphosphate
PKA	Protein kinase A
PKC	Protein kinase C
PKG	Protein kinase G
PLC	Phospholipase C
PMA	Phorbol 12-myristate 13-acetate
PP2A	Protein phosphatase 2A
PVDF	Polyvinylidene fluoride
RanBPM	Ran binding protein M
RT-PCR	Reverse transcriptase polymerase chain reaction
SCAMP	Secretory carrier membrane protein

SD	Synthetic dropout
SDS	Sodium dodecyl sulphate
SERT	Serotonin Transporter
SiRNA	Small interfering RNA
SNAP 25	synaptosomal associated protein of 25 kDa
SNARE	soluble N-ethylmaleimide-sensitive-factor attachment protein receptor
SSRI	Selective serotonin reuptake inhibitor
TCA	Tricyclic antidepressant
TfR	Transferrin receptor
TGN	Trans-Golgi network
TMD	Transmembrane domain
TNF	Tumor necrosis factor
TPH	Tryptophan hydroxylase
VAMP	Vesicle associated membrane protein
VMAT	Vesicular monoamine transporter
VNTR	Variable nucleotide tandem repeat
WGA	Wheat germ agglutinin
X-β-gal	5-Bromo-4-chloro-3-indolyl-b-D-galactoside in dimethyl formamide

1. INTRODUCTION

1.1 THE SEROTONERGIC SYSTEM

1.1.1 Serotonin

In 1948 Maurice M. Rapport and his co-workers Arda Alden Green and Irvine H. Page succeeded in isolating a substance from beef serum that was known to induce powerful contractions of the smooth muscles lining the walls of blood vessels, thereby causing an increase in blood pressure (Rapport et al., 1948). The substance was named serotonin, indicating a *ser*um agent affecting vascular *tone*. As Rapport and his fellow researchers tested the newly isolated vasoconstrictor, they noted that its chemical and biological activity resembled that of enteramine. In 1949 Rapport confirmed the chemical formula for serotonin as 5-hydroxytryptamine (5-HT) (Rapport, 1949). 5-HT was later recognized as a neurotransmitter, when Twarog and Page in 1953 identified 5-HT in the central nervous system (CNS) (Twarog and Page, 1953). Today, it is generally accepted that 5-HT has a widespread distribution in both the central and peripheral nervous systems.

1.1.2 Serotonergic pathways

Approximately 95% of the organism's total 5-HT is produced by enterochromaffin cells in the intestine and stored in platelets, where it functions as a peripheral hormone involved in vasoconstriction, haemostasis, and the control of immune responses. Dahlström and Fuxe provided the first detailed mapping of the serotonergic system in the mammalian brain and showed that cell bodies of serotonergic neurons are primarily found in the raphe nuclei of the brainstem (Dahlström and Fuxe, 1964). One of the key features of the serotonergic system, which distinguishes it from the major excitatory and inhibitory neurotransmitters, is this centralization of cell bodies. Out of the billions of neurons in the human brain, less than 300.000 appear to contain 5-HT (Tork, 1990).

Serotonergic pathways originating in the brainstem raphe nuclei project widely to almost all parts of the CNS. The innervations of widespread areas of the brain is consistent with the multitude of biological functions regulated by 5-HT, such as sleep, appetite, memory, learning and the variety of psychiatric disorders in which dysfunction of serotonergic neurotransmission has been observed, including depression, anxiety, obsessive-compulsive disorder, schizophrenia and migraine (Heinz et al., 2001; Hahn and Blakely, 2002; Murphy et al., 2004; Lesch and Gutknecht, 2005). Moreover, serotonin is a precursor for melatonin and is therefore synthesized in high amounts in the pineal gland (Reiter, 1991).

In addition to modulating functions in the adult brain, 5-HT controls important functions in brain development, where it regulates activities such as neural differentiation, axon outgrowth, and configuration of synaptic connections (Gaspar et al., 2003).

1.1.3 The synthesis, storage, and metabolism of 5-HT

5-HT belongs to a class of monoamines which also include the catecholamines dopamine (DA), norepinephrine (NE), epinephrine, and the imidazole histamine. 5-HT is a hydrophilic molecule that cannot cross the blood-brain barrier, and hence has to be synthesised locally within the serotonergic neurons.

5-HT is synthesised by a two-step process from the essential amino acid $_{L}$-tryptophan (Figure 1.1). The aromatic amino acid $_{L}$-tryptophan is obtained from the diet and is actively transported across the blood-brain barrier in competition with other neutral amino acids. The rate-limiting factor in 5-HT synthesis is the hydroxylation of $_{L}$-tryptophan to 5-hydroxytryptophan, catalysed by the enzyme tryptophan hydroxylase (TPH) (Boadle-Biber, 1993). Recently it was discovered that there are two different isoenzymes of TPH; TPH1 and TPH2, where TPH1 functions in the periphery and TPH2 in the central nervous system (Walther et al., 2003). 5-hydroxytryptophan is subsequently decarboxylated to form 5-HT by the relatively non-specific enzyme $_{L}$-amino acid decarboxylase.

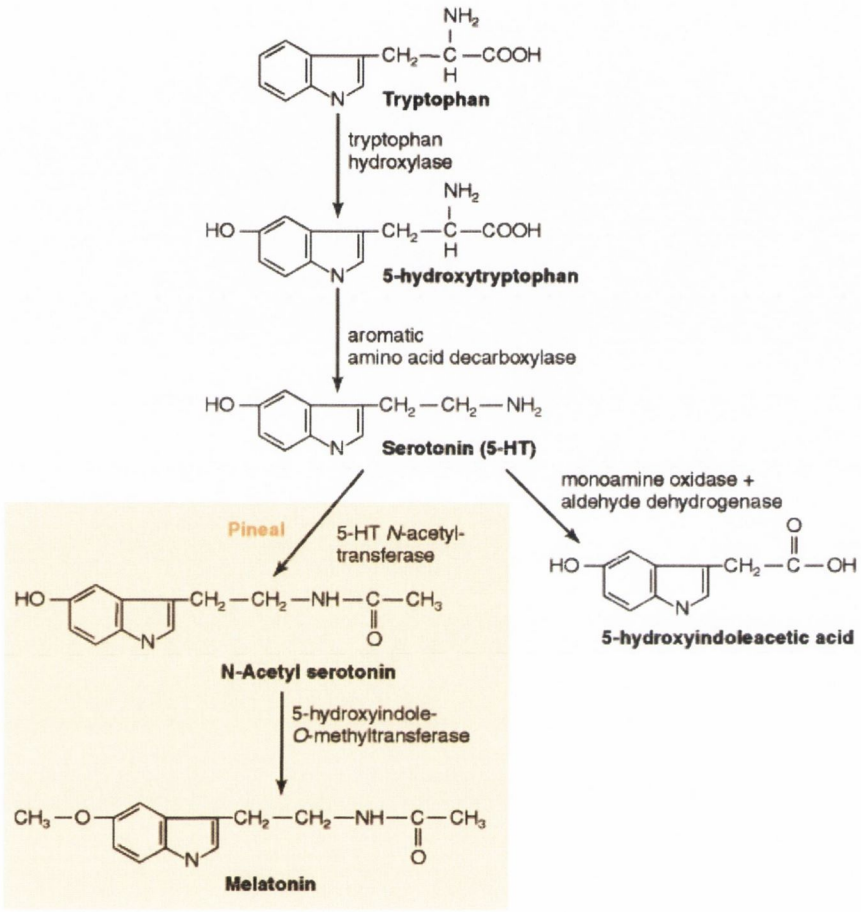


Figure 1.1 Biosynthesis of 5-HT. 5-HT is synthesised from the aromatic amino acid tryptophan. Tryptophan is hydroxylated to 5-hydroxytryptophan by tryptophan hydroxylase and then decarboxylated to form 5-HT by the non-specific enzyme aromatic amino acid decarboxylase. 5-HT serves as the precursor for melatonin in the pineal gland.

Following synthesis, 5-HT is stored within synaptic vesicles (Figure 1.2). The transport of 5-HT into synaptic vesicles is mediated by the vesicular monoamine transporter (VMAT). VMAT acts as an electrogenic antiporter of protons and monoamines by using a proton electrochemical gradient maintained by an ATP-dependent H^+ pump located in the secretory vesicles.

Like all monoamine neurotransmitters, 5-HT is released into the synaptic cleft via exocytosis. Synaptic vesicles containing 5-HT interact with the cytoskeleton and soluble vesicle-binding proteins, prior to docking at specialised membrane sites in the axon terminals (Südhof, 1995). When an action potential arrives at the axonal terminal, voltage-gated Ca^{2+} channels are activated causing an influx of Ca^{2+} ions. The increase in cytosolic Ca^{2+} triggers the fusion of synaptic vesicles with the presynaptic plasma membrane, resulting in 5-HT release.

Once 5-HT is released into the synaptic cleft it exerts its function by binding to receptors present in the plasma membrane of postsynaptic cells, or to receptors located in the presynaptic plasma membrane (autoreceptors) to generate or modulate intracellular events. In order to terminate serotonergic neurotransmission, 5-HT must be cleared from the synaptic cleft. This process is mediated by the serotonin transporter (SERT), which binds 5-HT and carries it across the plasma membrane back into the presynaptic neuron that released the 5-HT. Once back inside the serotonergic neuron, 5-HT is either re-stored in synaptic vesicles or metabolised by monoamine oxidase A (MAO-A) to 5-hydroxyindoleacetaldehyde, which is further oxidized to the major metabolite of 5-HT, namely 5-hydroxyindoleaceticacid (5-HIAA).

1.1.4 Serotonin receptors

Serotonin exerts its diverse actions by binding to 15 or more distinct 5-HT cell surface receptors. The 5-HT receptors are classified into seven groups, 5-HT_1 through 5-HT_7, largely on the basis of their structural and operational characteristics. With the exception of the 5-HT_3 receptor, which is a ligand-gated ion channel, all 5-HT receptor subtypes belong to the large family of seven transmembrane domain G-protein coupled receptors, that couple to and transduce signals via guanine nucleotide binding

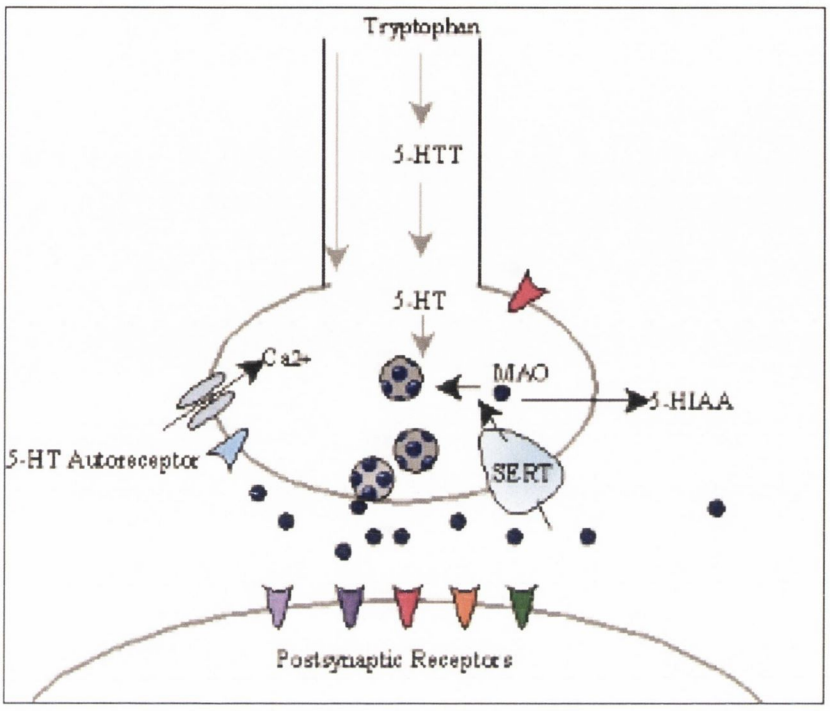


Figure 1.2 Schematic representation of the serotonergic synapse. Tryptophan is actively taken up into serotonergic neurons where it is converted to 5-HT by a two-step process. In the presynaptic terminal, 5HT is stored into synaptic vesicles and upon excitation, is released into the synaptic cleft via exocytosis. The released 5-HT exerts its function via binding to 5-HT receptors on the postsynaptic cell. The activity of 5-HT is terminated by the action of the serotonin transporter (SERT) which takes 5-HT up into the presynaptic terminal for metabolism by monoamine oxidases (MAO) located on the outer mitochondrial membrane or for re-storage into vesicles.

regulatory proteins (G-proteins). A number of signalling cascades are stimulated by the 5-HT receptors and affect a variety of intracellular proteins, such as adenylyl cyclase, phospholipase C (PLC), protein kinase C (PKC), voltage-gated N-type Ca^{2+} channels and the hyperpolarizing potassium channels (Adayev et al., 2005).

1.1.5 Serotonin and Depression

The monoamine theory of depression was first proposed during the 1960's based on the mood-altering effects of certain drugs. This theory suggested that the underlying biological basis for depression was a diminished neurotransmission involving NE and 5-HT and that targeting these neuronal lesions with antidepressants would restore normal function in depressed patients (Schildkraut, 1965).

The first two classes of drugs used for treating major depression were the monoamine oxidase inhibitors (MAOIs) and the tricyclic antidepressants (TCAs). Iproniazid (the first MAO inhibitor) was originally developed in the early 1950's to fight tuberculosis. Besides its ability to treat tuberculosis, iproniazid was observed to elevate mood and stimulate activity in many patients (Crane, 1956). These effects led scientists to investigate the ability of iproniazid to treat depression. Around the same time the first TCA, imipramine, was discovered in the search for drugs useful in the treatment of schizophrenia. It was ineffective in this regard, but had a remarkable mood elevating effect on certain patients with symptoms of depression (Kuhn, 1958). Subsequent studies demonstrated that imipramine acts as an inhibitor of NE and 5-HT re-uptake.

The primary effect of MAOIs and TCAs is an increase in the activity of monoamines and although a number of undesirable and harmful side effects were reported for both the MAOIs and the TCAs, they were used effectively for many years in the treatment of depression. Both MAOIs and TCAs were discovered by chance but the second generation of antidepressants, the selective serotonin re-uptake inhibitors (SSRIs), were designed specifically to target the re-uptake of 5-HT by blocking the 5-HT transporter. The idea was to produce agents that were more selective and therefore more effective and better tolerated than the older MAOIs and TCAs. The marketing of SSRIs began in

the 1980's with Fluoxetine or "Prozac" and SSRIs are today the most widely prescribed of all antidepressants (Hirschfeld, 2000).

There is substantial indirect evidence to support that alterations in the serotonergic neuronal system occur in many patients with depression. These findings include reduced concentrations of the major metabolite of 5-HT, 5-HIAA, in the cerebrospinal fluid (CSF) of unmedicated depressed patients and reduced concentrations of 5-HT and 5-HIAA in post-mortem brain tissue from depressed suicide victims, although these findings are subject to some controversy (Stanley and Stanley, 1990; Asberg, 1997). Changes in platelet SERT have been suggested as a possible biomarker for neurological disorders and the majority of studies concerning SERT densities in platelets from unmedicated depressed patients confirm a reduction in SERT density. Studies on post-mortem brain SERT binding sites in suicide victims and depressed patients have yielded inconsistent results with both decreases, increases, and no alterations in SERT binding sites (Plein and Berk, 2001; Purselle and Nemeroff, 2003). Also, an increase in the density of 5-HT_2 receptors has been shown in post-mortem brain tissue and in platelets from unmedicated depressed patients (Pandey, 1997).

The rate limiting enzyme for the synthesis of 5-HT in the brain, TPH2, is not saturated under normal physiological conditions. Therefore, any changes in brain tryptophan levels can lead to corresponding alterations in the ability of neurons to synthesise 5-HT. Results from such studies show that tryptophan depletion can eliminate the therapeutic efficacy of SSRIs, suggesting that increased availability of 5-HT is playing a direct role in maintaining the improvement in mood and other depressive symptoms. In contrast, tryptophan depletion does not worsen symptoms in depressed patients not taking medication, nor does it cause depression in healthy subjects with no depressive illness (Bell et al., 2001).

The symptomatic relief of depressive illness following treatments that alter the serotonergic system provide the most convincing evidence for serotonergic alterations in depressed patients. In general, all clinically efficacious SSRIs increase serotonergic neurotransmission following chronic treatment. However, while SSRIs block the re-uptake of 5-HT within a few hours of administration, a significant clinical antidepressant effect may not be observed for several weeks. Several studies have

shown that serotonergic autoreceptors are desensitised upon chronic treatment with SSRIs. This desensitisation occurs in a similar timeframe as the onset of the antidepressant response and thus it was hypothesised that the slow onset of clinical action may be ascribed to the inhibition of 5-HT release by 5-HT autoreceptors. When an SSRI is administered, the immediate consequence is an increase in extracellular levels of 5-HT leading to activation of 5-HT autoreceptors. 5-HT autoreceptor activation mediates a reduction in neuronal firing and thus a decrease in 5-HT release in projection areas. However, as treatment continues, the sustained increase of 5-HT causes the 5-HT autoreceptors to desensitise, reducing their ability to inhibit neuronal firing. Thus, neuronal firing is turned on and more 5-HT is released from the axon terminals where it is presumably needed to exert its therapeutic actions (Blier, 2003). The 5-HT autoreceptor hypothesis suggests that co-administration of an SSRI with a relevant 5-HT autoreceptor antagonist could mimic the dynamic changes established by chronic administration of SSRIs, thereby accelerating the onset of the antidepressant effect. Pindolol, an antagonist of autoreceptors of the 5-HT_{1A} subtype, has in fact been observed to induce a more rapid onset of antidepressant response when administrated in combination with an SSRI, although clinical studies of pindolol have produced inconsistent results and it has been questioned whether this compound is an appropriate ligand (Blier, 2003).

In summary, the connection between 5-HT and depression is likely to be more complicated and perhaps more indirect than the 5-HT hypothesis implies. SSRIs seem to be effective in the treatment of depression not because of their acute effects on extracellular 5-HT levels, but because of long-term adaptive changes in serotonergic neurotransmission. The superior efficacy of SSRIs in the treatment of depression has focused the attention on serotonergic neurotransmission and the structure and function of the serotonin transporter.

1.2 The Serotonin Transporter

1.2.1 Molecular cloning of Na^+/Cl^- dependent neurotransmitter transporters

The termination of neurotransmission is a critical component of neural signalling and depends on the rapid removal of neurotransmitters from the synaptic cleft by high affinity neurotransmitter transporters. SERT belongs to the family of Na^+/Cl^- dependent neurotransmitter transporters, which use sodium and chloride electrochemical gradients to drive the thermodynamically uphill movement of their substrates.

The molecular characterisation of members of the Na^+/Cl^- dependent family of neurotransmitter transporters began with the successful purification of a rat GABA transporter which in 1990 led to the isolation and sequencing of a clone encoding a neuronal γ-aminobutyric acid (GABA) transporter (GAT) (Guastella et al., 1990; Nelson et al., 1990). In 1991, the human NE transporter (NET) was cloned (Pacholczyk et al., 1991) and the high degree of sequence similarity between GAT and NET classified these two as belonging to the same gene family. Expression and homology cloning rapidly led to the enlargement of this family with transporters for the amino acids; glycine (GLYT) (Guastella et al., 1992; Smith et al., 1992a), proline (Fremeau et al., 1992) and taurine (Liu et al., 1992; Smith et al., 1992b; Uchida et al., 1992) and transporters for the monoamines; DA (DAT) (Giros et al., 1991; Kilty et al., 1991; Shimada et al., 1991; Usdin et al., 1991) and 5-HT (SERT) (Blakely et al., 1991; Hoffman et al., 1991) and transporters of the osmolytes; betaine (Yamauchi et al., 1992) and creatine (Guimbal and Kilimann, 1993).

Also, homology cloning revealed several orphan transporters whose substrates were initially unknown. Recent studies, however, suggest that these proteins transport neutral amino acids (Broer, 2006). Moreover, several subtypes of the GABA and glycine transporters derived from multiple genes and alternative splicing of gene products have been identified.

1.2.2 Cloning and expression of the serotonin transporter

In 1991 Blakely et al isolated a rat brain SERT cDNA by PCR using degenerate oligonucleotides derived from two highly conserved regions of GAT and NET (Blakely et al., 1991). At the same time, Hoffman et al isolated a SERT cDNA clone from a rat basophilic leukaemia cell line by screening subdivisions of cDNA pools for [^{3}H]5-HT uptake (Hoffman et al., 1991). Despite sequence differences in the original reports, the cDNA clones are now known to encode identical proteins. Subsequently, human SERT cDNAs were isolated from brain (Lesch et al., 1993b), platelet (Lesch et al., 1993a) and placenta (Ramamoorthy et al., 1993b) and found to be identical. Since then, SERT homologues have been cloned from a number of species including fruitfly (Corey et al., 1994a; Demchyshyn et al., 1994), mouse (Chang et al., 1996), sheep (Padbury et al., 1997), guinea pig (Chen et al., 1998b), cow (Mortensen et al., 1999a), monkey (Miller et al., 2001), nematode (Ranganathan et al., 2001), chicken (Larsen et al., 2004), zebrafish (Wang et al., 2006) and silkworm (Gu et al., 2006).

The human and other mammalian SERTs are proteins of 630 amino acid residues with approximately 90% cross-species identity. In humans, unlike rodents, three distinct SERT mRNA transcripts have been identified, resulting from both alternative splicing and usage of alternative polyadenylation sites (Ramamoorthy et al., 1993b; Austin et al., 1994).

In mammals SERT is expressed throughout the organism and in addition to the expression in serotonergic neurons, high levels of SERT are found in lung, placenta, and blood platelets (Brownstein and Hoffman, 1994).

Studies using Northern blot analysis and in situ hybridization in human (Austin et al., 1994) and rat (Blakely et al., 1991) brain demonstrated that expression of SERT mRNA closely parallels the distribution of TPH in serotonergic cell bodies of the midbrain and brainstem raphe nuclei (Hoffman et al., 1998). Furthermore, SERT mRNAs in regions associated with serotonergic terminals in rat brain have also been reported (Lesch et al., 1993c).

Immunocytochemistry in rat brain has been used to investigate the regional distribution of SERT expression. SERT immunoreactive fibres were found to be widely distributed throughout the brain with the highest density in forebrain regions, correlating with areas of high serotonergic activity (Qian et al., 1995).

The level of cytoplasmic SERT appeared to be high in soma and dendrites and low in axons, indicating that SERT is probably synthesized in soma and dendrites and then transported to the final destination in the axon. In contrast, plasma membrane levels of SERT were found to be higher in axon-derived membranes than in membranes from soma and dendrites, indicating that the axon is where most of the 5-HT uptake is taking place. Furthermore, the majority of SERT is located along the axon and not restricted to synapses, indicating that the regulation and termination of 5-HT neurotransmission extend beyond the synaptic cleft (Tao-Cheng and Zhou, 1999).

1.2.3 The serotonin transporter gene

The chromosomal location of the human SERT gene has been mapped to a single genomic locus at 17q11.2 (Ramamoorthy et al., 1993b). The gene is organised into 14 exons, spanning approximately 35 kb (Lesch et al., 1994). Translation of SERT initiates within exon 2 and extends partially into exon 14. An additional exon 1B located between exon 1A and 2 has been identified in the human SERT gene. SERT undergoes alternative splicing to give either a long (1A+1B+2) or short (1A+2) mRNA transcript. As the alternative splicing involves only non-coding regions, the primary structure of SERT is unaltered. Also, several polyadenylation sites at the 3'end of the human SERT gene have been identified, resulting in multiple mRNA species (Bradley and Blakely, 1997; Ozsarac et al., 2002). Alternative splicing and usage of alternate polyadenylation sites are factors likely to participate in tissue specific regulation of SERT expression by influencing mRNA stability and eventually the efficiency of protein synthesis.

The human SERT promoter contains a TATA-like motif and potential binding sites for transcription factors, including AP1, AP2, SP1, NFκB and a cAMP response element

(CRE)-like motif in the 5'-flanking regulatory region upstream of exon 1A. The information within 1.4 kb of the 5'-flanking region is sufficient to confer cell-specific expression regulated by a combination of positive and negative *cis*-acting elements (Heils et al., 1995; Mortensen et al., 1999b; Flattem and Blakely, 2000).

The expression of human SERT is also modulated by a repetitive element of varying length in the 5'-flanking region, termed the 5-HT transporter gene-linked polymorphic region (5HTTLPR). This polymorphism consists of a variable number of GC-rich repeat elements of 20-23 bp long. In humans the majority of alleles are composed of either 14 or 16 repeat elements differing in length by 44 bp involving repeat element 6 to 8. Compared with the long allele (16 repeats), the short allele has been reported to act as a dominant allele associated with lower transcriptional efficiency, resulting in reduced transporter levels and 5-HT uptake (Heils et al., 1996; Lesch et al., 1996; Greenberg et al., 1999). A variable nucleotide tandem repeat sequence (VNTR) in the intron following the first coding exon has also been described and seems to have enhancer-like properties (MacKenzie and Quinn, 1999).

SERT has long been suspected to play a role in various neurological and psychiatric diseases probably caused by a dysregulation of SERT expression rather than substitution of amino acids, which are thought to be critical to substrate transport. Consequently, a possible association of the two polymorphic regions 5HTTLPR and VNTR to susceptibility to various neuropsychiatric disorders has been studied intensively in recent years. Generally, these studies have produced conflicting results and no common replicated association has been detected (Anguelova et al., 2003). A possible explanation to the varying success in establishing a link between these polymorphisms and neuropsychiatric disorders is the large representative sample of individuals required to demonstrate significant levels of association. Also, it is likely that disorders are multifactorial caused by several different genetic abnormalities and that more than one genetic composition can form the basis for neurological and psychiatric disorders.

Several naturally occurring mutations have been identified within the coding region of human SERT. The coding variants are found at low frequencies and the functional consequences of the individual mutations are unknown. Two exceptions are I425V and L225M, which are rare SERT mutations in highly conserved transmembrane regions that were found to be associated with neuropsychiatric phenotypes (Di Bella et al., 1996; Glatt et al., 2001; Kilic et al., 2003; Ozaki et al., 2003; Torres and Caron, 2003; Prasad et al., 2005).

1.2.4 Transporter topology and structural analysis

The Na^+/Cl^- dependent transporters for the monoamines, GABA and the amino acids all share the same general topology. The primary sequence and hydropathy analysis (Kyte and Doolittle, 1982) predicts a membrane topology involving 12 transmembrane domains (TMDs) with cytosolic oriented N- and C- termini and a large extracellular loop (EL2) connecting TMD3 and TMD4 (Figure 1.3). This model is supported by experimental data on the topology of NET and SERT. The intracellular position of the N- and C- termini and the location of the predicted extracellular loops, EL2 and EL4, were confirmed in NET using sequence specific antibodies and selective membrane permeabilisation (Bruss et al., 1995). In 1998, Chen et al confirmed the position of the extracellular loops in SERT (Chen et al., 1998a) and more recently, the same group also confirmed the position of the intracellular loops in SERT (Androutsellis-Theotokis and Rudnick, 2002).

This overall topology has recently been confirmed by the crystallization of a bacterial homolog from *Aquifex aeolicus* ($LeuT_{Aa}$), the first structure of a member of the Na^+/Cl^- dependent neurotransmitter transporter family (Yamashita et al., 2005). This structure revealed a dimer with each monomer containing 12 TMDs organized in a unique fold. The binding site for the substrate, L-leucine, was buried inside the center of the $LeuT_{Aa}$ with TM 1, 3, 6, and 8 forming the binding pocket (Figure 1.4). This structure has provided valuable information for re-interpretation of years of molecular and pharmacological data and has provided new insight into the transport mechanism of neurotransmitter transporters.

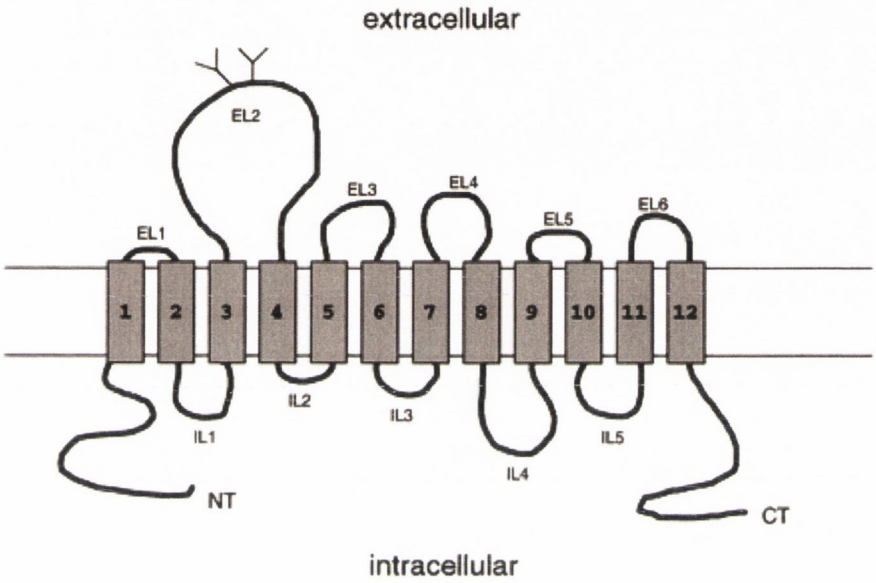


Figure 1.3 Two-dimensional representation of the serotonin transporter. The 12 membrane spanning domains are shown as cylinders representing α-helices. Glycosylation of SERT is indicated in the extracellular loop connecting transmembrane domains 3 and 4.

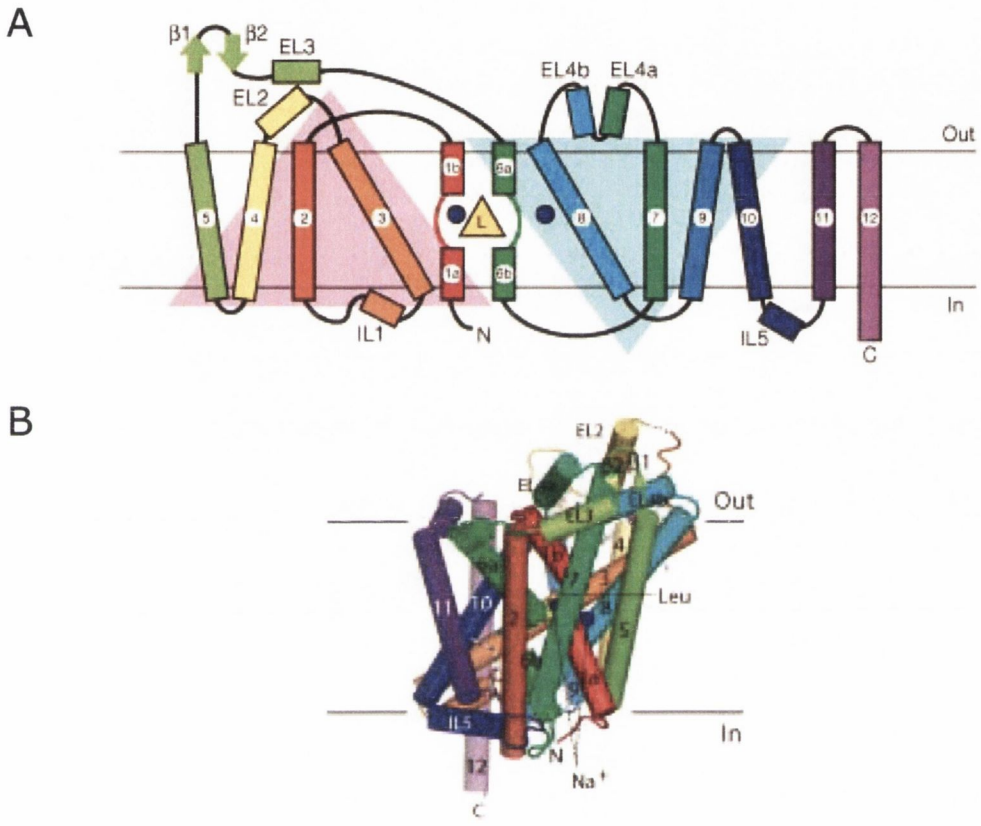


Figure 1.4 LeuT$_{Aa}$ structure. (A) The LeuT$_{Aa}$ topology with the 12 TMDs numbered 1-12. TMD1 and TMD6 are unwound halfway through the membrane to form the binding pocket for the sodium ions (blue circles) and the substrate, leucine. (B) Stereoview of LeuT$_{Aa}$ in the plane of the membrane. (Yamashita et al., 2005)

SERT together with DAT and NET comprise the subfamily of monoamine transporters characterised by similarity in sequence and pharmacological properties. The monoamine transporters are most conserved in the putative TMDs and least conserved at the cytoplasmic N- and C-termini and within the large extracellular loop connecting TMD3 and TMD4.

Members of the family of Na^+/Cl^- dependent neurotransmitter transporters are characterised by the presence of multiple *N*-glycosylation sites within the large extracellular loop connecting TMD3 and TMD4. *N*-glycosylation has been suggested to play an important role in the stability and trafficking of the transporters to the plasma membrane rather than being involved in transport activity.

Early studies using baculovirus-mediated expression of SERT glycosylation mutants in Sf9 insect cells indicated that glycosylation is required for optimal stability of the transporter in the membrane but not for transport activity or ligand binding (Tate and Blakely, 1994). However, mutation of both glycosylation sites in SERT reduced V_{max} to a greater extend than predicted from the B_{max} values, suggesting that unglycosylated SERT does not transport 5-HT as efficiently as wild-type SERT or that a fraction of the unglycosylated SERT is inactive. Similar studies with NET showed that the inability to *N*-glycosylate NET did not affect ligand recognition, but reduced the general protein stability and surface trafficking (Melikian et al., 1996; Nguyen and Amara, 1996).

Studies on the GLYT1 showed that removal of its glycosylation consensus sites resulted in the accumulation of unglycosylated transporter in intracellular compartments and that enzymatic deglycosylation of the transporter did not alter its transport activity (Olivares et al., 1995).

However, recent studies on DAT suggest that unglycosylated DAT at the plasma membrane does not transport substrate as efficiently as wild-type DAT (Li et al., 2004). This finding is in agreement with the initial observations made by Tate and Blakely and reported deviations between surface levels and uptake activity of unglycosylated NET (Melikian et al., 1996; Nguyen and Amara, 1996). Thus, removal of glycosylation sites seems to reduce the transport activity of the transporters. Interestingly, *N*-linked glycosylation has recently been suggested to play a role in GAT1 transport activity by affecting its affinity for sodium ions (Cai et al., 2005).

SERT monomers have been proposed to require *N*-linked glycosylation to associate with each other and to function in homo-oligomeric complexes (Ozaslan et al., 2003). The increased efficiency of folding of the glycosylated transporters is thought to facilitate oligomerization by mediating inter-subunit interactions or stabilising the oligomer in other ways. However, the quaternary status of Na^+/Cl^- dependent transporters has not yet been fully elucidated.

Na^+/Cl^- dependent transporters have been shown to form aggregated complexes when analysed by SDS-PAGE (Radian et al., 1986). A possible dimeric aggregate has been observed in heterologous expression studies of NET and DAT in COS cells (Bruss et al., 1995) and of SERT in HEK-293 cells (Jess et al., 1996) and in Sf9 insect cells (Tate and Blakely, 1994). Also, the effect of dominant negative-mutants upon wild-type transporter activities has suggested the existence of a quaternary structure of SERT (Chang et al., 1998).

Recent studies have provided more direct evidence for Na^+/Cl^- dependent transporters to engage in oligomeric complexes (Sitte et al., 2004). For instance, the use of fluorescence resonance energy transfer (FRET) microscopy has indicated oligomeric complexes of SERT and GAT1 (Schmid et al., 2001) and DAT (Sorkina et al., 2003) in living cells. Cross-linking studies demonstrated that DAT forms dimers and possible higher order oligomers when heterologously expressed in HEK-293 cells (Hastrup et al., 2001; Hastrup et al., 2003). Also, the ability of different epitope-tagged SERT (Kilic and Rudnick, 2000) and DAT (Sorkina et al., 2003) constructs to co-precipitate has supported oligomer formation of Na^+/Cl^- dependent transporters. In contrast, the glycine transporters GLYT1 and GLYT2 have been shown to exist in the plasma membrane exclusively as glycosylated monomers, whereas a significant fraction of the intracellular transporters were core-glycosylated and oligomeric in nature (Horiuchi et al., 2001). This study in particular suggests that neurotransmitter transporters do not require oligomerization for substrate translocation.

1.2.5 Transport mechanism of the serotonin transporter

It is well established that all Na^+/Cl^- dependent neurotransmitter transporters terminate synaptic transmission by using electrochemical gradients to drive the re-uptake of neurotransmitters from the synapse.

The uphill transport of 5-HT by SERT across the plasma membrane is coupled to the downhill influx of Na^+ and Cl^- and the efflux of K^+. The Na^+ and K^+ gradients are formed and maintained by the (Na^+/K^+)-ATPase resident in the plasma membrane. The energy obtained from the Cl^- gradient is negligible when compared to the energy derived from that of Na^+. Also while Cl^- can be replaced by Br^-, SCN^- or NO_2^-, Na^+ cannot be replaced by other cations. SERT exhibits an ion dependency with an apparent transport stoichiometry of 5-HT:Na^+:Cl^-:K^+ of 1:1:1:1. Given that 5-HT under physiological pH is transported in its cationic form, this stoichiometry predicts that no net charge crosses the membrane during a single transport cycle (Rudnick, 1998).

5-HT uptake has been thoroughly studied in platelets, synaptosomes and reconstituted vesicles and more recently also after stable expression of the cloned SERT cDNA in different heterologous expression systems. K_m values reported across different studies suggest that 5-HT accumulation saturates at low micromolar concentrations (Reith, 1998). Although the cloning of SERT cDNAs from several different species and their expression in heterologous systems has intensified characterization of recombinant SERT, the molecular mechanisms underlying 5-HT transport are still not well understood.

The most widely held conception of how SERT and related transporters function is founded on the alternating access model. In this model, the transporter binding site is alternately exposed to extracellular or cytoplasmic environments via conformational changes in the transporter protein. When the site is exposed to the external medium, a gate prevents access from the inside, and a similar external gate prevents access from the outside, when the binding site is exposed to the internal medium. The binding of 5-HT, Na^+, and Cl^- to SERT on the extracellular face of the membrane promotes a conformational change exposing the cargo to the interior thereby allowing the molecules to dissociate from the transporter. The reorienting of SERT to its original

state is thought to be facilitated by the outward movement of a K^+ (Rudnick, 1998). However, several groups have described transporter-associated currents that exceed the predictions of electroneutral transport. For instance, a study on the conducting states of rat SERT expressed in *Xenopus* oocytes showed that 5-HT uptake was associated with four types of currents, reflecting the existence of a permeation pathway similar to that of ionic channels (Mager et al., 1994; Cao et al., 1997). The 5-HT induced currents were found to be 7-12 fold larger than the influx of [^{3}H]5-HT, as though ions flow in excess of those that stoichiometrically accompany the 5-HT molecules. These currents were further characterised by Lin et al. They showed that channel openings took place several orders of magnitude less frequently than 5-HT transport cycles indicating that channel activity is not an essential step in 5-HT transport (Lin et al., 1996). This was supported by studies on drosophila SERT revealing 5-HT induced currents that could be linked to a channel-like conformation of SERT (Corey et al., 1994a; Galli et al., 1997). These results can not be explained by the alternating access model. Rather, the channel events indicate functional and structural similarities between transporters and ion channels. In any case, it appears that neurotransmitter transporters function in a far more complex fashion than what was originally thought.

SERT is the pharmacological target for TCAs (such as imipramine or paroxetine) and SSRIs (such as citalopram or fluoxetine) for treating symptoms associated with affective and mood disorders. These TCAs and SSRIs block SERT thereby enhancing serotonergic signalling. Although the inhibitory mechanisms of TCAs and SSRIs are poorly understood, pharmacological studies indicate the existence of distinct binding sites for these two classes of antidepressants and complex interactions between these sites as well as with the substrate translocation site have been postulated (Barker et al., 1994). Interspecies differences in pharmacological profiles, combined with construction of cross-species chimeras and site-directed mutagenesis, have been used as a strategy to localize domains and residues critical for ligand interaction (Demchyshyn et al., 1994; Barker and Blakely, 1996; Adkins et al., 2001; Mortensen et al., 2001; Rodriguez et al., 2003; Roman et al., 2003; Larsen et al., 2004).

In addition to being affected by antidepressants, SERT also represents the target for cocaine and amphetamines. While cocaine acts as an inhibitor of SERT, the effects mediated by amphetamines such as 3,4-methylenedioxy-methamphetamine (MDMA), better known as ecstasy, are attributed, in part, to high-affinity SERT-mediated transport of MDMA into serotonergic neurons followed by extensive release of 5-HT (Rudnick and Wall, 1993; Wall et al., 1995). Thus, both cocaine and amphetamines lead to increased levels of 5-HT in the synapse but in the case of amphetamines, cellular stores are actively released, while cocaine raises synaptic 5-HT levels by blocking the re-uptake.

1.2.6 Genetic regulation of the serotonin transporter

The delayed onset of a therapeutic effect associated with antidepressant therapy suggests that it is not the immediate 5-HT uptake inhibition, but rather long-term adaptive changes that underlie the therapeutic effect. These mechanisms may include regulation at the level of SERT gene expression and this idea has led to a series of studies investigating changes in SERT mRNA levels following antidepressant treatment. However, measurements of SERT mRNA in rats have yielded conflicting results, with some studies reporting no change (Burnet et al., 1994; Spurlock et al., 1994; Linnet et al., 1995), increases (Lopez et al., 1994) or decreases (Lesch et al., 1993c; Kuroda et al., 1994; Neumaier et al., 1996) in mRNA levels. The variability in results may be attributable to differences in the type and dosage of antidepressant or the route and frequency of administration. Changes in SERT mRNA levels may lead to alterations in SERT activity and density, and although alterations in SERT antagonist binding sites have been detected following chronic antidepressant treatment, there is no consensus in the literature. These conflicting findings led investigators to consider regulatory mechanisms in more defined cultured cell lines in the attempt to map some of the intracellular mechanisms underlying the effects of applied drugs and antidepressants.

The human placental choriocarcinoma cell lines JAR and BeWo, which functionally express SERT, have been used as models in a series of studies to investigate the genetic

regulation of SERT. For instance, in JAR cells SERT was found to be under specific regulation by cAMP, as 5-HT transporter activity was increased following treatment with cAMP elevating agents. The increase in 5-HT uptake was paralleled by a corresponding increase in membrane binding capacity for the SERT antagonist [^{125}I]RTI-55 and by increases in mRNA levels. Activation of the cAMP-dependent protein kinase (PKA) by the elevated levels of cAMP was suggested to be involved in the stimulation of SERT gene expression (Cool et al., 1991; Ramamoorthy et al., 1993a). The cAMP induction of 5-HT uptake and SERT mRNA levels was later verified in BeWo cells (Morikawa et al., 1998). The influence of cAMP on SERT has also been demonstrated in brain and is not selective for the choriocarcinoma cells (Foguet et al., 1993).

Also in JAR cells, staurosporine, a non-specific protein kinase inhibitor (Ramamoorthy et al., 1995a), herbimycin A, an inhibitor of tyrosine kinases (Prasad et al., 1997), and epidermal growth factor (EGF) (Kekuda et al., 1997; Kubota et al., 2001) have been demonstrated to be involved in transcriptional regulation of SERT. In all three cases, stimulation of 5-HT uptake was accompanied by increases in SERT mRNA levels and SERT plasma membrane density. Additional support for the participation of tyrosine kinases in the regulation of SERT gene expression came from studies on cytokines. For instance, interleukin-1β was found to be an activator of SERT gene expression in JAR cells as demonstrated by an increase in 5-HT uptake, SERT mRNA levels, and transporter density (Ramamoorthy et al., 1995b). The stimulatory effects of interleukin-1β were abolished by interleukin-1β receptor antagonists and by genistein, an inhibitor of tyrosine kinases, suggesting that interleukin-1β mediates signal transduction through the interleukin-1 receptor and that tyrosine phosphorylation is important at some point in the signalling pathway (Kekuda et al., 2000). A number of other proinflammatory cytokines, including tumor necrosis factor (TNF)-α (Mossner et al., 1998), interferon (IFN)-α, and IFN-γ (Morikawa et al., 1998) have also been shown to up-regulate SERT expression while for instance, interleukin-4 has been shown to down-regulate 5-HT uptake (Mossner et al., 2001).

1.3 TRAFFICKING AND REGULATION OF THE SEROTONIN TRANSPORTER

1.3.1 Membrane trafficking

In eukaryotic cells, proteins and membranes are sorted and delivered to specific cellular compartments through a series of interconnected membrane trafficking pathways (Figure 1.5). These compartments contain both resident proteins, which define each compartment according to its biochemical function, and proteins transiently passing through on the way to their final destinations. The secretory membrane compartments can be subdivided into two central membrane populations, the endoplasmic reticulum (ER)/Golgi system and the *trans*-Golgi network (TGN)/endosomal system. The ER/Golgi system performs the folding, oligomerization, and post-translational modifications of proteins transiting the secretory pathway. The TGN/endosomal system is central to the sorting, export, and recycling of numerous soluble and membrane-associated proteins. At the TGN, newly synthesized proteins are routed to endosomes and lysosomes, to regulated and constitutive exocytic pathways and, in polarized cells, to apical and basolateral membranes (Traub and Kornfeld, 1997).

Membrane proteins are transported to their site of function or cleared from there by membrane trafficking mediated by transport vesicles that are constantly circulating within the cell, budding off from one membrane and fusing with another. Membrane trafficking requires specialised proteins that regulate vesicle transport, docking and fusion. The protein families that mediate vesicle trafficking are conserved from yeast to man, as well as throughout the cell. The biogenesis of transport vesicles is initiated through the recruitment of large multi-subunit protein complexes termed coats. Coat components are recruited to the surface of the donor membrane through the action of a small Rab GTPase that, upon binding to GTP, associates with membranes and directs the assembly of the coat (Zerial and McBride, 2001). Distinct coat proteins and associated adaptor proteins mediate each budding event, serving both to shape the transport vesicle and to select the desired set of cargo molecules by direct or indirect interaction with sorting motifs located in the cytoplasmic domains of the cargo proteins (McMahon and Mills, 2004). The transport vesicles come in several different varieties,

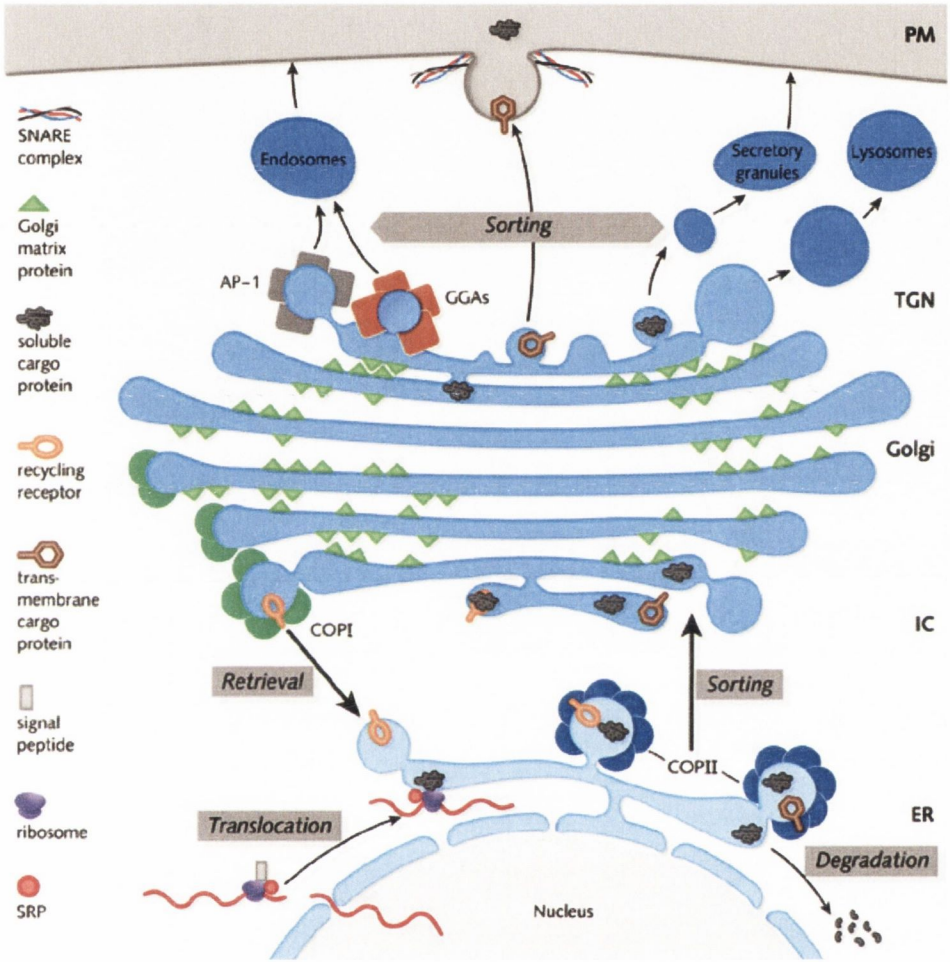


Figure 1.5 Schematic representation of the secretory pathway. Newly synthesized proteins enter the pathway at the ER and are subjected to repeated sorting and transport between membrane organelles until they arrive at their designated destination. (http://www.nature.com/embor/journal/v3/n9/fig_tab/embor073_f1.html).

which can be classified by the composition of the protein coat surrounding them. Three kinds of transport vesicle have been functionally characterized at a molecular level and can be defined by both their membrane origin and their coat proteins. Clathrin-coats are found on vesicles formed from both the plasma membrane and the Golgi and mediate vesicular trafficking within the endosomal membrane system. Coat protein complex I (COPI) and COPII vesicles direct traffic between early compartments of the secretory pathway. COPII vesicles emerge from the ER to export newly synthesized secretory proteins toward the Golgi, whereas COPI vesicles seem to be involved in both anterograde and retrograde transport within the Golgi complex, as well as mediating the recycling of proteins from the Golgi to the ER (McMahon and Mills, 2004). Also, most cells have biochemically distinct non-clathrin-coated flask-shaped invaginations in the plasma membrane characterised by the structural protein caveolin that oligomerizes to form the major component of the membrane coat. These particular invaginations, called caveolae, are examples of structures referred to as "lipid rafts" (Hommelgaard et al., 2005).

After vesicle formation, the coat components are released and the vesicle is then directed to its correct destination. This process is stimulated by Rab GTPases and a number of protein-protein and protein-lipid interactions. The disassembly of the coat is believed to expose the targeting machinery on the vesicle surface for subsequent delivery of the cargo to the appropriate organelle. Thus, it is not the coat proteins that determine the target of a transport vesicle. Instead, the final step in vesicle trafficking is the fusion of the vesicle with its target membrane; a process believed to be mediated by a large family of proteins termed SNAREs (soluble N-ethylmaleimide-sensitive-factor attachment protein receptor) (Gerst, 2003). Acting downstream of both tethering factors and Rab GTPases, which confer loose membrane attachment, SNAREs mediate tight docking and subsequent fusion of membrane bilayers. Most SNARE proteins are small integral membrane proteins characterised by a single membrane-spanning domain at their C-terminal end, a single SNARE motif located immediately adjacent to the C-terminal transmembrane anchor and an N-terminal domain. The SNARE motif is approximately 60–70 residues in length and consists of hydrophobic heptad repeats

spaced such that the adoption of a α-helical structure places all the hydrophobic side chains on the same face of the helix (Duman and Forte, 2003).

Different members of the SNARE family are localized to distinct membrane compartments of the secretory and endocytic trafficking pathways and thus contribute to the specificity of intracellular membrane fusion processes. SNAREs can be divided into two categories: vesicle or v-SNAREs, which are incorporated into the membranes of transport vesicles during budding, and target or t-SNAREs, which are located in the membranes of target compartments. Most intracellular membrane fusion reactions involve one v-SNARE and three t-SNARES. Interaction between the v-SNARE and the t-SNAREs leads to the formation of the SNARE complex, in which the four SNARE motifs assemble into a four-helical bundle bringing the two membranes into close proximity. The monomeric SNARE motifs are believed to be largely unstructured before complex assembly and become highly organised during the formation of the SNARE complex (Gerst, 2003). Thus, the SNARE formation is accompanied by a dramatic increase in α-helical secondary structure, an energetically favourable reaction that is believed to catalyse the fusion of the vesicle with the target membrane.

The best characterised neuronal SNARE complex is the one involved in exocytosis of synaptic vesicles (Li and Chin, 2003). The fusion of synaptic vesicles with the presynaptic nerve terminal is mediated by the formation of a complex comprising one helix each from syntaxin 1A and VAMP-2 (vesicle associated protein 2) and two helices from SNAP-25 (synaptosomal associated protein of 25 kDa). Syntaxin 1A and VAMP-2 are anchored in the plasma membrane and in the vesicular membrane respectively, by their C-terminal domains, whereas SNAP-25 is anchored to the plasma membrane by lipid-modified cysteine residues.

Membrane-resident SNARE proteins have been shown to localize to distinct microdomains, referred to as lipid rafts (Gil et al., 2005; Salaun et al., 2005). The association of SNARE proteins with lipid rafts has suggested a role for lipid rafts in regulating SNARE function and exocytosis. Lipid rafts are specialised membrane domains enriched in cholesterol and glycosphingolipids. They are present within membranes of most cell types and have also been implicated in the regulation of certain signal transduction and membrane trafficking pathways. For instance, lipid rafts have

been shown to be important platforms for fusion of vesicles containing the insulin-sensitive glucose transporter 4 (GLUT4) (Chamberlain and Gould, 2002). Furthermore, SERT has been shown to associate with lipid rafts in both intracellular and cell surface fractions suggesting that raft association may be important for trafficking and targeting of SERT (Magnani et al., 2004). The glutamate transporter has also been shown to associate with lipid rafts (Butchbach et al., 2004). A similar finding was reported for NET when it was found to undergo lipid raft-mediated internalisation (Jayanthi et al., 2004). Thus, lipid rafts appear to be involved in a variety of biological processes and may play a critical role in coordinating neurotransmitter release and re-uptake by regulating SNARE proteins and neurotransmitter transporter function and trafficking.

1.3.2 Serotonin transporter trafficking

Since the demand for a rapid fine-tuning of SERT in controlling serotonergic signalling cannot be attributed to the relatively slow process of transcriptional regulation it is most likely that SERT is also under some kind of acute regulation. Acute changes in 5-HT clearance are likely to originate from local variations in 5-HT concentrations, cell surface distribution and density of SERT proteins, interactions with regulatory proteins or reversible post-translational modifications.

Neurotransmitter transporters, including SERT, are not static components of synapses. On the contrary, they are continuously being delivered to and removed from the plasma membrane in response to various signals. Transporter trafficking involves an intricate network of protein-protein interactions starting with the biosynthesis of the transporters and their transport along the axon followed by their local insertion into the plasma membrane. Transporters located at the cell surface undergo endocytosis, and are either delivered to endosomes from where they are recycled back to the cell surface for another round of use (recycling pathway) or transported to lysosomes for degradation (degradation pathway). Such trafficking events either occurs constitutively (e.g. in the case of the transferrin receptor) or in a regulated manner dependent on intracellular or extracellular signals or ligands. However, the molecular and cellular mechanisms that

regulate each of these processes are largely unknown and are only now starting to be unravelled (Melikian, 2004).

Biochemical and immunochemical studies have revealed intracellular pools of SERT in both heterologous expression systems and in cultured neurons. These two approaches have been used extensively to measure or visualise subcellular redistributions of SERT in response to various signals or regulatory proteins. Although ultrastructural analyses have localized SERT to tubulo-vesicular membranes and SERT is easily detected in intracellular compartments using fluorescence microscopy, the exact identity of the endosomal compartments or transport vesicles involved in the intracellular trafficking of SERT has not yet been established (Melikian, 2004).

Studies on the GABA transporter and also on the choline transporter has suggested the presence of two populations of intracellular transporters, one that is cycling between the plasma membrane and the endosomal compartment and another static population of transporters that remains trapped intracellularly (Ribeiro et al., 2005; Wang and Quick, 2005). The existence of two distinct intracellular populations of transporters is also well-known from studies on GLUT4 (Dugani and Klip, 2005). These transporters reside intracellularly, both in vesicles that are sensitive to insulin and in vesicles that show no response to insulin. This intracellular accumulation of transporters may function as a mechanism to regulate changes in transport in response to increased neuronal activity and may also be relevant for SERT, which generally distribute between the cell surface and intracellular compartments in a ratio of 1:2 (Quick, 2002).

Proper sorting and targeting of membrane proteins to the cell surface and intracellular compartments and/or specific retention at specialised sites is thought to be mediated by specific sorting motifs. For instance, dileucine and tyrosine based motifs are well-characterised interaction motifs that are involved in the targeting of plasma membrane proteins to clathrin-coated vesicles via their association with adaptor protein complexes for trafficking and sorting along the endocytic pathway (Bonifacino and Traub, 2003). Most of the tyrosine-based signals conform to the consensus motif NPXY, or YXXΦ,

where X can be any amino acid and Φ is a large, bulky hydrophobic residue. Dileucine motifs are less strictly defined but they typically contain a leucine followed by another nonpolar residue, with upstream acidic amino acids usually positioned -4 or -5 relative to the first leucine.

Although SERT encodes for several candidate dileucine and tyrosine based motifs, none of these classical endocytic motifs have yet been identified to be involved in or necessary for transporter internalisation. While sorting of NET to the basolateral membrane of epithelial cells has been suggested to involve dileucine motifs located within the cytoplasmic N-terminal domain of NET a nonclassical endocytic signal has been identified within the C-terminal domain of DAT (Gu et al., 2001; Holton et al., 2005). Although the structural determinants targeting transporters to the various compartments are poorly understood it seems likely that the divergent cytoplasmic N- and C-termini of monoamine transporters contain signals conferring specific targeting of the transporters. For instance, the C-terminal of SERT has been implicated in proper trafficking of the transporter to the plasma membrane and has also been proposed to play a functional role at the cell surface by interacting with the actin cytoskeleton (Mochizuki et al., 2005; Larsen et al., 2006).

Ubiquitination can also be viewed as a regulatory mechanism for transporter function. The attachment of ubiquitin to lysine residues regulates protein transport between membrane compartments by serving as a sorting signal. The functional consequences of the type of ubiquitination vary, such that polyubiquitinated proteins are targeted for degradation by the proteasome, whereas monoubiquitination is implicated in other cellular functions, including endocytic trafficking (Hicke and Dunn, 2003). Evidence for direct ubiquitination of neurotransmitter transporters comes from studies on DAT where stimulation of PKC resulted in enhanced ubiquitination and degradation of DAT (Miranda et al., 2005; Miranda et al., 2006).

1.3.3 Regulation of the serotonin transporter by protein kinases

Reversible protein phosphorylation catalyzed by protein kinases is an essential regulatory mechanism involved in many biological processes. Amino acid sequence analysis of SERT reveals multiple intracellular consensus sites for protein kinases suggesting that phosphorylation plays a role in posttranslational regulation of SERT.

Early studies in bovine endothelial cells (Myers et al., 1989), human platelets (Anderson and Horne, 1992) and in rat basophilic leukaemia cells (Miller and Hoffman, 1994) demonstrated a substantial reduction in SERT mediated 5-HT transport after acute exposure to PKC activators. Thus down-regulation of 5-HT uptake by PKC activators appeared to be a consistent finding, arising in most cases from a reduction in V_{max} with no significant changes in K_m. However, the first evidence for altered cell surface expression of SERT as the result of PKC activation came from studies in HEK-293 cells stably expressing human SERT. Using a membrane impermeant biotinylation reagent Qian et al showed that the decrease in 5-HT uptake, observed after acute activation of PKC, was paralleled by a reduction in SERT cell surface abundance (Qian et al., 1997). PKC activation did not lead to enhanced degradation of SERT. Rather, activation of PKC resulted in a redistribution of SERT from the cell surface to intracellular compartments with no changes in total SERT.

A reduction in 5-HT uptake following PKC activation was also shown in BeWo cells and in COS cells transfected with rat SERT (Sakai et al., 1997). This group also reported that the phosphatase inhibitor calyculin A exerted the same effect on 5-HT uptake suggesting that a cycle of phosphorylation/dephosphorylation is involved in SERT regulation. Also, in an attempt to study whether PKC-mediated down-regulation of 5-HT uptake involves direct phosphorylation of SERT, they mutated putative PKC phosphorylation sites located within the cytoplasmic domains of SERT. However, none of these mutants showed decreased sensitivity to the PKC or phosphatase induced reduction in 5-HT uptake. This finding suggests that SERT is not directly phosphorylated by PKC or that phosphorylation occurs through kinases downstream of PKC or at non-consensus sites.

Using specific antibodies Ramamoorthy et al was the first to demonstrate that PKC activation is associated with direct phosphorylation of human SERT (Ramamoorthy et al., 1998). A basal level of SERT phosphorylation was detected when SERT was immunoprecipitated from transfected HEK-293 cells metabolically labelled with [^{32}P]-ortophosphate. The level of SERT phosphorylation increased when cells were treated with the PKC activator phorbol 12-myristate 13-acetate (PMA), an effect that was accompanied by a reduction in 5-HT transport. Activators of protein kinase A (PKA) and protein kinase G (PKG) also stimulated SERT phosphorylation, although no effect was observed on 5-HT uptake. Treatment of cells with okadaic acid, an inhibitor of protein phosphatase 2A (PP2A), also resulted in increased SERT phosphorylation and reduced 5-HT uptake. The stimulatory effects of PKC activation and PP2A inhibition on SERT phosphorylation were found to be additive. The effect of okadaic acid on SERT phosphorylation was not blocked by inhibitors of PKC, PKA, or PKG, suggesting that PP2A targets phosphorylation sites on SERT different from those affected by PKC, PKA, and PKG. Later, the same group reported that SERT exists in a complex with the catalytic subunit of PP2A (Bauman et al., 2000). PKC activation or PP2A inhibition abolished the interaction between SERT and PP2A, suggesting that the stability of this complex may influence SERT trafficking and phosphorylation.

In addition, the presence of extracellular SERT substrates was shown to attenuate the PKC-mediated phosphorylation and internalisation of SERT, an effect that was blocked by SERT antagonists (Ramamoorthy and Blakely, 1999). These findings indicate that SERT may be less sensitive to PKC-mediated phosphorylation during substrate translocation, which would provide a mechanism for maintaining SERT at the cell surface during periods of high transport demand.

Recently, Samuvel et al used a reversible biotinylation strategy to demonstrate that in HEK-293 cells, enhanced SERT endocytosis accounts for the PKC-mediated decrease in SERT cell surface expression (Samuvel et al., 2005). A similar finding was reported for the PKC-mediated down-regulation of SERT in platelets (Jayanthi et al., 2005). They showed enhanced endocytosis of SERT after 30 minutes incubation with PMA but also showed that there is a short-term effect after 5 minutes that does not involve endocytosis but rather is associated with inhibition of SERT intrinsic activity.

In summary, with the exception of the short-term effect of PMA in platelets, there appears to be general agreement that altered surface expression rather than reduced transport efficiency, mediates acute PKC-dependent modulation of 5-HT uptake. Similar findings are reported for other members of the family of Na^+/Cl^- dependent transporters and thus PKC activation may represent a general mechanism for regulating neurotransmitter transporters. Also these studies suggest that altered surface expression reflect an increase in SERT internalisation. However, whether reduced insertion or re-cycling of SERT into the plasma membrane is also involved in PKC-mediated SERT regulation is not evident from these studies. For instance, studies on DAT indicate that PKC activation drives DAT into the recycling endocytic pathway and that DAT sequestration is the result of simultaneously enhancing and suppressing DAT endocytic and recycling rates, respectively (Daniels and Amara, 1999; Melikian and Buckley, 1999; Loder and Melikian, 2003; Sorkina et al., 2005). Studies on endogenous NET in rat placental trophoblasts also revealed enhanced endocytosis of the transporter following PKC activation (Jayanthi et al., 2004). In addition, PKC-induced internalisation of NET in trophoblasts was shown to be dependent on the integrity of lipid-rafts but independent of dynamin and clathrin-mediated pathways. In contrast, co-expression of NET and a dominant-negative mutant of dynamin in HEK-293 cells completely blocked the effect of PKC activation on NET sequestration. This indicates the involvement of clathrin-mediated pathways in PKC-induced NET sequestration and suggests that the mechanisms underlying PKC-induced internalisation are cell type specific. Also, PKC has been shown to regulate DAT internalisation by clathrin-mediated and dynamin-dependent mechanisms in two different expression systems (Daniels and Amara, 1999; Sorkina et al., 2005). Furthermore, PKC-mediated internalisation of SERT has been shown to involve a redistribution of the transporter from lipid rafts to non-lipid rafts (Samuvel et al., 2005). This led to the hypothesis that PKC-mediated phosphorylation of transporters may be a signal leading to intracellular sequestration, possibly by acting as a binding motif for endocytic proteins. However, there seems to be some controversy over whether phosphorylation is actually required for transporter sequestration. For instance, site-directed mutagenesis of predicted PKC phosphorylation sites does not affect sequestration of SERT (Sakai et al., 1997), DAT

(Chang et al., 2001; Granas et al., 2003) or GAT (Corey et al., 1994b). Therefore, it could be speculated that PKC may exert its function by targeting transporter associated proteins. Recently it was suggested that PKC-induced phosphorylation is not required for PKC-induced transporter sequestration but rather that PKC activation traps transporters in a subcellular compartment in which they are normally in their phosphorylated state (Melikian, 2004).

Protein kinase pathways, different from PKC, have also been implicated in SERT regulation. Miller and Hoffman reported that acute stimulation of A_3 adenosine receptors increased 5-HT uptake in rat basophilic leukaemia cells (Miller and Hoffman, 1994). The increase in 5-HT uptake was not associated with an increase in total ligand binding, suggesting increased catalytic activity of SERT. However, these experiments suffered from limitations and more recent studies indicate an increase in SERT cell surface expression following A_3 adenosine receptor stimulation in rat basophilic leukaemia cells (Zhu et al., 2004). Furthermore, the increase in SERT surface density was proposed to arise from enhanced insertion of SERT into the plasma membrane rather than reduced endocytosis. The same group reported that the stimulatory effect of A_3 adenosine receptor activation on 5-HT uptake was mimicked by a membrane-permeant analog of cGMP and fully blocked by a selective inhibitor of PKG and partially blocked by an inhibitor of p38 mitogen-activated protein kinase (MAPK). This suggests that both PKG and p38 MAPK signalling pathways are involved in A_3 adenosine receptor induced SERT regulation. Activation of p38 MAPK was shown to play a role in catalytic activation of SERT rather than in supporting SERT trafficking to the plasma membrane (Zhu et al., 2004; Zhu et al., 2005). While inhibitors of p38 MAPK blocked the A_3 adenosine receptor mediated increase in SERT catalytic activity they failed to block the A_3 adenosine receptor mediated increase in SERT surface density. This suggests that SERT is regulated by A_3 adenosine receptors via two PKG-dependent pathways, one leading to enhanced insertion of SERT into the plasma membrane and one p38 MAPK-dependent pathway that increases SERT intrinsic activity (Zhu et al., 2004). Thus, PKG and p38 MAPK may work in concert to achieve

a balance between the number and catalytic activity of SERT molecules at the cell surface.

Samuvel et al showed that inhibition of p38 MAPK in rat synaptosomes resulted not only in a decrease in 5-HT uptake, but also in a decrease in SERT phosphorylation and SERT cell surface levels (Samuvel et al., 2005). Furthermore, reduction of p38 MAPK expression by small interfering RNAs (siRNAs) in HEK-293 cells transiently expressing SERT resulted in decreased 5-HT uptake and SERT cell surface expression. PKC- and p38 MAPK-mediated SERT down-regulation was shown to be additive, indicating distinct pathways for PKC and p38 MAPK. While PKC activation leads to enhanced internalisation of SERT in HEK-293 cells, inhibition of p38 MAPK leads to decreased delivery of SERT to the cell surface.

Thus, the mechanisms underlying p38 MAPK-mediated regulation of SERT are poorly understood and there seems to be some discrepancy between these studies. However, together these studies suggest that both trafficking-dependent and independent mechanisms are involved in p38 MAPK-induced SERT regulation.

1.3.4 Regulation of the serotonin transporter by interacting proteins

Only little is known about the mechanisms underlying constitutive and regulated trafficking of SERT and related transporters. Protein kinases appear to play a critical role in transporter trafficking and transporters may be regulated through their direct association with interacting proteins by phosphorylation dependent or independent pathways. However, only a few proteins have been identified that interact directly with SERT.

As mentioned earlier, SERT was found to interact with the catalytic subunit of PP2A (Bauman et al., 2000). PP2A co-immunoprecipitated with SERT in native tissue and in extracts from transfected cells. The interaction between SERT and PP2A was inhibited by PKC activators and also by phosphatase inhibitiors, indicating a regulated association of SERT and the catalytic subunit of PP2A. Both DAT and NET were also reported to interact with the catalytic subunit of PP2A.

The PKC substrate MacMARCKS has also been isolated as a binding partner of the C-terminus of SERT. Heterologous expression of SERT with MacMARCKS caused a reduction in 5-HT uptake and reduced sensitivity to PKC-mediated down-regulation (Jess et al., 2002).

Syntaxin 1A is another such protein that has been reported to interact with a number of ion channels and transporter proteins. Syntaxin 1A has been studied extensively because of its role in neurotransmitter vesicle fusion. It was first reported to interact with the N-terminal cytoplasmic domain of GAT1 and to function as a positive modulator of GAT1 expression but a negative regulator of transport rates (Beckman et al., 1998; Deken et al., 2000; Horton and Quick, 2001). The presence of syntaxin 1A was shown to be required for PKC-mediated modulation of GAT1 and PKC activation was in fact shown to enhance GAT1 association with syntaxin 1A (Beckman et al., 1998).

GLYT1 and GLYT2 have also been reported to engage in a physical and functional interaction with syntaxin 1A (Geerlings et al., 2000). Furthermore, syntaxin 1A was found to be involved in the transport of GLYT2 to, but not its retrieval from, the plasma membrane (Geerlings et al., 2001).

These studies led researchers to explore the possibility that syntaxin 1A also influences SERT function. Using GST-pulldown experiments, Haase et al showed a direct interaction between the N-terminal domain of SERT and syntaxin 1A (Haase et al., 2001). The first TMD of SERT was required for efficient binding of syntaxin 1A, suggesting that the TMD contributes to the interaction with syntaxin 1A or somehow stabilises the conformation of the remaining N-terminal domain for proper binding to syntaxin 1A. Heterologous expression of syntaxin 1A and SERT in HEK-293 cells resulted in a V_{max} reduction of 5-HT transport, suggesting changes in the number of transporter molecules at the cell surface or changes in SERT catalytic activity. Unpublished data (Magnani, 2004) from our group suggest that syntaxin 1A disturbs SERT trafficking to the plasma membrane. Confocal microscopy of transfected HEK-293 cells revealed an accumulation of SERT and syntaxin 1A in intracellular structures positive for ER-markers. Syntaxin 1A appeared to inhibit transporter post-translational glycosylation without affecting total levels of SERT. A decrease in SERT cell surface

expression upon co-expression with syntaxin 1A was also supported by cell surface biotinylation studies. However, overexpression of syntaxin affected the morphology of the ER and Golgi and also resulted in accumulation of the non-related toll-like receptor 2. Thus, the effects of syntaxin 1A appeared rather unspecific making it difficult to interpret the results.

The opposite effect was reported for syntaxin 1A in thalamocortical neurons endogenously expressing SERT (Quick, 2002). Co-immunoprecipitation of SERT with syntaxin 1A supported formation of a complex containing the two proteins in neurons. Incubation with botulinum toxin C1, an endoprotease that specifically cleaves and functionally inactivates syntaxin 1A, resulted in a decrease in 5-HT uptake which was accompanied by a decrease in SERT cell surface expression, suggesting that syntaxin 1A functions as a positive regulator of SERT cell surface expression.

In contrast to the findings reported on GAT1, syntaxin 1A is not necessary for PMA-mediated down-regulation of SERT in HEK-293 cells (Haase et al., 2001). Also, PKC activation does not change the syntaxin 1A-mediated inhibition of 5-HT uptake suggesting that PKC and syntaxin 1A mediate their regulatory actions via a common saturable pathway or that the presence of syntaxin 1A renders SERT inaccessible to PKC-mediated down-regulation. PKC activation has been shown to inhibit SERT association with syntaxin 1A (Samuvel et al., 2005) and thus it could also be speculated that activation of PKC displaces syntaxin 1A from SERT thereby abolishing the effect of syntaxin 1A.

Syntaxin 1A has also been shown to interact with the N-terminal domain of both DAT (Lee et al., 2004) and NET (Sung et al., 2003). Similar to the data reported for GAT1, syntaxin 1A supports surface expression of NET but inhibits NET catalytic activity. Also, the presence of syntaxin 1A was required for PKC-mediated inhibition of NE uptake (Sung et al., 2003).

Furthermore syntaxin 1A has been shown to regulate two of the previously mentioned SERT associated currents (Quick, 2003). Binding of syntaxin 1A to the N-terminal domain of SERT seems to alter the stoichiometry of the transport cycle, thus converting 5-HT uptake from an electrogenic to an electroneutral process. These findings are supported by studies on NET, where syntaxin 1A was shown to eliminate NET

associated currents (Sung et al., 2003). Also, the N-terminal domain of NET has been shown to regulate and define the ionic specificity of a NET-mediated current further supporting a potential regulatory role of syntaxin 1A (Binda et al., 2006).

In summary, syntaxin 1A appears to interact specifically with the N-terminal domain of a number of transporters, although the interaction domain responsible for the binding to syntaxin 1A seems to vary from transporter to transporter. The effect of syntaxin 1A on SERT and related transporters is likely to be cell-type specific but also transporter specific and may depend on the presence and availability of other transporter specific interacting proteins. However, the general finding of syntaxin 1A as a binding partner of neurotransmitter transporters may provide a link between exocytosis of neurotransmitters and the re-uptake by transporters (Deken et al., 2000).

1.4 AIM OF STUDY

Neurotransmitter transporters are thought to exist in large multimeric protein complexes. However, only a few proteins have been identified that engage in direct protein-protein interactions with SERT or the related proteins DAT and NET. Interaction with associating proteins is thought to play an important role in constitutive and regulated trafficking as well as being involved in the functional properties of the transporter. Thus, the aim of the present study is to identify novel SERT interacting proteins and to explore the functional consequences of such interactions. The yeast two-hybrid system has become a widely used approach in the search for novel protein-protein interactions. Here the yeast two-hybrid approach is used in an attempt to identify novel protein interacting partners of SERT. Positive interactions obtained in the yeast two-hybrid system are being verified in non-yeast based assays. A number of molecular assays including confocal laser-scanning microscopy are employed in the attempt to elucidate the functional effects of confirmed interactions between SERT and associating proteins.

2. MATERIALS AND METHODS

2.1 MATERIALS

2.1.1 Plasmids

The pcDNA3-hSERT, the pcDNA3-hNET and the pcDNA3-hDAT constructs were obtained from Ove Wiborg (Centre for Basic Psychiatric Research, Aarhus Psychiatric University Hospital, Risskov, Denmark). The pGBKT7 (Appendix A) and the pACT2 (Appendix B) shuttle vectors were obtained from Clontech. The control vectors pGBKT7-p53 and pTD1-1 were isolated from the pretransformed yeast strains AH109 and Y187 respectively, which were provided by Clontech. The pGEX-KG vector (Appendix C) is derived from the pGEX-2T vector (Pharmacia Biosystems) and was obtained from Dr. Tim Mantle, Biochemistry Department, Trinity College Dublin. The pcDNA3 vector was purchased from Invitrogen (Appendix D). The mammalian constructs pcDNA3-PICK1-FLAG, pcDNA3-Hic5-Myc and the yeast construct pGAD10-PICK1 and pGAD10-Hic5 were kindly provided by Dr. Gonzalo Torres (Department of Neurobiology, University of Pittsburgh School of Medicine, Pittsburgh, USA). The mammalian construct pCMV5-rMint3, was provided by Dr. Thomas Südhof (Howard Hughes Medical Institute, Texas, USA).

2.1.2 *Escherichia coli* and *Saccharomyces cerevisiae* strains

Chemically competent *Escherichia coli* DH5α cells were obtained from Invitrogen. The *Saccharomyces cerevisiae* strain Y187 containing a human brain cDNA library in pACT2 (Appendix E), the AH109 and the control strains AH109[pGBKT7-53] and Y187[pTD1-1] were obtained from Clontech. The Y187 yeast strain was obtained from Dr. Seamus Martin (Smurfit Institute of Genetics, Trinity College Dublin, Ireland).

2.1.3 Enzymes

Deep Vent Polymerase, T4 DNA ligase and DNA restriction endonucleases were purchased from New England Biolabs. Reverse Transcriptase was obtained from Promega, DNase was obtained from Invitrogen and Pfu DNA polymerase was obtained from Stratagene.

2.1.4 Antibodies

Mouse anti-FLAG, mouse anti-β-actin, mouse anti-syntaxin 1A and horseradish peroxidase-conjugated goat anti-rabbit IgG, goat anti-mouse IgG and rabbit anti-goat IgG were obtained from Sigma. Rabbit anti-HA, rabbit anti-myc, goat anti-SERT (C-20) and goat anti-SCAMP2 were purchased from Santa Cruz. Mouse anti-transferrin receptor (TfR) and mouse anti-trans-Golgi network (TGN) 38 were obtained from Zymed Laboratories and Affinity BioReagents, respectively. Mouse anti-GAPDH was from Abcam. Mouse anti-flotillin-1 and mouse anti-Mint3 were obtained from BD Transduction Laboratories. Mouse anti-SERT (AB-N09) was purchased from Advanced Targeting Systems. An antiserum raised against the fourth extracellular loop of rat SERT, denoted anti-SERT (EL4), (Unpublished data; Tate CG, Wynne S, Magnani F) was kindly provided by Dr. Christopher G. Tate (Medical Research Council Laboratory of Molecular Biology, Cambridge, UK). All Fluorophore-conjugated antibodies were raised in donkey and obtained from Jackson ImmunoResearch (Table 2.1)

2.1.5 Other Materials

Adenine hemisulphate	Sigma
Agar	Sigma
Agarose	Pronadisa
Ammonium Persulfate	Sigma
Ampicillin	Sigma

Table 2.1 List of Antibodies

Antibody	*Host*	*Reactivity*	*Manufacturer*	*Application*
Primary Antibodies				
Anti-FLAG	Mouse	-	Sigma	WB 1:1000
Anti-HA	Rabbit	-	Santa Cruz	WB 1:1000
Anti-myc	Rabbit	-	Santa Cruz	WB 1:1000
Anti-β-actin	Mouse	Hu,Ms,Rt	Sigma	WB 1:5000
Anti-GAPDH	Mouse	Hu,Ms,Rt	Abcam	WB 1:5000
Anti-syntaxin 1A	Mouse	Hu, Rt	Sigma	WB 1:2000 IF 1:100
Anti-TfR	Mouse	Hu,Ms,Rt	Zymed Laboratories	WB 1:500 IF 1:100
Anti-flotillin 1	Mouse	Hu,Ms,Rt	BD Transduction Laboratories	WB 1:2000 IF 1:100
Anti-TGN38	Mouse	Rt	Affinity BioReagents	IF 1:100
Anti-Mint3	Mouse	Hu,Ms,Rt	BD Transduction Laboratories	IF 1:100
Anti-SERT (C20)	Goat	Hu, Rt	Santa Cruz	WB 1:1000
Anti-SERT (AB-N09)	Mouse	Hu,Rt	Advanced Targeting System	IF 1:100
Anti-SERT (EL4)	Rabbit	Hu,Rt	Christopher Tate	IF 1:100-1:250
Anti-SCAMP2 (N-20)	Goat	Hu,Ms,Rt	Santa Cruz	WB 1:1000 IF 1:100-1:250
Anti-hESO3	Rabbit	Hu	Sigma (Custom-made)	WB 1:1000-1:10000 IF 1:500
Secondary Antibodies				
HRP conjugated Anti-Rabbit IgG	Goat	Rabbit	Sigma	WB 1:5000
HRP conjugated Anti-Mouse IgG	Goat	Mouse	Sigma	WB 1:2500
HRP conjugated Anti-Goat IgG	Rabbit	Goat	Sigma	WB 1:20000
FITC labelled Anti-Goat IgG	Donkey	Goat	Jackson ImmunoResearch	IF 1:2000
Cy5 labelled Anti-Goat IgG	Donkey	Goat	Jackson ImmunoResearch	IF 1:2000
FITC labelled Anti-Rabbit IgG	Donkey	Rabbit	Jackson ImmunoResearch	IF 1:2000
Texas Red labelled Anti-Rabbit IgG	Donkey	Rabbit	Jackson ImmunoResearch	IF 1:2000
Texas Red labelled Anti-Mouse IgG	Donkey	Mouse	Jackson ImmunoResearch	IF 1:2000

Hu:Human, Ms:Mouse, Rt:Rat, WB:Western Blot, IF:Immunofluorescence

L-Arginine HCl	Sigma
Bacto Agar	Difco Laboratories
Bacto-peptone	Difco Laboratories
Bacto-tryptone	Difco Laboratories
Bacto-yeast extract	Difco Laboratories
Brij-58	Sigma
Bovine Serum Albumin	Sigma
Carrier DNA	Clontech
CHAPS	Sigma
Complete™ Protease Inhibitor Cocktail	Roche
Coomassie Brilliant Blue R-250	Sigma
Deoxynucleotides	New England Biolabs
DMSO	Sigma
Dimethyl formamide	Sigma
DNA ladders	New England Biolabs
DTT (dithiothreitol)	Sigma
Dulbecco's Modified Eagle's Medium	Sigma
Donkey Serum	Sigma
EDTA	Sigma
Ethidium Bromide	Sigma
Foetal calf serum	Sigma
GeneJuice™ Transfection Agent	Novagen
Glass beads	Sigma
Glass cover slips	BDH
L-Glutamine	Sigma
Glucose	Sigma
Glutathione-agarose	Sigma
Glycerol	Sigma
Glycine	Sigma
L-Histidine HCL	Sigma
5-Hydroxy[G-^{3}H]tryptamine creatine sulphate	Amersham Pharmacia

5-Hydroxytryptamine creatine sulphate	Sigma
Hydrogen peroxide	Sigma
IPTG	Apollo Scientific
L-Isoleucine	Sigma
Kanamycin	Sigma
L-Leucine	Sigma
Lithium Acetate	Sigma
L-Lysine	Sigma
Lysozyme	Sigma
Nitrocellulose membrane	Sigma
2-Mercaptoethanol	Sigma
L-Methionine	Sigma
Microscope slides	BDH
Oligo-dT Primer	Promega
ONPG	Sigma
OPTI-MEM®I	Invitrogen
Optiphase Supermix Scintillation Cocktail	Perkin Elmer
Para-p-phenylendiamine	Sigma
Paroxetine	SmithKline Beecham
PEG 3350	Sigma
PEG 8000	Sigma
Penicillin/Streptomycin	Sigma
Petri dishes	Greiner
L-Phenylalanine	Sigma
Phorbol 12-myristate 13-acetate (β-PMA)	Sigma
PIPES	Sigma
Protein molecular weight markers	New England Biolabs
Protogel	National Diagnostics
PVDF membrane	Millipore
RNase Inhibitor	Promega
Sarkosyl	Sigma

SDS	Sigma
Spermidin	Sigma
Sucrose	Sigma
Sulfo-NHS-Biotin	Pierce
TEMED	Sigma
L-Threonine	Sigma
Tissue culture flasks and plates	Greiner
Tris-HCL	Sigma
Triton X-100	Sigma
L-Tryptophan	Sigma
Trypsin-EDTA solution	Sigma
Tween-20	Sigma
L-Tyrosine	Sigma
UltraLink-Immobilised NeutrAvidin	Pierce
Uracil	Sigma
L-Valine	Sigma
X-gal	Apollo Scientific
Yeast Nitrogen base without amino acids	Difco Laboaratories

All oligonucleotides were purchased from MWG (listed in Appendix F). All reagents and chemicals used were of molecular biology or analytical grade.

2.2 METHODS

2.2.1 *E. coli* media recipes

LB (Luria-Bertani) medium

1% (w/v) bacto-tryptone
0.5% (w/v) bacto-yeast extract
1% (w/v) NaCl

Sterilised by autoclaving at 120°C for 20 minutes.

LB agar plates: LB medium containing 1.5% (w/v) bacto-agar

SOB medium

2% (w/v) bacto-tryptone

0.5% (w/v) bacto-yeast extract

0.05% (w/v) NaCl

2.5 mM KCl

10 mM $MgCl_2$

10 mM $MgSO_4$

1 litre was prepared by dissolving tryptone (20g), yeast-extract (5g) and NaCl (0.5g) in 950 ml H_2O. 10 ml of a 250 mM solution of KCl was added and pH was adjusted to 7 before autoclaving. $MgCl_2$ and $MgSO_4$ were added to a final concentration of 10 mM each (10 ml of a 1 M solution).

2.2.2 Antibiotics

Antibiotics were prepared as stock solutions; filter sterilized and stored at -20°C.

Antibiotic	**Stock Solution**	**Working Concentration**
Ampicillin	50 mg/ml in H_2O	100 μg/ml
Kanamycin	10 mg/ml in H_2O	50 μg/ml

2.2.3 *Saccharomyces cerevisiae* media recipes

YPAD medium

1% (w/v) bacto-yeast extract
2% (w/v) bacto-peptone
2% (w/v) glucose
0.006% (w/v) adenine hemisulphate

1 litre of medium was prepared by the addition of yeast-extract (10g) and peptone (20g) to 940 ml H_2O and adjustment of pH to 5.8 before autoclaving, followed by the addition of 50 ml of a 40% (w/v) sterile solution of glucose and 10 ml of a 0.6% (w/v) adenine hemisulphate solution.

YPAD agar plates: YPAD medium containing 2% (w/v) bacto-agar.

Synthetic dropout (SD) medium

0.67 % (w/v) yeast nitrogen base without amino acids
2% (w/v) glucose
10% (v/v) appropriate10X dropout solution

1 litre of medium was prepared by mixing 6.7 g yeast nitrogen base with 100 ml of dropout solution in 850 ml H2O. The pH was adjusted to 5.8 before autoclaving, followed by the addition of 50 ml of a 40% (w/v) sterile glucose solution.

SD agar plates: SD medium containing 2% (w/v) bacto-agar.

X-β-gal plates

0.67% (w/v) yeast nitrogen base without amino acids
2% (w/v) glucose
10% (v/v) appropriate 10X dropout solution
2% (w/v) bacto-agar

1 litre of agar solution was prepared by mixing 6.7 g yeast nitrogen base and 20 g bacto-agar with 100 ml of dropout solution in 750 ml H_2O. The medium was autoclaved and allowed to cool off to about 55°C, before 50 ml of a 40% (w/v) sterile glucose solution was added together with 100 ml Na-phosphate buffer (0.5 M Na_2HPO_4, 0.25 M NaH_2PO_4) and 0.8 ml X-β-gal solution (100 mg/ml 5-Bromo-4-chloro-3-indolyl-b-D-galactoside in dimethyl formamide).

10X dropout solution

Adenine hemisulphate	200 mg/L
L-Arginine HCl	200 mg/L
L-Histidine HCL	200 mg/L
L-Isoleucine	300 mg/L
L-Leucine	1000 mg/L
L-Lysine HCl	300 mg/L
L-Methionine	200 mg/L
L-Phenylalanine	500 mg/L
L-Threonine	2000 mg/L
L-Tryptophan	200 mg/L
L-Tyrosine	300 mg/L
Uracil	200 mg/L
L-Valine	1500 mg/L

The appropriate amino acids were dissolved in H_2O, autoclaved and stored at 4°C.

2.2.4 Growth and maintenance of *E. coli* and *Saccharomyces cerevisiae*

Liquid cultures of *E. coli* and *Saccharomyces cerevisiae* were grown in a shaking incubator, typically at 37°C for *E. coli* and 30°C for *Saccharomyces cerevisiae*. Growth was monitored using a spectrophotometer by measurement of the optical density (OD) at a wavelength of 600 nm.

E. coli and *Saccharomyces cerevisiae* strains grown on agar plates were incubated up-side-down at 37°C for *E. coli* and 30°C for *Saccharomyces cerevisiae* and stored for up to 4 weeks at 4°C on plates sealed with parafilm. For long-term maintenance *E. coli* and *Saccharomyces cerevisiae* strains were stored in aliquots of liquid cultures containing 25% (v/v) sterile glycerol in cryogenic vials at -80°C.

2.2.5 Preparation of competent *E. coli* cells

A single *E. coli* colony was transferred into 25 ml SOB medium in a 250 ml flask and incubated for 7 hours at 37°C with vigorous shaking at 280 rpm. 2 ml of this culture was used to inoculate 250 ml SOB medium in a 1.5 litre flask and incubated overnight at 18°C with moderate shaking at 230 rpm until the OD_{600} had reached 0.55. At this point the culture flask was transferred to an ice-water bath for 10 minutes and cells were harvested by centrifugation in pre-chilled centrifuge tubes at 4,000 rpm in a Sorvall GSA rotor for 10 minutes at 4°C. The supernatant was carefully removed and the pellet was suspended in 80 ml of ice-cold sterile transformation buffer (55 mM $MnCl_2$, 15 mM $CaCl_2$, 250 mM KCl, 10 mM PIPES pH 6.7). The suspension was centrifuged at 4,000 rpm for 10 minutes at 4°C, the supernatant was removed and the pellet was re-suspended in 20 ml of ice-cold transformation buffer. 1.5 ml of DMSO (dimethylsulphoxide) was added and the bacterial suspension was incubated on ice for 10 minutes. Aliquots of 100 µl were dispensed into chilled sterile microfuge tubes and freezed immediately in liquid nitrogen and stored at -80°C.

2.2.6 Transformation of competent *E. coli* cells

The appropriate number of tubes containing 100 µl competent cells, prepared as described in section 2.2.5, were removed from the freezer and immediately placed on ice where they were allowed to thaw for 5 minutes. 2 µl of ligation mixture or approximately 50 ng of purified plasmid DNA was added directly to the cells and each tube was gently stirred before it was returned to the ice. The cells were incubated on ice for 30 minutes and heat-shocked for 30 seconds in a 37°C water bath and placed on ice for 2 minutes. 0.8 ml of room temperature SOC medium was added to each tube and the cells were incubated at 37°C for 60 minutes prior to plating. Cells were plated at a desired density, depending on the expected frequency of transformation, onto LB agar plates containing the appropriate antibiotic and were incubated overnight at 37°C.

2.2.7 Preparation of plasmid DNA from *E. coli*

Maxi-prep of plasmid DNA (Endotoxin free)

Maxi-preps of endotoxin free DNA was performed using the EndoFree Plasmid Maxi Kit from Qiagen. A single colony was inoculated into 250 ml of LB medium containing the appropriate antibiotic and incubated overnight at 37°C (280 rpm). The cells were harvested by centrifugation at 6,000 rpm in a Sorvall GSA rotor for 15 minutes at 4°C and the pellet was re-suspended in 10 ml Buffer P1. 10 ml Buffer P2 was added and the solutions were mixed by inverting 4-6 times. The suspension was incubated at room temperature for 5 minutes followed by the addition of 10 ml cold Buffer P3 and inversion 4-6 times. This lysate was poured into a QIAfilter cartridge and incubated at room temperature for 10 minutes before it was forced through the filter into a 50 ml tube. 2.5 ml Buffer ER was added to the filtered lysate, the solutions were mixed by inversion and incubated on ice for 30 minutes. This suspension was applied to an equilibrated QIAGEN-tip and allowed to enter the DNA binding resin by gravity flow. The flow-through was discarded and the QIAGEN-tip washed twice with 30 ml Buffer QC before the DNA was eluted with 15 ml Buffer QN. The DNA was precipitated by

the addition of 10.5 ml room-temperature isopropanol followed by centrifugation at 11,000 rpm in a Sorvall SS-34 rotor for 30 minutes at 4°C. The precipitated DNA was washed with 5 ml of endotoxin free, room temperature 70% ethanol and centrifuged at 11,000 rpm for 10 minutes. The pellet was air-dried for 10 minutes and re-suspended in 100 µl endotoxin free Buffer TE.

Miniprep of plasmid DNA

Mini-preps of plasmid DNA were performed using a modified boiling method (Holmes and Quigley, 1981). A single colony was inoculated into 3 ml of appropriate medium and incubated overnight at 37° (300 rpm). 2 ml of the bacterial culture was harvested in a microfuge tube by centrifugation at 12,000 g for 1 minute. The supernatant was removed and the cells were re-suspended in the residual medium. 500 µl of solution C, freshly prepared by a 1:1 mixture of solution A (50 mM Tris-HCl, pH 8.0, 20% w/v Sucrose) and solution B (10% w/v Triton X-100, 50 mM EDTA), was added to the cells and the suspension was vortexed briefly followed by the addition of 10 µl lysozyme solution (50 mg/ml lysozyme in 20 mM NaOAc, pH 4.6, 50% glycerol). The tube was inverted 3-4 times before it was placed in a boiling water bath for 90 seconds. The sample was centrifuged at 12,000 g for 15 minutes and the supernatant was transferred into a new microfuge tube. 700 µl ice-cold isopropanol was added to the supernatant and the tube was placed at -20°C for 20 minutes followed by centrifugation at 12,000 g for 30 minutes. The resulting pellet was washed once in 100 µl 70 % ethanol and once in 100 µl 100 % ethanol and air-dried for 10 minutes before it was re-suspended in 20 µl of distilled H_2O or TE buffer.

2.2.8 DNA enzymatic manipulations

General DNA manipulations and molecular biology techniques were performed essentially as described by (Sambrook and Russel, 2001).

Restriction analysis

Restriction analysis of plasmids was carried out in a total volume of 20 µl. 2 µl of the appropriate buffer (10X stock) was added to 0.5-1 µg DNA followed by the addition of 5 units of enzyme. The reaction mixture was incubated at the optimum temperature (usually 37°C) for 3 hours. To obtain 100% activity 0.2 µl of BSA (100X stock) was added when using BSA requiring enzymes.

DNA ligation

Ligation of cohesive ends was carried out by mixing approximately 100 ng vector with insert DNA in a 1:3 molar ratio of vector to insert in a total volume of 9 µl. 1 µl 10X T4 DNA ligase buffer was added followed by the addition of 200 units of T4 DNA ligase and the reaction was left to incubate overnight at 16°C.

2.2.9 Agarose electrophoresis

Agarose gels (1% w/v) were prepared in, and run with, TBE buffer (45 mM Tris-borate, 1 mM EDTA, pH 8.0). DNA samples were mixed with 0.2 volume of loading buffer (0.25% w/v bromophenol blue, 30% glycerol) and loaded onto the gel. A size marker was loaded into a well adjacent to the samples and the DNA was electrophoresed at a constant voltage (100 V). The gel was removed from the electrophoresis apparatus and placed in H_2O containing 0.5 µg/ml ethidium bromide for 10 minutes. The gel was washed in H_2O for 10 minutes before the fluorescent DNA-ethidium bromide complex was visualized under ultraviolet light.

2.2.10 Purification of DNA fragments from agarose gels

The Agarose Gel DNA Extraction Kit from Roche was used to isolate individual DNA fragments that had been separated by agarose gel electrophoresis. The desired band was excised from the gel, transferred into a pre-weighted Eppendorf tube, and its weight

and volume (1g ~ 1 ml) was determined. 3 volumes of agarose solubilisation buffer were added and the tube was incubated at 55°C for 5 minutes to dissolve the agarose. 10 µl of a silica suspension was added and the tube was incubated for 10 minutes at 55°C with vortexing every 2-3 minutes. The suspension was centrifuged at 12,000 g for 30 seconds to pellet the DNA/silica complex and the supernatant was discarded. The complex was re-suspended in 500 µl nucleic acid binding buffer, centrifuged at 12,000 g for 30 seconds and the supernatant was removed. The pellet was washed twice in 500 µl washing buffer and air-dried for 15 minutes. To elute the DNA, the pellet was suspended in 10 µl of distilled H_2O and incubated at 55°C for 10 minutes with vortexing every 2-3 minutes. The suspension was centrifuged at 12,000 g for 30 seconds and the supernatant was transferred into a new tube. This step was repeated once and the supernatant was combined with that of the first elution to obtain the purified DNA in a total volume of 20 µl.

2.2.11 Purification of RNA from mammalian cells

Cells were grown to 60-70% confluence in 10-cm plates or 6-well plates. The medium was removed and 1 ml of Tri-Reagent was added to the cells. The cell suspension was transferred to an eppendorf tube and incubated for 10 min at room temperature. 200 µl of chloroform was added and the mixture was vortexed for 15 seconds and spun at 12,000 g for 15 min at 4°C. The aqueous phase was transferred to a fresh eppendorf tube and combined with 500 µl of isopropanol by gentle inversion. The mixture was incubated at room temperature for 10 min and spun at 12,000 g for 8 min at 4°C. The pellet was washed in 1 ml of 75 % cold ethanol, spun at 7500 g for 5 min at 4°C and air-dried for 5 min. The pellet was dissolved in RNAse free H_2O and stored at -80°C.

2.2.12 Reverse Transcriptase Polymerase chain reaction (RT-PCR)

Prior to RT-PCR the RNA was treated with DNAse by combining 1 µg of RNA with 1 µl of 10X DNAse buffer and 1 µl of DNAse I (1 µnit/µl) in a total of 10 µl. The

mixture was incubated for 15 min at room temperature and the DNAse was inactivated by addition of 1 µl 25 mM EDTA and incubation for 10 min at 65°C. The 10 µl reaction was combined with 1 µl oligo-dT primer (0.5 µg/µl), 4 µl of 5X Reverse Transcriptase Buffer, 1 µl of 10 mM dNTPs, 1 µl of RNase inhibitor (20 units/µl) and 1 µl of Reverse Transcriptase (200 units/µl) in a total of 20 µl. The mixture was transferred to a thermal cycler preheated to 37°C and incubated for 60 min followed by 10 min at 75°C. The first strand cDNA was stored at -20°C or used directly for amplification by PCR.

2.2.13 Polymerase chain reactions (PCR)

Polymerase chain reactions were carried out on a programmable Gene Amp 2400 Thermal cycler (Perkin Elmer) in sterile 0.2 ml tubes by mixing the following components:

10X Reaction Buffer	2 µl
10 mM dNTPs	1 µl
10 µM forward primer	1 µl
10 µM reverse primer	1 µl
1-5 units/µl thermostable DNA polymerase	2 units
Template DNA (10 ng of plasmid DNA or 2 µl cDNA)	-
H_2O	-
Total volume	20 µl

The DNA was amplified using the denaturation, annealing, and polymerization times and temperatures listed below.

Cycle Number	Denaturation	Annealing	Polymerization
First cycle	5 min at 94°C	-	-
20-32 cycles	30 sec at 94°C	30 sec at 53-60°C	30 sec - 90 sec at 72°C
Last cycle	-	-	7 min at 72°C

Following the amplification, the reaction mixture was submitted to agarose electrophoresis and when desired, the DNA was isolated using the Agarose Gel DNA Extraction Kit.

2.2.14 Site directed mutagenesis

Site directed mutagenesis was performed by PCR using complementary primers containing the desired mutation. The following components were mixed and subjected to PCR according to the cycles given below:

10X Reaction Buffer	5 µl
10 mM dNTPs	2 µl
Forward primer (100 ng/µl)	1.25 µl
Reverse primer (100 ng/µl)	1.25 µl
1-5 units/µl thermostable DNA polymerase	2 units
Template DNA (20 ng of plasmid DNA)	-
H_2O	-
Total volume	50 µl

Cycle Number	Denaturation	Annealing	Polymerization
First cycle	5 min at 94°C	-	-
17 cycles	1 min at 94°C	1 min at 55°C	18 min at 72°C
Last cycle	-	-	7 min at 72°C

Following PCR the mixture of newly synthesized mutant constructs and template DNA is incubated with the methylation-specific endonuclease to remove the wild-type template DNA (1 µl DpnI for 1 h at 37°C). The mixture is then transformed into competent *E.coli* cells and grown overnight in order to allow individual colonies to grow. The presence of point mutations is verified by DNA sequencing.

2.2.15 DNA sequencing

DNA sequencing was performed by MWG Biotech, Anzinger Str. 7, 85560 Ebersberg, Germany, using MWG standard primers.

2.2.16 Preparation of yeast competent cells

A 250 ml flask containing 50 ml of YPAD medium was inoculated with a single yeast colony and incubated at 30°C (250 rpm) for 18 hours. Approximately 30 ml of this culture was transferred to a 2 litre flask containing 300 ml of YPAD to produce an OD_{600} = 0.2-0.3. The culture was incubated at 30°C (230 rpm) for 3 hours to an OD_{600} = 0.4-0.6, and harvested by centrifugation at 1,000 g for 5 minutes at room temperature. The pellet was washed by suspension in 30 ml sterile H_2O, centrifuged at 1,000 g for 5 minutes at room temperature and re-suspended in 1.5 ml of freshly prepared, sterile 1 x TE/1 x LiAc (10 mM Tris-HCl, 1 mM EDTA, 100 mM lithium acetate, pH 7.5). The competent cells were used immediately for transformation.

2.2.17 Transformation of yeast competent cells

For each transformation 5 µl of herring testes carrier DNA (10mg/ml) was transferred into a sterile 1.5 ml tube and mixed with 0.1 µg of plasmid DNA (for cotransformation 0.1 µg of each plasmid was used). 100 µl of yeast competent cells were added and the cells were mixed by vortexing. 600 µl of a sterile PEG/LiAc solution (40% PEG 3350, 10 mM Tris-HCl, 1 mM EDTA, 100 mM lithium acetate) was added to each tube and the cells were vortexed briefly. The cells were incubated at 30°C (200 rpm) for 30 minutes followed by the addition of 70 µl DMSO. The suspension was then mixed gently and incubated in a water bath at 42°C for 15 minutes. The tubes were placed on ice for 2 minutes before the cells were harvested by centrifugation at 12,000 g for 10 seconds. The cells were re-suspended in 1 ml of sterile H_2O and plated at a desired density onto appropriate SD agar plates.

2.2.18 Isolation of DNA from yeast

A single yeast colony was transferred into 10 ml of the appropriate SD medium and incubated at 30°C (250 rpm) overnight to saturation. The cells were harvested by centrifugation at 4500 rpm for 5 minutes and re-suspended in 500 µl H_2O. The cell suspension was transferred into a 1.5 ml eppendorf tube and the cells were collected by a 10 second spin. The supernatant was removed and the cells were suspended in the residual liquid and mixed with 200 µl of buffer A (2% Triton X-100, 1% SDS, 100 mM NaCl, 10 mM Tris-HCl pH 8.0, 1 mM EDTA pH 8.0) followed by addition of 200 µl acid-washed glass beads and 200 µl phenol:chloroform:isoamyl alcohol (25:24:1). The organic and aqueous phases were mixed by vortexing for 3 minutes followed by addition of 200 µl TE buffer (10 mM Tris-HCl, 1 mM EDTA). The tubes were centrifuged at maximum speed for 5 minutes and the upper aqueous phase was transferred to a fresh tube. The DNA was precipitated with 1 ml of 100% ethanol and the precipitate was recovered by centrifugation at maximum speed for 3 minutes. The pellet was re-suspended in 400 µl TE buffer followed by addition of 40 µl 3 M NaOAc, vortexing, addition of 1 ml 100% ethanol and vortexing. The DNA was recovered by

centrifugation at maximum speed for 2 minutes and the pellet was air-dried for 10 minutes before it was re-suspended in 20 µl distilled H_2O. 2 µl of total yeast DNA was used to transform competent *E. coli* cells and plasmid was isolated using the mini-prep method described in section 2.2.7.

2.2.19 Yeast Two-Hybrid Screening

Construction and testing of bait plasmid

The DNA encoding the protein domain to be used as bait was cloned into the multiple cloning site of pGBKT7 to generate an in-frame fusion to GAL4 DNA-binding domain. This bait plasmid was transformed into the yeast strain AH109 to generate AH109[bait] and selected on SD/-Trp plates. The bait fusion protein was tested for toxicity effects by comparing its growth rate in liquid culture with yeast transformed with the "empty" pGBKT7 vector. The bait fusion protein was also tested for transcriptional auto-activation by plating the AH109[bait] strain onto SD/-Trp/-His and SD/-Trp/-Ade plates.

Screening of pretransformed library

One colony of the AH109[bait] was transferred into a 500 ml flask containing 50 ml SD/-Trp medium and incubated at 30°C (260 rpm) for 18-24 hours. When the OD_{600} of the cell culture had reached a value above 0.8 the cells were harvested by centrifugation at 1000 g for 5 minutes and re-suspended in the residual medium. Just prior to use, 1 ml of the pretransformed human brain library (Y187[library]) was thawed and gently vortexed. 10 µl of the library was transferred to a microfuge tube and set aside for library titering. The re-suspended AH109[bait] culture was mixed with the 1 ml library culture in a sterile 2 litre flask with 45 ml of 2X YPAD medium containing 50 µg/ml kanamycin and incubated at 30°C (40 rpm) for 20-24 hours. The cells were harvested by centrifugation at 1000 g for 10 minutes and re-suspended in 10 ml 0.5X YPAD containing 50 µg/ml kanamycin. In order to determine mating

efficiencies and number of clones screened dilutions of the mating mixture were plated on SD/-Leu, SD/-Trp and SD/-Leu/-Trp plates. The mating mixture was plated on 60 large (150-mm) SD/-Leu/-Trp/-His/-Ade plates (SD/-Leu/-Trp/-His plates in the four screens performed previously) and incubated at 30°C for 7-10 days (primary screen). Colonies were re-streaked onto SD/-Leu/-Trp/-His/-Ade plates and grown for 3-5 days at 30°C (secondary screen) before they were replica plated (or re-streaked) onto SD/-Leu/-Trp/-His/-Ade plates and SD/-Leu/-Trp/-His/-Ade plates containing X-β-gal. β-galactosidase activity was monitored directly from the X-β-gal plates while the SD/-Leu/-Trp/-His/-Ade plates were assayed for β-galactosidase activity by using the colony-lift filter assay as described in section 2.2.21.
Total DNA was purified from positive yeast clones and transformed into competent *E. coli* cells for further plasmid isolation.

2.2.20 Mating assay – verification of two-hybrid clones

The empty vector pACT2 and selected prey constructs (pACT2-library cDNA) were re-transformed into the Y187 yeast strain and selected on SD/-Leu plates. The empty pGBKT7 vector and the relevant pGBKT7 bait constructs were transformed into AH109 and selected on SD/-Trp plates. The control strains AH109[pGBKT7-53] and Y187[pTD1-1] were plated onto SD/-Trp and SD/-Leu plates respectively. The plates were incubated at 30°C for 3 days and three colonies from each individual transformation were re-streaked onto fresh plates. The three colonies were combined and suspended in 300 µl sterile H_2O. 30 µl of each bait construct including the two controls AH109[pGBKT7] and AH109 [pGBKT7-53] were used to generate horizontal parallel streaks, 3-5 mm wide, on SD/-Trp plates. Vertical parallel streaks of the prey constructs and the control strains Y187[pACT2] and Y187[pTD1-1] were generated on SD/-Leu plates. The plates were incubated at 30°C for 2 days and the two haploid yeast strains were brought into contact by placing one bait plate orthogonally to one prey plate on the same replica velvet. The double imprint was transferred to an YPAD plate and incubated overnight at 30°C before it was replica plated onto SD/-Trp/-Leu plates for diploid selection. The plates were incubated at 30°C for 2 days and replica plated

onto SD/-Trp/-Leu, SD/-Trp/-Leu/-His/-Ade, and SD/-Trp/-Leu/-His/-Ade + X-β-gal and SD/-Trp/-Leu + X-β-gal plates. Plates were incubated at 30°C for 5 days and growth and colour development was monitored every day.

2.2.21 Colony-lift filter assay

A Whatman #5 filter was placed in a clean petri dish and soaked in 2.5-5 ml Z-buffer/X-gal solution (100 ml Z buffer [60 mM Na_2HPO_4, 40 mM NaH_2PO_4, 10 mM KCl, 1 mM $MgSO_4$], 0.27 ml β-mercaptoethanol and 1.67 ml X-β-gal solution [20 mg/ml 5-bromo-4-chloro-3-indolyl-β-D-galactopyranoside in N,N-dimethyl-formamide]). Another Whatman #5 filter was placed over colonies growing on a SD/-Trp/-Leu/-His/-Ade plate and left for 10 seconds. The filter was submerged in liquid nitrogen for 10 seconds and allowed to thaw at room temperature. This step was repeated once and the filter was placed, colony side up, on the pre-soaked filter and incubated at 30°C. Colour development was monitored periodically for 8 hours.

2.2.22 Liquid β-galactosidase assay

Selected cDNA clones were co-transformed into the AH109 yeast strain with each of the four bait constructs pGBKT7[hSERT(1-87)], pGBKT7[hSERT(1-108)], pGBKT7[hSERT(596-577)], pGBKT7[hSERT(577-630)], the empty vector pGBKT7 and the control vector pGBKT7-p53. As a positive control pGBKT7-p53 was co-transformed with pTD1-1. The transformants were selected on SD/-Leu/-Trp plates, incubated for 3 days at 30°C and three colonies from each transformation were re-streaked onto fresh plates. By combining the three colonies each strain was inoculated in 5 ml SD/-Leu/-Trp medium and grown to stationary phase. Cultures were diluted 10-fold and grown to a final OD_{600} of 0.8-1.0. 2 ml of cells were harvested by centrifugation at 10,000 g for 30 seconds and washed once in H_2O. The cells were re-suspended in 500 µl Z-buffer (60 mM Na_2HPO_4, 40 mM NaH_2PO_4, 10 mM KCl, 1 mM $MgSO_4$) and OD_{600} was measured. 300 µl of cells were transferred into 700 µl Z-buffer

containing 0.27 % v/v β-mercaptoethanol. 40 µl 0.1% SDS and 80 µl of chloroform were added and the suspension was vortexed for 15 seconds and incubated at 30°C for 15 minutes. 2 ml ONPG solution (4 mg/ml o-Nitrophenyl-β-D-galactopyranoside in 0.1 M Na-phosphatebuffer [0.06 M Na_2HPO_4, 0.04 M NaH_2PO_4]) was added and the solution was vortexed and incubated in a 30°C water bath for 5-30 minutes. The reaction was terminated by adding 500 µl 1 M Na_2CO_3 and the cells were allowed to settle for 30 minutes before the absorbance was measured at 420 nm and 550 nm. Results were normalized against cell density and incubation time using the following equation: β-galactosidase activity = $1000 \times [(OD_{420} - 1.75 \times OD_{550})] / (t \times v \times OD_{600})$, where OD_{420} and OD_{550} is the absorbance of the reaction mixture; OD_{600} reflects cell density in the re-suspended cell suspension; t is the time of the reaction in minutes; and v is the volume of the culture in millilitre used in the assay.

2.2.23 Preparation of yeast crude extract for Western blotting

Three colonies from each yeast strain were transferred into 3 ml of selective medium and grown for 2 days at 30°C. The yeast culture was diluted 1:1 in YPAD medium and grown for additional 6 hours. 3 OD of each culture was harvested by centrifugation at 14,000 rpm for 2 minutes, washed once with H_2O and re-suspended in 100 µl H_2O. 5 µl of 2% SDS and 4 µl of 25 x Protease Inhibitor cocktail were added to the cells and cell lysis was performed by vortexing the cells with approximately 100 µl glass beads (425-600 microns) for 90 seconds. Following addition of 50 µl of 3 X SDS gel loading buffer the mixture was boiled for 3 minutes and centrifuged at 14,000 rpm for 1 minute. The supernatant was transferred to a new tube and used for SDS gel analysis.

2.2.24 Maintenance and storage of mammalian cells

HEK-293 cells were grown in Dulbecco's Modified Eagle's Medium (DMEM) supplemented with 10% (v/v) fetal bovine serum, 100 units/ml penicillin, 2 mM glutamine and 100 µg/ml streptomycin. A172 cells were grown essentially as HEK-293

cells but supplemented with 1% non-essential amino acids. SH-SY5Y cells were grown in DMEM:Ham's F-12 (1:1) medium supplemented with 15% (v/v) fetal bovine serum, 100 units/ml penicillin, 2 mM glutamine, 100 µg/ml streptomycin and 1% non-essential amino acids. All three cell lines were maintained at 37°C and 5% CO_2 in a humidified incubator. RN46A-B14 cells (White et al., 1994) were cultured at 33°C in DMEM:Ham's F-12 (1:1) medium containing 10% (v/v) fetal bovine serum, 250 µg/ml G418, and 100 µg/ml hygromycin. Cells were split every 3-4 days, when they reached 80-90% confluency. The growth medium was removed and the cells were washed once with prewarmed (37°C) sterile PBS. Trypsin-EDTA solution was added and distributed over the cells and left for 1-2 minutes until the cells detached. The cells were gently resuspended in growth medium and transferred into new culture plates and the desired density.

For cryopreservation, cells were trypsinized as described above and centrifuged at 1000 rpm for 5 minutes. The supernatant was removed and the cells were washed in medium and spun again at 1000 rpm for 5 minutes. The pellet was resuspended in growth medium containing 10% DMSO and aliquots of 0.5 ml were dispensed into sterile cryovials and placed in a polystyrene holder at -80°C for 12 h. The vials were then placed in liquid nitrogen for long-term storage.

Removal of cells from liquid nitrogen was carried out by rapidly thawing a vial by adding pre-warmed serum-free medium. The cells were transferred to 40 ml of pre-warmed serum-free medium and centrifuged at 1200 rpm for 5 minutes. The cells were resuspended in 5 ml of growth medium and seeded into a 6-well plate at the desired density.

2.2.25 Transient transfection of mammalian cells

Cells were seeded 24-48 hours prior to transfection. Transfections were performed using GeneJuice™ transfection reagent according to the manufacturer's instructions. GeneJuice was mixed with serum-free medium (3µl GeneJuice in 100 µl medium) and

incubated at room temperature for 5 minutes. DNA was added to the mixture in a ratio of: 1 μg of DNA to 3μl of GeneJuice. The mixture was incubated at room temperature for 15 minutes and added to the cells dropwise. Cells were incubated for 30-72 hours before processing. For all transfection experiments, pcDNA3 vector was used to equalize total DNA input to the same level.

2.2.26 Preparation of cell lysates

The growth medium was removed and the cells were washed twice in PBS. Cells were kept on ice and lysed in detergent-containing buffer (5 mM CHAPS or 1% Triton in 150 mM NaCl, 50 mM Tris-HCl, pH 7.4, (2mM EDTA), 1x Complete™ Protease Inhibitor mixture, Roche) for 20 minutes followed by centrifugation at 13,000 rpm for 20 minutes. The supernatant was transferred into a fresh tube and used either immediately for experiments or stored at -20°C.

2.2.27 Preparation of rat brain extract

Brain homogenate was prepared from one adult rat following decapitation. One brain was homogenized in 10% (w/v) of ice-cold TNE buffer (50mM Tris-HCl, pH 7.4, 150mM NaCl, 5mM EDTA) in the presence of protease inhibitors (1 x Complete™ protease Inhibitor Mixture) using 15 strokes of a Dounce homogeniser. Total homogenate was centrifuged at 1000 rpm for 10 min at 4°C and the supernatant was subsequently centrifuged at 13,000 rpm for 20 min at 4°C. The pellet was resuspended in TNE buffer containing 5mM CHAPS and incubated for 30 min at 4°C. Finally, the lysate was centrifuged at 13,000 rpm for 20 min at 4°C and the supernatant was recovered and used for experiments.

2.2.28 Markwell protein assay

Protein concentrations were assayed using a modification of the Lowry method. Samples were diluted to reach a final volume of 500 μl and compared against a series

of dilutions of BSA (0-100 µg/ml) in a total of 500 µl. 1.5 ml of solution C (freshly prepared by mixing 100 volumes of solution A [2% (w/v) $NaCO_3$, 0.4% (w/v) NaOH, 0.16% (w/v) sodium Potassium Tartrate, 1% (w/v) SDS] with 1 volume of solution B [4% (w/v) $CuSO_4$]) was added to each sample and standard solution and the mixtures were incubated for 10 minutes at room temperature followed by the addition of 150µl of Folin-Ciocalteu reagent (diluted 1:1 with H_2O). The tubes were incubated at room temperature for 45 minutes before the absorbance was measured at 600 nm.

2.2.29 SDS-polyacrylamide gel electrophoresis (SDS-PAGE)

Sodium dodecyl sulphate-polyacrylamide gel electrophoresis (SDS-PAGE) was carried out in a discontinuous denaturing system using a 5% stacking gel and 8-15% resolving gels. Components of a 10% resolving gel are as follows: 3.3 ml Protogel™ (Ultra-pure 30% w/v acrylamide and 0.8% w/v bisacrylamide solution), 4.0 ml H_2O, 2.5 ml 1.5 M Tris-HCl (pH 8.7), 100 µl 10% SDS, 100 µl 20% ammonium persulphate and 10 µl TEMED. The amount of acrylamide was adjusted in gels of higher percentage. The stacking gel was prepared with 0.65 ml Protogel™, 2.75 ml H_2O, 0.5 ml Tris-HCl (pH 6.8), 40 µl 10% SDS, 50 µl 20% ammonium persulphate and 5 µl TEMED.
Samples were mixed with 3 x SDS gel-loading buffer (125 mM Tris-HCl (pH 6.8), 4% (w/v) SDS, 20% glycerol, 0.02% bromphenol blue, and 125 mM DTT), incubated 1 h at 37°C or boiled for 3 minutes before they were loaded into separate wells and electrophoresed at a constant current (60 mA) for 2-3 hours. A prestained protein marker was used for molecular weight determination. Gels were then either stained using Coomassie Blue R-250 (0.25% (w/v) in 50% (v/v) methanol and 10% (v/v) acetic acid) or used for Western Blotting.

2.2.30 Western Blotting

Following SDS-PAGE, resolved proteins were blotted onto either a polyvinylidene fluoride (PVDF) or a nitrocellulose membrane at 160 mA for 1 hour and 30 minutes.

Following transfer the membrane was first incubated in 50 ml blocking solution (either 5% (w/v) Marvel and 0.5% (w/v) TWEEN 20 in TBS buffer [50 mM Tris-HCL, pH 8.0, 150 mM NaCl] or 3% (w/v) BSA, 0.5% (w/v) Marvel and 0.5% (w/v) TWEEN 20 in TBS buffer) for 1 hour at room temperature and then incubated in primary antibody (diluted in blocking solution) overnight at 4°C. The membrane was washed extensively in TWB buffer (TBS buffer containing 0.5% TWEEN 20) and incubated in secondary antibody (diluted in blocking solution) for 1 hour at room temperature. The membrane was washed in TBW buffer and immunoreactive bands were visualized using ECL Western Blotting Detection Reagent (Amersham Biosciences) or Supersignal west femto maximum sensitivity substrate (Pierce).

2.2.31 GST Pull-down assay

For glutathione *S*-transferase (GST) pull-down assays the relevant PCR fragments were fused to GST by subcloning into the pGEX-KG bacterial expression vector. A 50 ml overnight culture of *Escherichia coli* expressing a GST fusion protein was diluted into 500 ml to an OD=0.2 and further grown to an OD=0.6-0.8. The culture was induced with 1mM isopropyl-1-thio-β-D-galactopyranoside (IPTG) at 30°C for 4 h. The cells were harvested by centrifugation at 6,000 rpm for 15 minutes and resuspended in 150 OD/ml of Spermidin-mix (20 mM Spermidin, 200 mM NaCl, 2 mM EDTA). 2 volumes of 10% sucrose in PBS (containing 0.1 mM DTT and 1 x Proteinase inhibitor mixture) were added to the mixture followed by addition of Brij-58 to a final concentration of 0.25%. Lysozyme was added to a final concentration of 0.5 mg/ml and the mixture was incubated on ice for 1 hour. The mixture was homogenized using 15 strokes of a Dounce homogeniser and the homogenate was centrifuged at 15,000 rpm for 45 min at 4°C. For GST alone, the supernatant was kept on ice (contains the GST protein) and the pellet was discarded. For the GST fusion proteins, the supernatant was discarded and the pellet was homogenized in 5 ml of STE buffer (10 mM Tris-HCL, pH 8.0, 1 mM EDTA, 150 mM NaCl). 0.7 ml of 10% sarkosyl in STE buffer and 40 µl of 1.25 M DTT were added to the homogenate and the mixture was incubated on ice for 15 minutes. The mixture was homogenized again before centrifugation at 15,000 rpm for

45 min at 4°C. The supernatant was transferred to a fresh tube and mixed with 2 ml of 10% Triton-X 100 in STE. The volume was adjusted to 10 ml with STE and the mixture was incubated for 30 minutes at room temperature. Fusion proteins were purified by affinity chromatography, using glutathione-agarose beads. 2-3 ml of glutathione-agarose beads were washed in 10 ml PBS and incubated with the 10 ml of soluble protein fractions. The mixture was incubated on a roller for 2 hours at room temperature and the beads were washed 3 times in 10 ml of PBS. The beads were resuspended in 1-2 ml PBS and stored at 4°C for up to two weeks. The amount of immobilised protein was estimated by SDS-PAGE using coomassie staining.
Approximately 20 micrograms of GST or GST fusion protein, coupled to agarose, were incubated with 500 µg of total protein from transfected HEK-293 cells. The mixture was incubated 3 hours at room temperature or overnight at 4°C. The agarose was washed three times in lysis buffer and proteins were eluted in SDS-sample buffer and analysed by Western blotting.

2.2.32 Co-immunoprecipitaion

For co-immunoprecipitation assays on transfected HEK-293 cells, 500 µg of total protein was incubated with 1 µg control IgG or 1 µg anti-SERT (C-20). Co-immunoprecipitation on rat brain was performed by incubating rat brain extract (1 mg of total protein) with 10 µl of anti-SERT (EL4) antiserum or 10 µl rabbit non-immune serum for 2 h at 4°C. Immunocomplexes were captured by incubating with G-agarose beads at 4°C overnight. Beads were washed three times with 5mM CHAPS and proteins were eluted in SDS-sample buffer.

2.2.33 5-HT uptake assay (on transiently transfected cells)

Cells were grown in poly-L-lysine-coated (0.1 mg/ml) 24-well plates and transfected 36-48 hours prior to the uptake assay or the cells were transfected in 6-well plates, and trypsinized and seeded into 24-well plates 14-20 hours after transfection. The cells

were then grown for a further 36-48 hours before the uptake assay was performed. Medium was removed from the cells by aspiration and the cells were washed once with TB buffer (10 mM Hepes, pH 7.5, 150 mM NaCl, 2 mM KCl, 1 mM $CaCl_2$, 1 mM $MgCl_2$) and further incubated in TB buffer for 15 minutes at 37°C. The uptake assay was performed at room temperature and started by the addition of [^{3}H]5-HT and terminated 6 min later by three washes of ice-cold TB buffer containing 1 μM paroxetine. Cells were solubilised with OptiPhase scintillation fluid and [^{3}H]5-HT accumulation was quantified using a 1450 Microbeta scintillation counter. Specific [^{3}H]5-HT uptake was determined by subtracting the amount of [^{3}H]5-HT accumulated in the presence of 10 μM paroxetine. The radiolabelled 5-HT used in this study was 5-[1,2-^{3}H(N)] -hydroxytryptamine creatine sulphate with specific activities between 20 and 50 Ci/mmol. Accumulated [^{3}H]5-HT did not exceed 10% of the total radioactivity present in the assay buffer. Data were analysed using SigmaPlot 8.0 software package using the Michaelis-Menten equation. Kinetic parameters were determined by non-linear regression.

2.2.34 Cell surface biotinylation

Transiently transfected HEK-293 cells were washed three times in ice-cold PBS^{++} (PBS containing 1 mM $MgCl_2$ and 0.1 mM $CaCl_2$) and incubated in 1.0 mg/ml sulfo-NHS-biotin (Pierce) in PBS^{++} on ice for 30 min with gentle agitation. The biotinylating agent was removed by washing the cells three times with ice-cold quench buffer (100 mM glycine in PBS^{++}) and incubated for a further 30 min in quench buffer on ice. The cells were washed three times in ice-cold PBS^{++} and lysed in 1% Triton X-100 prepared in PBS^{++} containing protease inhibitors. Lysates were centrifuged at 13,000 rpm for 30 minutes at 4°C, and the supernatants were incubated with NeutrAvidin beads (Pierce) for 1 h at room temperature. The beads were washed three times in lysis buffer, and bound proteins were eluted with SDS-sample buffer. Samples were analysed by Western blotting and quantified with Gene Tools Image Analysis Software (Syngene).

2.2.35 Sucrose Gradient Fractionation

Brain from one adult rat was removed immediately following decapitation and placed in TNE buffer. The brain was homogenized in 10% (w/v) TNE buffer in the presence of protease inhibitors (1 x Complete^{TM} protease Inhibitor Mixture) using 15 strokes of a Dounce homogeniser. The homogenate was centrifuged at 10,000 *g* for 10 min at 4°C. The pellet was resuspended in TNE buffer containing 2% Brij-58 and incubated for 30 min at 4°C. The sample was then sonicated and homogenized again before centrifugation at 2000 *g* for 10 min at 4°C to remove cell debris. 0.5 ml of the supernatant was mixed with an equal volume of 80% (w/v) sucrose in TNE, transferred into an ultracentrifuge tube and overlaid successively with 1 ml of 30% (w/v) sucrose and 0.5 ml of 5% (w/v) sucrose. The gradients were centrifuged for 17 h at 134,400 *g* in a Beckman Coulter Optimal L-100 XP ultracentrifuge using a SW55Ti swing-out rotor. Eight fractions of 312 µl were collected from the top of the gradient and processed for Western blotting.

2.2.36 Confocal Microscopy

RN46A cells or transfected HEK-293 cells were grown on glass coverslips to 60-70% confluence. Cells were washed in PBS and fixed with 4% paraformaldehyde in PBS, pH 7.5, for 10 min at room temperature. Residual fixative was quenched with 50 mM NH_4Cl for 10 min. Cells were incubated with blocking solution (0.2% Triton X-100, 5% donkey serum in PBS) at 4°C overnight followed by incubation with primary antibody diluted in blocking solution for 1 h at room temperature. Cells were washed extensively in PBS and incubated with the appropriate fluorophore-conjugated secondary antibody diluted in blocking solution for 1 h at room temperature. After washing, the cells were mounted onto microscope slides in 2 µg/µl p-phenylenediamine in 1:1 glycerol:PBS. Samples were imaged on a Zeiss LSM510 laser scanning confocal microscope. Confocal images (xy-scans) were acquired with a confocal laser scanning microscope LSM510 (Zeiss) using 488 nm (Argon), 543 nm (HeNe), and 633 nm (HeNe2) laser lines for FITC, Cy3 and Cy5 excitation and BP 500-530 nm, BP 560-615

nm, and 644-718 nm emission filters for detection, respectively. Images were processed using the Zeiss LSM Image Browser version 3.

2.2.37 siRNA interference

The GAPDH control siRNA was purchased from Ambion as a validated siRNA that had already been verified experimentally to reduce the expression of the GAPDH gene. The three ESO3 siRNAs (A:GGGUGGUUGGGAAGGAUCU; B:GCCACUCACUG UGAGAUCC, and C:GGAAUUCCCACAGUUGCUA) were pre-designed by Ambion using an algorithm developed by Cenix BioScience and owned by Ambion. The effectiveness of this algorithm has been tested on 1,100 algorithm-designed siRNAs in the silencing of 400 endogenously expressed human transcripts. At least two of the three pre-designed siRNAs are guaranteed to reduce mRNA levels by 70% or more.
All siRNAs were purchased as validated or predesigned from Ambion and transfected into HEK-293 cells using Lipofectamine 2000 transfection reagent (Invitrogen). Transfections were performed according to the manufacturer's instructions with minor modifications. Cells were seeded 24 hours prior to transfection in growth medium without antibiotics and grown to 70% confluence. The medium was aspirated from the cells and replaced with 1 volume of OPTI-MEM®I before cells were transfected with siRNA (50nM) as specified by the manufacturer. After 4 hours, 1 volume of growth medium (without antibiotics) was added to the cells. At 12 hours after siRNA transfection medium was replaced with fresh medium and cells were transfected with SERT in a ratio of 1:4 with pcDNA3 (50 ng SERT and 200 ng pcDNA3 per well in a 24-well plate). Cells were incubated for a further 36 h before they were processed for RNA isolation, Western blotting and 5-HT uptake assays.

3. IDENTIFICATION OF POTENTIAL SEROTONIN TRANSPORTER BINDING PROTEINS

3.1 INTRODUCTION

3.1.1 The Yeast Two-Hybrid system

Most physiological processes in living cells are largely governed by the regulated interaction of specific proteins with other proteins in order to achieve a particular function. Proteins associate with one another, either to form lasting functional complexes, or in transient interactions that result in modifications of one of the proteins, such as interactions of protein kinases with their substrates. The function of a protein is therefore reflected in its biological interactions with other proteins. Abnormal protein-protein interactions appear to be a common manifestation in a number of neurological disorders such as Creutzfeld-Jacob and Alzheimer's disease (Trojanowski and Lee, 2000). Because of their importance in normal cellular functioning and their implications in various diseases, protein-protein interactions have been the object of intense research for many years. Numerous procedures have been developed to identify the interaction network of a protein of interest. The most powerful genetic method available today is the well-known yeast two-hybrid system, which has been widely used to study interactions between two known proteins as well as identifying novel binding partners of specific proteins. The assay is a genetic method conducted in yeast that uses transcriptional activity as a measure of protein-protein interactions. The principle of this system was first described in 1989 by Fields and Song (Fields and Song, 1989) and is based on the observation that many transcription factors are composed of two physically separable domains, a site-specific DNA-binding domain and a transcriptional activation domain. The DNA-binding domain serves the targeting of the transcription factor to specific promoter sequences whereas the activation domain facilitates assembly of the transcription complex. Neither of the two domains can function as a transcription factor but if they are brought into close proximity to one

another they can reconstitute transcriptional activity. Thus, if a protein X (denoted the bait) is expressed as a fusion to a DNA-binding domain of a transcription factor and a protein Y (denoted the prey) is expressed as a fusion to an activation domain, an active transcription factor will only be reconstituted if the two proteins X and Y interact with each other (Figure 3.1). This technique can be used to identify novel protein interactions, confirm suspected interactions, and define interacting domains. When the yeast two-hybrid system is used to identify novel interacting partners of a protein of interest, an appropriate cDNA library is cloned in fusion with the activation domain and substituted for the prey construct. The commonly used systems rely upon either the yeast GAL4 or the *Escherichia coli* LexA DNA binding domain in combination with either the yeast GAL4, the herpes simplex virus VP16 or the bacterial B42 transcription activation domain (Van Criekinge and Beyaert, 1999).

In order to detect proteins that interact with the bait the yeast strain is modified to contain specific reporter genes. The reporter genes are only expressed when the prey (in this case a protein encoded by the cDNA library) interacts with the bait protein. Commonly used reporter genes are yeast genes involved in amino acid biosynthesis, such as *URA3, HIS3*, *LEU2* and *ADE2*, allowing yeast containing a positive interaction to grow on media lacking the corresponding amino acids. In addition, the *E.coli LacZ* gene encoding β-galactosidase is often used as an enzymatic reporter gene. Yeast containing a positive interaction produces blue colonies on plates or filters containing the β-galactosidase substrate 5-bromo-4-chloro-3-indolyl-β-D-galactoside (X-β-gal), which allows a convenient qualitative identification of positive colonies. A quantitative assay for β-galactosidase activity can also be performed on extracts of liquid cultures using for example ortho-nitrophenyl-β-D-galactoside (ONPG) as substrate. Cleavage of ONPG produces a yellow product, which is readily monitored by a spectrophotometer. One major advantage of the two-hybrid system is that the assay is performed *in vivo*, which makes the proteins involved more likely to be in their native conformations. In addition, the cDNA library screen provides immediate access to the genes encoding the interacting proteins. The smallest domain necessary for interaction may already be apparent through isolation of multiple clones encoding different regions of the same protein allowing precise mapping of an interacting protein. Also, weak and transient

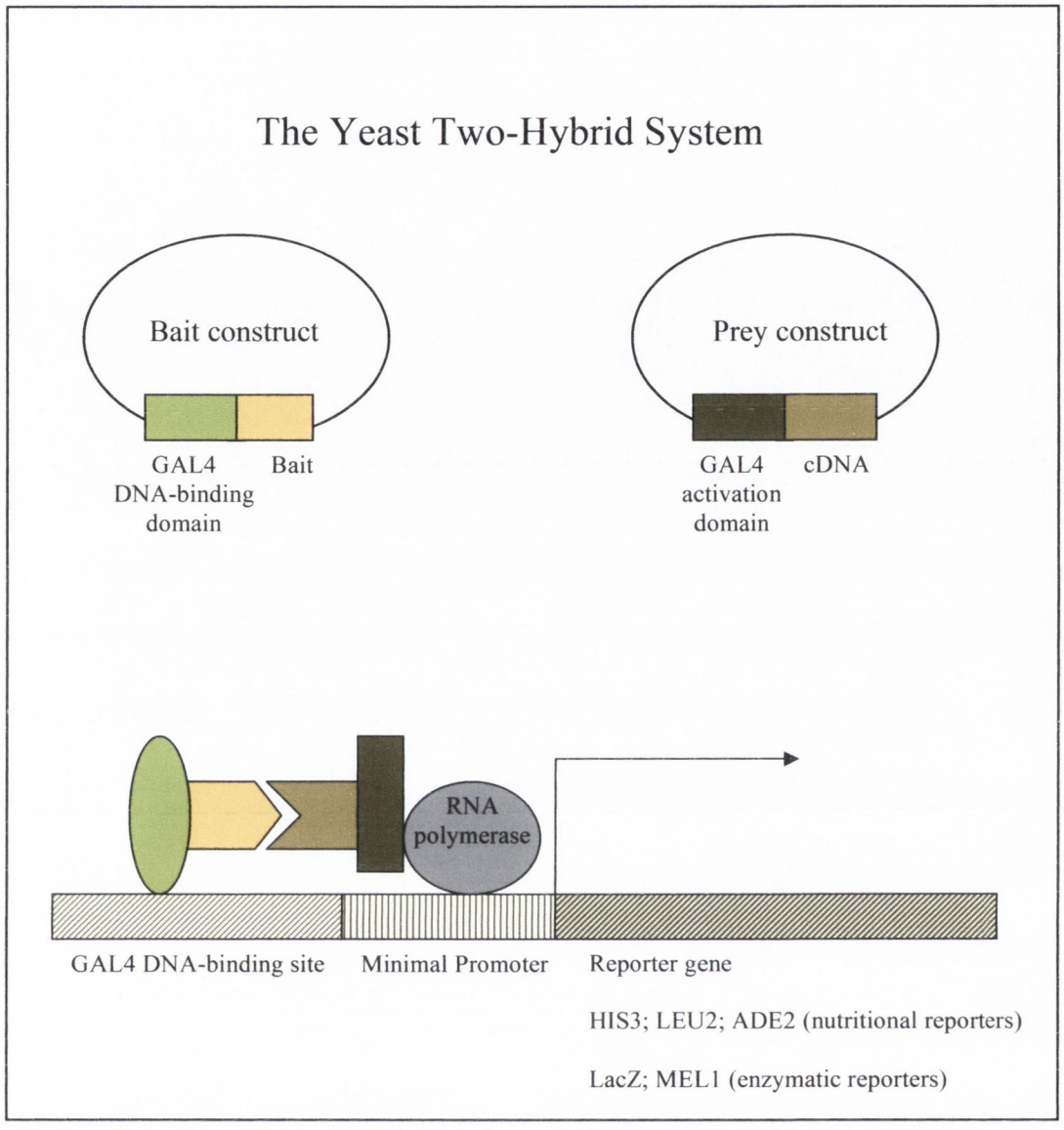


Figure 3.1 Principle of the yeast two-hybrid system. The protein of interest (bait) is expressed as a fusion to the GAL4 DNA-binding domain while inserts from a cDNA library are expressed as fusions with the GAL4 activation domain. The bait construct binds the GAL4 DNA binding site upstream of the reporter gene. The GAL4 activation domain fusion protein binds transcription factors and RNA polymerase in the nucleus but does not localize to the GAL4 DNA binding site. When a cDNA encoded protein interacts with the bait construct, the two transcription factor domains are brought into close contact and can act together to initiate transcription of reporter genes from the GAL4 DNA-binding site.

interactions are more readily detected in the yeast two-hybrid system since the genetic reporter gene strategy results in a significant amplification. Unfortunately the yeast two-hybrid system is also associated with several limitations and problems giving rise to false positives and furthermore making some real positives impossible to detect. False positives may occur due to a number of reasons. For instance, some proteins can activate transcription if they bind directly to the promoter sequence of the reporter genes. However, using a system with various reporter genes driven by different promoters can eliminate many of these false positives. Some proteins may also bind directly to the DNA-binding domain of the bait fusion construct thereby activating transcription of reporter genes. In addition, some proteins seem to be particularly "sticky" and interact not only with the bait but also with a number of unrelated proteins. The yeast two-hybrid system may also reveal interactions between proteins that display affinity for each other but never associate unless artificially co-expressed if they *in vivo* localize to different compartments or are expressed in different cell types. Thus, all positive candidates should be tested against several controls and it is imperative to confirm interactions that have been detected using the yeast two-hybrid approach by alternative non-yeast based assays and eventually demonstrate a functional significance of the interaction.

3.1.2 Aim of study

Regulated trafficking, specific localization and activity of neurotransmitter transporters are thought to be maintained by protein-protein interactions although little is known about the components involved. The intracellular N- and C-termini of neurotransmitter transporters are likely to be targets for interacting proteins and these domains have previously been used as baits in a number of yeast two-hybrid screens in attempts to identify novel interacting partners.

The aim of this study was to use the yeast two-hybrid system to identify novel SERT interacting proteins. The yeast two-hybrid screens were performed by using a special mating protocol which exploits that yeast can exist as haploids of either mating type a (MATa) or mating type α (MATα). Haploid cells of different mating types will mate

with one another and form diploids if they are physically juxtaposed. Thus, by expressing the bait and prey constructs (cDNA library) in haploid yeast strains of opposite mating type, a diploid yeast strain containing both the bait and the prey construct is easily obtained. An interaction between the bait and in this case a library encoded protein is determined by detecting activation of reporter genes in the diploid strain. The primary advantage of this technique is that it reduces the number of yeast transformations needed to test individual interactions. It also provides the possibility of screening commercial pre-transformed libraries thereby avoiding a commonly encountered problem of achieving optimal transformation efficiency of the cDNA library. The system is based on the GAL4 DNA-binding domain and the GAL4 activation domain with *TRP1* and *LEU2* as selective markers for the bait and prey constructs respectively. The nutritional markers *ADE2* and *HIS3* are used as reporter genes in combination with the enzymatic reporter gene *LacZ*.

This study includes results obtained from five individual yeast two-hybrid screens. Four screens were performed as part of the project leading to my MSc, although only to the point where DNA from positive clones obtained in the primary screens had been isolated and sequenced. The last screen was carried out as part of this study. As mentioned earlier, the intracellular N- and C-termini of neurotransmitter transporters are normally chosen as baits in yeast two-hybrid screens. However, in addition to the conventional intracellular N- and C-termini, longer N- and C-terminal domains containing the first and twelfth predicted transmembrane domain, respectively, were also used as baits.

3.2 RESULTS

3.2.1 Analysis of clones identified using the yeast two-hybrid system

3.2.1.1 Yeast two-hybrid screening

By using PCR, pcDNA3-hSERT was used as a template to amplify the following four SERT domains.

SERT domain	Base pairs	Amino acid residues	Selection
A: Short N-terminal domain	1-261	1-87	Low stringency
B: Long N-terminal domain	1-324	1-108	Low stringency
C: Short C-terminal domain	1786-1890	596-630	Low stringency
D: Long C-terminal domain	1729-1890	577-630	Low stringency
E: Long C-terminal domain	1729-1890	577-630	High stringency

To generate the bait plasmids the four cDNA fragments were cloned into the multiple cloning site of pGBKT7 (Figure 3.2) to generate an in-frame fusion to the GAL4 DNA-binding domain. Bait constructs were tested for protein expression and auto-activation prior to library screening. Five independent two-hybrid screens were performed; one with each of the four bait-constructs described above (referred to as screen A, B, C, and D) and a fifth screen also using the long C-terminal domain as bait (screen E). The screens were performed according to the manufacturer's instructions as described in section 2.2.19. In short, using the screen performed as part of this study as an example; the AH109 yeast strain was transformed with the bait construct encoding the GAL4 DNA-binding domain in fusion with the long C-terminal domain of SERT (residues 577-630). The AH109 bait construct was mated with the Y187 yeast strain

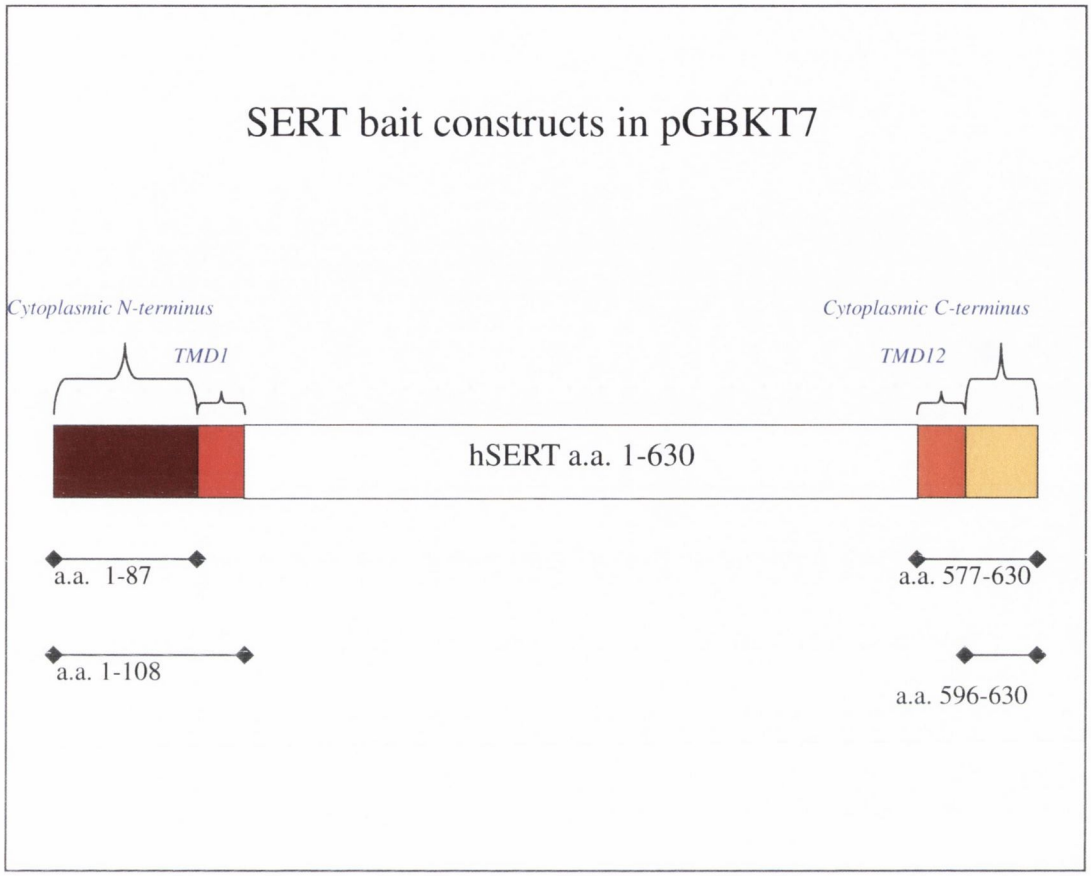


Figure 3.2 SERT bait constructs generated in pGBKT7. Schematic representation of the human serotonin transporter protein illustrating the four SERT domains used as baits in the yeast two-hybrid screens. The four domains were amplified by PCR using specific primers and inserted into the pGBKT7 vector to generate fusion proteins of the GAL4 DNA-binding domain and the four SERT domains respectively.

pretransformed with the human brain cDNA library. The mating mixture was plated onto high stringency selection plates and incubated for 7-10 days. Colonies isolated from the primary screen were re-streaked onto high stringency selection plates (secondary screen) and finally screened for β-galactosidase activity as described in section 2.2.21.

The original human brain cDNA library (in *E.coli*) used in the present study is guaranteed to have at least 1 x 10^6 independent clones before amplification (Clontech). To ensure a representative yeast library, the titre should be at least 10-fold higher than the number of independent clones in the original library. Prior to yeast mating an aliquot of the cDNA library was taken out and used for titering. Using dilutions of the cDNA library, the titre was determined to approximately 5.9 x 10^7 colony-forming units (cfu) per ml, indicating that the library was of acceptable quality.

Dilutions of the mating mixture were plated onto control plates for calculating mating efficiency as well as the number of clones screened. Colonies were counted on plates with preferably 30-300 cfu (Table 3.1) and the viabilities of the haploid and diploid yeast strains were calculated as follows:

$$\frac{\text{cfu x 1000 µl/ml x dilution factor}}{\text{volume plated (µl)}} = \text{number of viable cfu/ml}$$

$$\text{Viability of Y187 library strain = cfu/ml on SD/-Leu} = \frac{91 \text{ cfu x } 1000 \text{ µl/ml x } 10000}{100 \text{ µl}} = 9.1 \text{ x } 10^6 \text{ cfu/ml}$$

$$\text{Viability of AH109 bait strain = cfu/ml on SD/-Trp} = \frac{2500 \text{ cfu x } 1000 \text{ µl/ml x } 10000}{100 \text{ µl}} = 2.5 \text{ x } 10^8 \text{ cfu/ml}$$

$$\text{Viabiliy of diploids = cfu/ml on SD/-Trp/-Leu} = \frac{107 \text{ cfu x } 1000 \text{ µl/ml x } 1000}{100 \text{ µl}} = 1.1 \text{ x } 10^6 \text{ cfu/ml}$$

$$\textbf{Mating efficiency} \text{ (\% diploids)} = \frac{\text{viability of diploids}}{\text{viability of limiting factor}} = \frac{1.1 \text{ x } 10^6 \text{cfu/ml}}{9.1 \text{ x } 10^6 \text{cfu/ml}} = 12\%$$

Number of clones screened = cfu/ml of diploids x total volume of mating mixture (ml)

$$= 1.1 \text{ x } 10^6 \text{cfu/ml x } 12 \text{ ml} = 1.32 \text{ x } 10^7$$

Table 3.1 Calculation of mating efficiency and the number of clones screened[1]

Selective Plates	Number of colonies		
	Dilutions		
	1:100	1:1000	1:10000
SD/-Leu	> 5000	650	91
SD/-Trp	Confluent	Almost confluent	~ 2500
SD/-Trp/-Leu (diploids)	920	107	11

[1]Numbers are from screen E using the long C-terminal domain of SERT as bait.

Similar mating efficiencies and number of diploids were obtained for all five screens. According to Clontech, a library mating efficiency above 5% is acceptable. Also, if the number of diploids obtained is more than 5 x 10^6, at least 3 x 10^6 clones of the original yeast library have been screened, which in most cases is greater than or approximately equal to the number of independent clones in the original cDNA library prepared in *E.coli*. Thus, the yeast two-hybrid mating approach applied in this study can be considered successful, at least in terms of library quality and the number of clones tested for interaction with SERT.

3.2.1.2 Sequence analysis of selected clones isolated in the yeast two-hybrid screens

A total of 5464 clones were picked up from the five primary screens. After a secondary screen on high stringency selection plates and testing for β-galactosidase activity, 597 clones were selected for sequence analysis. Thus, only about 10% of the clones originally appearing as positive colonies in the primary screens survived the second and third round (β-galactosidase activity) of selection. A great number of clones failed the second screening process indicating the importance of this step in the analysis of yeast two-hybrid clones. The identities of the 597 inserts were determined by automated DNA sequencing and compared against the National Center for Biotechnology Information (NCBI) database using the BLAST search programme. The number of clones from the individual libraries that were selected for sequence analysis and the distribution of cDNAs encoding parts of known proteins *versus* cDNAs that do not correspond to any known protein sequence is summarised in Table 3.2.

Table 3.2 also illustrates the consequence of using either low or high stringency selection plates in a yeast two-hybrid screen. The first four screens, A to D, were performed on low stringency selection plates, only selective for activation of the HIS3 reporter gene. The large number of positive colonies observed in each of the four screens suggested the use of high stringency selections plates when performing screen E. As expected, fewer colonies appeared in the primary screen when selecting for both the HIS3 and the ADE2 reporter genes.

Table 3.2 Number of clones isolated in the yeast two-hybrid screens

Screen (bait)	Number of clones in primary screen	Number of clones selected for analysis	cDNA for known proteins[1]	cDNA for unknown proteins[2]	Not determined[3]
1-87	945	87	67	21	-
1-108	1023	127	99	28	-
596-630	2398	181	111	70	-
577-630 (I)	867	132	71	12	49
577-630 (II)	231	70	52	11	7

[1] Including clones encoding fragments corresponding to the 3'-UTR

[2] Clones that could only be assigned to a chromosome region

[3] Clones that failed DNA sequencing or remain to be sequenced

Based on the assigned identity of each insert, the 597 clones were classified into two main groups: one group containing clones of potential interest and a second group comprising clones unlikely to represent interaction partners of SERT. The first group consists of clones encoding proteins of known function that are likely to participate in a complex with SERT but also clones encoding uncharacterised proteins or hypothetical proteins provided that several clones encoding the particular protein were isolated from independent cDNAs. The second group includes proteins known to reside extracellular or within the mitochondrion as well as clones encoding fragments corresponding to 3'-untranslated regions (3'-UTR). Also, clones that encode proteins that are frequently found in yeast two-hybrid screens, independently of the bait construct, were included in the second group. A list of frequently occurring false positives is available from the website (http://www.fccc.edu/research/labs/golemis/InteractionTrapInWork.html). Clones that could only be assigned to a chromosome region and only appeared once were also included in this group. Yeast allows translational frameshifting and thus even in cases where stop codons or frameshifts are present within a cDNA sequence, significant expression of the correct reading frame may still occur. For this reason, stop codons and incorrect reading frames were not used as criteria to eliminate clones from further analysis.

Some proteins were detected in several of the yeast two-hybrid screens, and thus appeared to interact with both the N- and the C-terminal domain of SERT. For example, COPS5 (COP9 constitutive photomorphogenic homolog subunit 5) was detected in all five screens. COPS5 has been reported to interact directly with the DNA-binding domain of GAL4 (Nordgard et al., 2001) and is therefore likely to give rise to false positive interactions. Clones encoding part of the Na^+/K^+-ATPase β-subunit also appeared in all five screens. However, these clones only comprised the extracellular C-terminal half of the β-subunit, indicating that the isolation of Na^+/K^+-ATPase represent a false positive result. In general, clones that appeared to interact with both the N- and the C-terminal domain of SERT were treated with suspicion and initially categorized as false positives or clones of secondary interest.

Based on these criteria, 116 clones were assigned to group number one. The 116 clones were subjected to further analysis in order to confirm the yeast two-hybrid results and to test the specificity of the individual interactions.

3.2.1.3 Verification of protein interactions by yeast mating

The 116 selected clones were all transformed into the Y187 yeast strain and re-tested for specific interaction with the original bait by using the yeast-mating assay described in section 2.2.20 and illustrated in Figure 3.3.

In order to test the specificity of the interactions all clones were tested against the empty pGBKT7 vector, the unrelated bait vector pGBKT7-53 and all of the four SERT bait constructs. The pACT2 vector and the pTD1-1 vector were included as negative and positive controls, respectively. The pTD1-1 vector encodes a fusion of the GAL4 activation domain and SV40 large T antigen that specifically interacts with p53 encoded by pGBKT7-53.

For every four clones to be tested one prey plate and one bait plate were generated; each plate also containing the two corresponding controls. Thus, in order to test all 116 clones, a total of 29 prey plates and 29 bait plates were generated. By using pieces of sterile velvet and a replicating block the two haploid yeast strains were mated and the resulting diploid strains were selected on SD plates lacking tryptophan and leucine. The diploid yeast was replica-plated onto plates selective for activation of the nutritional reporter genes HIS3 and ADE2 and onto plates sensitive to activation of the enzymatic reporter gene LacZ. Activation of reporter genes was scored visually and based on the degree of growth and β-galactosidase activity (blue colour development).

The results of the mating experiments are listed in Appendix G. 91 of the 116 clones were successfully tested using the yeast mating approach. Clones that failed the validation procedure either did not form diploids, appeared to be contaminated or were eliminated due to experimental reasons such as different yeast strains growing too close to each other resulting in uncertainties in assigning positive interactions to specific clones.

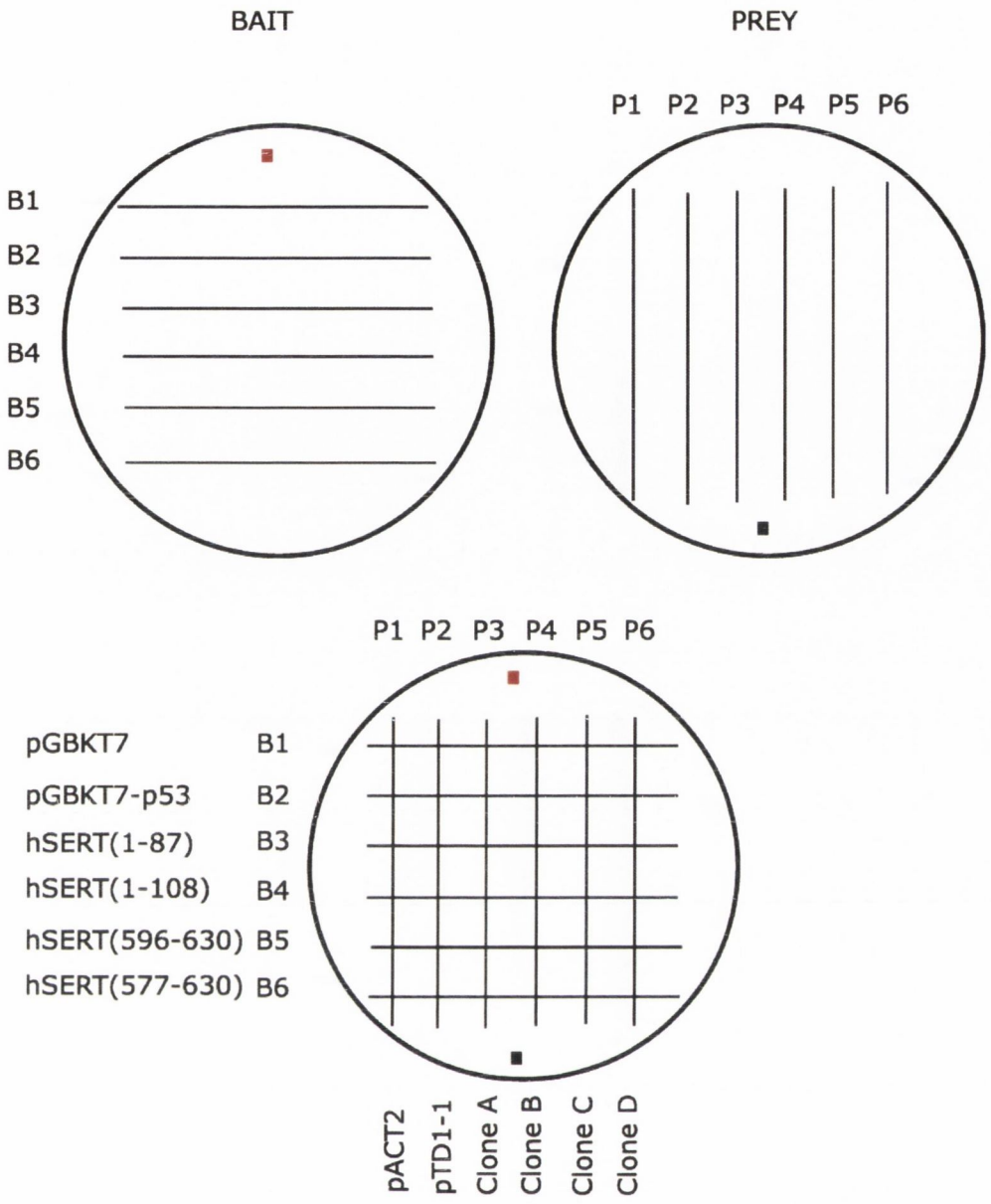


Figure 3.3 Illustration of yeast mating by replica plating. Bait and prey constructs are expressed in yeast strains of opposite mating type. The bait constructs (B1-B6) are streaked horizontally on SD/-Trp plates while the prey constructs (T1-T6) are streaked vertically on SD/-Leu plates. The individual plates are incubated for 2 days at 30°C and the two haploid yeast strains are brought into contact by placing the bait plate orthogonally to the prey plate on the same replica velvet. Diploids form in the patches and are selected on SD/-Trp/-Leu plates.

The most common clone isolated in the yeast two-hybrid screens was the Ran binding protein M (RanBPM), also known as Ran binding protein 9. A total of 26 clones were isolated; 13 in screen A using hSERT(1-87) as bait and 13 in screen B using hSERT(1-108) as bait. Although RanBPM did not appear in any of the screens using the C-terminal domain of SERT as bait, the re-testing analysis revealed that clones encoding RanBPM were able to activate all reporter genes regardless of the nature of the bait construct, including the two controls (Appendix G; A:854, B:15, and B:1013). RanBPM is a multi-adaptor scaffolding protein originally characterized as a binding protein for the small GTPase Ran and reported to localize both in the nucleus and in the cytoplasm (Nishitani et al., 2001). RanBPM has been reported to interact with a broad spectrum of functionally unrelated transmembrane and intracellular molecules. In particular, RanBPM has been suggested to interact with steroid hormone and tyrosine kinase receptors and to affect their signalling properties and transcriptional activities (Rao et al., 2002; Wang et al., 2002). It is interesting to note that most of the interactions reported for RanBPM have been detected in GAL4 based yeast two-hybrid systems similar to the one used in this study. Considering that RanBPM interacts non-specifically with all bait constructs used in this study, including the GAL4 DNA-binding domain alone, it seems reasonable to suggest that RanBPM may represent a common false positive in GAL4 based yeast two-hybrid studies.

The second most abundant clone appearing in the yeast two-hybrid screens was the high molecular mass microtubule-associated protein 1A (MAP1A). MAP1A is expressed predominantly in cells of the nervous system and is thought to play a role in regulating the cytoskeleton in mature neurons (Schoenfeld et al., 1989; Wiche et al., 1991). A total of 19 clones encoding part of the MAP1A light chain, LC2, were isolated. 11 clones were isolated using the N-terminal domain (residues 1-108) of SERT while four clones encoding MAP1A were isolated in each of the two screens with the C-terminal domain of SERT (residues 577-630). Despite the fact that MAP1A appeared to bind both to the N- and the C-terminal domain of SERT, MAP1A was still included in the re-testing analysis. When independent clones encoding MAP1A were tested in the mating assay, they nearly all exhibited specific interaction with the

C-terminal domain of SERT (Appendix G; B:120, D:295, D:399, D:458, E:49H, E:50H, and E:84K). Only two of the seven MAP1A clones that were examined in the mating assay, showed activation of reporter genes in combination with the N-terminal domain of SERT (E:49H and E:50H). This however, was only scored as weak activation compared to the strong activation of reporter genes observed when the two clones were combined with the C-terminal domains of SERT. These results seem confusing considering the large number of clones isolated in the screen using the N-terminal domain of SERT. MAP1A was only isolated in screens using constructs containing either TMD1 or TMD12. Using these constructs as bait involves the possibility of identifying proteins that bind non-specifically to SERT through interactions between hydrophobic residues. However, although MAP1A did not appear in the screen using the short C-terminal domain of SERT as bait, the mating assay revealed activation of reporter genes when MAP1A was expressed together with the short C-terminal domain. Thus, in the case of MAP1A, the yeast two-hybrid screens and the mating assays seemed to yield conflicting results.

MAP1A LC2 has been reported to interact with the C-terminal domain of stargazin, a protein involved in regulation of cell surface trafficking and synaptic targeting of AMPA receptors (Ives et al., 2004). In the same study MAP1A LC2 was also shown to interact directly with the AMPA receptor. Interestingly, the interaction between stargazin and the MAP1A light chain was identified in a GAL4 based yeast two-hybrid system similar to the one used in the present study. Also, the MAP1A clones isolated in the stargazin yeast two-hybrid screen were almost identical in length to some of the clones isolated in this study. Thus, MAP1A may very well represent a true interacting partner of SERT and could possibly be involved in linking the transporter to the cytoskeleton. In relation to this, it is interesting to note that the cytoskeleton has been suggested to play a role in the regulation of SERT (Sakai et al., 2000). However, a potential functional interaction between MAP1A and SERT was not examined in greater detail during the course of this study but considering the growing body of evidence that MAP1A plays a role in membrane trafficking it would be interesting to include this protein in future studies.

3.2.1.4 Selection of clones for further analysis

Based on their identity and the results obtained in the yeast mating experiments 15 of the 91 clones were selected for a third round of examination. The identities of the 15 clones are listed in Table 3.3. To add more credibility to individual proteins several clones encoding parts of the same protein were included.
The mating assay was repeated with the 15 selected clones and positive interactions were detected on plates selective for activation of the nutritional reporter genes HIS3 and ADE2. The 15 clones were also subjected to β-galactosidase colony-lift filter assay as described in section 2.2.21. Finally the 15 clones were co-transformed into the AH109 yeast strain in combination with each of the four bait vectors and the two controls. Positive interactions in co-transformants were scored on plates selective for activation of the nutritional reporter genes HIS3 and ADE2 and also on plates sensitive to activation of the enzymatic reporter gene LacZ. The results of the three assays are listed in Table 3.4.

A final evaluation of the results obtained throughout all the yeast experiments combined with the identity and integrity of the clones suggested the following proteins as candidates for further analysis: *Mint3* (D:258), a PDZ (postsynaptic density protein-95, postsynaptic discs large, and zona occludens-1) containing protein that function in membrane transport and organisation (Tanahashi and Tabira, 1999); *ESO3* (B:20, B:283 and B:790), an ubiquitous expressed protein belonging to the NY-ESO-1 gene family (Alpen et al., 2002); *Lipocalin-type prostaglandin D2 synthase* (L-PGDS) (B:489), a brain enzyme involved in sleep that acts both as a PGD2-synthesizing enzyme and as an extracellular transporter of various lipophilic small molecules (Urade and Hayaishi, 2000); *MAP1S* (E:7B, E:47E and E:129F), a member of the microtubule-associated protein 1 family, which for example has been reported to interact with ubiquitin-protein ligase E3A (Wong et al., 2002; Orban-Nemeth et al., 2005); *C-terminal binding protein 2* (CTBP2) (E:58H), a dually functioning protein, acting both as a major component of synaptic ribbons and as a transcriptional repressor (Schmitz et al., 2000; Piatigorsky, 2001).

Table 3.3 Identity of 15 selected clones

Clone No.[1]	Accession No.	Name
B: 20	Q14657	ESO3
B: 283	Q14657	ESO3
B: 447	Q1LZN2	Nodal modulator previously known as pM5
B: 489	P41222	Prostaglandin D2 synthase 21kDa (brain)
B: 790	Q14657	ESO3
B: 891	(NM_006288)	Thy-1 cell surface antigen
D: 258	O96018	Amyloid beta A4 precursor protein-binding family A member 3 (Mint3)
D: 285	O75781	Paralemmin
D: 507	P51957	Homology to serine/threonine-protein kinase Nek4
D: 320	Q9UBK5	Transmembrane adapter protein KAP10
E: 7A	P62745	Ras-related small GTPase
E: 7B	Q66K74	MAP1S (BPY2 interacting protein 1) (VCY2 interacting protein-1)
E: 47E	Q66K74	MAP1S (BPY2 interacting protein 1) (VCY2 interacting protein-1)
E: 58H	P56545	C-terminal binding protein 2
E: 129F	Q66K74	MAP1S (BPY2 interacting protein 1) (VCY2 interacting protein-1)

[1] Screens; B: hSERT(1-108), D: hSERT(577-630), E: hSERT(577-630)

Table 3.4 Re-testing of selected clones

Clone No.[1]	Mating Assay SD/-Trp/-Leu/His/-Ade						Colony lift-filter assay						Co-transformations in AH109 SD/-Trp/-Leu/His/-Ade						Co-transformations in AH109 SD/-Trp/-Leu + X-β-gal					
	pGBKT7	pGBKT7-p53	N-SERT 1-87	N-SERT 1-108	C-SERT 596-630	C-SERT 577-630	pGBKT7	pGBKT7-p53	N-SERT 1-87	N-SERT 1-108	C-SERT 596-630	C-SERT 577-630	pGBKT7	pGBKT7-p53	N-SERT 1-87	N-SERT 1-108	C-SERT 596-630	C-SERT 577-630	pGBKT7	pGBKT7-p53	N-SERT 1-87	N-SERT 1-108	C-SERT 596-630	C-SERT 577-630
B: 20				+++						+++						+++						+++		
B: 283				+++						+++						+++						+++		
B: 447				+++						++			+			+++		++				++		++
B: 489				+++						+++						+++								
B: 790				+++						+++						+++						+++		
B: 891				++		++				++			+			++	+	++	+			++		++
D: 258						++						++						++						+
D: 285				++		++				++		++	+			++	++	++				++	++	+
D: 507						++						++						++						+
D: 320				++		++				++		++				++		++				+		+
E: 7A						++						++						++						++
E: 7B						+++						+						++						++
E: 47E						++						++						++						++
E: 58H						++						++						++						+
E: 129F						+++						++						++						++

[1] Screens; B: hSERT(1-108), D: hSERT(577-630), E: hSERT(577-630)

[2] +++/+++, major growth/intense dark blue; ++/++, moderate growth/aquamarine blue; +/+ little growth/faint blue

When the BLAST search was repeated for clone D:507 it revealed high similarity to Alu repeats and the library insert did not appear to represent a real protein. Clone E:7A was found only to encode a few residues of the C-terminal end of the Ras-related GTPase and thus, also does not seem to represent a genuine interacting partner.

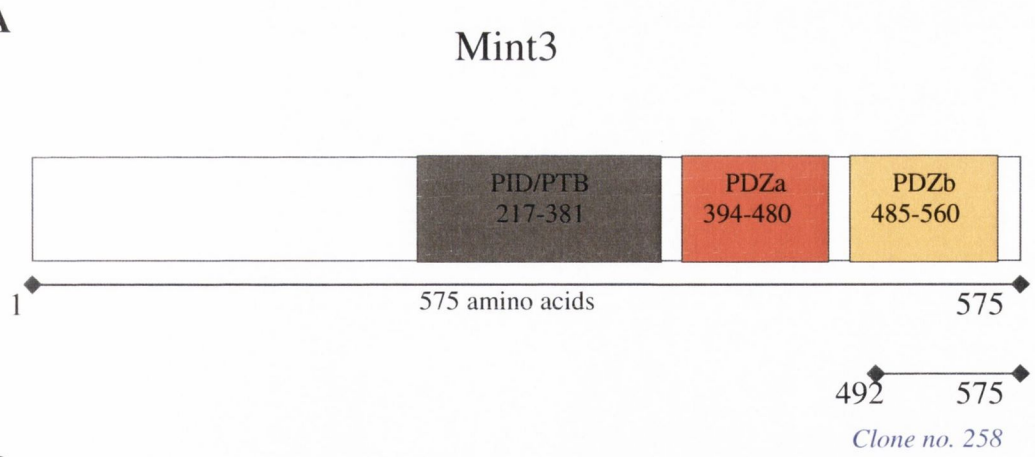
While, PGDS, CTBP2, and MAP1S are being investigated by other members of the group, Mint3 and ESO3 were chosen as first priorities for a detailed analysis in this study. Although interesting results have emerged from studies on PGDS (Anja Fjorback, personal communication), neither PGDS nor CTBP2 or MAP1S have been included in any of the experiments carried out in this study and thus, the three proteins are not discussed any further.

The secretory carrier membrane protein 2 (SCAMP2) was also identified as a positive candidate in the yeast two-hybrid system. However, the SCAMP2 clones failed the re-testing analysis in yeast and the interaction between SERT and SCAMP2 was only verified later in the project. The binding of SCAMP2 to SERT and the functional consequences of this interaction is described in chapter 5.

Mint3 was isolated with the long C-terminal domain of SERT. Only one clone encoding part of the second PDZ domain present within the Mint3 protein was isolated in the yeast two-hybrid screen (Figure 3.4). Three independent clones encoding various lengths of ESO3 were isolated using the long N-terminal domain of SERT as bait (Figure 3.5). In yeast, both Mint3 and ESO3 appeared to bind specifically to the long C-terminal and long N-terminal domain of SERT, respectively. When combined with the long C-terminal domain bait construct, the Mint3 clone displayed medium growth on plates selective for activation of the nutritional reporter genes HIS3 and ADE2 and weak to medium activation of the LacZ gene. All three ESO3 clones revealed strong activation of the three reporter genes when combined with the long N-terminal domain (Table 3.4).

Evaluation of proper expression levels of bait constructs in yeast had previously been carried out. In order to test whether the ESO3 and Mint3 clones encode proteins of the expected size, protein extracts from yeast transfected individually with the ESO3 and

A



B

```
        10          20          30          40          50          60
MDFPTISRSP SGPPAMDLEG PRDILVPSED LTPDSQWDPM PGGPGSLSRM ELDESSLQEL

        70          80          90         100         110         120
VQQFEALPGD LVGPSPGGAP CPLHIATGHG LASQEIADAH GLLSAEAGRD DLLGLLHCEE

       130         140         150         160         170         180
CPPSQTGPEE PLEPAPRLLQ PPEDPDEDSD SPEWVEGASA EQEGSRSSSS SPEPWLETVP

       190         200         210         220         230         240
LVTPEEPPAG AQSPETLASY PAPQEVPGPC DHEDLLDGVI FGARYLGSTQ LVSERNPPTS

       250         260         270         280         290         300
TRMAQAREAM DRVKAPDGET QPMTEVDLFV STKRIKVLTA DSQEAMMDHA LHTISYTADI

       310         320         330         340         350         360
GCVLVLMARR RLARRPAPQD HGRRLYKMLC HVFYAEDAQL IAQAIGQAFA AAYSQFLRES

       370         380         390         400         410         420
GIDPSQVGVH PSPGACHLHN GDLDHFSNSD NCREVHLEKR RGEGLGVALV ESGWGSLLPT

       430         440         450         460         470         480
AVIANLLHGG PAERSGALSI GDRLTAINGT SLVGLPLAAC QAAVRETKSQ TSVTLSIVHC

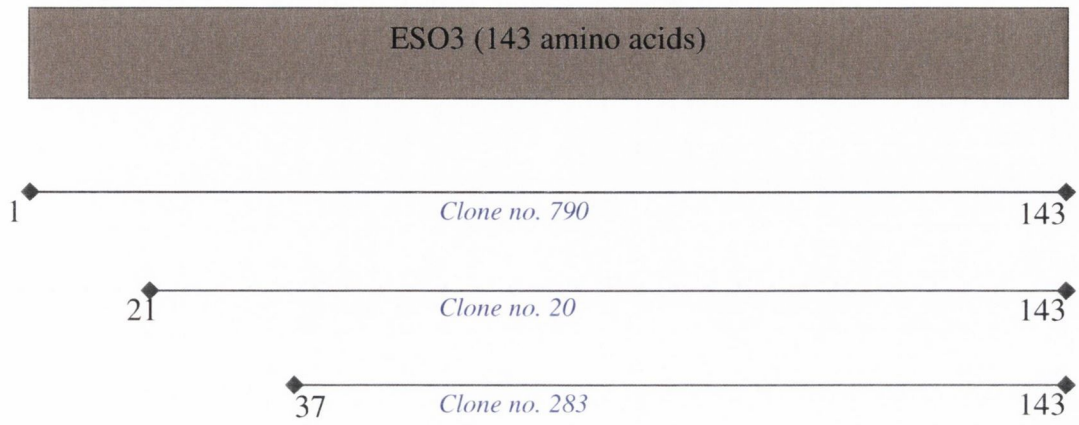
       490         500         510         520         530         540
PPVTTAIIHR PHAREQLGFC VEDGIICSLL RGGIAERGGI RVGHRIIEIN GQSVVATPHA

       550         560         570
RIIELLTEAY GEVHIKTMPA ATYRLLTGQE QPVYL
```

Figure 3.4 Illustration of Mint3. (A) Schematic representation of the human Mint3 protein illustrating the localization of the phosphotyrosine interaction domain (PID/PTB) and the two PDZ domains (Swiss-Prot entry 096018). The sequence encoded by clone no. 258 comprises the last 84 amino acids of the Mint3 protein. (B) Mint3 amino acid sequence. The sequence encoded by clone no. 258 is underlined and the carboxylate-binding motif of PDZb is shown in bold.

ESO3

A



B

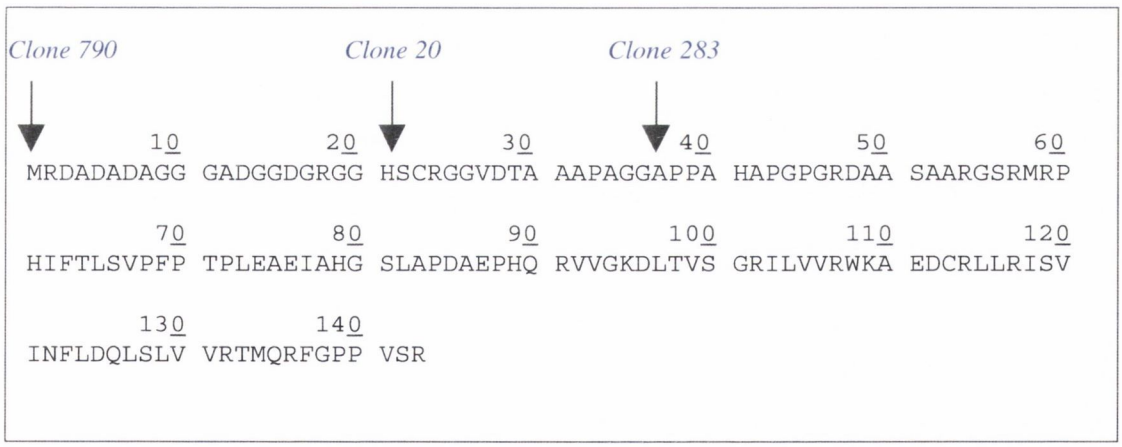


Figure 3.5 Illustration of ESO3. (A) Schematic representation of the ESO3 protein illustrating the regions encoded by the three clones. (B) ESO3 amino acid sequence (Swiss-Prot entry Q14657). Arrows indicate the position of the first amino acid encoded by each of the three clones identified in the yeast two-hybrid screen.

Mint3 clones, were prepared and analysed by Western blotting. The fusion proteins were detected with an antibody recognizing the HA-epitope positioned C-terminal to the GAL4 activation domain (Appendix B). As shown in Figure 3.6, both ESO3 and Mint3 fusion proteins were properly expressed in yeast at the expected size.

3.2.2 Further evaluation of Mint3 and ESO3 in yeast

3.2.2.1 Liquid β-galactosidase assays on Mint3 and ESO3

A simple method to assess the strength of protein-protein interactions is by quantifying the activity of the LacZ reporter gene using the liquid β-galactosidase assay. Using the Mint3 and ESO3 co-transformants generated in the AH109 yeast strain, β-galactosidase activity was measured and compared against the positive control as described in section 2.2.22. These experiments confirmed the original observation of a specific interaction between Mint3 and the long C-terminal domain (Figure 3.7) and between ESO3 and the long N-terminal domain of SERT (Figure 3.8). The level β-galactosidase activity detected in cells expressing ESO3 in combination with the long N-terminal domain of SERT was almost 2 fold greater than the positive control suggesting a strong interaction between ESO3 and SERT. In contrast, the Mint3 clone displayed only moderate β-galactosidase activity when compared to the positive control, which corresponds well with the results obtained in the previous β-galactosidase assays on plates and filters (Table 3.4).

3.2.2.2 Liquid growth assays on Mint3 and ESO3

A liquid growth assay was performed on the Mint3 and ESO3 AH109 co-transformants by inoculating three colonies of each strain into liquid SD/-Leu/-Trp medium. The cultures were grown for 1 day and diluted into selective SD/-Leu/-Trp/-Ade/-His medium and incubated for a further 2 days before cell density was measured. Activation of reporter genes facilitate growth in the selective medium, and thus, the cell density reflects the ability of the bait and prey proteins to interact.

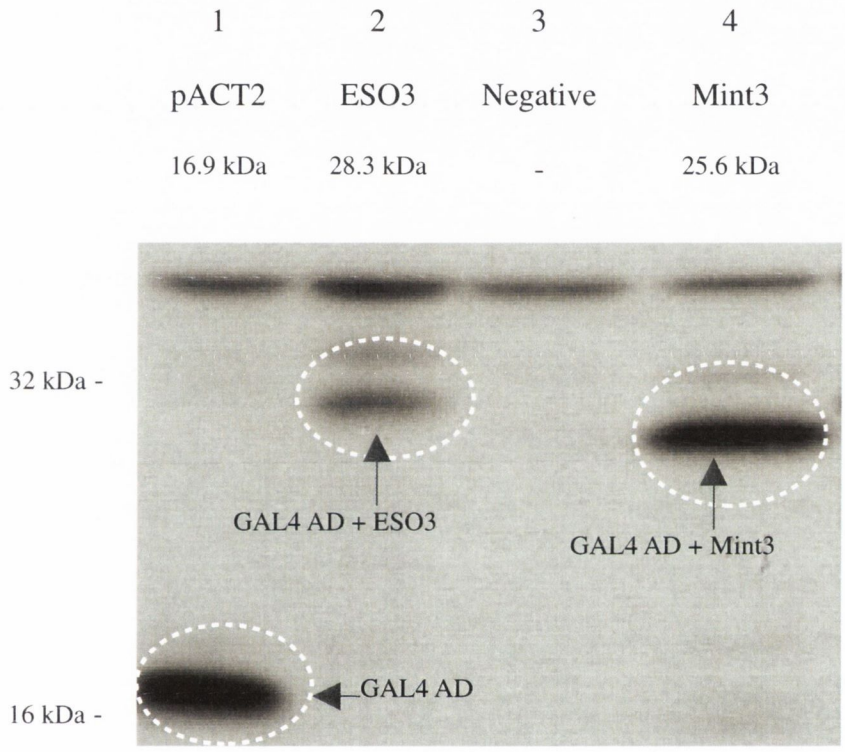


Figure 3.6 Verification of ESO3 and Mint3 protein expression. Y187 yeast strains containing the ESO3 clone 283 and the Mint3 clone 258 were grown in selective medium (SD/-Leu). Crude yeast extract was prepared and analysed by Western blotting using an anti-HA antibody recognizing the HA-epitope positioned C-terminal to the GAL4 activation domain (GAL4 AD). The Y187 yeast strain containing the empty pACT2 vector was used as a positive control (lane 1) and Y187 alone (lane 3) was used as a negative control. The constructs and the expected size of the GAL AD fusion proteins are indicated above each lane.

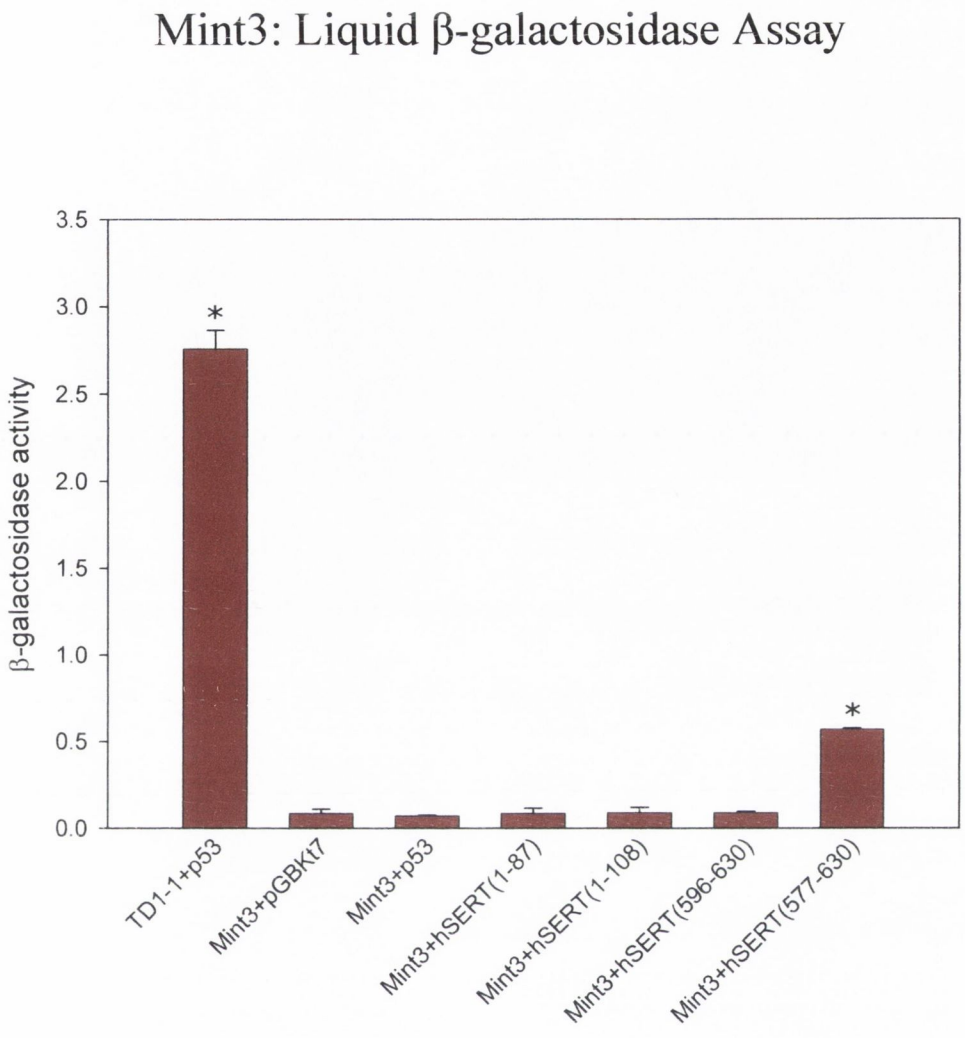


Figure 3.7 Liquid β-galactosidase assay on Mint3. The quantitative liquid β-galactosidase assay verifies specific interaction between the long C-terminal domain of SERT and Mint3. AH109 yeast co-transformants were grown in SD/-Trp/-Leu medium and prepared for liquid β-galactosidase assay. The β-galactosidase activity is expressed in standard units given by the equation: β-galactosidase activity = $1000 \times [(OD_{420} - 1.75 \times OD_{550})] / (t \times v \times OD_{600})$, where OD_{420} and OD_{550} is the absorbance of the reaction mixture; OD_{600} reflects cell density in the re-suspended cell suspension; t is the time of the reaction in minutes; and v is the volume of the culture in millilitre used in the assay. Values are expressed as the mean ± S.E. of triplicate samples from a single experiment and are representative of three independent experiments. *Asterisk* indicates significant difference compared with the negative control (Mint3+pGBKT7) ($p < 0.01$, one-way ANOVA followed by Bonferroni post hoc analysis).

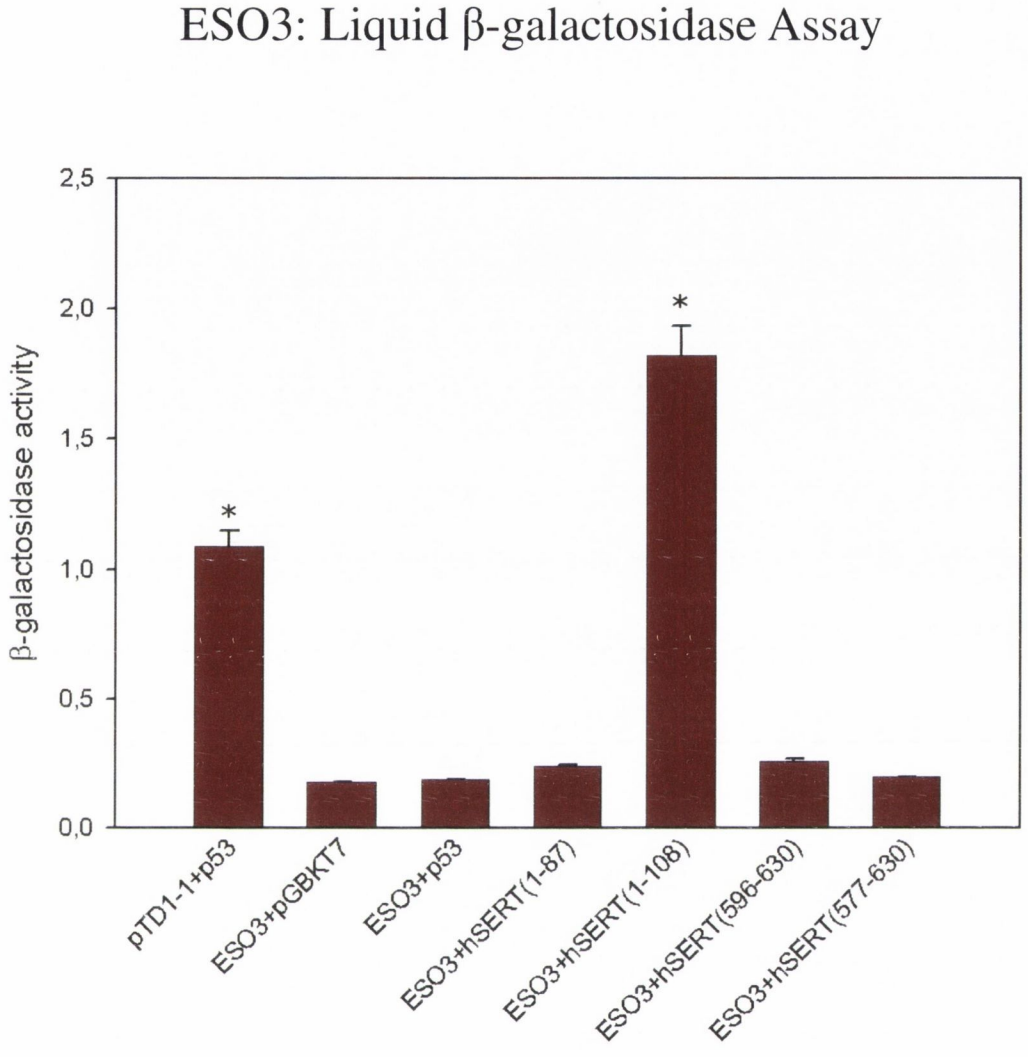


Figure 3.8 Liquid β-galactosidase assay on ESO3 (clone no. 790). The quantitative liquid β-galactosidase assay verifies specific interaction between the N-terminal domain of SERT and ESO3. AH109 yeast co-transformants were grown in SD/-Trp/-Leu medium and prepared for liquid βgalactosidase assay. The βgalactosidase activity is expressed in standard units given by the equation: β-galactosidase activity = $1000 \times [(OD_{420} - 1.75 \times OD_{550})] / (t \times v \times OD_{600})$, where OD_{420} and OD_{550} is the absorbance of the reaction mixture; OD_{600} reflects cell density in the re-suspended cell suspension; t is the time of the reaction in minutes; and v is the volume of the culture in millilitre used in the assay. Values are expressed as the mean ± S.E. of triplicate samples from a single experiment and are representative of three independent experiments. *Asterisk* indicates significant difference compared with the negative control (ESO3+pGBKT7) ($p < 0.01$, one-way ANOVA followed by Bonferroni post hoc analysis).

Again these experiments confirmed specific interaction between Mint3 (Figure 3.9) and the long C-terminal domain and between ESO3 and the long N-terminal domain of SERT (Figure 3.10). In the liquid growth assay the Mint3 interaction with the C-terminal domain of SERT appeared stronger than indicated by the results obtained in the liquid β-galactosidase assay. However, this observation corresponds well with the fact that the *ADE2* and *HIS3* reporter genes are under control of the GAL1 promoter, which is stronger than the MEL1 promoter that drives the expression of the *LacZ* reporter gene in the AH109 yeast strain in which the co-transformants are generated. There is no differentiation between levels of β-galactosidase activity detected in diploid *versus* haploid yeast cells containing ESO3 and the N-terminal domain of SERT. The degree of LacZ gene activation is most likely indistinguishable above a certain level and thus, if the interaction between ESO3 and the N-terminal domain of SERT is very robust, the strength of the promoters probably becomes irrelevant.

Since one of the ESO3 clones isolated in the yeast two-hybrid screen represented the entire coding sequence, ESO3 was easily subcloned into a mammalian expression vector. The immediate assess to a mammalian ESO3 construct resulted in more emphasis on this protein and a wide array of experiments were carried out in order to explore the functional effects of the interaction between ESO3 and SERT. The experiments on ESO3 are presented in chapter 4.

3.2.3 Analysis of known transporter interacting proteins for binding to SERT

3.2.3.1 PICK1 and Hic-5

The two proteins PICK1 and Hic-5 have previously been isolated in a yeast two-hybrid screen using the C-terminus of DAT as bait (Torres et al., 2001). Using the yeast two-hybrid approach, the authors showed that PICK1 also binds to the C-terminal domain of NET and SERT. PICK1 contains a single PDZ domain, is a substrate for PKC, and is known to interact with a broad range of proteins including receptors, ion channels and transporters. From the same yeast two-hybrid screen, the authors also reported the

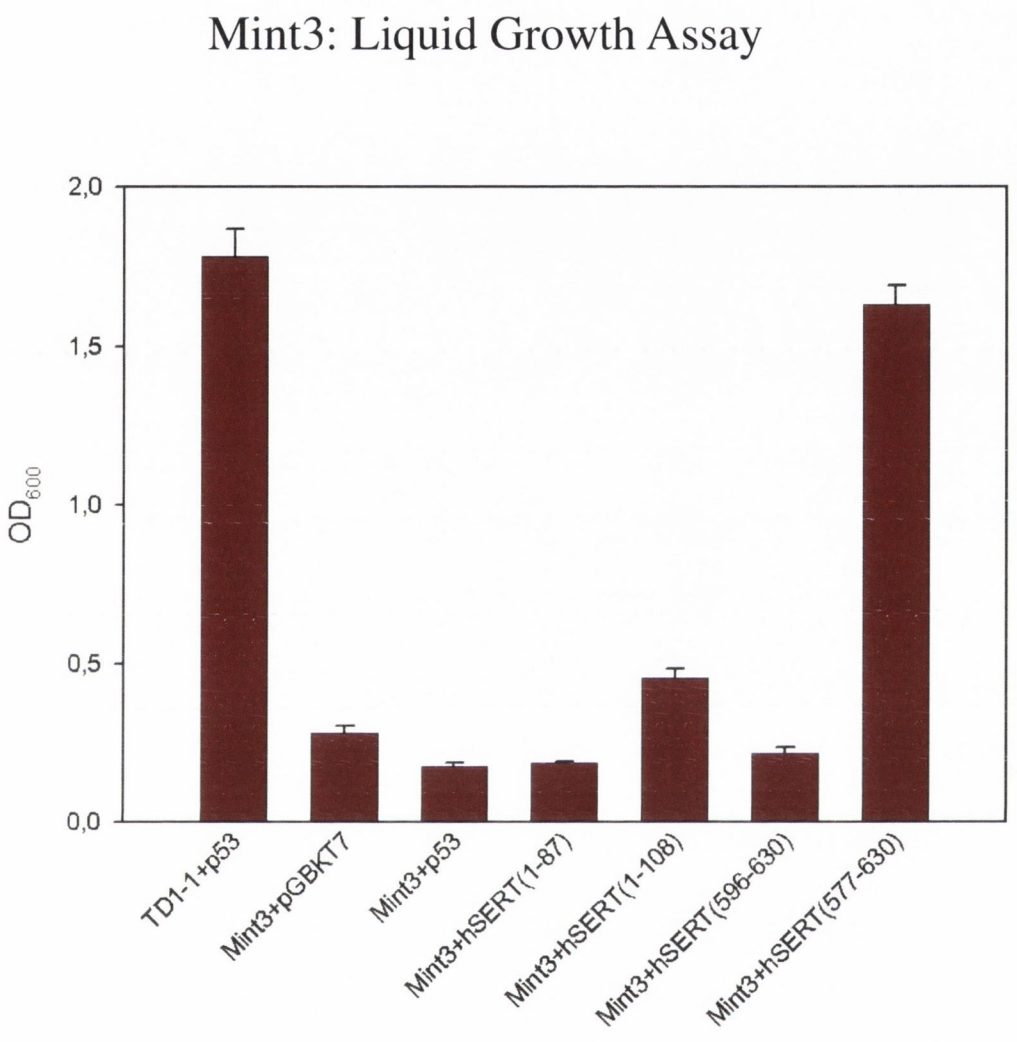


Figure 3.9 Liquid growth assay on Mint3. AH109 yeast co-transformants were grown in selective SD/-Trp/-Leu/-Ade/-His medium and the optical density was measured at 600nm (OD_{600}). Values are expressed as the mean ± S.E. of duplicate samples from a single experiment and are representative of two independent experiments. *Asterisk* indicates significant difference compared with the negative control (Mint3+pGBKT7) ($p < 0.01$, one-way ANOVA followed by Bonferroni post hoc analysis).

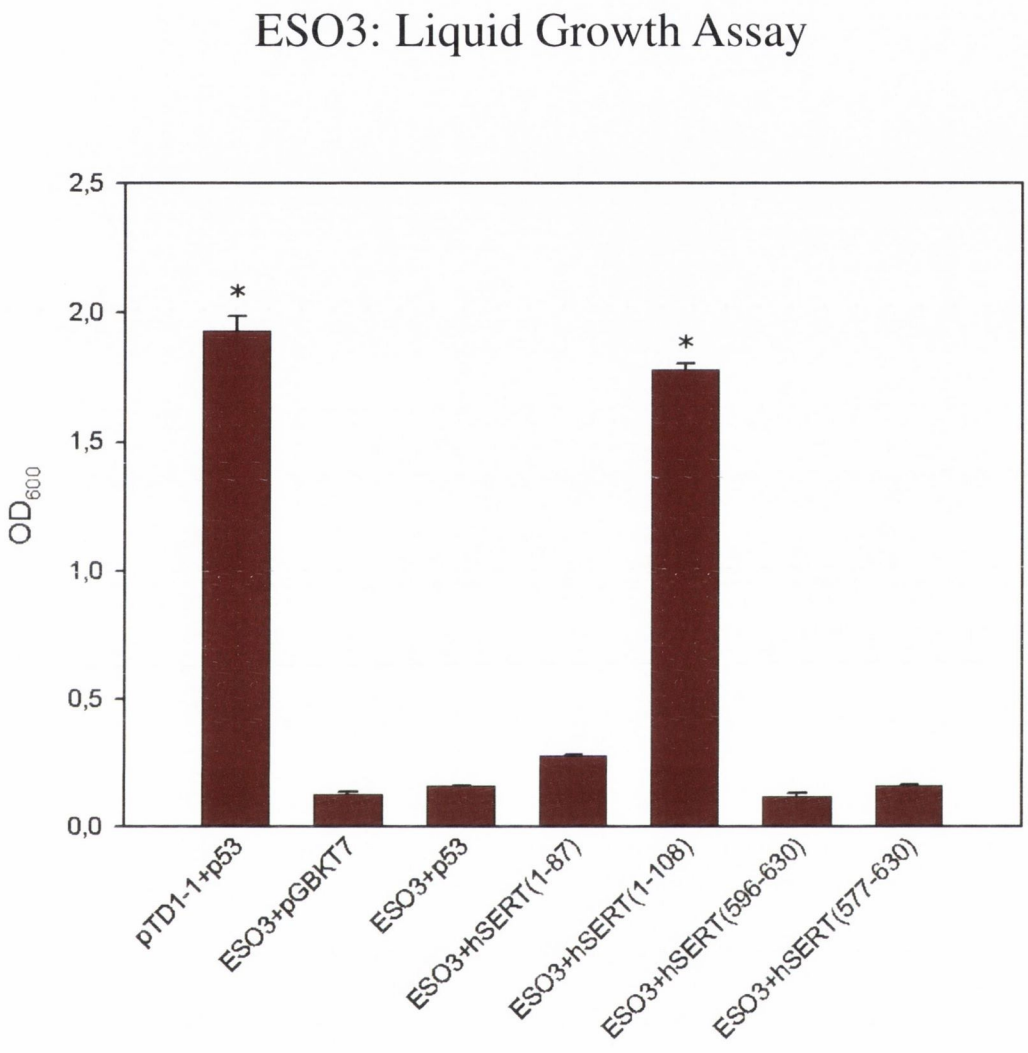


Figure 3.10 Liquid growth assay on ESO3 (clone no. 790). AH109 yeast co-transformants were grown in selective SD/-Trp/-Leu/-Ade/-His medium and the optical density was measured at 600nm (OD_{600}). Values are expressed as the mean ± S.E. of duplicate samples from a single experiment and are representative of two independent experiments. *Asterisk* indicates significant difference compared with the negative control (ESO3+pGBKT7) ($p < 0.01$, one-way ANOVA followed by Bonferroni post hoc analysis).

finding of the LIM domain-containing protein Hic-5 (Carneiro et al., 2002). Using the yeast two-hybrid approach, they also showed that Hic-5 binds to both NET and SERT. Hic-5 is a focal adhesion protein with striking similarity to paxillin, which functions at focal adhesion complexes as well as in the nucleus as a nuclear receptor coactivator (Shibanuma et al., 2003). Recently, Hic-5 was shown to interact directly with SERT in platelets and proposed to play a role in internalisation of the transporter upon activation of PKC (Carneiro and Blakely, 2006).

In order to test whether the binding of SERT to PICK1 and Hic-5 could be verified in our laboratory, the two proteins were tested for interaction with the C-terminal domain of SERT, NET and DAT in the yeast two-hybrid system as well as for binding to the C-terminal domain of SERT in a GST pull-down assay.

3.2.3.2 Yeast Two-Hybrid analysis of PICK1 and Hic-5

Using the yeast two-hybrid mating approach the proteins PICK1 and Hic-5 were tested for their ability to interact with the C-terminal domain of SERT, NET and DAT, respectively. Constructs encoding the C-terminal domain of NET (residues 557-617), the C-terminal domain of DAT (residues 560-620), and constructs encoding the N- and C-terminal domains of SERT including two SERT deletion constructs, C-SERT-$_{V}$ and C-SERT-$_{NAV}$, lacking the last amino acid and the last three amino acids, respectively, were transformed into the AH109 yeast strain (Appendix F). The PICK1 and Hic-5 constructs generated in the pGAD10 vector (similar to pACT2) were transformed into the Y187 yeast strain and mated with each of the bait constructs. Co-transformatants of PICK1 and Hic-5 and each of the bait constructs were also generated in the AH109 yeast strain. Hic-5 failed to interact with any of the bait constructs in both the yeast mating assay and in co-transformants. However, PICK1 was found to interact with the C-terminal domain of DAT in both assays, confirming previous reports, whereas the reported associations of PICK1 with NET and SERT could not be detected using this approach.

3.2.3.3 GST-pulldown assays on PICK1 and Hic-5

GST pull-down assays were carried out in order to test whether the full-length proteins PICK1 and Hic-5 interact with the C-terminal domain of SERT.

GST alone and a fusion protein of GST and the C-terminal domain of SERT, GST-hSERT (577-630) (Appendix F), immobilised onto glutathione-agarose, were incubated with cell extracts prepared from HEK-293 cells expressing PICK1 or Hic-5. Each assay was performed under three different conditions by using either Triton-X 100 (T), CHAPS (C), or deoxycholic acid (D) in the lysis buffer. As shown in Figure 3.11, the C-terminal construct of SERT, but not GST alone, was able to bind PICK1. The binding of PICK1 to the C-terminal domain of SERT dramatically increased when exchanging Triton with CHAPS whereas the use of deoxycholic acid appeared to abolish the interaction under conditions where total levels of PICK1 were unchanged.

Using the same three conditions, the C-terminal construct of SERT was also found to bind Hic-5 (Figure 3.12). However, Hic-5 exhibited considerable binding to the GST control construct, in particular when using CHAPS as detergent, indicating a possible non-specific interaction. The binding of Hic-5 to the GST control construct was highly reduced when increasing the concentration of CHAPS from 2 mM to 5 mM (Figure 3.13). This increase in concentration of detergent had no effect on the binding of Hic-5 to the C-terminal construct of SERT suggesting that Hic-5 does bind specifically to SERT in agreement with the recent study by Carneiro and Blakely (Carneiro and Blakely, 2006).

Although the interaction of SERT with PICK1 and Hic-5 could not be reproduced in our yeast two-hybrid system, the GST pull-down assays demonstrated binding of both PICK1 and Hic-5 to the C-terminal domain of SERT. This finding also verified that the GST pull-down assay can be used successfully in the analysis of the novel SERT interacting proteins identified in this study.

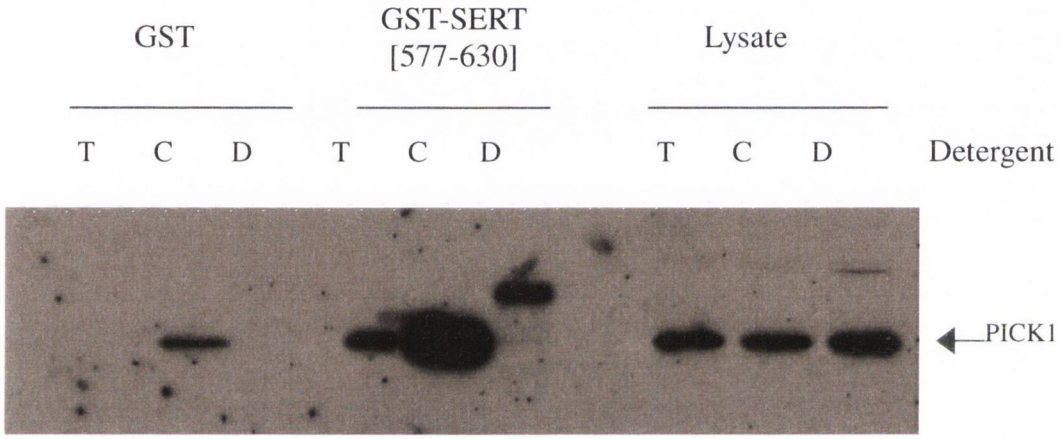


Figure 3.11 PICK1 binds to the C-terminal domain of SERT. GST and GSTSERT[577-630] immobilised on glutathione sepharose beads were incubated with cell extracts from HEK-293 cells transfected with PICK-FLAG. Bound protein was eluted with SDS sample buffer and analysed by Western blotting using an anti-FLAG antibody. Cell extracts were prepared using different detergents: (T), Triton-X 100; (C), CHAPS; (D), and deoxycholic acid.

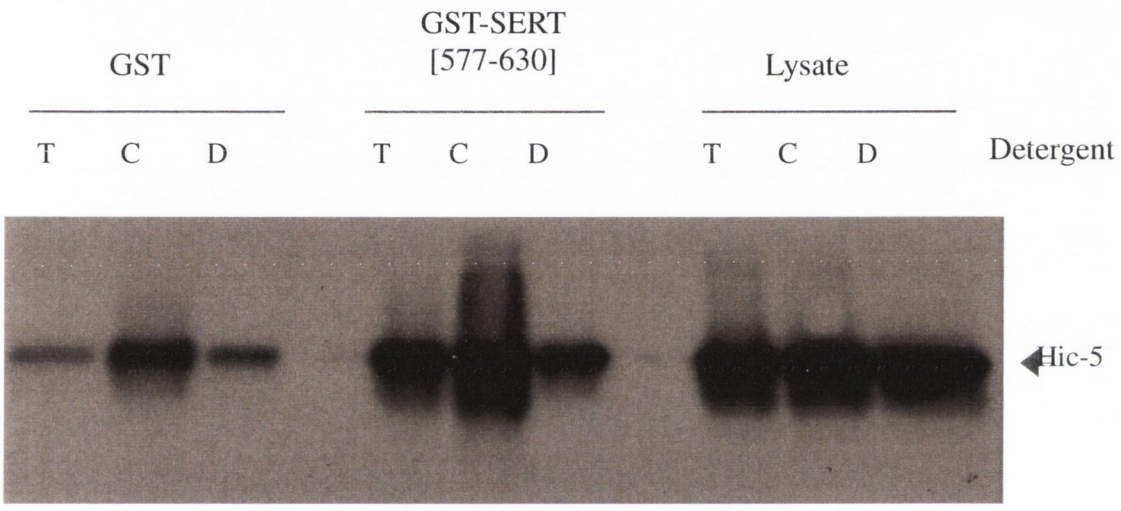


Figure 3.12 Hic-5 binds to the C-terminal domain of SERT. GST and GSTSERT[577-630] immobilised on glutathione sepharose beads were incubated with cell extracts from HEK-293 cells transfected with myc-tagged Hic-5. Bound protein was eluted with SDS sample buffer and analysed by Western blotting using an anti-myc antibody. Cell extracts were prepared using different detergents: (T), Triton-X 100; (C), CHAPS; (D), deoxycholic acid.

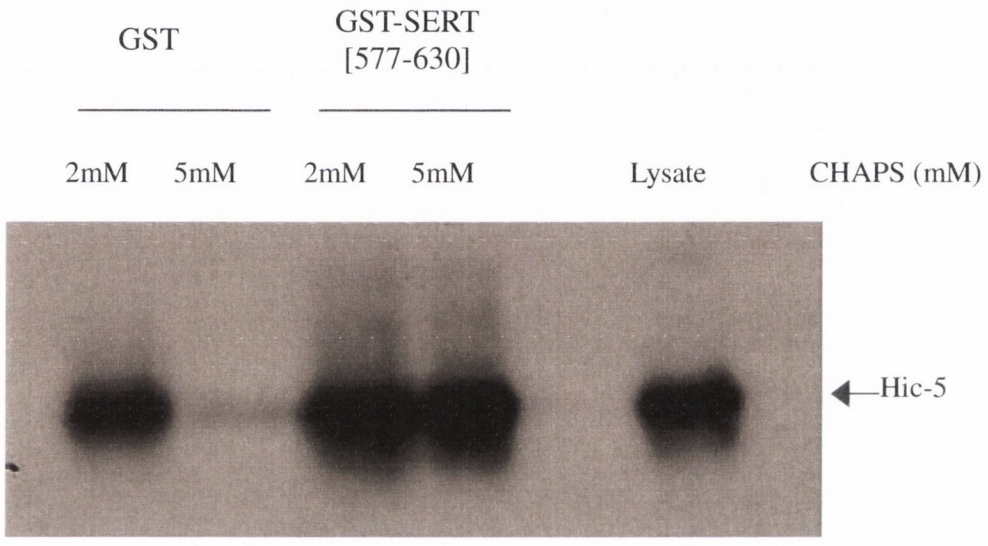


Figure 3.13 Increased concentration of detergent eliminates non-specific binding between Hic-5 and GST. GST and GSTSERT[577-630] immobilised on glutathione sepharose beads were incubated with cell extracts from HEK-293 cells transfected with myctagged Hic-5. Bound protein was eluted with SDS sample buffer and analysed by Western blotting using an anti-myc antibody. The HEK293 cells were lysed in 10 mM CHAPS and cell extracts were diluted to obtain concentrations of CHAPS as indicated in each lane before incubation with GST fusion constructs.

3.3 Discussion

Since its invention in 1989, the yeast two-hybrid system has proven to be a powerful tool to study protein-protein interactions. However, the system presents a high prevalence of false positives as well as false negatives and thus numerous variations have been developed to overcome technical limitations of the classical yeast two-hybrid system. First of all, in the classical yeast two-hybrid system the fusion proteins need to be targeted to the yeast nucleus. Although most yeast two-hybrid constructs encode nuclear localization signals, some proteins may not be suited for this system. For instance extracellular proteins or proteins that contain strong targeting signals to different compartments of the cell as well as proteins that possess strong hydrophobic domains may cause problems in this system. Two of the bait constructs used in this study contain a stretch of hydrophobic residues. In the LexA system an assay has been developed to test whether the bait actually localizes to the nucleus and binds the LexA operator (Brent and Ptashne, 1984) but a similar system was not available for the GAL4 based system. Previous results showed that all bait constructs used in this study were properly expressed in yeast but there are no evidence proving that the baits actually localize to the yeast nucleus. However, since positive clones were identified and shown to interact specifically with the hydrophobic bait constructs, it strongly indicates proper localization of the bait fusion proteins. One could argue that testing well-characterised interacting partners could validate proper nuclear localization. However, false negatives are also a common problem in the yeast two-hybrid assay. For instance, syntaxin 1A, which has been shown to physically interact with SERT in biochemical assays (Haase et al., 2001; Quick, 2003) and co-immunoprecipitate with SERT in neurons (Quick, 2002) did not interact with SERT in a LexA based yeast two-hybrid system (Jana Haase, personal communication). Thus, some known interactions simply cannot be detected in the yeast two-hybrid system. This may be due to sterical hindrance caused by the fusion of transcription factor domains, failure of nuclear localization or arise from protein instability or incorrect folding of protein domains. Furthermore, some interactions may be dependent on posttranslational modifications such as glycosylation, phosphorylation, acetylation or disulfide bond formation and

although many cellular functions are highly conserved from yeast to mammals, yeast does not perform these modifications in an equivalent manner to mammalian cells. Despite the successful and widespread use of the classical yeast two-hybrid system a wide range of other genetic techniques have been developed to overcome some of the limitations of the conventional system. For instance, the problem with nuclear localization is eliminated in the split-ubiquitin system in which interactions take place outside the nucleus allowing identification of proteins interacting with integral membrane proteins (Thaminy et al., 2004).

Ideally, an interaction that has been identified in a yeast two-hybrid screen should be reproducible in any other yeast two-hybrid assay. However this is far from the case. For instance, the previously reported yeast two-hybrid interactions between SERT and PICK1 (Torres et al., 2001), and SERT and Hic-5 (Carneiro et al., 2002) could not be verified using the yeast two-hybrid approach in this study. Also, in the present study, the lack of reproducibility of yeast two-hybrid results is illustrated by the fact that the two screens with the C-terminal domain of SERT, did not result in isolation of similar clones. Although reproducibility is known to be a general problem in genetic screens such as the yeast two-hybrid system, it was unexpected to find that two screens performed with identical bait constructs only revealed few similar results. The only difference between the two screens was that screen D was performed on low stringency selection plates while screen E was performed on high stringency selection plates (section 2.2.19). Also there did not seem to be any similarity between the results obtained in a yeast two hybrid screen with the N-terminal domain of rat SERT (Jana Haase, personal communication), and the two screens with the N-terminal domains of human SERT performed in this study. However, this can possibly be attributed to different cDNA libraries and to differences between the yeast two-hybrid systems, LexA *versus* GAL4 based systems and perhaps also to differences in bait constructs, rat *versus* human SERT.

An interesting aspect of this study is the parallel screening of both the N- and C-terminal domains of SERT as well as the application of bait constructs containing

not only the conventional cytoplasmic domains but also a transmembrane domain. This approach, although fairly laborious, provided a unique opportunity to compare results obtained using different domains of the same protein as bait. For instance, the results clearly revealed promiscuous proteins interacting with all bait constructs and conversely added credibility to clones that were only detected using either the N- or C-terminal domain of SERT. The possibility of some proteins interacting independently with both the N- and the C-terminal domain of SERT or that a single protein interacts simultaneously with the two domains cannot be excluded. The N- and C-termini of human SERT have in fact been shown to locate close together (Just et al., 2004), which in theory would allow proteins to position themselves and bind simultaneously to both termini.

However, in this study one of the major criteria for selecting clones was specificity. For instance, the hydrophobic bait constructs may engage in non-specific hydrophobic interactions and thus, proteins interacting with both the transmembrane containing constructs were initially categorized as false positives.

In general, categorisation of proteins isolated in a yeast two-hybrid screen is rather subjective. Activation of reporter genes is scored visually and decisions are based on relative parameters such as growth and colour, which is likely to result in loss of some weaker but genuine positive interactions. Also, some interactions that do not make immediate sense may actually occur inside living cells and contribute to as-yet-undiscovered regulatory pathways. The sequencing of the human genome resulted in the identification of a large number of novel proteins, whose function and interactions with other proteins are being investigated. Each day proteins are assigned to particular pathways or multimeric structures or become associated with a particular function. Therefore, yeast two-hybrid results should routinely be compared with the literature and available databases.

ESO3 and Mint3, the two proteins prioritised in this study, were isolated using the long N- and C-terminal domain of SERT, respectively. One could argue that since the proteins did not appear in the yeast two-hybrid screens with the corresponding shorter fragments or exhibited binding to the shorter fragments in the mating assays, the

transmembrane domain or part of the transmembrane domain, present within each of the two bait constructs, is necessary for interaction with ESO3 and Mint3. As described in chapter 5, that is actually the case with ESO3. The Mint3 clone isolated in the yeast two-hybrid screen only comprised the second PDZ domain of Mint3. PDZ domains are protein-protein interaction motifs that bind to short peptide sequences often located at the extreme C-terminus of their target proteins. Thus, if Mint3 binds to a peptide located at the extreme C-terminus of SERT, it would be expected not only to bind to the long C-terminal construct of SERT but also to the short C-terminal construct. However, the binding of Mint3 to the extreme C-terminus may depend on some structural stability induced by the presence of the hydrophobic domain or the Mint3 PDZ domain may bind an internal not yet identified PDZ domain binding motif. This question could have been addressed by testing the Mint3 yeast clone for binding to C-terminal deletion constructs of SERT.

In general, the short C-terminal domain of SERT seemed to attract a huge number of proteins (Table 3.2). Compared to the three screens performed in parallel two to three times as many colonies were isolated in the primary screen using this construct. The short C-terminal construct is only 35 amino acids long and it could be speculated that it adopts a random configuration and consequently engage in a large number of non-specific interactions. In the case of the two N-terminal domain constructs, the GAL4 DNA-binding domain prevents accessibility to the extreme N-terminus of SERT. Therefore, interactions dependent on the free N-terminus of SERT would not be detected using neither the short nor the long N-terminal construct. However, one particular protein, although not described in this study, was found to bind both to the short and the long N-terminal domain of SERT (and neither of the two C-terminal domains) indicating the presence of an interaction domain within the cytoplasmic region functioning independently of a free N-terminus (Appendix G; A:191, A:361 and B:123). In total, 14 clones encoding different lengths of this particular protein appeared in the two N-terminal screens. The reason why this protein was not included in the present study is that at the time the yeast two-hybrid results were analysed, the 14 clones could only be assigned to a specific chromosome region and there was no

information available regarding a corresponding protein. Recent reports, however, suggest a role for this protein in regulating receptor function and activity of voltage-dependent Ca^{2+} channels. A potential role of this protein in the regulation of SERT will be explored in future studies.

In general, the strength of an interaction predicted by the yeast two-hybrid approach correlates well with affinity data determined using in vitro measurements (Estojak et al., 1995). However, isolation of a large number of clones encoding parts of the same protein does not necessarily reflect the strength of the interaction with the bait. It may reflect the importance of the interaction but that is highly dependent on the quality of the cDNA library. Also, it is more likely to isolate abundant preys several times, whereas rare preys may only be isolated once, independent of their actual importance or affinity for the bait. Ideally, a cDNA library should contain full-length DNA copies of every mRNA expressed in the starting sample, in abundances representative of the original source. However, many of the clones found in cDNA libraries contain only partial gene fragments with low representation of 5'-ends and the libraries are often missing rare clones that have been lost in amplification.

While only ESO3 and Mint3 are described here (and a third one in chapter 5) other members of the group are investigating several other proteins identified in this study. Only a few interacting partners of monoamine transporters have been described in the literature. Thus, the finding of three novel binding partners of SERT could potentially contribute to the understanding of the complex mechanisms underlying the regulation of SERT and related transporters.

4. FUNCTIONAL INTERACTION BETWEEN ESO3 AND THE SEROTONIN TRANSPORTER

4.1 INTRODUCTION

ESO3 is a member of the NY-ESO-1 gene family, which has three distinct members, NY-ESO-1 (ESO1), LAGE-1 (ESO2), and ESO3. All three genes lie within a 400kb region on chromosome Xq28 and have similar exon-intron structures (Alpen et al., 2002). While ESO1 and ESO2 share 84% amino acid identity, ESO3 shares less than 50% amino acid identity with the two other members. Unlike ESO1 and ESO2, which are well known cancer/testis antigens expressed only in testis and a variety of human cancers, ESO3 is ubiquitously expressed in somatic tissues, including brain. The latter, combined with the finding that it is highly conserved in mouse and rat, suggests that the encoded protein is functionally important. There is no information available regarding the function, localization or structure of ESO3. The amino acid sequence of ESO3 shows no obvious similarity to any other protein sequences that could hint at potential relationships of ESO3 to any previously characterised proteins. Also no protein sorting signals or localization sites could be predicted for ESO3 using software available from the ExPASy web site (Gasteiger et al., 2003).

In chapter 3, ESO3 was described as a novel binding partner of SERT and shown to interact specifically with the N-terminal domain of the transporter in the yeast two-hybrid system. In this study the interaction between ESO3 and SERT was examined in more detail and the effect of ESO3 on SERT function was investigated.

4.2 RESULTS

4.2.1 Endogenous expression of ESO3 and SERT in different cell lines

Using RT-PCR various cell lines were tested for endogenous expressions of ESO3 and SERT. The cell lines included were human neuroblastoma SHSY5Y cells, human glial A172 cells, human JAR choriocarcinoma cells, and human HEK-293 fibroblast-like cells and for ESO3, also rat RN46A neuronal cells.

Using gene specific primers, RT-PCR was performed on total RNA isolated from each of the five cell lines according to the procedure described in sections 2.2.11 – 2.2.13.

ESO3 was found to be expressed in all five cells lines, including HEK-293 cells (Figure 4.1), whereas SERT was detected in SHSY5Y, A172, and JAR cells but not in HEK-293 cells (Figure 4.2).

4.2.2 PCR cloning of human and rat ESO3

The human ESO3 coding sequence was PCR amplified from yeast clone number 790 (isolated in the yeast two-hybrid screen, chapter 3), using gene-specific primers containing restriction sites for cloning into the EcoRI and XhoI sites of the mammalian expression vector pcDNA3 (construct pcDNA3-hESO3, Appendix F). The human ESO3 sequence was also sub-cloned into pcDNA3 with an N-terminal HA-tag and the construct was denoted pcDNA3-HA-hESO3. As shown in Figure 4.1, the RN46A cell line expresses ESO3 endogenously. Total RNA was isolated from RN46A cells and primers specific for the rat ESO3 sequence were used to amplify the coding region of rat ESO3. Rat ESO3 was inserted into the pcDNA3 vector and the construct was denoted pcDNA3-rESO3. The rat ESO3 sequence was also cloned into pcDNA3 with an N-terminally located HA-tag to generate the construct pcDNA3-HA-rESO3. The integrity of all ESO3 constructs was verified by DNA sequencing.

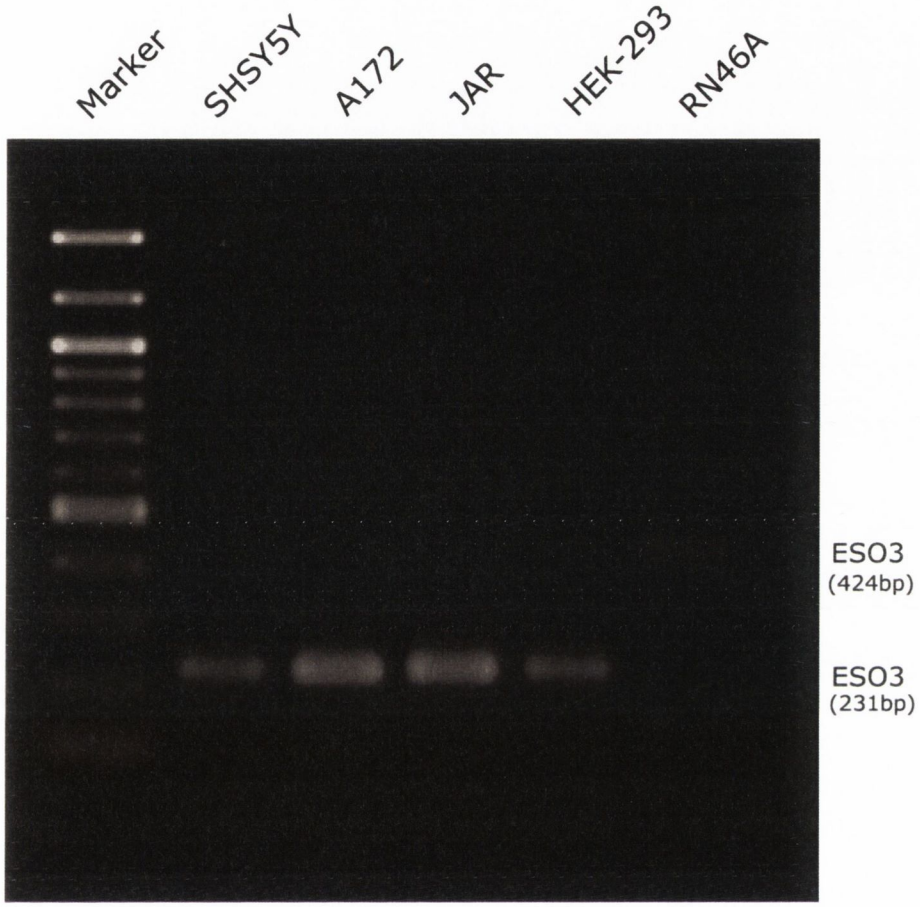


Figure 4.1 Endogenous expression of ESO3 in various cell lines. Total RNA was isolated from the cell lines indicated above each lane and RT-PCR was performed using specific primers for human and rat ESO3 as described in experimental procedures.

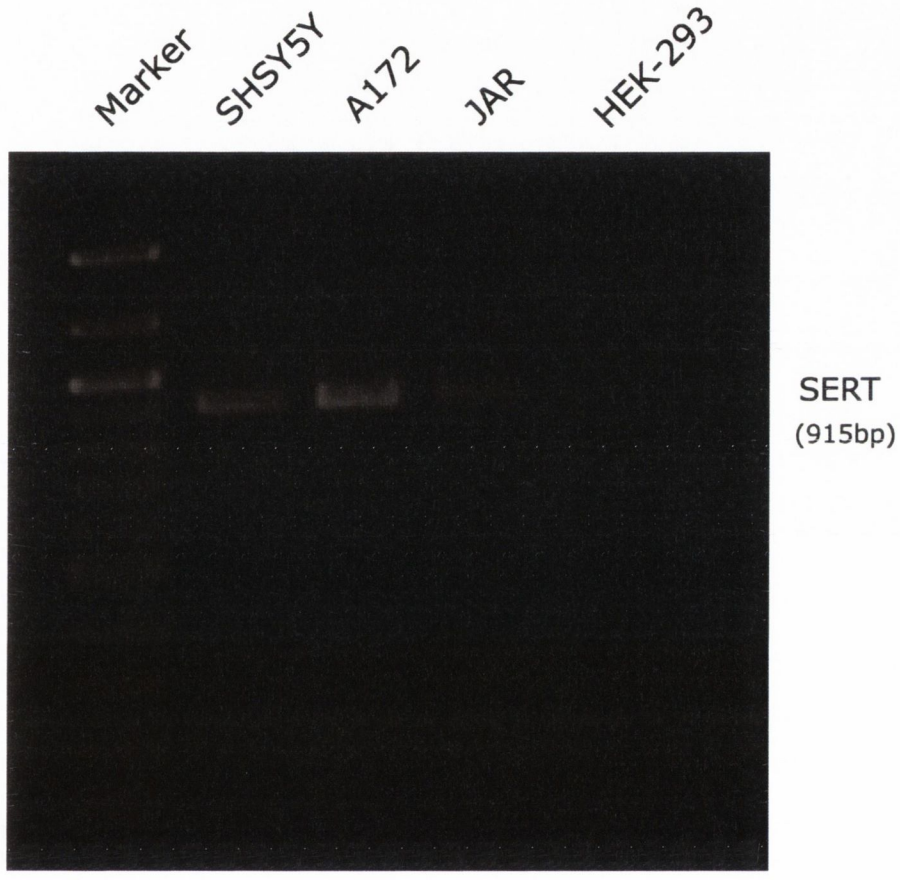


Figure 4.2 Endogenous expression of SERT in various cell lines. Total RNA was isolated from the cell lines indicated above each lane and RT-PCR was performed using SERT specific primers according to the protocol described in sections 2.2.10-2.2.12

4.2.3 Characterisation of an antibody raised against the C-terminal of ESO3

4.2.3.1 Prediction of antigenic peptide

Since there were no commercial antibodies available, a custom-made antibody was generated against human ESO3. An antibody directed against a single peptide of ESO3 was chosen rather than having the antibody raised against the full-length protein. A suitable peptide sequence within ESO3 was predicted using a series of programmes as described below while Sigma Genosys performed the peptide synthesis, immunisation and collection of antibodies.

The secondary structure of ESO3 was predicted using the PredictProtein (Rost et al., 2004), Sspro (Cheng et al., 2005) and the DNAstar software (DNAstar inc., Madison, USA) package. All three programmes predicted a secondary structure essentially as illustrated in Figure 4.3 with a highly ordered C-terminal part and an N-terminal part that assumes no stable shape. In order to identify an antigenic peptide sequence the ESO3 protein sequence was analysed using the DNAStar software package. When combining the information of the secondary structure of ESO3 with the predicted hydrophilicity, surface probability and antigenicity (Figure 4.4) both the N- and C-termini were good candidates for generating an anti-peptide antibody. Because the N- and C-termini of proteins are often found to be exposed and possess a high degree of flexibility they are usually a good choice for generating anti-peptide antibodies. However, because of the multiple glycine and aspartate residues in the N-terminus of ESO3, the C-terminus seemed to represent the most suitable peptide sequence. By using the Antigen Profiler at Open Biosystems the peptide comprising the last 12 residues of ESO3 (RTMQRFGPPVSR) were determined to be the most antigenic sequence. These 12 residues were therefore chosen as the peptide sequence for antibody generation. For experimental reasons it had been preferable to generate an antibody that recognized both human and rat ESO3. However, there are no suitable segments within human ESO3 that are 100% identical to rat ESO3 and only 7 out of the 12 chosen residues in the C-terminus of human ESO3 are identical in the C-terminus of rat ESO3.

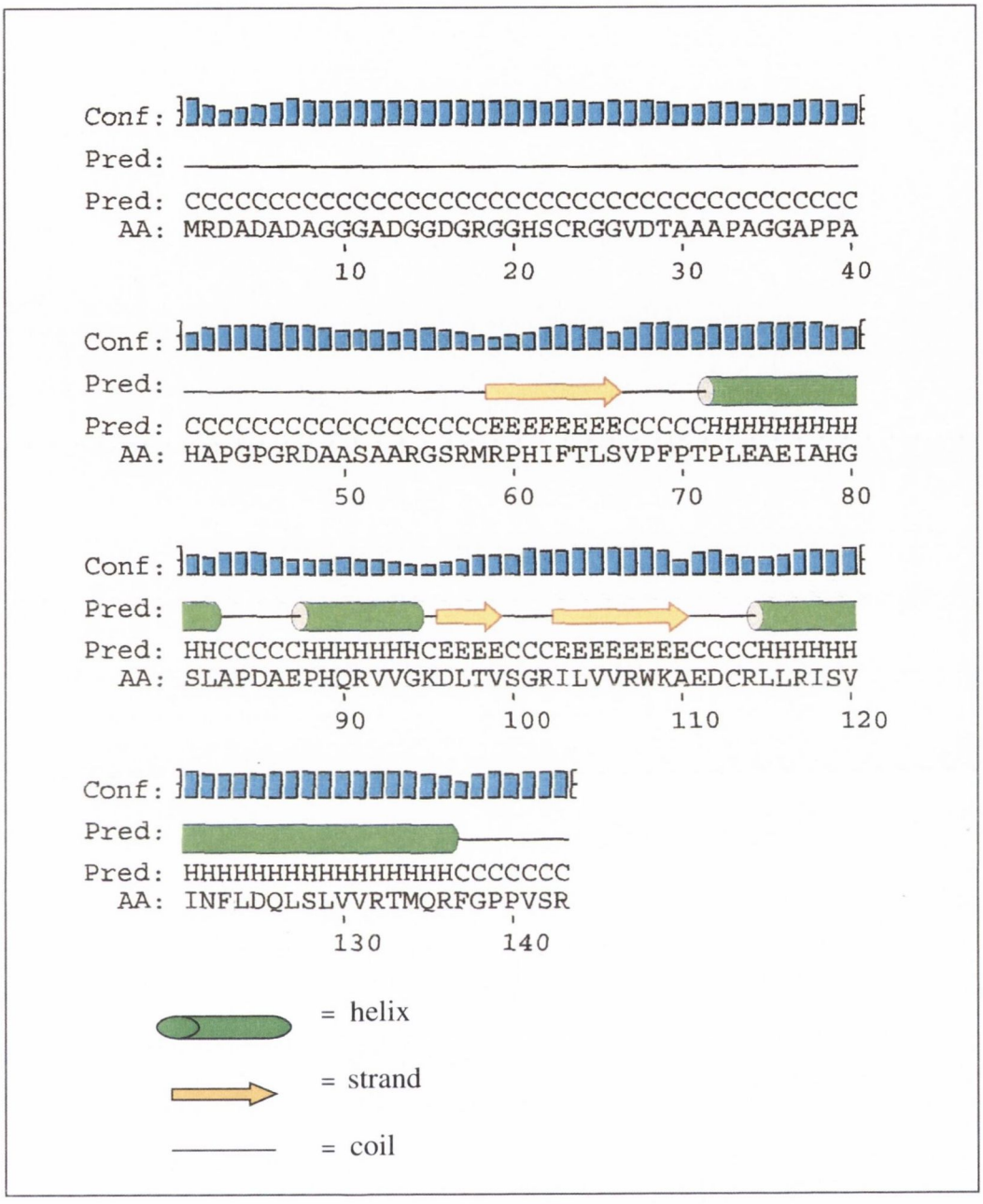


Figure 4.3 Secondary structure prediction of human ESO3. The PredictProtein, Sspro and DNAstar softwares were used to predict the secondary structure of ESO3. Shown above the amino acid sequence is the predicted structure: H, helix; C, coil; E, extended β strand and a measure of confidence of prediction.

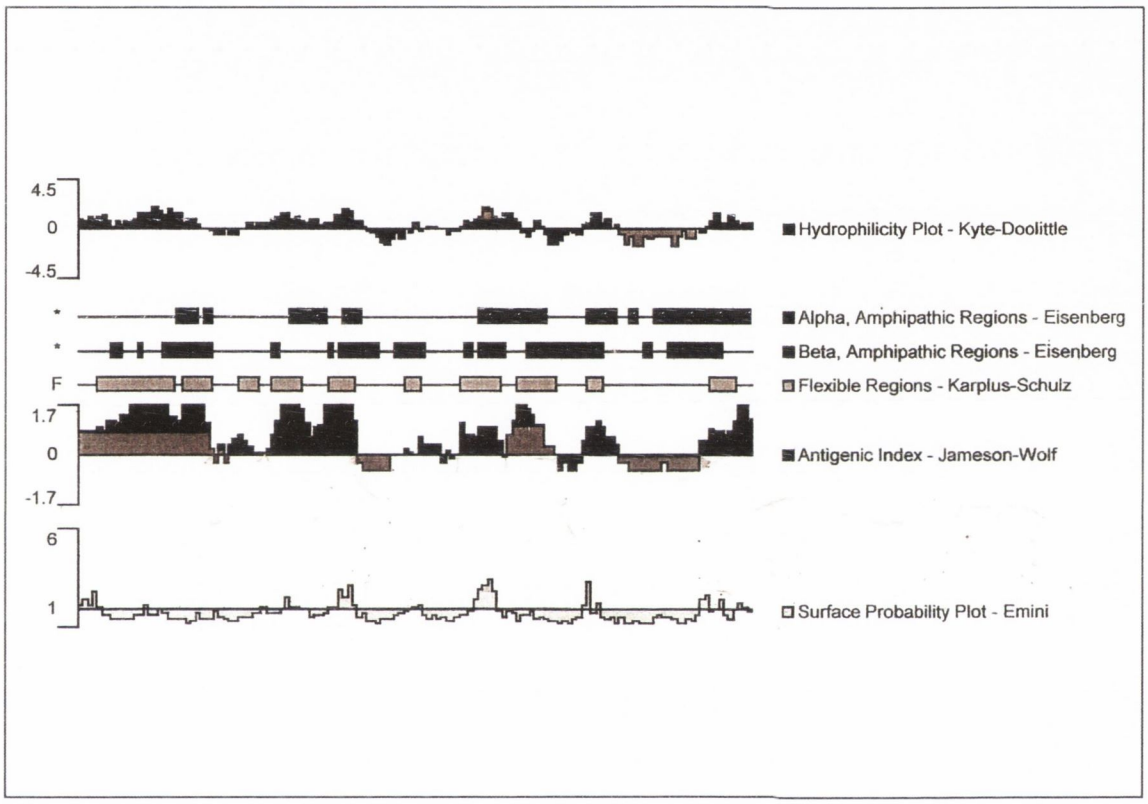


Figure 4.4 Prediction of antigenic peptide. The DNAStar sequence analysis software package was used for predicting hydrophilicity, surface probability, flexibility, and antigenic index for human ESO3.

4.2.3.2 Western blot analysis of ESO3 polyclonal antibody

At Sigma Genosys two rabbits were immunised six times with two weeks intervals. Blood samples were collected one week after the third, fourth, fifth and sixth immunisation and the samples were denoted test bleed number 1, 2, 3 and 4 respectively.

The four test bleeds were analysed by testing their specificity for ESO3. Western blots of cell extracts from HEK-293 cells transfected with pcDNA3 or pcDNA3-hESO3 where incubated with pre-immune serum or test bleeds number 1 to 4. While test bleed number 1 resulted in non-specific bands, test bleeds number 2, 3 and 4 detected a single band of the expected apparent molecular weight demonstrating that the three test bleeds specifically recognize human ESO3 (Figure 4.5). There did not appear to be any differences in the affinity or specificity for ESO3 between anti-sera collected from the two rabbits. For all subsequent experiments test bleed number 4 was used to detect human ESO3 on Western blots and therefore, is referred to as the anti-ESO3 antibody. In spite of the non-identical C-termini in human and rat ESO3, anti-ESO3 could potentially recognize an epitope within the C-terminus of rat ESO3. Therefore, anti-ESO3 was tested for its ability to recognize rat ESO3 on Western blots of cell lysates from HEK-293 cells transfected with pcDNA3-HA-hESO3 or pcDNA3-HA-rESO3. The blot was first incubated with the anti-ESO3 antibody and then re-probed with an anti-HA antibody in order to verify proper expression of the rat construct. As shown in Figure 4.6, anti-ESO3 does not recognize rat ESO3 on Western blots.

The C-terminus of rat ESO3 possess little antigenicity and thus the sequence corresponding to the peptide of human ESO3 used for the generation of anti-ESO3 was not suitable for generating an antibody against rat ESO3. Instead, an attempt to generate an antibody recognizing rat ESO3 was made using an internal peptide sequence (residues 42-60) selected for its predicted antigenic properties (by Alpha Diagnostic International). However, the rat ESO3 polyclonal antibody was unsuccessful in detecting rat ESO3 in RN46A cells using immunocytochemistry or by Western blotting on cell extracts from HEK-293 cells transiently expressing rat ESO3. The reason why this antibody failed to detect rat ESO3 in the two applications is not

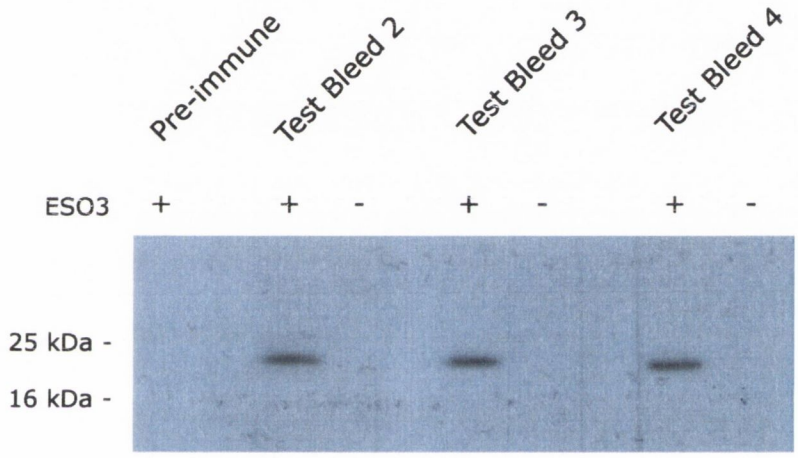


Figure 4.5 Evaluation of ESO3 anti-sera. Total protein lysates were prepared from HEK-293 cells transfected with human ESO3 or pcDNA3**.** Samples were separated by SDS-PAGE and transferred to a PVDF membrane for immunoblot analysis. The PVDF membrane was cut into four pieces and incubated with pre-immune serum or test bleed number 2, 3 and 4, respectively. The anti-sera were all diluted 1:10,000 in blocking solution and detected using HRP-conjugated anti-rabbit antibody. All three anti-sera specifically recognized ESO3.

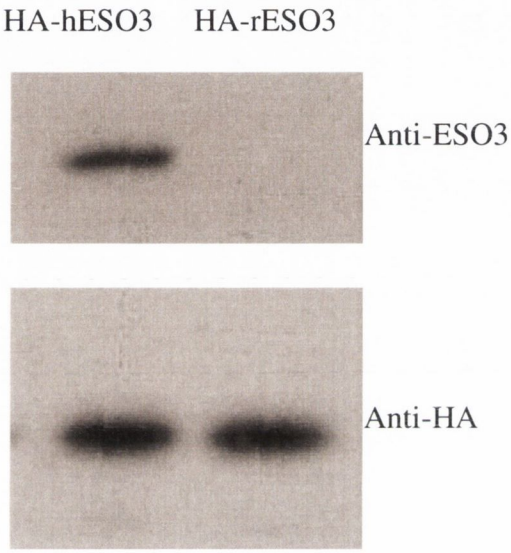


Figure 4.6 Anti-ESO3 does not recognize rat ESO3. Total protein lysates were prepared from HEK-293 cells transfected with HA-tagged human ESO3 or HA-tagged rat ESO3. The samples were separated by SDS-PAGE and transferred onto a PVDF membrane. Immunoreactive bands were first revealed using the anti-ESO3 antibody (1:5000). The blot was then stripped and re-probed with an anti-HA antibody to verify proper expression of both constructs.

clear. Although polyclonal antibodies generated against a peptide sequence may not recognize the native protein these antibodies are generally a good choice for immunoblotting where the protein is denatured.

4.2.4 Direct interaction between ESO3 and SERT

4.2.4.1 GST pull-down assays

In the yeast two-hybrid system ESO3 was shown to interact specifically with the N-terminal domain of SERT (residues 1-108). GST pull-down assays were performed to confirm the interaction between ESO3 and the N-terminal domain of SERT. A number of GST fusion proteins were generated in the pGEX-KG vector (Appendix F). The four bait domains used in the yeast two-hybrid screens were all cloned into the pGEX-KG vector to generate the following constructs: GST-SERT(1-87), GST-SERT(1-108), GST-SERT(596-630), and GST-SERT(577-630). The N-terminal domains of the closely related monoamine transporters NET and DAT were also cloned into pGEX-KG and denoted GST-NET(1-85) and GST-DAT(1-89), respectively.

SDS-PAGE and Coomassie staining was used to assess proper expression and immobilisation of the fusion proteins onto glutathione beads. An example of a Coomassie stained gel is given in Figure 4.7, showing immobilized GST, GST-SERT(1-108), GST-SERT(596-630), and GST-SERT(577-630). The concentrations of immobilized fusion proteins were estimated by comparison to BSA. The GST-NET(1-85) fusion protein failed to be properly expressed in *E.coli* and therefore could not be included in these studies.

All GST pull-down experiments were carried out essentially as described in section 2.2.31 by incubating 20 micrograms of GST or GST fusion protein, coupled to glutathione agarose, with approximately 500 µg of total protein. Bound proteins were eluted from the beads and analysed by Western blotting.

Cell extracts were prepared from HEK-293 cells transfected with pcDNA3-hESO3 in either 10 mM CHAPS or 1% Triton X-100 in a standard Tris-buffer. Before incubation with the fusion proteins, the Triton cell extracts were diluted to obtain different

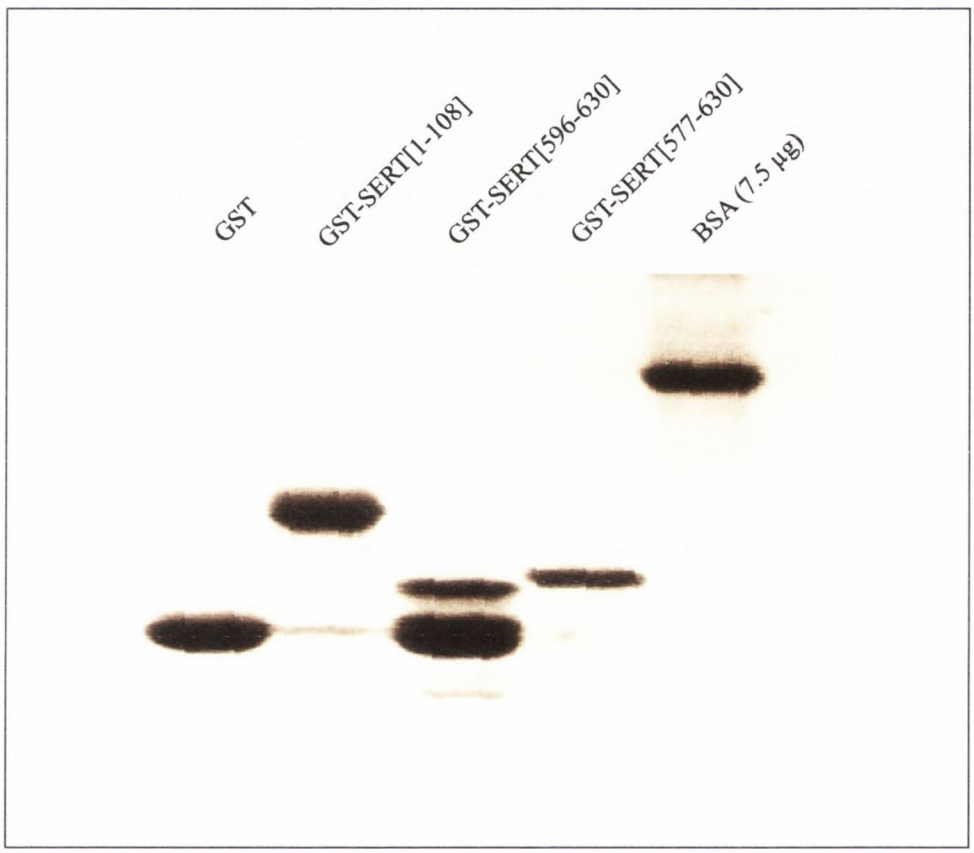


Figure 4.7 Coomassie staining of immobilized GST-fusion proteins. GST-fusion proteins were expressed in *E.coli* and affinity purified using glutathione beads. A sample of glutathione beads with immobilised GST-fusion protein was boiled in SDS sample buffer. The supernatant was recovered and GST-fusion proteins were analysed by SDS-PAGE followed by staining with Coomassie blue. The amount of protein present in each sample was estimated by comparison with BSA.

concentrations of detergent and salt: *Standard Triton*: 0.2% Triton and 150 mM NaCl; *High Salt*: 0.2% Triton and 1 M NaCl; *High Triton*: 1.0% Triton and 150 mM NaCl. The CHAPS cell extracts were diluted to either 2 mM or 10 mM CHAPS.

As shown in Figure 4.8 GST-SERT(1-108) but not GST alone was able to precipitate ESO3. A decrease in binding of ESO3 was observed when increasing the concentration of Triton, whereas an increase in the concentration of salt had no effect on the binding. Furthermore, a dramatic increase in precipitated ESO3 was observed when exchanging Triton with CHAPS. There was no difference in the amount of ESO3 present in the cell extracts prepared with the two detergents. Thus, the zwitterionic detergent CHAPS appears to improve the binding of ESO3 to the N-terminal domain of SERT. The short N-terminal cytoplasmic construct of SERT, GST-SERT(1-87) was unable to bind ESO3 under conditions where ESO3 showed strong association with the GST-SERT(1-108) construct (Figure 4.9). Also, the C-terminal construct, GST-SERT (577-630), was unable to bind ESO3 further supporting the specificity of the binding between ESO3 and the N-terminal domain of SERT (Figure 4.9). ESO3 was also shown to interact with the corresponding N-terminal domain of DAT, GST-DAT(1-89) (Figure 4.10).

4.2.4.2 Co-immunoprecipitaion

To determine whether ESO3 also associates with full-length SERT, co-immunoprecipitation assays were performed on transfected HEK-293 cells using the anti-SERT (C-20) antibody. The GST pull-down experiments indicated that CHAPS is a better choice of detergent for stabilizing the interaction between ESO3 and SERT. Therefore, co-immunoprecipiations were performed on cell extracts prepared in 5 mM CHAPS. As shown in Figure 4.11, both endogenous ESO3 and heterologously expressed ESO3 co-immunoprecipitates with SERT. In contrast, ESO3 was not detected in immunoprecipitates from cells expressing ESO3 alone, or when using control IgG.

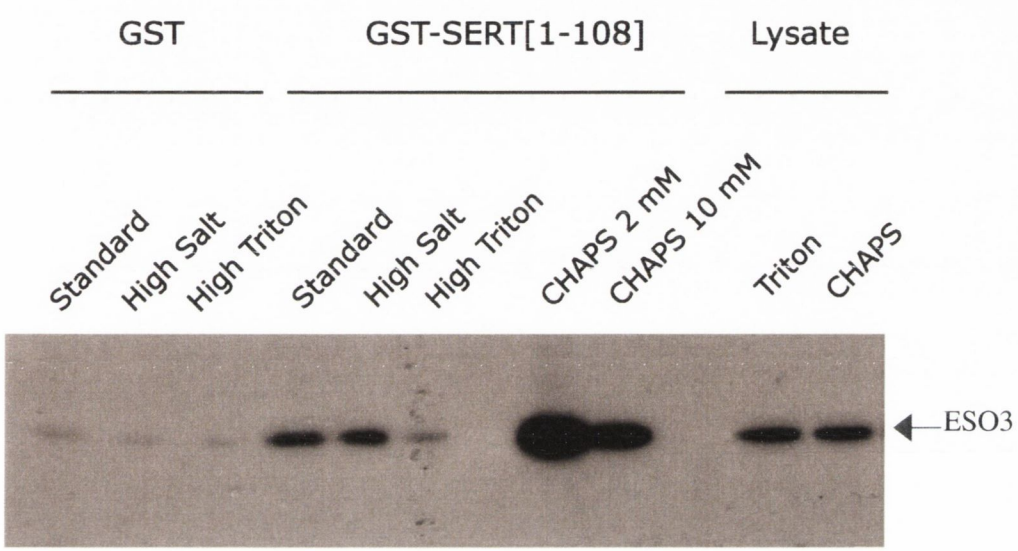


Figure 4.8 ESO3 interacts with the N-terminal domain of SERT. GST and GST-SERT(1-108) immobilised on glutathione beads were incubated with extracts from HEK-293 cells transfected with ESO3. Cell extracts were prepared using either 10 mM CHAPS or 1% Triton-X 100 and diluted to the following concentrations before incubation with the glutathione beads: *Standard Triton*: 0.2% Triton and 150 mM NaCl; *High Salt*: 0.2% Triton and 1 M NaCl; *High Triton*: 1.0% Triton and 150 mM NaCl. The CHAPS cell extracts were diluted to either 2 mM or 10 mM. Bound protein was eluted with SDS sample buffer and analysed by Western blotting using the anti-ESO3 antibody (1:5000).

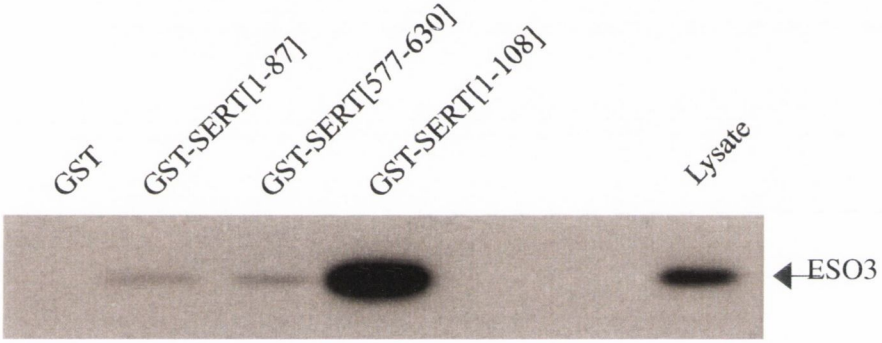


Figure 4.9 ESO3 binds specifically to the long N-terminal domain of SERT. GST, GST-SERT(1-87), GST-SERT(577-630) and GST-SERT(1-108) immobilised on glutathione beads were incubated with extracts from HEK-293 cells transfected with ESO3. Cell extracts were prepared in 5 mM CHAPS and used directly for GST-pulldown experiments. Bound protein was eluted with SDS sample buffer and analysed by Western blotting using the anti-ESO3 antibody (1:5000).

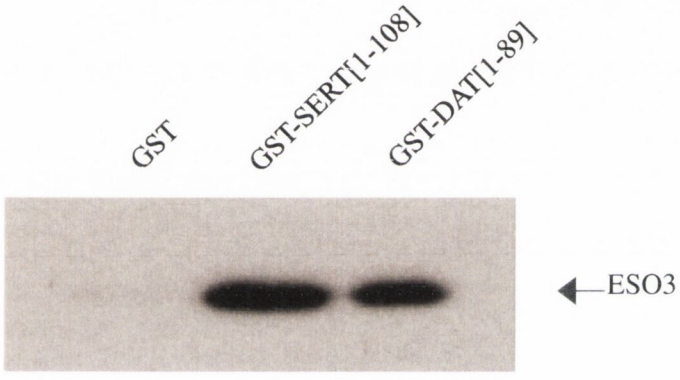


Figure 4.10 ESO3 interacts with the N-terminal domain of DAT. GST, GST-SERT(1-108), and GST-DAT(1-89) immobilised on glutathione beads were incubated with extracts from HEK-293 cells transfected with ESO3. Cell extracts were prepared in 5 mM CHAPS and used directly for GST-pulldown experiments. Bound protein was eluted with SDS sample buffer and analysed by Western blotting using the anti-ESO3 antibody (1:5000).

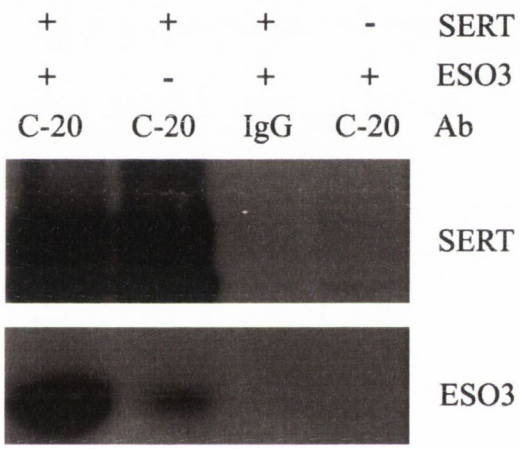


Figure 4.11 The full-length SERT interacts with ESO3 in HEK-293 cells. HEK-293 cells transfected with either SERT or ESO3 alone or in combination were immunoprecipitated with anti-SERT(C-20) antibody or control IgG. Immunoprecipitated SERT and co-immunoprecipitated ESO3 were detected by immunoblotting using anti-SERT (C-20) antibody and anti-ESO3 antibody (1:1000).

4.2.5 Mapping of binding domains in ESO3 and SERT

The yeast two-hybrid system was used to define the region of ESO3 involved in the interaction with SERT. Possible interactions between the N-terminal domain of SERT and deletions of ESO3 were tested for their ability to grow on selective media. The nature of the three ESO3 clones identified in the yeast two-hybrid screen (Figure 3.5) suggested that the N-terminal part of ESO3 is not required for interaction with SERT. Also, the N-terminal part of ESO3 appears to be the least conserved when comparing the human sequence to that of mouse and rat (Figure 4.12). As shown in Figure 4.13, no interaction was observed between an N-terminal construct of ESO3 (residues 1-60) and the N-terminal domain of SERT (residues 1-108). A longer construct encoding amino acids 1-101 of ESO3 also showed no interaction with SERT, whereas an N-terminal deletion construct (residues 61-143) behaved similar to the full-length protein, displaying a strong interaction with SERT.

To map the binding domain of SERT involved in the interaction with ESO3, possible interactions between full-length ESO3 and truncated versions of the N-terminal domain of SERT were tested (Figure 4.14). Deletion of residues 1-40 and 1-60 of SERT had no effect on the binding to ESO3, whereas further deletion of residues 1-78 abolished the interaction with ESO3. Also, removal of residues 101-108 had no effect on the interaction, whereas removal of residues 88-108 resulted in complete loss of binding to ESO3. These results demonstrate that the region spanning residues 61-100 of SERT, or at least part of that region, is necessary for interaction with ESO3 (Appendix H).

4.2.6 Effect of ESO3 on SERT function

4.2.6.1 5-HT transport assay

The effect of ESO3 overexpression on SERT-mediated 5-HT uptake was assessed in HEK-293 cells. Co-transfection of SERT (50 ng/well in a 24-well plate) with increasing amounts of ESO3 (0 – 150 ng/well) caused a dose-dependent reduction in 5-HT uptake. When SERT was co-transfected with ESO3 in a ratio of 1:1, specific

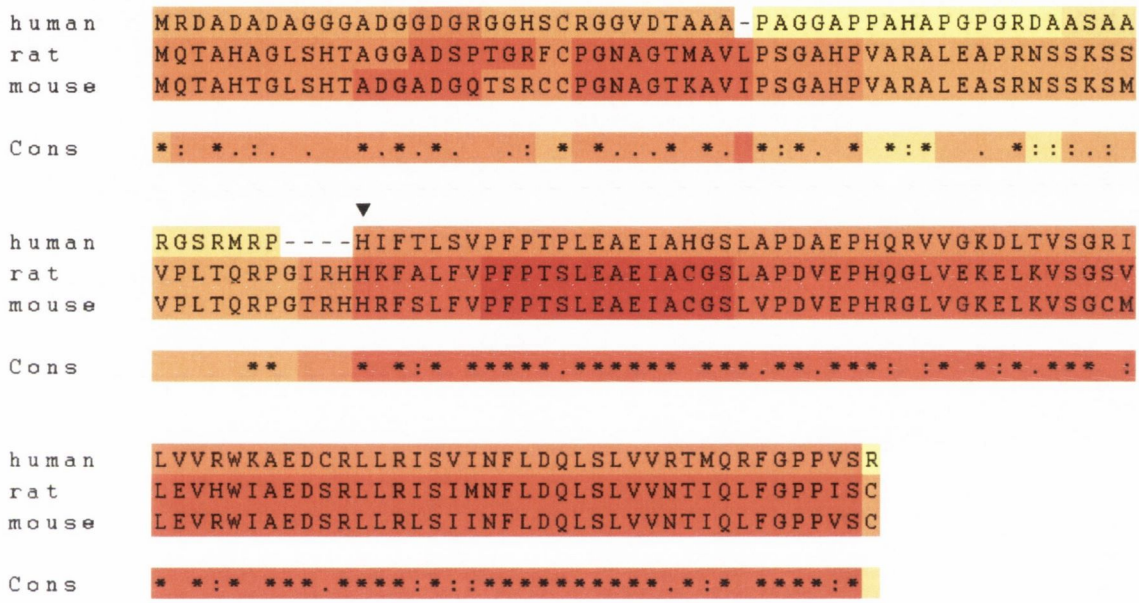


Figure 4.12 Protein sequence comparison of human, rat, and mouse ESO3. The multiple sequence alignment program T-COFFEE was used to align ESO3 protein sequences from human, rat, and mouse. The arrowhead indicates the first amino acid of the highly conserved region of ESO3.

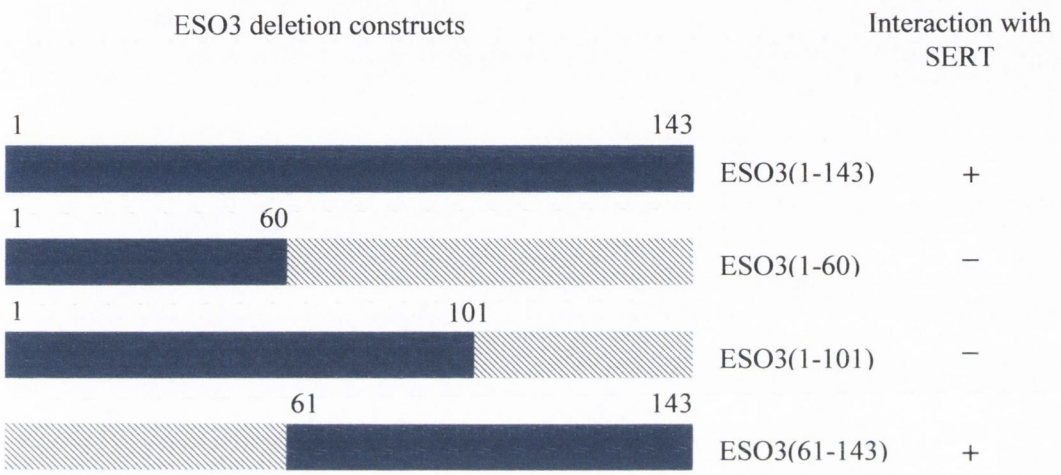


Figure 4.13 Mapping of ESO3 region responsible for interaction with SERT. Schematic diagram of ESO3 deletion constructs. Using the yeast two-hybrid system, the ESO3 deletion constructs were tested for their ability to bind the N-terminal domain of SERT. The C-terminal part of ESO3 was found to be involved in the interaction with the N-terminal domain of SERT.

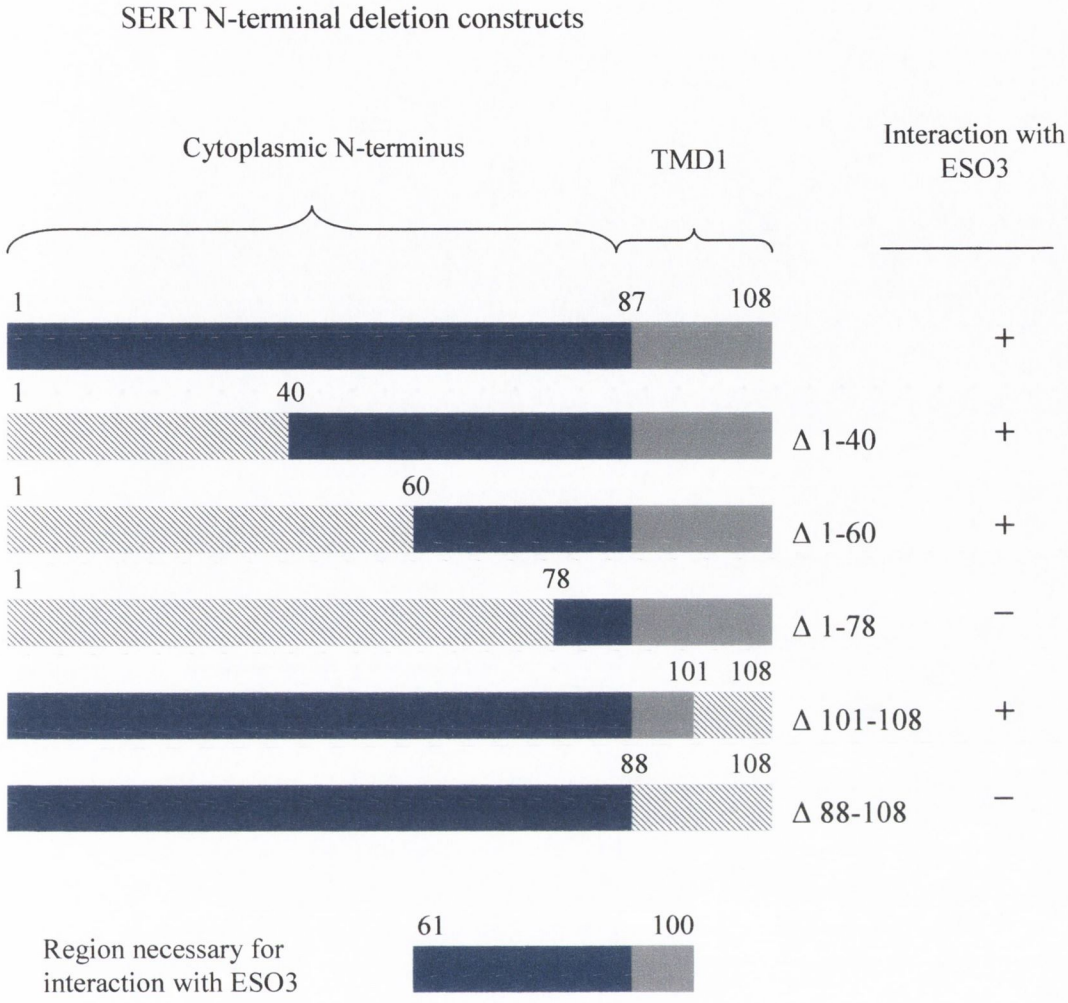


Figure 4.14 Mapping of SERT binding domain involved in the interaction with ESO3. Schematic diagram of SERT deletion constructs. Using the yeast two-hybrid system, the SERT deletion constructs were tested for their ability to interact with full-length ESO3. Residues 61-100 were found to be critical for interaction with ESO3.

5-HT uptake was reduced by approximately 50% (Figure 4.15). No further reduction in 5-HT uptake was observed at higher concentrations of ESO3. The increasing expression of ESO3 did not affect the total levels of SERT protein as quantified by Western blotting (Figure 4.16).

In cells co-transfected with SERT (50 ng/well in a 24-well plate) and ESO3 (50 ng/well), the maximal 5-HT uptake capacity (V_{max}) was reduced by an average of 50% when compared to cells expressing SERT alone (V_{max} 12.8 ± 0.3 pmol/min/10^6 cells in cells expressing SERT alone *versus* 6.7 ± 0.5 pmol/min/10^6 cells in cells expressing SERT and ESO3) (Figure 4.17). No reduction in total 5-HT uptake was observed in cells co-expressing SERT and a C-terminally truncated ESO3 construct, ESO3(1-101), (V_{max} 14.5 ± 0.3 pmol/min/10^6). On the contrary, a small increase of 10% was consistently observed when SERT was expressed in combination with the C-terminally truncated construct. No significant changes in the apparent affinity of 5-HT for the transporter were observed (control, K_m 484 ± 41 nM; ESO3, K_m 401 ± 101 nM; ESO3(1-101), K_m 482 ± 36 nM).

4.2.6.2 Cell surface biotinylation

Cell surface biotinylation experiments were performed in order to test whether the observed decrease in 5-HT uptake in the presence of ESO3 is paralleled by changes in transporters expressed on the cell surface. HEK-293 cells transfected with SERT (0.5 µg/well in a 6-well plate) alone or in combination with ESO3 (0.5 µg/well) were labelled with the membrane impermeant biotinylation reagent sulfo-NHS-biotin. Cells were solubilised and biotinylated proteins were collected with avidin beads. Bound protein was eluted and analysed by Western blotting using the anti-SERT (C-20) antibody. When SERT is expressed alone approximately 30% is localized to the cell surface. As shown in Figure 4.18A and B, the amount of SERT on the cell surface (biotinylated) was reduced by an average of 50% when co-expressed with ESO3, reducing the cell surface amount of SERT to 15% of total SERT. Also, an increase in intracellular (non-biotinylated) SERT equivalent to the expected value of

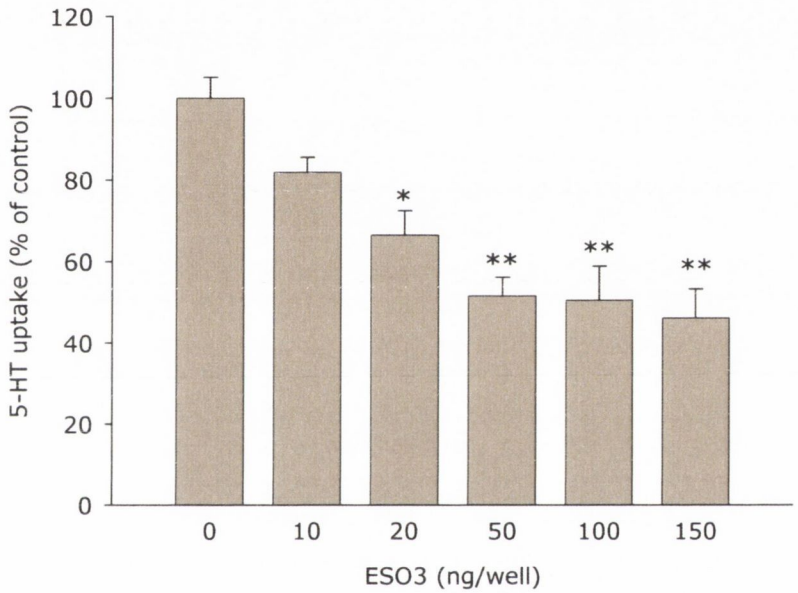


Figure 4.15 SERT uptake activity is reduced by ESO3 in a dose-dependent manner. SERT (50 ng/well in a 24-well plate) was co-transfected with increasing amounts of ESO3 (0150 ng/well) as indicated and specific [^{3}H]5-HT uptake was determined at a single concentration of 5-HT (1μM). Values are expressed as percentage of control ± S.E. of triplicate samples. Data are representative of three independent experiments. *Asterisks* indicate statistically significant reduction in SERT uptake from control (* $p < 0.05$; ** $p < 0.01$, one-way ANOVA with Bonferroni post hoc analysis).

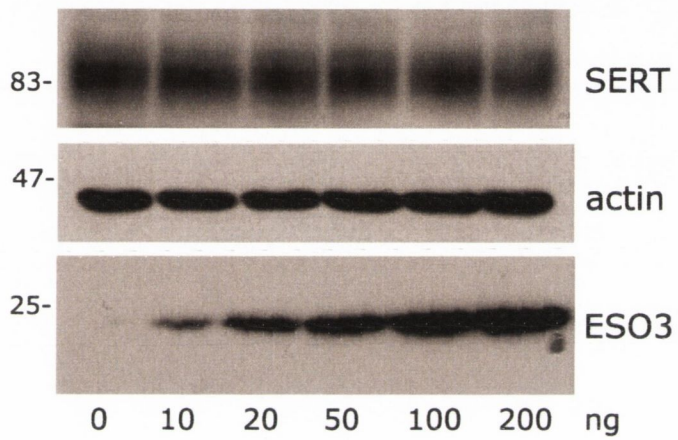


Figure 4.16 Western blot of whole cell lysates from co-transfected HEK-293 cells. The blot was cut into two pieces and the upper part was probed with anti-SERT (C-20) antibody and the lower part was incubated with anti-ESO3 antibody. The ESO3 blot was stripped and re-probed with anti-β-actin to verify equal protein loading between samples. Expression levels of SERT are not affected by ESO3 overexpression within the 0-150 ng range used in this experiment. The blot is a representative of two experiments.

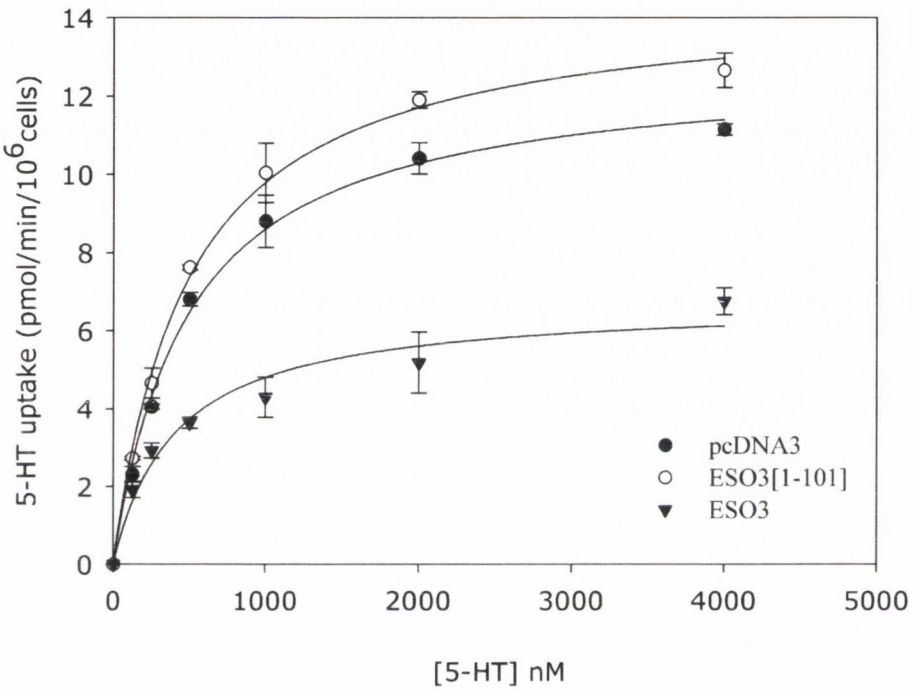


Figure 4.17 Overexpression of ESO3 down-regulates SERT uptake activity. [^{3}H]5-HT uptake experiments in HEK-293 cells transfected with SERT (50 ng/well) alone or SERT in combination with full-length ESO3 (50 ng/well) or the deletion mutant ESO3(1-101) (50 ng/well). The data represents the mean ± S.E. of triplicate samples from a single experiment and are representative of five independent experiments.

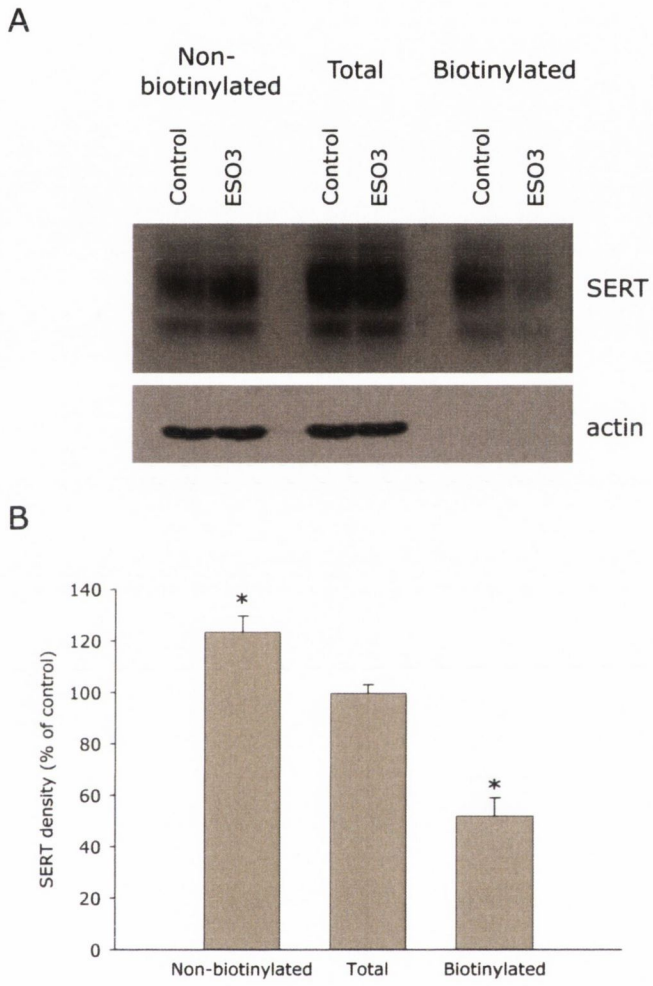


Figure 4.18 ESO3 overexpression downregulates SERT uptake activity by decreasing the cell-surface levels of the transporter. (A) Representative immunoblot of biotinylation experiment of cells transfected with SERT alone (0.5 μg/well in a 6-well plate) or in combination with ESO3 (0.5 μg/well), showing SERT immunoreactivity in non-biotinylated, total, and biotinylated fractions. The blot was stripped and reprobed for β-actin. (B) Quantification of signals based on densitometry measurements of immunoblots from five separate biotinylation experiments. Data are expressed as percentage of control ± S.E. *Asterisk* indicates statistically significant change in SERT protein compared to control ($p < 0.05$; student's *t* test).

approximately 20% was observed. Immunoblots were re-probed for β-actin confirming that no intracellular proteins were labelled with biotin.

4.2.6.3 Confocal microscopy

The decrease in SERT levels on the cell surface corresponds well with the changes in SERT uptake activity suggesting that overexpression of ESO3 causes a redistribution of SERT. To test this hypothesis confocal microscopy was used to investigate the localization of SERT when expressed alone or in combination with ESO3 in HEK-293 cells. When expressed alone SERT primarily localized at or near the plasma membrane (Figure 4.19A). In contrast, ESO3 localized to intracellular compartments resembling the ER or Golgi apparatus (Figure 4.19B). The co-expression of SERT with ESO3 resulted in a dramatic redistribution of the transporter where SERT co-localized with ESO3 in these intracellular structures (Figure 4.19C). Using confocal microscopy markers for the ER and the Golgi apparatus were used to identify the intracellular compartment in which SERT accumulates and co-localizes with ESO3. The lectin Concanavalin A (ConA), which binds to mannose-rich glycans was used to label the ER, whereas the lectin wheat germ agglutinin (WGA), which recognizes complex glycans was used to localize the Golgi apparatus (Virtanen et al., 1980; Parkkinen et al., 1997). HEK-293 cells transfected with SERT and ESO3 were stained with anti-ESO3 in combination with ConA or WGA. As shown in Figure 4.20, ESO3 accumulated mainly in ConA-positive structures.

4.2.7 Effect of PKC activation on ESO3-mediated SERT down-regulation

Activation of PKC has been shown to regulate cell surface expression of a number of neurotransmitter transporters. To investigate whether the ESO3-mediated down-regulation of SERT is linked to the PKC pathway, the effect of the PKC activator β-PMA on SERT-uptake activity was examined in the presence and absence of ESO3. HEK-293 cells transfected with SERT alone or in combination with ESO3 (ratio 1:1) were treated with vehicle (DMSO) or 1 μM β-PMA for 30 minutes prior to the 5-HT

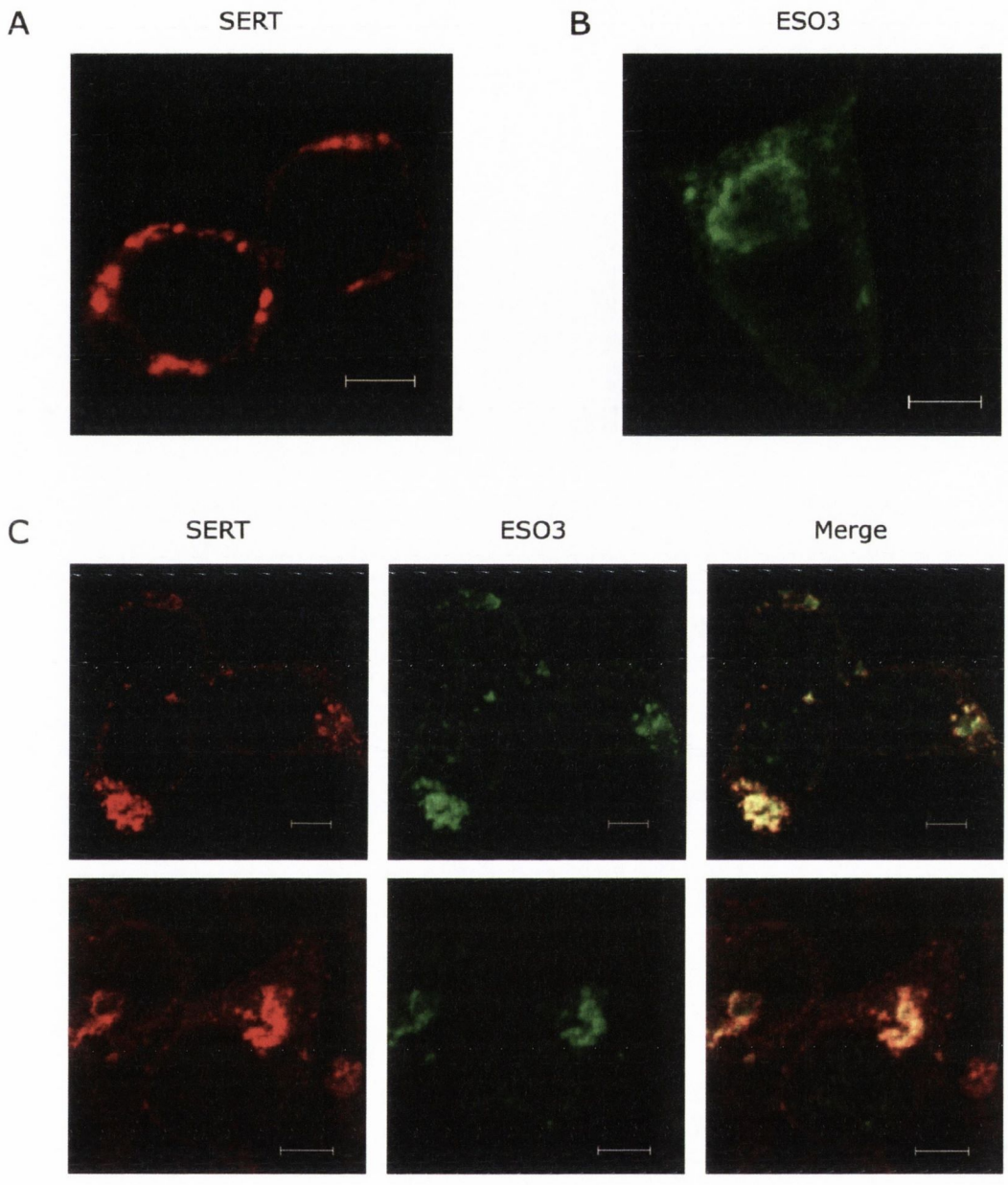


Figure 4.19 Overexpression of ESO3 changes SERT subcellular localization. The distribution pattern of SERT (A) and ESO3 (B) when expressed alone or in combination in HEK-293 cells (C). Immunostaining was performed using mouse anti-SERT (AB-N09) antibody and rabbit anti-ESO3 antibody. Bar, 5 μm.

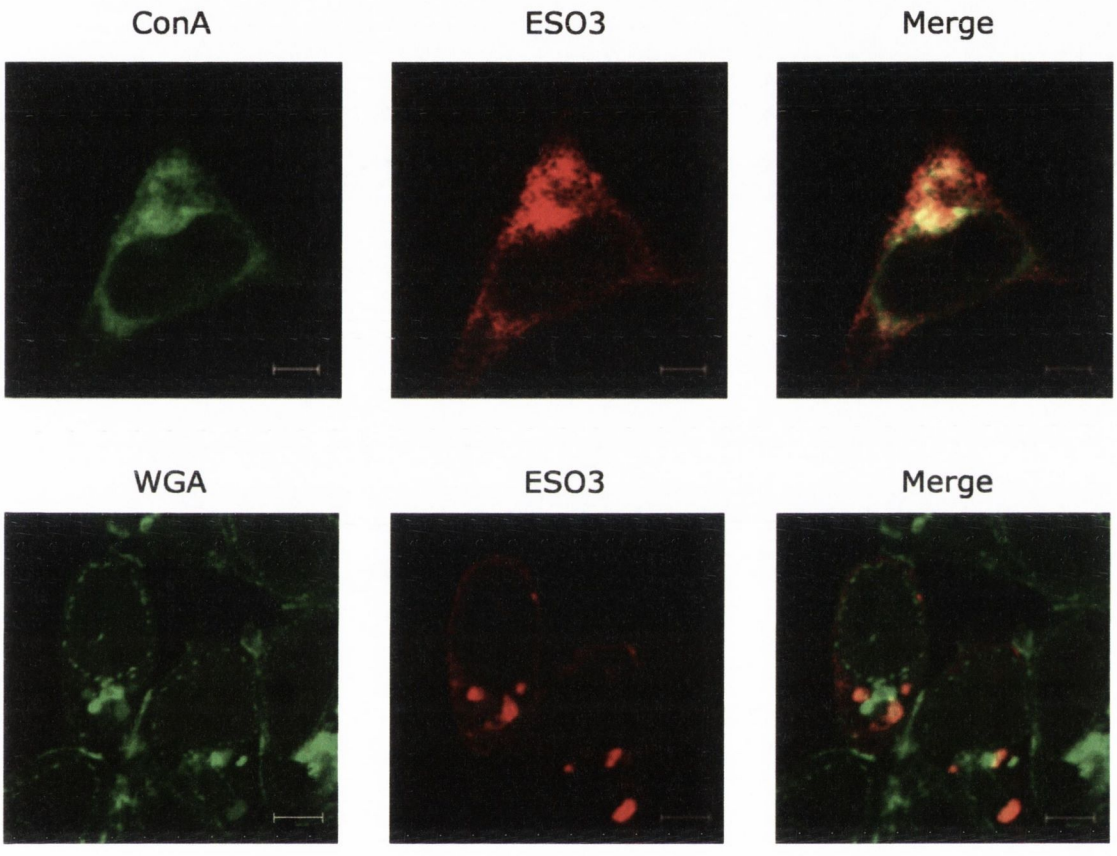


Figure 4.20 ESO3 accumulates in the ER. The distribution pattern of ESO3 in HEK-293 cells transfected with both SERT and ESO3 was compared with staining for the ER and the Golgi apparatus. Immunostaining was performed using rabbit anti-ESO3 antibody, ConA-FITC (1:150) and WGA-FITC (1:200). Bar, 5 μm.

transport assay. PMA treatment of cells expressing SERT alone reduced 5-HT uptake by approximately 35% consistent with previous findings of PKC-mediated down-regulation of 5-HT transport in HEK-293 cells (Qian et al., 1997; Ramamoorthy et al., 1998) (Figure 4.21). As before, 5-HT uptake was reduced by an average of 50% when SERT was co-expressed with ESO3. However, the 5-HT uptake in cells co-expressing SERT and ESO3 was further reduced by the treatment with PMA. Thus, activation of PKC in the presence of ESO3 showed an additive inhibitory effect, indicating that the ESO3 mediated down-regulation of SERT is not linked to the PKC signalling pathway.

4.2.8 Suppression of endogenous ESO3 by siRNA

4.2.8.1 Optimisation of semi-quantitative RT-PCR

The effect of siRNA-mediated knockdown of endogenous ESO3 on SERT uptake activity was analysed to further establish a role for ESO3 in the regulation of SERT function. As shown in Figure 4.1 and 4.2, both ESO3 and SERT are expressed in the human neuroblastoma SHSY5Y cell line. Thus, this cell line appeared to be suitable for studying the regulation of SERT when expressed endogenously in neuronal cells. However, difficulties in assessing specific 5-HT uptake led to the compromise of using HEK-293 cells transiently expressing SERT for the siRNA experiments.

A semi-quantitative RT-PCR approach was used to assess the expression levels of endogenous ESO3 and the control glyceraldehyde-3-phosphate dehydrogenase (GAPDH). Total RNA was isolated from HEK-293 cells and the RT-PCR reaction was optimised for semi-quantitative detection (Marone et al., 2001). To determine the optimal concentration of PCR primers, primers for ESO3 (Figure 4.22) and GAPDH (Figure 4.23) were tested in a concentration range of 0.02 to 0.60 μM according to the procedures described in section 2.2.12 and 2.2.13. The lowest concentration of primers, which produced a robust PCR product without being limiting, was chosen as the optimal concentration. For ESO3, the optimal concentration was determined to be 0.50 μM and for GAPDH it was 0.16 μM. Next, increasing numbers of PCR cycles were assayed to determine the exponential range for the amplification of the ESO3 and

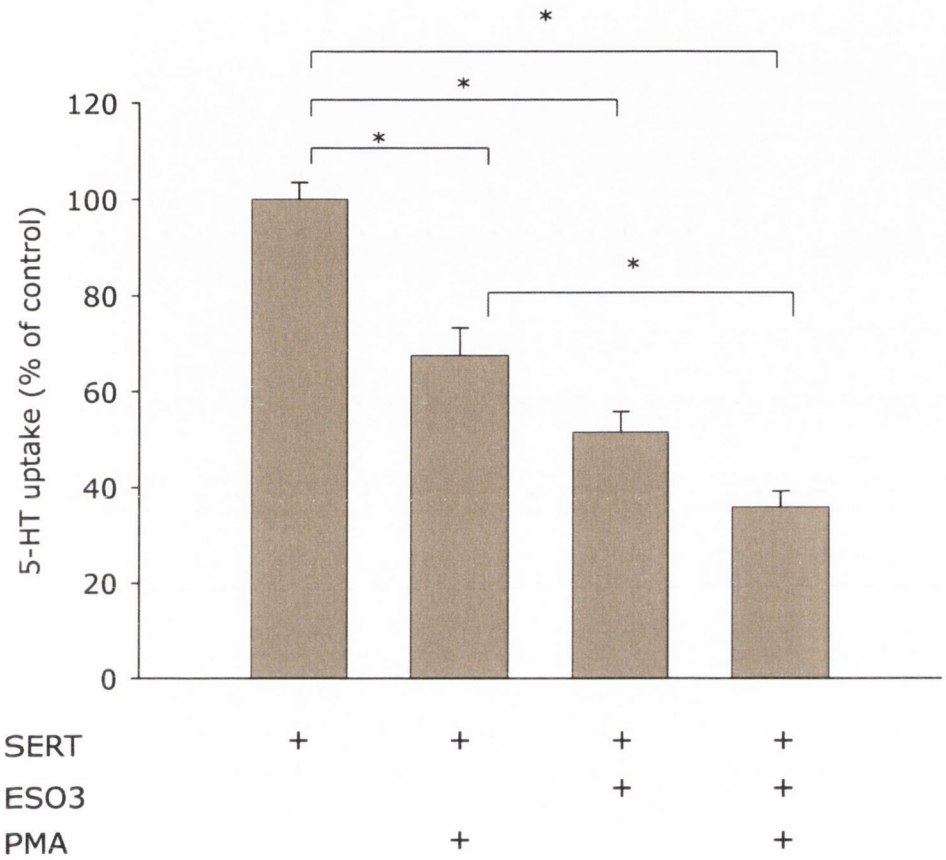


Figure 4.21 Down-regulation of SERT by ESO3 and PKC is mediated by distinct mechanisms. HEK-293 cells were transfected with SERT alone or in combination with ESO3 and treated with vehicle or 1 μM β-PMA for 30 minutes before specific [^{3}H]5-HT uptake was determined at a single concentration of 5-HT (1μM). Values are expressed as percentage of control ± S.E. of triplicate samples. Data are representative of four independent experiments. Experimental conditions that resulted in a significant change from control value or between indicated groups are denoted by *asterisks* (*p <0.01, one-way ANOVA with Bonferroni post hoc test).

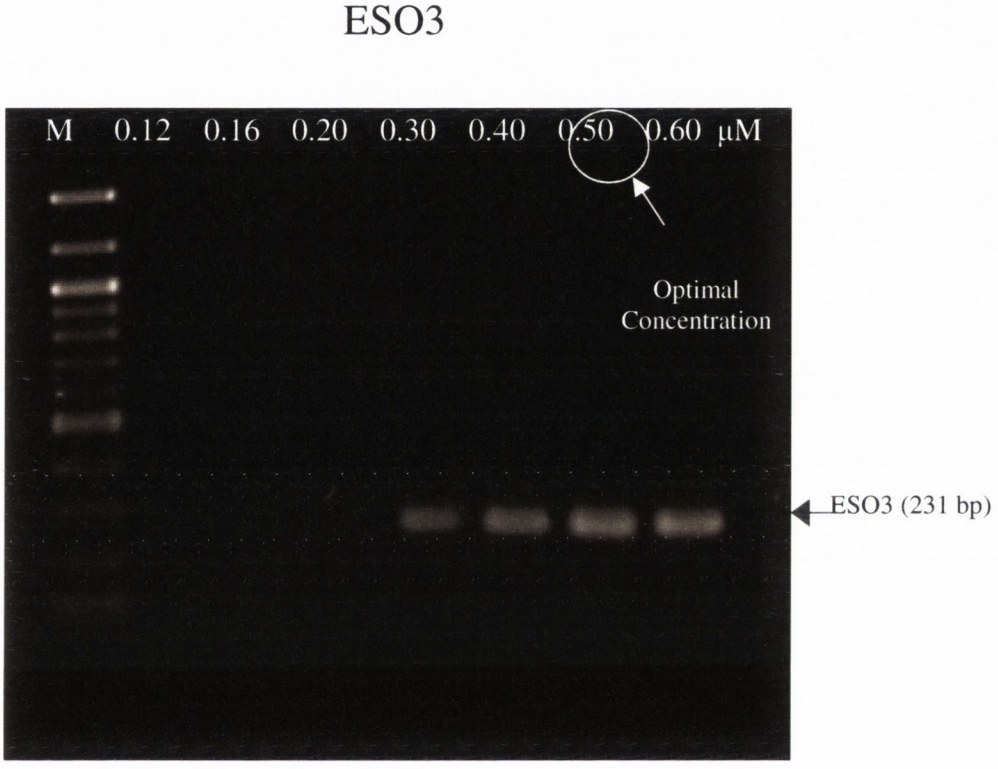


Figure 4.22 Determination of the optimal concentration of ESO3 primers. In order to determine the optimal primer concentration for use in the RT-PCR experiments ESO3 primers were tested in a concentration range of 0.12 to 0.60 μM. Within that range 0.50 μM was determined to be the lowest concentration of primers capable of producing a robust PCR product without being limiting.

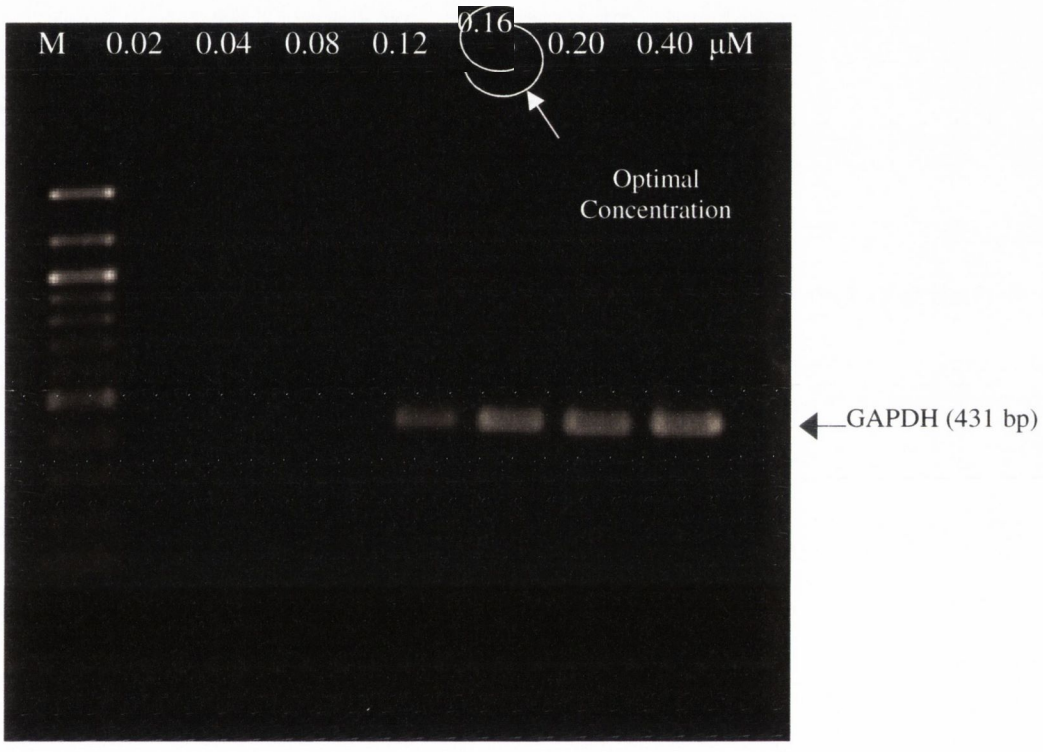


Figure 4.23 Determination of the optimal concentration of GAPDH primers. In order to determine the optimal GAPDH primer concentration for use in the RT-PCR experiments GAPDH primers were tested in a concentration range of 0.02 to 0.40 μM. Within that range 0.16 μM was determined to be the lowest concentration of primers capable of producing a robust PCR product without being limiting.

GAPDH PCR products. PCR cycles ranging from 20 to 32 revealed that both the ESO3 (Figure 4.24) and the GAPDH amplification products (Figure 4.25) reached a plateau at 28-30 cycles. The PCR band intensities were quantified by densitometry and plotted as log versus PCR cycle number (Figure 4.26). The graphs revealed that the linear range of amplification for both ESO3 and GAPDH was within 20 to 26 cycles and 24 cycles were chosen for all subsequent experiments. To determine whether the selected conditions were suitable for semi-quantitative RT-PCR when including both primer pairs in the same reaction, PCR products from reactions with ESO3 and GAPDH primers alone were compared to PCR products obtained from a reaction containing both primer pairs. As shown in Figure 4.27, the amplification products obtained with each separate primer pair were of similar intensity as those obtained from a reaction containing both primer pairs demonstrating that there is no competition between the two primer pairs. Thus, when using the optimised conditions, quantitative analysis of ESO3 levels could be assessed by using GAPDH as an internal control to normalise between individual PCR reactions.

4.2.8.2 Optimisation of siRNA transfection

Small interfering RNAs (siRNAs) are small RNA duplexes of 21-23 nucleotides, homologous to a region within a gene of interest. SiRNAs are introduced into cells by transfection where they target RNA-degrading enzymes to destroy transcripts complementary to the siRNAs. RNA interference is a powerful tool for silencing a gene of interest providing an experimental procedure for testing the function of a specific protein. A pre-validated GAPDH siRNA and a GAPDH negative control siRNA (Ambion) were used to optimise transfection conditions in HEK-293 cells. First, the transfection efficiency of two of Ambion's transfection reagents, siPORT Lipid and siPORT Amine were compared to the efficiency of Lipofectamine 2000 from Invitrogen, which is probably the most widely used transfection reagent for siRNAs. HEK-293 cells were seeded in growth medium without antibiotics and grown to 50%-60% confluence and transfected with siRNAs using each of the three reagents according to the instructions provided by the manufacturers. After 36 hours, GAPDH

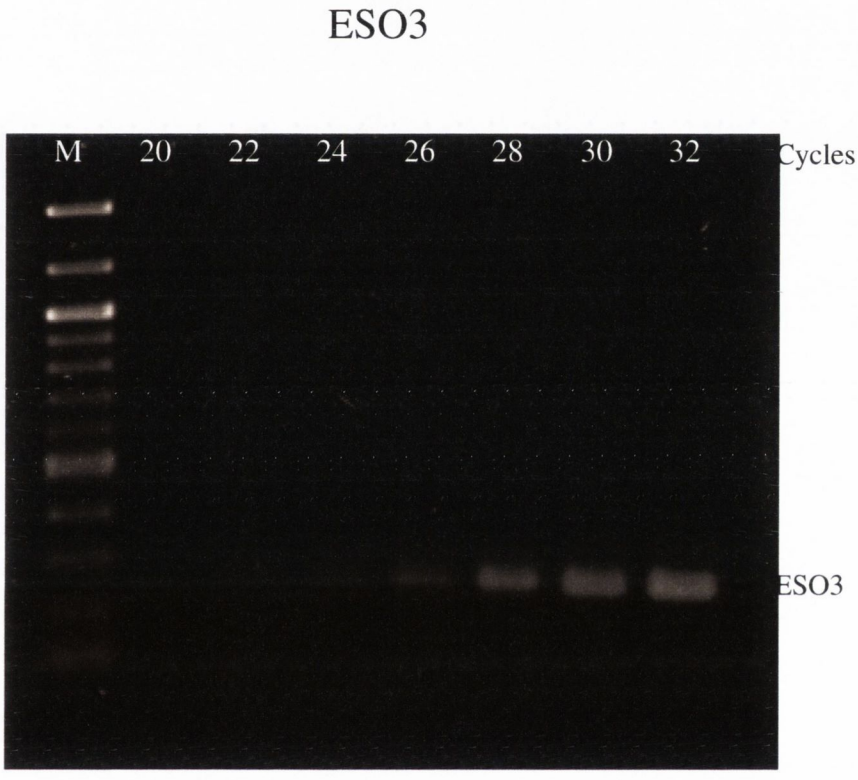


Figure 4.24 Determination of the linear range of ESO3 amplification. A PCR mastermix was prepared and split into 7 aliquots (50µl each), and then subjected to PCR as normal using the optimised concentration of ESO3 primers. Aliquots were removed from the thermal cycler at the indicated cycle number and transferred to a water bath at 72ºC for 7 minutes before cooling on ice.

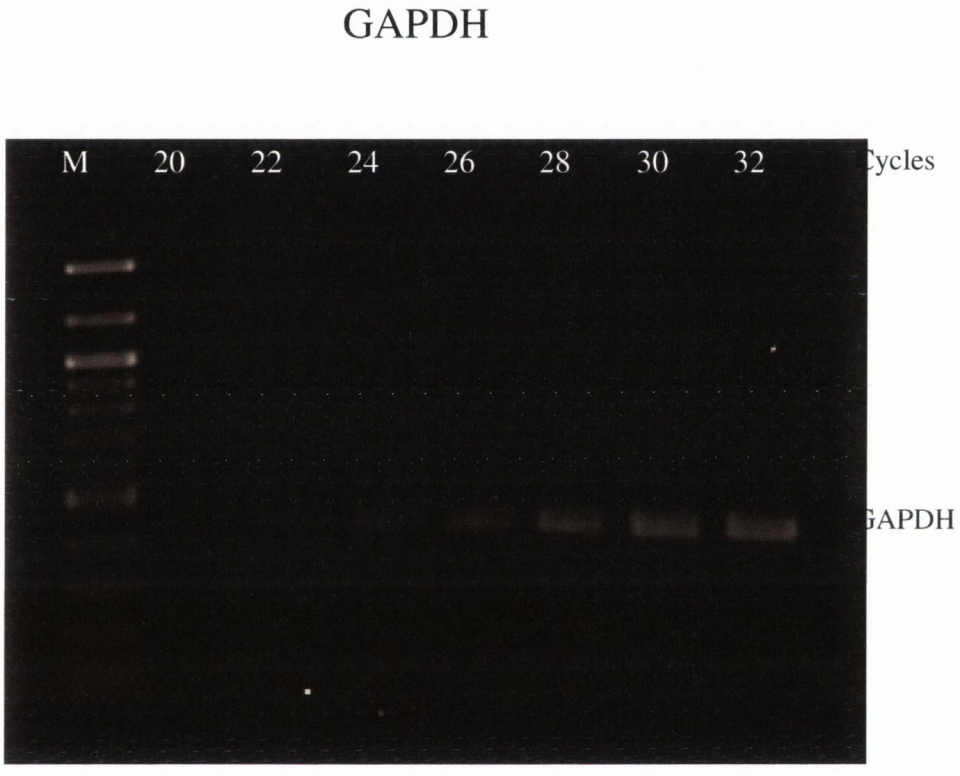


Figure 4.25 Determination of the linear range of GAPDH amplification. A PCR mastermix was prepared and split into 7 aliquots (50µl each), and then subjected to PCR as normal using the optimised concentration of GAPDH primers. Aliquots were removed from the thermal cycler at the indicated cycle number and transferred to a water bath at 72°C for 7 minutes before cooling on ice.

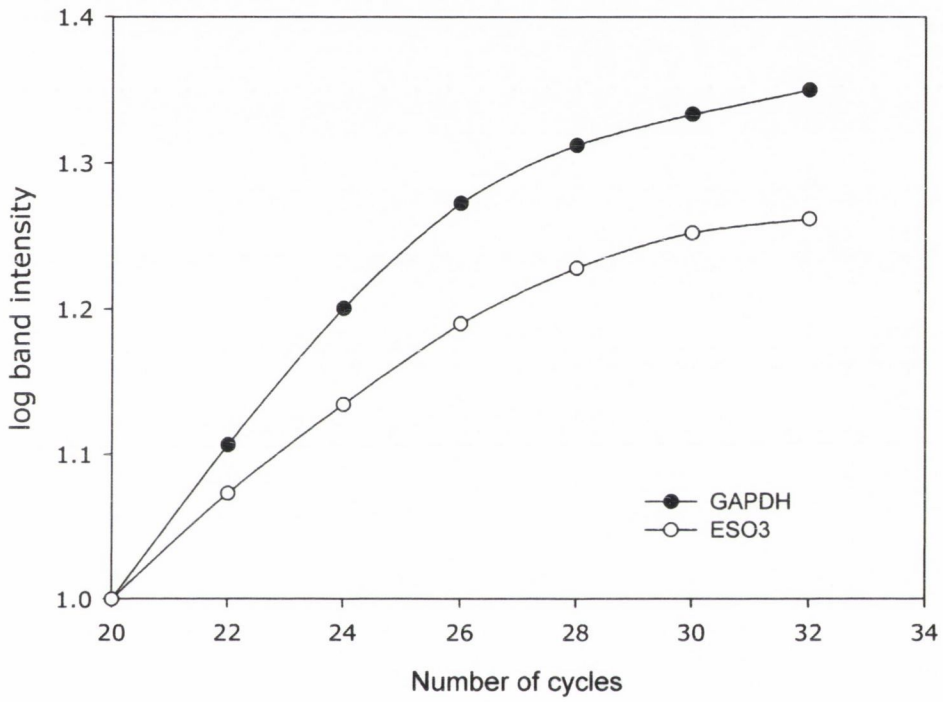


Figure 4.26 Determination of the linear range of amplification for ESO3 and GAPDH. The band intensities of ESO3 and GAPDH PCR products shown in Figure 5.24 and 5.25 were quantified by densitometry and plotted as log versus PCR cycle number relative to the point at 20 cycles. The linear segments correspond to the range of exponential amplification of the PCR products.

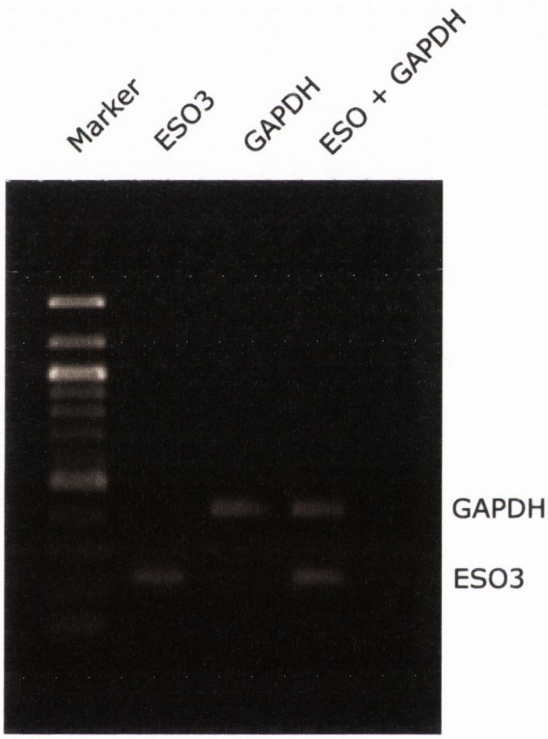


Figure 4.27 Control for competition between primer pairs. PCR reactions were performed under the same conditions with the ESO3 primer pair, the GAPDH primer pair or both primer pairs together. There is no competition between ESO3 and GAPDH primer pairs.

protein levels were analysed by Western blotting and normalised against levels of actin. When siRNA transfection was performed using Lipofectamine, GAPDH protein levels were reduced by approximately 80% in cells transfected with siRNA targeted at GAPDH (50 nM) compared to cells transfected with the GAPDH negative control siRNA (50 nM) (Figure 4.28). In contrast, no reductions in GAPDH levels were observed when either siPORT Lipid or siPORT Amine were used for siRNA transfection. Thus, Lipofectamine was used for further optimisation of siRNA transfection. For instance, when compared to cells in suspension the transfection efficiency of adherent cells was found to be almost three times higher. Also, the optimal cell density for transfection of adherent HEK-293 cells was determined to be 80%-90% resulting in a consistent reduction of GAPDH protein levels by approximately 95% (Figure 4.29).

4.2.8.3 Suppression of endogenous ESO3 expression in HEK-293 cells increases 5-HT uptake

The silencing efficiency of three different siRNA sequences (siRNA sequence A, B, and C, Ambion) targeted at the ESO3 gene was compared against a non-specific control siRNA. The siRNAs were transfected into HEK-293 cells using the conditions optimised for the GAPDH siRNA. After 24 hours total RNA was isolated from the cells and mRNA levels were analysed by semi-quantitative RT-PCR. Compared to the control siRNA all three ESO3 siRNAs resulted in a decrease of ESO3 PCR product demonstrating efficient silencing of ESO3 mRNA (Figure 4.30). However, siRNA sequence B resulted in a greater reduction of ESO3 levels compared to siRNA sequence A and C. Thus, siRNA sequence B was used for all subsequent experiments. ESO3 siRNA sequence B or control siRNA was transfected into HEK-293 cells and levels of ESO3 mRNA were quantified at 12, 24 and 36 hours after transfection (Figure 4.31). At 12 hours after transfection levels of ESO3 mRNA were reduced by an average of 60%. After 24 hours a reduction of 75% was observed and after 36 hours ESO3 mRNA levels were inhibited by 95%. To verify changes in protein expression, total cell extracts were prepared in parallel and equal amounts of total protein were

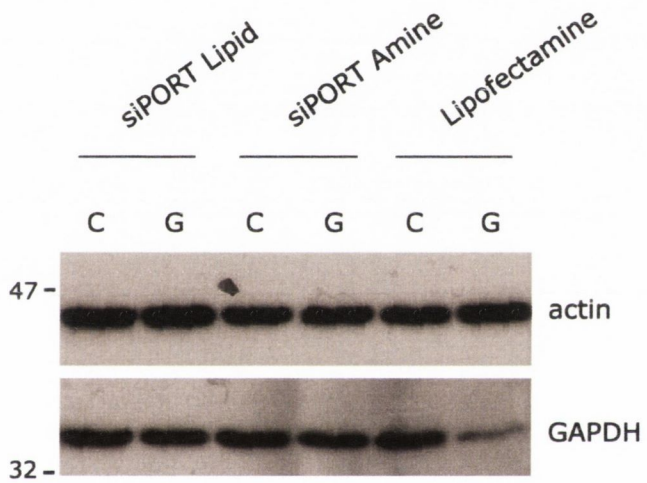


Figure 4.28 Comparison of three different reagents for siRNA transfection. HEK-293 cells were grown to 60% confluence and transfected using one of three transfection reagents; siPORT Lipid, siPORT Amine, or Lipofectamine with either 50 nM control siRNA (C) or 50 nM of pre-validated GAPDH siRNA (G). After 36 hours GAPDH protein levels were analysed by Western blotting. Only siRNA transfection performed with Lipofectamine resulted in significant reduction of GAPDH protein levels.

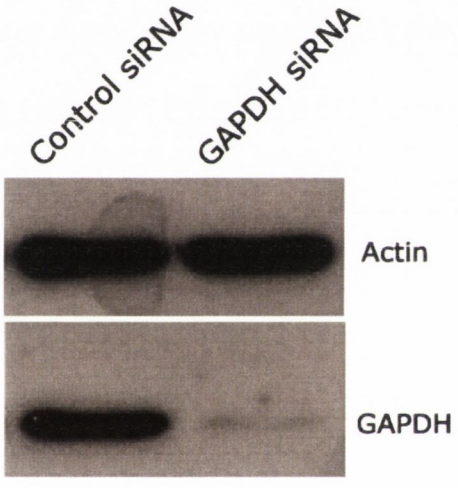


Figure 4.29 Optimised conditions for GAPDH siRNA transfection. HEK-293 cells were grown to 80-90% confluence and transfected with either 50 nM control siRNA (C) or 50 nM of GAPDH siRNA (G). After 36 hours GAPDH protein levels were analysed by Western blotting. Using these optimised conditions, a consistent reduction of GAPDH protein levels of 95% was observed.

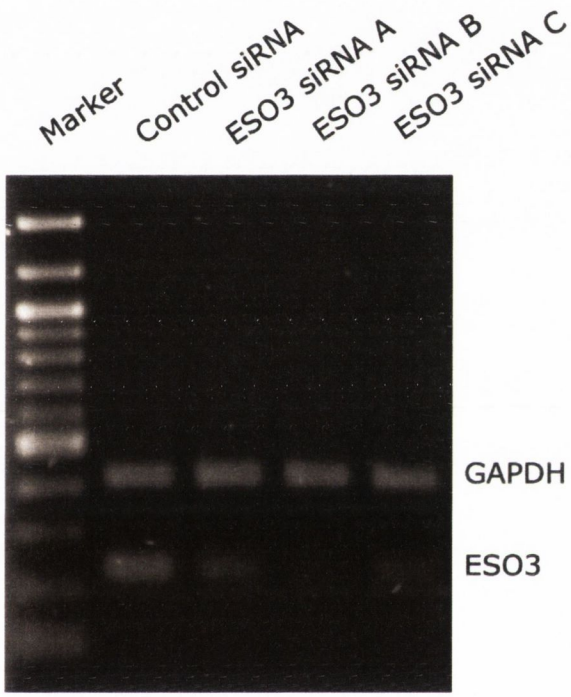


Figure 4.30 Comparison of the effect of three siRNAs on ESO3 mRNA levels. HEK-293 cells were grown to 80% confluence and transfected with control siRNA (50 nM) or ESO3 siRNA sequence A, B, or C (each 50 nM). After 24 hours total RNA was isolated and subjected to RT-PCR for quantitative analysis of mRNA levels.

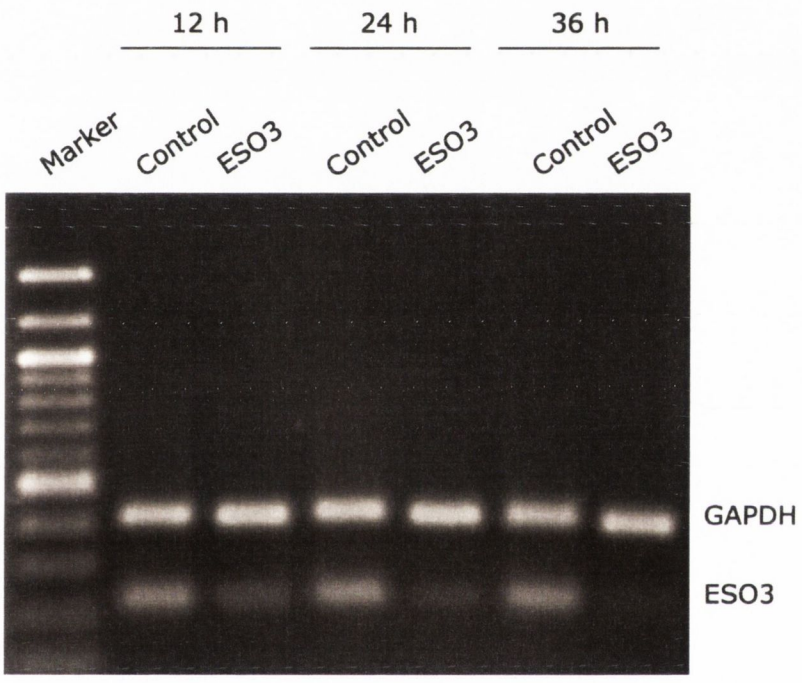


Figure 4.31 Time course effect of siRNA sequence B on ESO3 mRNA levels. HEK293 cells were grown to 80% confluence and transfected with control siRNA (50 nM) or ESO3 siRNA sequence B (50 nM). Total RNA was isolated at 12, 24, and 36 hours after transfection and subjected to semi-quantitative RT-PCR for analysis of ESO3 mRNA levels.

analysed by Western blotting (Figure 4.32). In order to detect the small levels of endogenous ESO3, Western blots were developed using the highly sensitive Supersignal West Femto Maximum Sensitivity Substrate. ESO3 protein levels were reduced in a time-dependent manner consistent with the inhibition of ESO3 mRNA levels. In contrast, levels of GAPDH, which also serves as a control for non-specific effects of the gene knockdown process, were unchanged.

Next, the effect of siRNA-mediated knockdown of ESO3 on 5-HT uptake was examined in HEK-293 cells heterologously expressing SERT. HEK-293 cells were transfected with ESO3 siRNA sequence B or control siRNA. 12 hours after siRNA transfection cells were transfected with SERT in a ratio of 1:4 with pcDNA3 (50 ng SERT and 200 ng pcDNA3 per well in a 24-well plate). Cells were incubated for a further 36 hours before 5-HT uptake assays were performed (Figure 4.33). In cells transfected with the active siRNA directed against ESO3, 5-HT uptake was significantly increased by an average of 15% compared to cells transfected with non-specific siRNA. In parallel suppression of ESO3 protein levels was verified by Western blotting (Figure 4.34). In contrast, total SERT and GAPDH protein expression levels were not affected by transfection with ESO3 siRNA.

4.3 Discussion

In this study a functional role for ESO3 in the regulation of SERT trafficking was established. GST pull-down experiments demonstrated a direct interaction between ESO3 and the N-terminal domain of SERT. Neither the C-terminal domain nor the cytoplasmic N-terminal domain of SERT was able to bind ESO3 consistent with the results obtained using the yeast two-hybrid approach (chapter 3). Also, both endogenous and heterologously expressed ESO3 co-immunoprecipiated with SERT in HEK-293 cell extracts demonstrating an interaction between ESO3 and the full-length SERT. The binding between ESO3 and the N-terminal domain of SERT was sensitive to increased concentrations of both the non-ionic detergent Triton X-100 and the zwitterionic detergent CHAPS as demonstrated in the GST pull-down assays. This may suggest that the binding between ESO3 and SERT involves hydrophobic interactions.

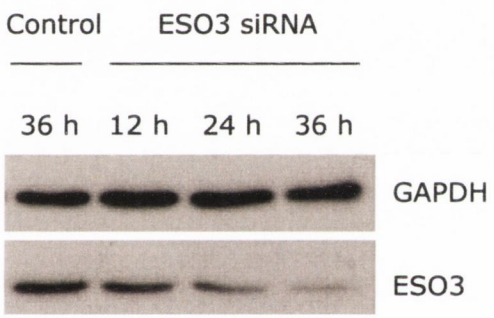


Figure 4.32 Western blot of whole cell lysates from siRNA transfected HEK-293 cells. Cell extracts were prepared from HEK-293 cells transfected with control siRNA (50 nM) or ESO3 siRNA sequence B (50 nM) at 12, 24, and 36 hours after transfection. Equal amounts of protein were analysed by Western blotting and the time-dependent inhibition of ESO3 expression was compared to the control at 36 hours.

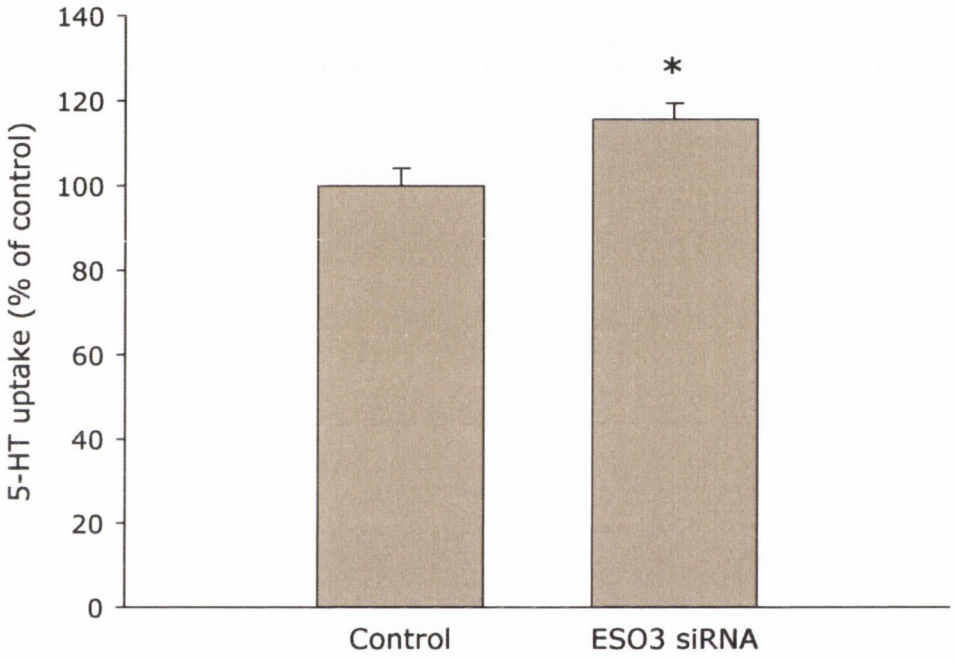


Figure 4.33 5-HT uptake is increased by suppression of ESO3. HEK293 cells were transfected with 50 nM siRNA targeted at ESO3 or 50 nM control siRNA. 12 hours after siRNA transfection cells were transfected with SERT in a ratio of 1:4 with pcDNA3 (50 ng SERT and 200 ng pcDNA3 per well in a 24-well plate). The cells were cultured for a further 36 hours before specific [^{3}H]5-HT uptake was determined at a single concentration of 5-HT (1μM). Data represent the mean ± S.E. of four independent experiments performed in triplicates. *Asterisk* indicates statistically significant increase in 5-HT uptake (* $p < 0.05$, student's *t* test).

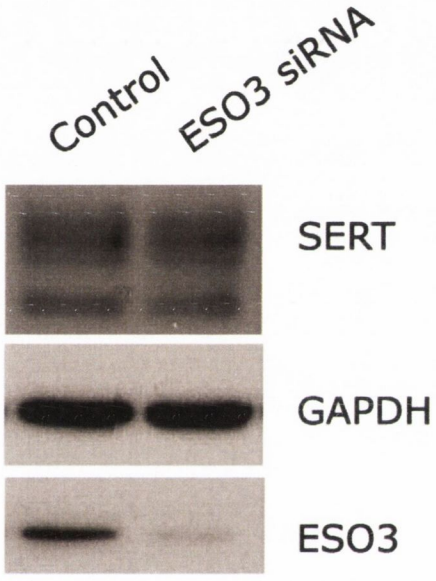


Figure 4.34 Western blots of whole cell lysates from siRNA transfected HEK-293 cells. Cell extracts were prepared from HEK-293 cells transfected with control siRNA (50 nM) or ESO3 siRNA sequence B (50 nM) followed by transfection with SERT. Samples were separated by SDS-PAGE and transferred to a PVDF membrane for immunoblot analysis. The PVDF membrane was cut into three pieces and incubated with antibodies against SERT, GAPDH and ESO3, respectively.

Both Triton and CHAPS are two very commonly used mild detergents for membrane protein purification. However, compared to Triton, CHAPS appeared to improve the binding of ESO3 to the N-terminal domain of SERT. This apparent increase in binding of ESO3 was also observed in preliminary co-immunoprecipitation experiments. This might be explained by the unique properties of each detergent such as their ability to solubilise membrane proteins and to stabilise proteins in general. The concentration of CHAPS used in the biochemical experiments was just below the critical-micelle-concentration (CMC) whereas the concentration of Triton was 10 times above the CMC value. Thus, the apparent inhibiting effect of Triton may be due to the relatively high concentrations of this detergent.

GST pull-down experiments also showed that ESO3 interacts directly with the N-terminal domain of DAT suggesting that the interaction with ESO3 is not unique to SERT, but may be a common feature of monoamine transporters. This also indicates that the ESO3 binding site is located in a region conserved between SERT and DAT. The segment or at least part of the segment comprising residues 61-100 of the N-terminal domain of SERT was found to be essential for interaction with ESO3. The amino acid sequence is almost completely conserved between SERT and DAT within residues 79-100 (Appendix H), suggesting that this domain could be sufficient for interaction with ESO3. The yeast two-hybrid studies revealed that deletion of amino acids 1-60 of SERT had no effect on the binding of ESO3 whereas deletion of amino acids 1-78 abolished the interaction with ESO3. This indicates that residues 61-78 of SERT participate in the binding of ESO3. Because there is no sequence similarity between SERT and DAT within that region it could be speculated that residues located N-terminally to the conserved region do not participate directly in the binding of ESO3 but may confer some structural stability necessary for the interaction with ESO3.

In HEK-293 cells SERT mediated 5-HT uptake was reduced by ESO3 in a dose-dependent manner. There were no changes in SERT protein expression excluding the possibility of non-specific effects due to protein overexpression. A 50% reduction in 5-HT uptake was observed when SERT was co-transfected with ESO3 in a ratio of 1:1. The co-expression of ESO3 with SERT resulted in a V_{max} reduction consistent with the

observed decrease in cell-surface exposure of SERT as revealed by cell surface biotinylation and confocal microscopy. The apparent co-localization of SERT and ESO3 in the ER suggests that ESO3 may exert its function on SERT early in the secretory pathway.

Higher ratios of transfected ESO3 to SERT did not result in further reductions in 5-HT uptake indicating that SERT is regulated by ESO3 via a saturable mechanism. This may suggest the involvement of a limiting endogenous factor of which the ESO3 mediated down-regulation of SERT is dependent on. It could also be speculated that a number of transporters escape before ESO3 is ready or in place to exert its function on SERT, a scenario that is likely to be independent, at least to a certain extent, of the amount of ESO3.

No cleavable N-terminal signal for transport to the ER was predicted for the ESO3 sequence. However, ESO3 was predicted to contain a C-terminally positioned alpha helical domain (Figure 4.3 and 4.4) that could potentially represent a transmembrane domain and serve as a signal for targeting to the ER.

The intracellular transport of membrane proteins starts with their integration into the ER membrane. During ER insertion, the correct folding of the proteins is established and checked by a quality control system that allows only correctly folded proteins to leave the ER. In the case of multimeric complexes, retention ensures that only properly folded assembled multimers are exported from the ER to the Golgi. In some cases, the masking of specific ER retention/retrieval motifs during protein assembly regulates the forward trafficking of membrane proteins through the secretory pathway. For instance oligomerization of neurotransmitter transporters appears to be essential for ER export providing an additional regulatory step in the forward trafficking of transporters (Sitte et al., 2004). Thus, regulation of the export of transporters from the ER may influence the number of transporters expressed at the plasma membrane. The mechanism by which ESO3 sequesters SERT in the ER can only be speculated. The binding of ESO3 to SERT could mask an export signal within SERT required for efficient recruitment to vesicles mediating export from the ER or the binding of ESO3 could induce a conformational change in SERT resulting in exposure of an ER retention signal.

However, when co-expressed with ESO3, SERT displays a glycosylation pattern characteristic of mature transporter. As oligosaccharide side chains are sequentially processed from a high mannose form in the ER to the complex-glycosylated form in the Golgi apparatus, the presence of complex oligosaccharides are often used to monitor the efficiency of the exit of a protein from the ER. Thus, the detection of what appears to be fully glycosylated SERT implies that SERT has been modified by Golgi specific enzymes. This seems to contradict the hypothesis of ESO3 sequestering SERT in the ER. However, several studies suggest that proteins that are retained in the ER can acquire Golgi-specific carbohydrate modifications by enzymes that have been transported from the Golgi to the ER via a retrograde transport mechanism (Storrie et al., 1998; Girod et al., 1999; Karhinen and Makarow, 2004). Perhaps a more likely explanation to the appearance of complex glycosylated SERT could be that ESO3 does not simply retain the transporter in the ER but rather mediates rapid retrieval of SERT from the Golgi to the ER. This scenario allows Golgi-specific modifications of SERT and was originally demonstrated by studies on proteins tagged with the well-known ER retention/retrieval signal KDEL (Pelham, 1988, 1991; Lewis and Pelham, 1992). A faint staining of the ER was in fact obtained with the Golgi marker WGA, suggesting the presence of complex carbohydrates in the ER. ER retention/retrieval signals also include the classic cytoplasmic C-terminal dilysine (KKXX) motif and the cytoplasmic arginine-based RXR motif, which has been implicated in the forward trafficking of ion channels and other membrane proteins through the secretory pathway (Zerangue et al., 1999; Margeta-Mitrovic et al., 2000; Standley et al., 2000). Interestingly, ESO3 does in fact contain an RXR motif positioned at residues 57-59. These cytoplasmic RXR motifs differ from the KKXX motifs in that location of RXR motifs are not limited to the most C-terminal domain of the protein (Shikano and Li, 2003; Gassmann et al., 2005).

Although not very well characterised, COPI and two isoforms of the 14-3-3 proteins, a class of proteins that function as regulators of a wide range of biological processes, have been found to recognise the RXR motif (Yuan et al., 2003). Interestingly, 14-3-3 proteins have been shown to interact with both SERT (Haase et al., 2001) and NET (Sung et al., 2005) via the N-terminal domain.

Thus, ESO3 might be inserted into or anchored to the ER membrane by its putative C-terminally positioned transmembrane domain. If ESO3 is oriented with its N-terminus towards the cytoplasm, thereby exposing the RXR motif, it can interact with SERT at the proposed region located adjacent to and including part of the first transmembrane domain of SERT.

A recent BLAST search with the human ESO3 cDNA sequence revealed identity to a "mRNA similar to guanine nucleotide binding protein-like 1". This entry is provided by the Mammalian Gene Collection as part of a study generating full-length human cDNA sequences (Strausberg et al., 2002). There is no protein sequence associated with this entry and thus, the annotation of this cDNA clone to guanine nucleotide binding protein-like 1 is not evident from the available information. However, this information is very interesting considering the important role of GTPases in regulating ER to Golgi transport (Duden, 2003) and thus, ESO3 may represent a cytosolic factor that regulate incorporation into COPI and/or COPII vesicles.

Co-expression of SERT with the C-terminally deleted ESO3 mutant resulted in an increase in 5-HT uptake similar to what was observed following ESO3 siRNA treatment. This could suggest that the ESO3 mutant impairs the binding of endogenous ESO3 with SERT thereby "rescuing" a fraction of transporter molecules from being retained by endogenous ESO3. The ESO3 deletion mutant might associate with endogenous ESO3, perhaps through a dimerisation motif retained in the deletion mutant, resulting in a dimer or complex unable to bind to SERT.

The siRNA experiments suggest an essential role for ESO3 in the functional regulation of SERT. Unfortunately the siRNA assays could not be performed in a cell line endogenously expressing SERT. Originally the ESO3 siRNAs were intended for use in the human neuroblastoma cell line SHSY5Y. This cell line was found to express small levels of SERT and TPH2 as well as VMAT2, MAO-A and MAO-B (determined by RT-PCR, data not shown). However, because SHSY5Y cells express high levels of NET it was difficult to obtain reliable results of SERT specific 5-HT uptake in these cells. The rat immortalised serotonergic cell line, RN46A (White et al., 1994), would

provide an excellent endogenous system for both SERT and ESO3. However, the human ESO3 siRNA sequence was not suitable for the rat ESO3 mRNA sequence and although an antibody was in fact also raised against rat ESO3 it did not work very well for either immunocytochemistry or Western blotting making it difficult to analyse endogenous rat ESO3.

For the siRNA experiments it was hypothesised that in order to be able to actually measure an effect of the inhibition of endogenous ESO3 on 5-HT uptake, the amount of SERT molecules present per cell should be relatively low. Since transient transfection of SERT normally involves high levels of expression of the transporter, SERT cDNA was diluted with vehicle but kept at the same total amount to achieve transfection of more cells with less SERT cDNA per cell. Using these conditions a significant increase in 5-HT uptake of approximately 15 % was obtained. Using cell surface biotinylation, attempts were also made to verify the expected increase in SERT protein expressed at the cell surface. However, due to the relatively low sensitivity of this method a significant increase in biotinylated SERT could not be demonstrated (data not shown).

ESO3 did not appear to be involved in PKC mediated down-regulation of SERT consistent with the hypothesis that ESO3 regulates SERT at an early stage in the secretory pathway, whereas activation of PKC accelerates the endocytosis of SERT. However, recently both PKC and PKA phosphorylation of specific residues adjacent to a RXR motif in the NMDA receptor subunit NR1 was demonstrated to suppress the retention of NR1, thereby releasing NR1 from the ER to the cell surface (Scott et al., 2001; Scott et al., 2003). Whether this could also be the case with ESO3 is not evident from the experiments performed in this study. However, one interesting observation should be noted in relation to this. When HEK-293 cells transfected with SERT alone was treated with PMA for 30 minutes we observed a 35% maximal reduction in 5-HT uptake consistent with previous reports (Qian et al., 1997). However, when the treatment with PMA was prolonged to 60 minutes a consistent recovery in 5-HT uptake of 10% was observed (data not shown) contradicting previous reports (Ramamoorthy et al., 1998). This recovery in 5-HT uptake could reflect suppression of ER retention via phosphorylation of endogenous ESO3 thereby promoting the release of SERT from the

ER and delivery of SERT to the cell surface. 60 minutes incubation with PMA before recovery in 5-HT uptake would also be consistent with previously reported transport kinetics of membrane proteins through the secretory pathway (Hirschberg et al., 1998; Dahm et al., 2001).

5. SUBCELLULAR REDISTRIBUTION OF THE SEROTONIN TRANSPORTER BY SECRETORY CARRIER MEMBRANE PROTEIN 2

5.1 INTRODUCTION

When going through the list of putative SERT interacting proteins that failed the yeast two-hybrid re-testing analysis in chapter 3, the *s*ecretory *c*arrier-*a*ssociated *m*embrane *p*rotein 2 (SCAMP2) appeared as a likely candidate for participating in a functional interaction with SERT.

SCAMP2 belongs to a family of non-glycosylated membrane proteins characterised by four transmembrane domains and cytoplasmically located N- and C-termini (Brand et al., 1991; Brand and Castle, 1993; Hubbard et al., 2000). The SCAMP family consists of five SCAMP isoforms; SCAMP1, 2 and 3, which all contain an extended N-terminus with three conserved Asp-Pro-Phe (NPF) repeats and SCAMP4 and 5, which lack most of this N-terminal domain present in the other SCAMPs. SCAMP1-4 are all ubiquitously expressed while SCAMP5 is only detectable in brain (Fernandez-Chacon and Südhof, 2000). The NPF repeats have been suggested to play an important role in SCAMP-mediated endocytosis (Fernandez-Chacon et al., 2000). NPF repeats are binding sites for EH (for EPs15 homology) domain-containing proteins. The EH domain is a highly conserved motif comprising approximately 100 residues that is involved in a variety of cellular functions including endocytic recycling of membrane proteins (Montesinos et al., 2005).

SCAMP proteins are conserved across the animal and plant kingdom and exhibit a broad distribution among membranes of the cell surface recycling system, including the endosomal compartment, constitutive secretory vesicles, and regulated secretory

granules, such as large dense-core vesicles of neuroendocrine cells and GLUT4-containing vesicles (Hubner et al., 2002). Furthermore, in neuroendocrine PC12 cells, SCAMP2 has been shown to concentrate along with syntaxin 1A at putative docking/fusion sites for large dense-core vesicles at the cell surface, suggesting a role for SCAMP2 in exocytosis (Liu et al., 2002; Liu et al., 2005).

SCAMP1 and SCAMP3, but not SCAMP2 have been found to be phosphorylated on tyrosine residues (Wu and Castle, 1998) consistent with the prediction of tyrosine phosphorylation sites in SCAMP1 and SCAMP3 but not in SCAMP2. Treatment with EGF of fibroblasts overexpressing the EGF receptor induced phosphorylation of SCAMP1 and SCAMP3, but not SCAMP2, and led to enhanced colocalization of SCAMP3 with the EGF receptor (Wu and Castle, 1998). This suggest that phosphorylation of SCAMPs could play a functional role in the internalisation of membrane proteins.

The cytoplasmic segment linking transmembrane 2 and 3 is unique to SCAMPs and is highly conserved among SCAMP isoforms. This particular segment is known as the E peptide and is thought to compose part of the functional domain of SCAMPs (Hubbard et al., 2000). E peptide derived from SCAMP2 (201-CWYRPIYKAFRSDNS-215) function as an inhibitor of exocytosis in permeabilised mast cells and in neuroendocrine PC12 cells when studied as a free peptide (Guo et al., 2002; Liu et al., 2002). Two mutational variants of the SCAMP2 E peptide (C201A, W202A+Y203A) were not able to inhibit exocytosis demonstrating that the sequence of the E peptide is critical to its ability to block exocytosis. Interestingly, E peptide has been shown to bind lipid bilayers (Hubbard et al., 2000; Zhang et al., 2003) and particularly membranes containing phosphatidylinositol 4,5-biphosphate, $PI(4,5)P_2$, an essential regulator of plasma membrane trafficking (Cremona and De Camilli, 2001), further supporting a role for SCAMP2 in membrane trafficking.

5.2 RESULTS

5.2.1 Cloning of human SCAMP2

HEK-293 cells were tested for expression of the three SCAMP isoforms, SCAMP1, SCAMP2, and SCAMP3. Total RNA was isolated from HEK-293 cells and cDNA was synthesised using oligo dT primers and reverse transcriptase (+RT). A control reaction was included without reverse transcriptase to test for contaminating genomic DNA (-RT). PCR was performed on both +RT and -RT reaction mixtures using gene specific primers for SCAMP1, SCAMP2, and SCAMP3. Analysis of PCR products by gel electrophoresis revealed endogenous expressions of SCAMP2 and SCAMP3 but not SCAMP1 (Figure 5.1). The primers used for amplification of SCAMP2 contained the restriction sites HindIII and NotI for cloning into the expression vector pcDNA3. Thus, the band corresponding to SCAMP2 was excised from the gel, purified and ligated into the pcDNA3 vector and the integrity of the resulting clone was verified by DNA sequencing.

5.2.2 SCAMP2 interacts directly with SERT

5.2.2.1 GST pull-down assay

GST pull-down experiments were carried out as described in section 2.2.31. GST alone or fusion proteins of GST and the N-terminal domain of SERT (amino acids 1-108; GST-NSERT), the C-terminal domain of SERT (amino acids 577-630; GST-CSERT), or the N-terminal domain of DAT (amino acids 1-89; GST-NDAT) were coupled to agarose beads and incubated with cell extracts from HEK-293 cells heterologously expressing SCAMP2. As shown in Figure 5.2, the N-terminal construct but neither GST alone nor the C-terminal construct of SERT was able to bind SCAMP2. Also, SCAMP2 interacts with the N-terminal domain of DAT suggesting a common association of monoamine transporters with SCAMP2.

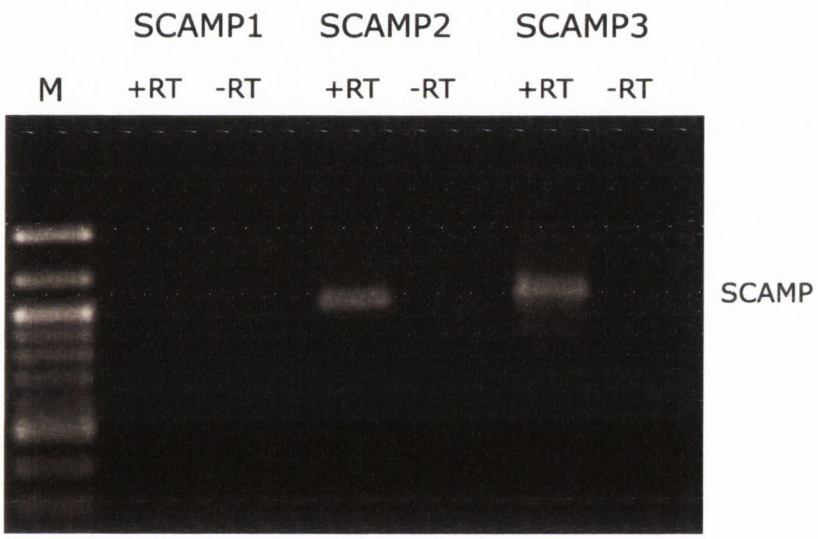


Figure 5.1 Endogenous expressions of SCAMP2 and SCAMP3 but not SCAMP1 in HEK-293 cells. Total RNA was isolated from HEK-293 cells and cDNA was synthesised using oligi-dT primers and reverse transcriptase (+RT) as described in section 2.2.11. A control reaction without reverse transcriptase (-RT) was included. The PCR reactions were performed using gene specific primers recognising SCAMP1, SCAMP2, and SCAMP3, respectively.

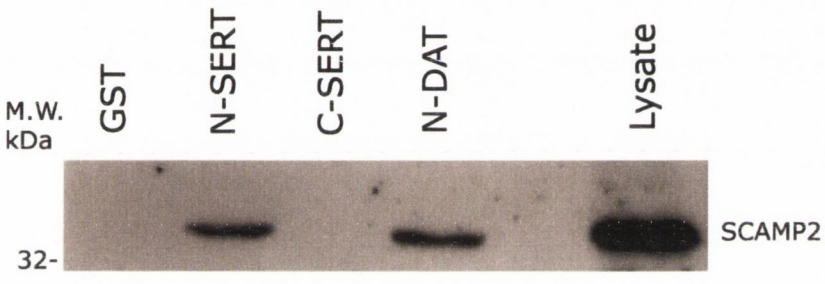


Figure 5.2 SCAMP2 interacts with the N-terminal domain of SERT and DAT. Cell lysate prepared from HEK-293 cells transfected with SCAMP2 was incubated with various GST constructs immobilised on glutathione-agarose beads. Bound proteins were eluted and analysed by immunoblotting using the anti-SCAMP2 antibody.

5.2.2.2 Co-immunoprecipitation

The association of SCAMP2 with SERT was further examined by co-immunoprecipiatation experiments from transfected cells and rat brain homogenate. Using the anti-SERT (C-20) antibody initial experiments were performed on extracts of HEK-293 cells transfected with SCAMP2 alone or in combination with SERT. As shown in Figure 5.3, SCAMP2 co-immunoprecipitated with the SERT antibody, but not with control IgG, only when both SERT and SCAMP2 were expressed in HEK-293 cells.

Further investigations showed that SCAMP2 and SERT also interact in rat brain tissue. Membrane fractions from rat brain were solubilised, and the supernatant was immunoprecipitated with the anti-SERT (EL4) antiserum or control non-immune serum. As shown in Figure 5.4, SCAMP2 co-immunoprecipitated with SERT when using anti-SERT (EL4), whereas no protein was precipitated using control-serum.

5.2.3 Overexpression of SCAMP2 causes a reduction in 5-HT uptake resulting from a cellular redistribution of SERT

5.2.3.1 5-HT transport assay

The effect of SCAMP2 on SERT mediated 5-HT uptake was assessed in HEK-293 cells. Co-transfection of SERT (0.5 μg/well in a 6 well plate) with increasing amounts of SCAMP2 (0-1 μg/well) caused a dose-dependent reduction in 5-HT uptake (Figure 5.5). When SERT was co-transfected with SCAMP2 in a ratio of 1:1, specific 5-HT uptake was reduced by approximately 30%. 5-HT uptake was further reduced at increasing ratios of SCAMP2 to SERT. The increasing expression of SCAMP2 had no effect on total levels of SERT as quantified by Western blotting (Figure 5.6).

In cells transfected with SCAMP2 and SERT, the maximal 5-HT uptake capacity was decreased by an average of 30% when compared to cells expressing SERT alone (V_{max} 7.7 ± 0.4 pmol/min/10^6 cells in cells expressing SERT alone *versus* 5.4 ± 0.5 pmol/min/10^6 cells in cells expressing SERT and SCAMP2) (Figure 5.7). No

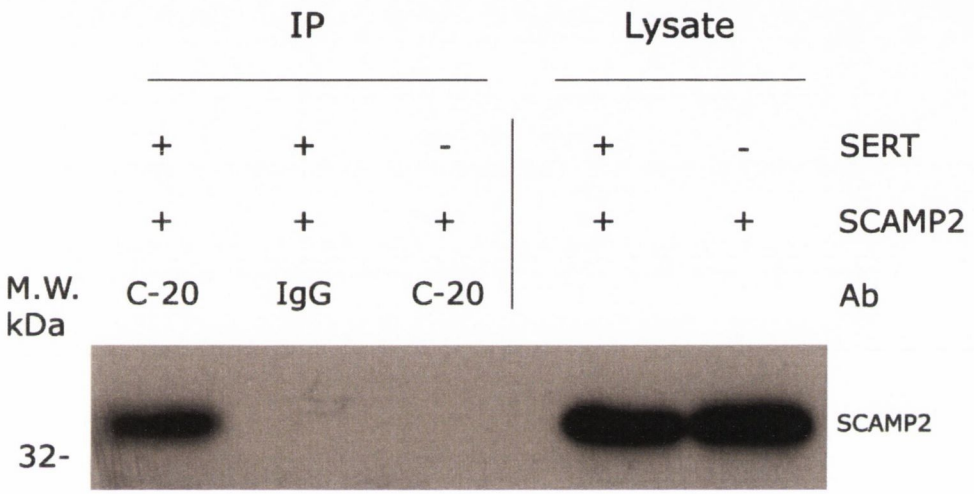


Figure 5.3 SCAMP2 co-immunoprecipitates with the full-length SERT in transfected HEK-293 cells. HEK-293 cells transiently expressing SERT and SCAMP2 or SCAMP2 alone were immunoprecipitated using anti-SERT(C-20) antibody or control IgG. Co-immunoprecipitated SCAMP2 was detected by immunoblotting.

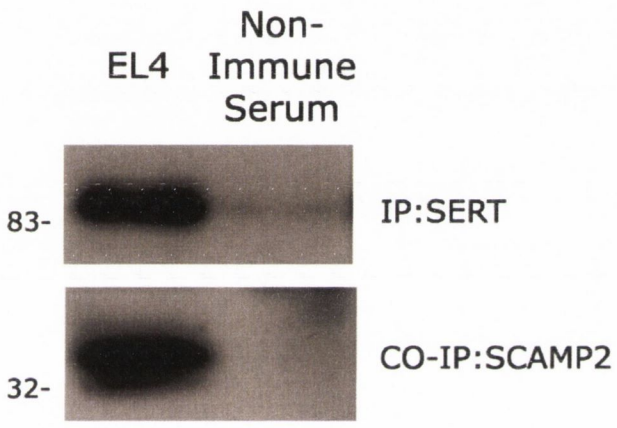


Figure 5.4 SERT interacts with SCAMP2 in rat brain. Rat brain extracts were immunoprecipitated with anti-SERT(EL4) serum or rabbit non-immune serum. Co-immunoprecipitated SCAMP2 was visualised by Western blotting.

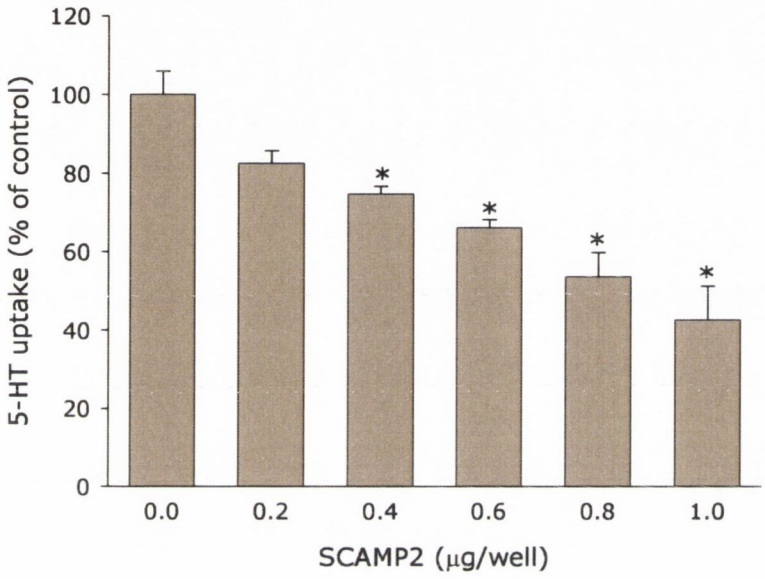


Figure 5.5 5-HT uptake is reduced by SCAMP2 in a dose-dependent manner. SERT (0.5 μg/well for a 6-well plate) was co-transfected with increasing amounts of SCAMP2 (0-1 μg/well) as indicated and specific [^{3}H]5-HT uptake was determined at a single concentration of 5-HT (1μM). Values are expressed as percentage of control ± S.E. of triplicate samples from a single experiment and are representative of three independent experiments. *Asterisk* indicates statistically significant reduction in 5-HT uptake compared to control (* $p < 0.01$, one-way ANOVA with Bonferroni post hoc analysis).

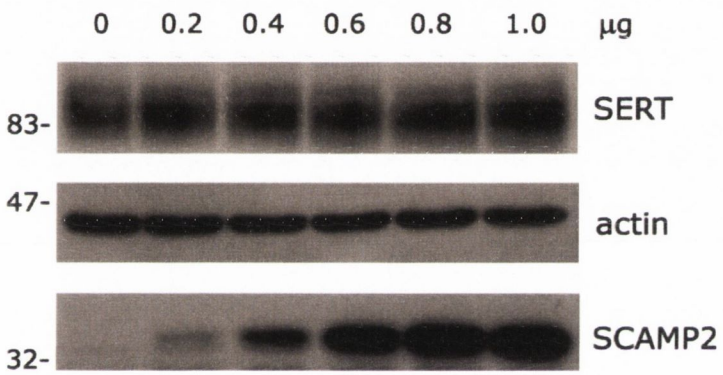


Figure 5.6 Western blot of whole cell lysates from co-transfected HEK-293 cells. Expression levels of SERT are not affected by SCAMP2 overexpression within the 0-1 μg range used in the dose-dependent 5-HT uptake experiments. β-actin was used as a control to verify equal protein loading.

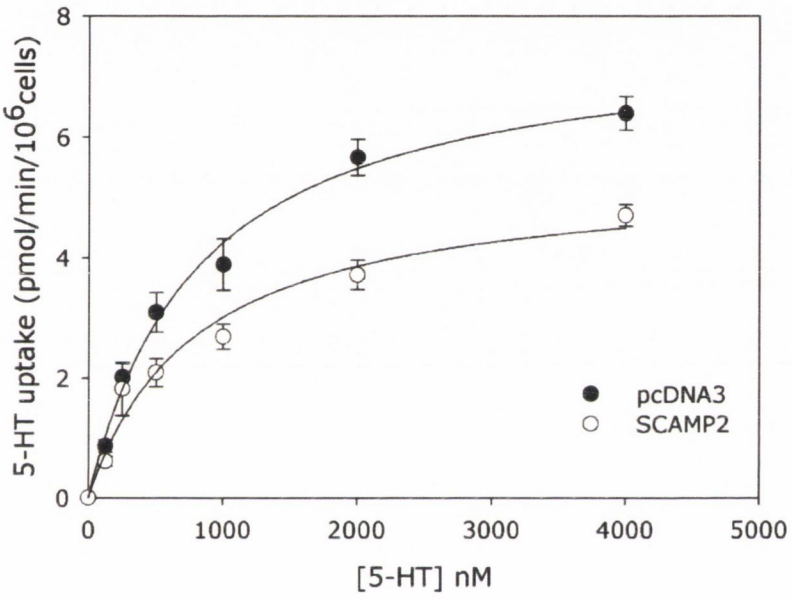


Figure 5.7 Overexpression of SCAMP2 decreases SERT uptake activity. HEK-293 cells were transfected with SERT (0.5 μg/well) and either pcDNA3 control vector or SCAMP2 (each 0.5 μg/well) in 6-well plates. Kinetic parameters of [^{3}H]5-HT were assessed as described in experimental procedures. Each data point was determined in triplicate and was plotted as mean value ± S.E. The saturation curves are representative of four independent experiments.

significant changes in the apparent affinity for the transporter were observed (K_m 814 ± 107 nM in cells expressing SERT alone *versus* 783 ± 193 nM in cells expressing SERT and SCAMP2).

5.2.3.2 Cell surface biotinylation

Cell surface biotinylation experiments were performed to establish whether the observed decrease in V_{max} in the presence of SCAMP2 is paralleled by changes in the number of SERT molecules expressed on the cell surface. Surface proteins of HEK-293 cells transfected with SERT (0.5 μg/well in a 6-well plate) alone or in combination with SCAMP2 (0.5 μg/well) were biotinylated with the membrane impermeant biotinylation reagent sulfo-NHS-biotin Cells were then solubilised and biotinylated proteins were collected with avidin beads. Equal volumes of total protein lysates and non-biotinylated protein and two to three times the volume of biotinylated protein were analysed by Western blotting using the anti-SERT (C-20) antibody (Figure 5.8A). Immunoblots were re-probed for β-actin, confirming that no intracellular proteins were labelled with biotin. Blots were analysed by densitometry and the relative amounts of SERT were quantified taking into account the volumes used of each fraction. When SERT alone was transfected, cell surface and intracellular protein was distributed on average in a ratio of 30%:70%. When co-tranfected with SCAMP2, the distribution of SERT changed to a ratio of 20%:80% cell surface *versus* intracellular protein. Thus, cell-surface (biotinylated) SERT was decreased by approximately one third under conditions where total levels of transporter molecules remain unchanged (Figure 5.8B). The reduction in SERT levels on the cell surface corresponds well with the changes in SERT uptake activity, suggesting that SCAMP2 exert its function by causing a redistribution of SERT.

5.2.4 SERT and SCAMP2 co-localize in HEK-293 cells

Confocal laser-scanning microscopy was used to examine the subcellular steady-state localization of SERT and SCAMP2 in HEK-293 cells. In cells transfected with SERT

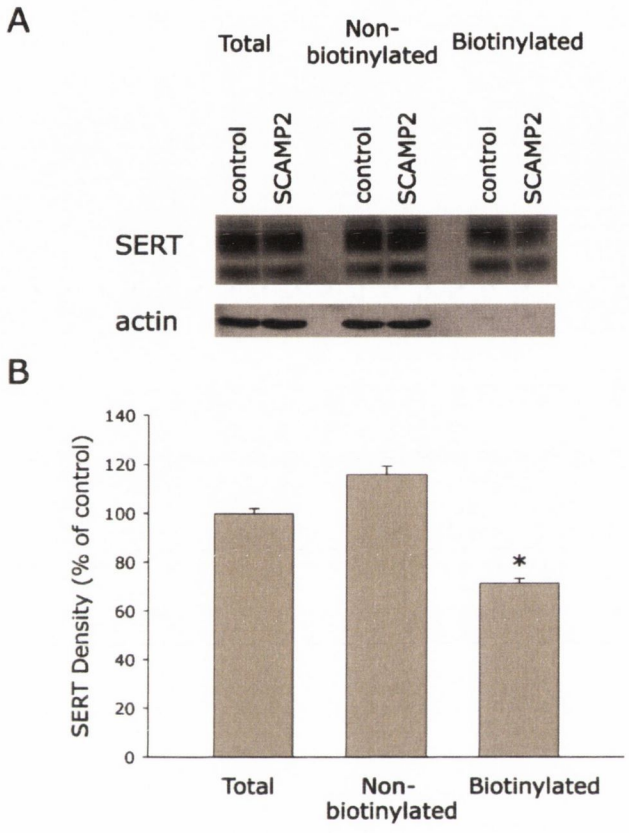


Figure 5.8 Overexpression of SCAMP2 decreases SERT cell surface expression. (A) Representative immunoblot of biotinylation experiment using cells transfected with SERT alone (0.5 μg/well) (control) or in combination with SCAMP2 (0.5 μg/well), showing SERT immunoreactivity in total, nonbiotinylated and biotinylated fractions. The blot was stripped and re-probed for β-actin. (B) Quantification of signals is based on densitometry measurements of immunoblots from four separate biotinylation experiments. Data are expressed as percentage of control ± S.E. *Asterisk* indicates statistically significant reduction in biotinylated SERT protein compared to control ($p < 0.05$; student's *t* test).

alone, the transporter partially co-localized with endogenous SCAMP2 both at the cell surface in well-defined punctuate structures and in intracellular compartments (Figure 5.9A). When overexpressing SCAMP2 in the absence of SERT, SCAMP2 exhibited an overall distribution similar to the endogenously expressed protein. In cells overexpressing both SERT and SCAMP2, SERT co-localized extensively with SCAMP2 in intracellular structures. Under these conditions it appeared that the amount of SERT at the cell surface is diminished, but this apparent change in distribution cannot be easily quantified from confocal microscopy images, and is much better assessed by cell surface biotinylation as demonstrated in the previous paragraph. However, the extensive co-localization between SERT and SCAMP2 supports a direct role for SCAMP2 in regulating the subcellular distribution of SERT.

Using triple labelling the localization of SERT and SCAMP2 was compared with the staining pattern of the transferrin receptor (TfR), a marker of the general endocytic recycling pathway (Figure 5.9B). While SERT almost completely co-localized with SCAMP2, there was very little overlap with the TfR, which exhibited a punctuate staining throughout the cell. In summary, SERT appears to co-localize with SCAMP2 in discrete intracellular structures that are largely distinct from TfR-positive endosomes.

5.2.5 Endogenous SERT co-localizes with SCAMP2 in RN46A cells

To further characterise the co-localization between SERT and SCAMP2 the endogenous distribution of SERT and SCAMP2 was examined in an immortalised serotonergic rat raphe cell line RN46A-B14 (White et al., 1994). RT-PCR revealed endogenous expression of SCAMP2 as well as SCAMP1 and SCAMP3 in RN46A cells (data not shown). Immunostaining followed by confocal microscopy demonstrated extensive co-localization of SERT and SCAMP2 in discrete structures near the plasma membrane and in intracellular compartments (Figure 5.10A).

Next, triple labelling was used to compare the localization of SERT and SCAMP2 with different organelle markers (Figure 5.10B). Similar to the findings in HEK-293 cells, there was no overlap with the endosomal marker TfR and also not with TGN38, a

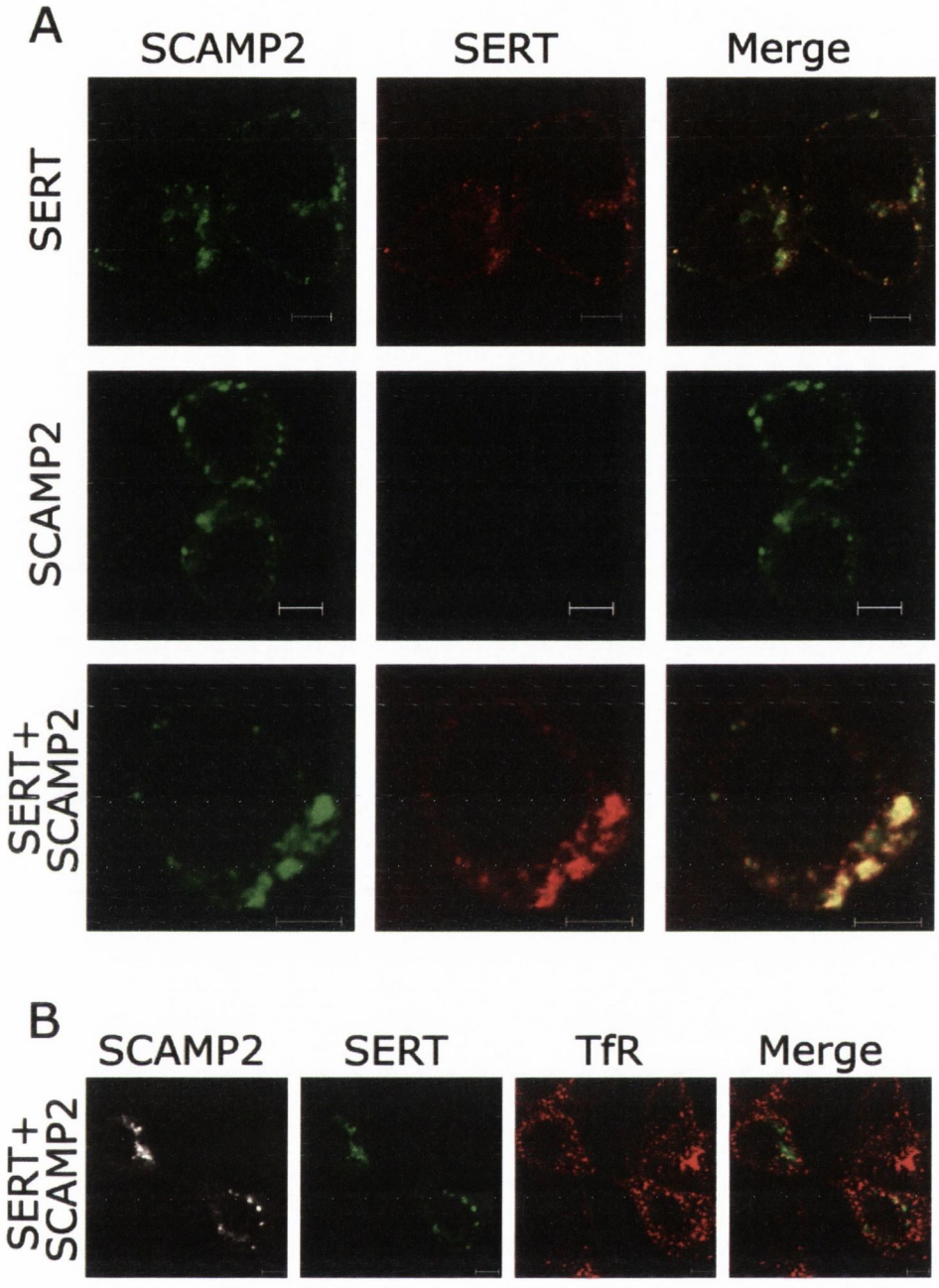


Figure 5.9 SERT co-localizes with SCAMP2 in HEK-293 cells. (A) SERT and SCAMP2 were transfected individually or in combination (in a 1:1 ratio) into HEK-293 cells and their distribution patterns were assessed by confocal microscopy as described in experimental procedures. Double immunostaining was performed with the primary antibodies: mouse anti-SERT(AB-N09) and goat anti-SCAMP2. Secondary antibodies used were: anti-mouse-Texas Red and anti-goat-FITC (B) Comparison of the distribution of SERT and SCAMP2 with the endosomal marker TfR. Immunostaining was performed using the primary antibodies: rabbit anti-SERT(EL4), goat anti-SCAMP2, and mouse anti-TfR. Secondary antibodies were: anti-rabbit-FITC, anti-Goat-Cy5, and anti-mouse-Texas Red. Bar, 5 μm.

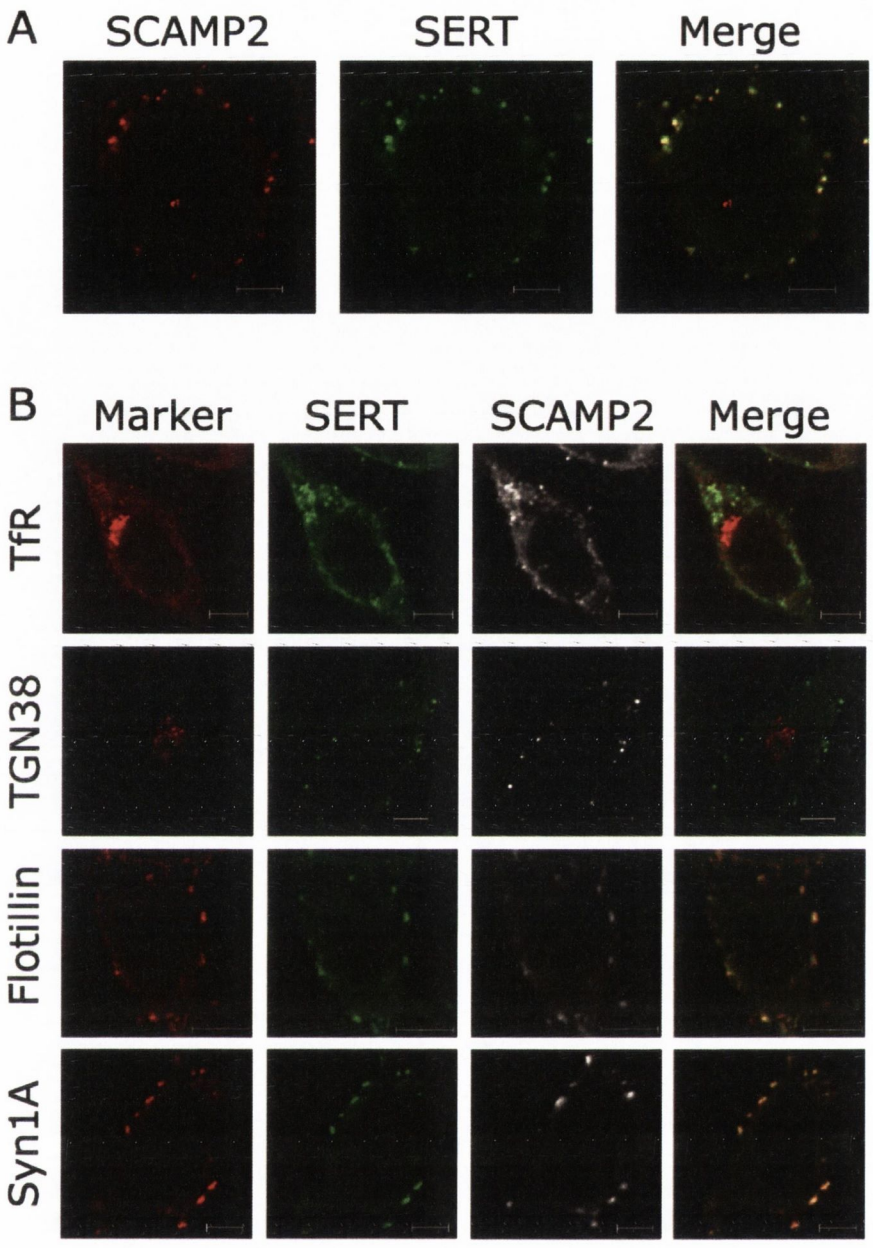


Figure 5.10 Co-localization of endogenous SERT with SCAMP2 in immortalised neurons. (A) Double staining was performed on RN46A cells to demonstrate co-localisation between endogenous SCAMP2 and SERT. (B) Triple labelling comparing the distribution of SERT and SCAMP2 with the indicated markers. Immunostaining was performed using rabbit anti-SERT(EL4), goat anti-SCAMP2, and mouse antibodies against the indicated markers. Secondary antibodies were: Cy5 anti-goat, FITC anti-rabbit, and Texas Red anti-mouse. Bar, 5 μm.

commonly used marker for the trans-Golgi network. In contrast, the lipid raft marker flotillin-1 (Bickel et al., 1997) co-localized extensively with SERT in SCAMP2-containing vesicles. Likewise, syntaxin 1A, which has previously been shown to interact directly with SERT (Haase et al., 2001; Quick, 2003) and to co-localize with SCAMP2 in PC12 cells (Liu et al., 2002), also showed extensive co-localization with SERT and SCAMP2.

5.2.6 Similarly to SERT, SCAMP2 is present in lipid rafts

Confocal microscopy demonstrated extensive co-localization between SERT and SCAMP2 and the lipid raft marker flotillin-1. SERT was previously demonstrated to associate with lipid rafts at both the cell surface and in intracellular compartments (Magnani et al., 2004). To examine the distribution of SCAMP2, rat brain was homogenised and lysed in 2% Brij-58 and fractionated through a discontinuous sucrose gradient. Detergent-resistant membrane fractions and their associated proteins migrate to the upper, low-density region of the gradient, whereas solubilised proteins remain in the lower, high-density fractions. As expected, flotillin-1 was found in the upper low-density raft fractions (1 to 3), whereas the non-raft protein TfR was present only in high-density fractions (6 to 8) confirming that this procedure effectively separates raft from non-raft proteins (Figure 5.11). Both SERT and syntaxin 1A were also found in low-density fractions, confirming previous findings (Magnani et al., 2004). More importantly, SCAMP2 was also enriched in raft fractions, suggesting the possibility that SERT and SCAMP2 associate in specialised domains within cellular membranes.

5.2.7 The presence of SCAMP2 prevents PKC-mediated down-regulation of SERT in HEK-293 cells

The down-regulating effect of SCAMP2 on SERT cell surface expression resembles the decrease in cell surface SERT observed upon activation of PKC by phorbol esters (Qian et al., 1997). To examine a potential link between the PKC- and SCAMP2-

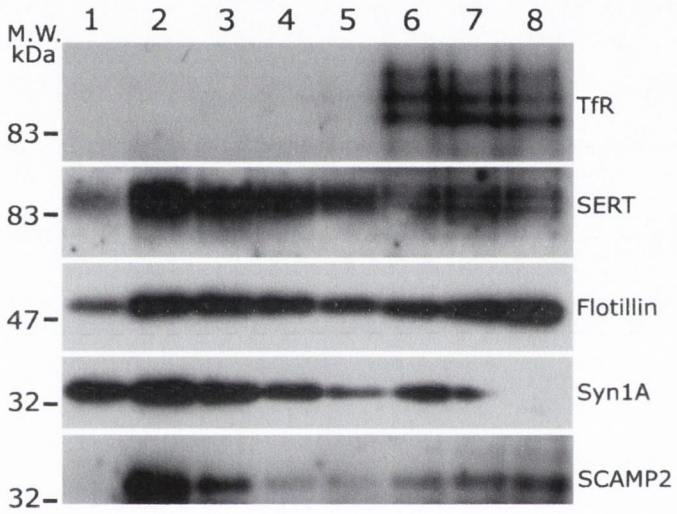


Figure 5.11 SCAMP2 associates with lipid rafts in rat brain tissue. Crude homogenate from rat brain was lysed in 2% (w/v) Brij-58 and fractionated on a discontinuous sucrose gradient, as detailed in experimental procedures. Aliquots of gradient fractions were separated by SDS-PAGE and analysed using the antibodies against the indicated proteins.

mediated down-regulation of SERT, HEK-293 cells expressing SERT in the presence or absence of SCAMP2 were treated with vehicle (DMSO) or 2 μM β-PMA for 10 or 30 minutes (Figure 5.12). In cells expressing SERT alone 5-HT uptake was reduced by approximately 25% and 50% after 10 and 30 minutes incubation with PMA, respectively. 5-HT uptake was reduced by approximately 30% in cells expressing SERT in combination with SCAMP2 (ratio 1:1). However, no further reduction in 5-HT uptake was observed following incubation with PMA, suggesting that SCAMP2 and PKC activation regulate SERT through the same saturable pathway or, that the presence of SCAMP2 renders SERT resistant or inaccessible to PKC-mediated down-regulation. It should be noted that this experiment was only repeated twice and therefore is considered as a preliminary result.

5.2.8 Cysteine-201 within the highly conserved E peptide of SCAMP2 is critical for the cellular redistribution of SERT

The most conserved structural segment within the SCAMP2 family is the so-called E peptide, which is positioned at the cytoplasmic membrane surface linking the second and third transmembrane domain. This segment has been demonstrated to play a critical role at a late step in exocytosis in neuroendocrine (Liu et al., 2002) and mast cells (Guo et al., 2002). Mutations of selected residues within the E peptide greatly affected its ability to regulate exocytosis when studied as a free peptide (Guo et al., 2002). Therefore, to test whether the E peptide is involved in the SCAMP2 mediated down-regulation of SERT two critical single amino acid mutations (C201A and W202A) were generated within the E peptide. Using the anti-SERT (C-20) antibody, co-immunoprecipitation experiments were performed on HEK-293 cells transfected with SERT in combination with C201A or W202A. As shown in Figure 5.13, both the C201A and the W202A mutant co-immunoprecipitated with SERT, suggesting that these residues do not participate or influence the binding of SCAMP2 to SERT.

Next, the effect of the two mutants on SERT uptake activity was examined in HEK-293 cells (Figure 5.14). While the W202A mutant behaved similar to wild-type SCAMP2,

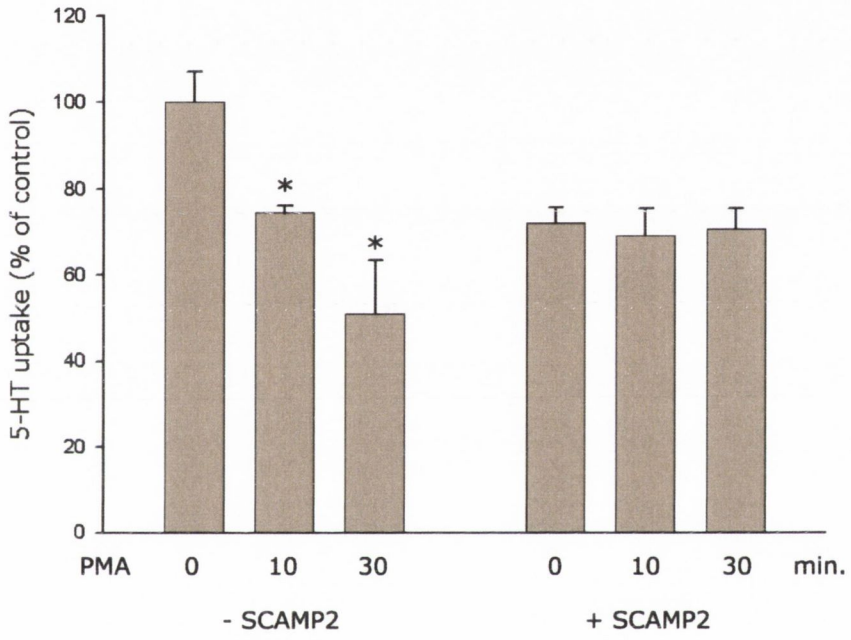


Figure 5.12 SCAMP2 prevents PKC-mediated SERT down-regulation. HEK-293 cells transfected with SERT alone or in combination with SCAMP2 were treated with vehicle or 2 μM β-PMA for 10 or 30 minutes before specific [^{3}H]5-HT uptake was determined at a single concentration of 5-HT (1μM). Values are expressed as percentage of control ± S.E. of triplicate samples. Data are representative of two independent experiments. *Asterisk* indicates statistically significant reduction in 5-HT uptake compared to PMA at t_0 ($p < 0.01$; one-way ANOVA with Bonferroni post hoc test).

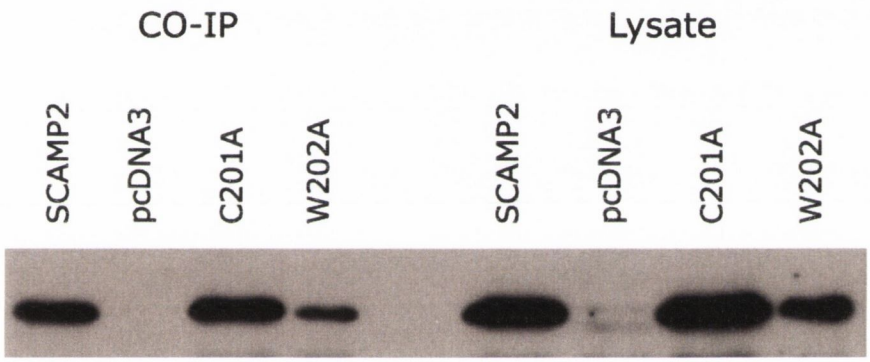


Figure 5.13 Mutations of C201 or W202 do not affect the binding of SCAMP2 to SERT. HEK293 cells transfected with SERT in combination with control vector, wild-type SCAMP2, C201A or W202A were immunoprecipitated using anti-SERT (C-20) antibody. Co-immunoprecipitated SCAMP2 was visualised by Western blotting.

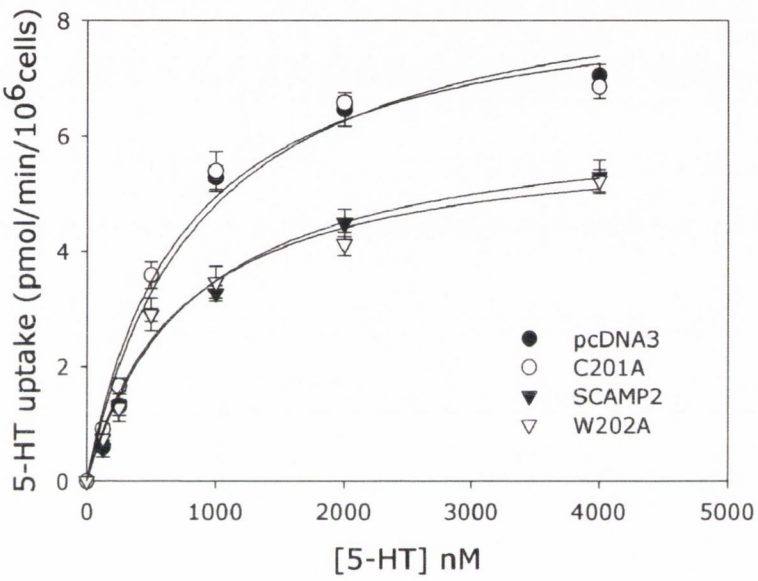


Figure 5.14 The SCAMP2 mutant C201A has no affect on SERT uptake activity. HEK-293 cells were transfected with SERT in combination with control vector, wild-type SCAMP2, C202A or W202A. Kinetic parameters of [^{3}H]5-HT were assessed as described in experimental procedures. Each data point was determined in triplicate and was plotted as mean value ± S.E. The saturation curves are representative of five independent experiments.

i.e. causing a decrease in V_{max} of approximately 30% compared to the control (V_{max} 8.9 ± 0.8 pmol/min/10^6 cells in cells expressing SERT alone *versus* 6.3 ± 0.5 pmol/min/10^6 cells in cells expressing SERT in combination with wild-type SCAMP2 and 6.1 ± 0.4 pmol/min/10^6 cells in cells expressing SERT together with W202A), overexpression of the C201A mutant had no effect on SERT uptake activity, exhibiting a profile similar to the control (V_{max} 8.6 ± 0.6 pmol/min/10^6 cells). There were no significant changes in K_m values among any of the constructs (control, K_m 870 ± 221 nM; wild-type SCAMP2, K_m 817 ± 160 nM; C201A, K_m 734 ± 150 nM; W202A, K_m 723 ± 143 nM). Although the W202A mutant was consistently found to be expressed at lower levels, there was no difference in expression levels between wild-type SCAMP2 and the C201A mutant (Figure 5.15). This suggests that the inability of the C201A mutant to inhibit SERT-mediated 5-HT uptake is not due to reduction of SCAMP2 protein expression, but rather due to impaired function of SCAMP2. Surface biotinylation experiments confirmed that the C201A mutant was unable to reduce the cell surface expression of SERT (Figure 5.16A and B).

Together these results demonstrate that a single amino acid replacement in SCAMP2 completely abolishes the functional effect of SCAMP2 on SERT function without disrupting the interaction with SERT.

5.3 Discussion

This study reveals SCAMP2 as a novel SERT-interacting protein that affects SERT subcellular distribution via binding to the N-terminal domain of the transporter.

In fibroblasts, SCAMPs are concentrated in compartments involved in endocytosis and recycling of membrane proteins while in neurons and other cell types having regulated transport pathways, SCAMPs are also found on secretory organelles involved in regulated exocytosis, such as synaptic vesicles, secretion granules and transporter vesicles (Brand et al., 1991; Brand and Castle, 1993).

SCAMP2 directly interacts with SERT both in a heterologous expression system and in brain tissue. SCAMP2 binds to the N-terminal domain of SERT and also to the

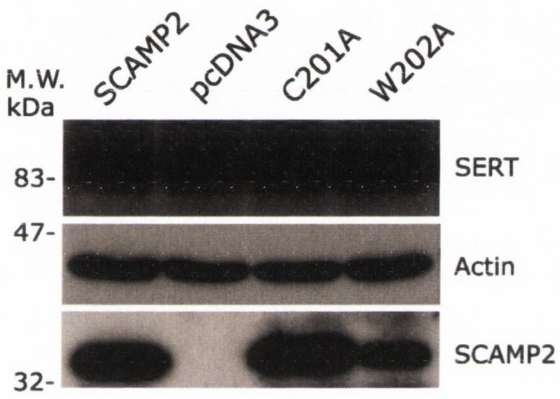


Figure 5.15 Western blots of whole cell lysates from co-transfected HEK-293 cells. Cell extracts from HEK-293 cells transfected with SERT in combination with pcDNA3, wild-type SCAMP2, C201A, or W202A were analysed by Western blotting. The blot was cut into two pieces and the upper part was probed with anti-SERT (C-20) antibody and the lower part was incubated with anti-SCAMP2 antibody. The SCAMP2 blot was re-probed for β-actin to verify equal loading between samples.

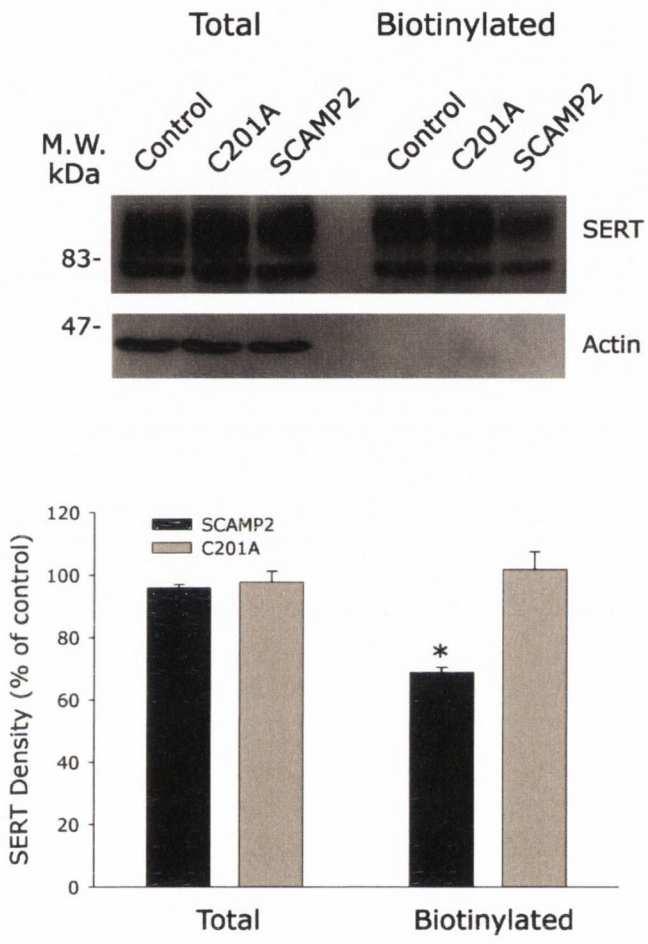


Figure 5.16 The C201A mutant is unable to down-regulate SERT cell surface expression. (A) Representative immunoblot of biotinylation experiment of cells transfected with SERT alone (0.5 μg/well in a 6-well plate) or in combination with SCAMP2 (0.5 μg/well) or C201A (0.5 μg/well) showing SERT immunoreactivity in total and biotinylated fractions. The blot was stripped and reprobed for β-actin. (B) Quantifications are based on densitometry measurements from three separate experiments. Data are expressed as percentage of control ± S.E. *Asterisk* indicates statistically significant change in SERT protein level compared to control ($p < 0.05$; student's *t* test).

corresponding domain of DAT, suggesting that the interaction with SCAMP2 is a common feature of monoamine transporters.

Overexpression of SCAMP2 along with SERT in HEK-293 cells resulted in a dose-dependent down-regulation of 5-HT uptake. The decrease in 5-HT uptake was attributed to a reduction in V_{max} rather than changes in the affinity of 5-HT for the transporter. No reduction in total SERT protein expression was observed when SCAMP2 was co-expressed with SERT, excluding the possibility of non-specific effects due to protein overexpression. This conclusion is further supported by the observation that the SCAMP2 mutant C201A, although expressed at similar levels as wild-type SCAMP2 did not affect SERT function. Also, no change in SERT glycosylation pattern was detected, indicating that SCAMP2 does not have an influence on the maturation of SERT or its transport through the quality control system within the ER. Rather the reduction in 5-HT uptake corresponds well with the observed cellular redistribution of SERT as revealed by cell surface biotinylation and confocal microscopy.

Although SCAMPs have been shown to localize at least to a certain extend to the plasma membrane (Guo et al., 2002; Liu et al., 2002), SCAMP2 could not be biotinylated under the conditions used in this study. This may be due to the fact that the extracellular domains of SCAMPs are very small, rendering them inaccessible for the biotinylation reagent, or because exposure of SCAMP2 to the cell surface is limited and/or transient (Laurie et al., 1993; Castle and Castle, 2005).

In neuronal RN46A cells endogenous SERT localized almost exclusively in SCAMP2-positive compartments. In these cells, as well as in HEK-293 cells, SERT and SCAMP2 staining did not overlap significantly with either TfR-postive endosomes, nor with the Golgi marker TGN38. These data are in general agreement with a recent study by Castle and Castle, in which SCAMP2 showed limited co-localization with TfR in NRK cells (Castle and Castle, 2005). These authors also show that the various SCAMP isoforms accumulate in perinuclear compartments as well as in peripheral early and recycling endosomes and suggest that the individual SCAMP isoforms mark distinct pathways that diverge from the constitutive recycling route. Thus, SCAMPs are

predominantly associated with recycling rather than degradation pathways, suggesting that through the interaction with SCAMP2, SERT might be targeted to a distinct recycling compartment. Thus, in HEK-293 cells the effect of SCAMP2 overexpression on the subcellular distribution of SERT might be the result of more transporter molecules being directed into SCAMP2-containing intracellular compartments.

The finding that SERT/SCAMP2-positive structures contain the lipid raft marker flotillin-1, also supports the idea that these vesicular structures could be recycling endosomes, as such compartments have previously been shown to be enriched in lipid raft markers, including flotillin-1 (Gagescu et al., 2000). Previous work in our laboratory revealed that SERT associates with lipid rafts in a cholesterol-dependent manner. Lipid raft associated SERT was found to originate from both cell surface and intracellular compartments, suggesting that lipid rafts may also play a role in SERT trafficking (Magnani et al., 2004). This idea is further supported in the current study, as also SCAMP2 was found to be present in SERT-containing lipid raft fractions. Thus, the SERT/SCAMP2 complex may be formed within intracellular detergent-resistant membrane domains. Also, flotillin-1 has recently been identified to define a clathrin-independent endocytic pathway in mammalian cells (Glebov et al., 2006). In this context it is interesting to note, that NET appears to undergo PKC-mediated internalisation in a dynamin- and clathrin-independent, but lipid-raft-dependent manner (Jayanthi et al., 2004).

SERT/SCAMP2-positive structures also strongly overlap with syntaxin 1A staining in RN46A cells. Syntaxin 1A, which is a crucial component in synaptic vesicle fusion, has been shown to regulate a number of neurotransmitter transporters, which has led to the hypothesis that neurotransmitter release and re-uptake are tightly coupled events (Deken et al., 2000). Syntaxin 1A has been suggested to recycle with synaptic vesicles (Walch-Solimena et al., 1995), however recent data suggest that in neurons syntaxin 1A predominantly localize to the plasma membrane and only a small fraction of syntaxin 1A is present in intracellular synaptic-like vesicles that do not undergo action potential-dependent recycling (Mitchell and Ryan, 2004). Since SCAMPs have also

been identified in vesicles rich in synaptic vesicle marker proteins (Thoidis et al., 1998), the observed SERT/SCAMP2-positive structures might in fact represent synaptic vesicles or synaptic-like vesicles, a possibility that may apply to neurotransmitter transporters in general. GLYT2 for example was shown to be present on vesicles that also contain the synaptic vesicle marker synaptophysin, as well as syntaxin 1A (Geerlings et al., 2001). In neurons, GAT1 was found to recycle to and from the plasma membrane in similar fashion and time-scale as synaptic vesicles (Deken et al., 2003). In PC12 cells, exogenous DAT and GLUT4 (and also endogenous GLUT1 and GLUT3) were found in primary endocytic vesicles containing synaptic vesicle proteins (Provoda et al., 2000). Thus, synaptic vesicle proteins may be endocytosed along with recycling membrane proteins, including neurotransmitter transporters, and delivered to the endosomal compartment. Alternatively, since SERT/SCAMP2-positive vesicles, in particular in RN46A cells appear to be located very close to the plasma membrane, their co-localization with syntaxin 1A could represent SNARE complex-mediated vesicle attachment sites. This possibility is supported by a previous study showing that in PC12 cells SCAMP2 associates with dense-core vesicles at putative vesicle fusion sites, where it co-localizes with syntaxin 1A in the plasma membrane (Liu et al., 2002; Liu et al., 2005).

The enhanced intracellular accumulation of SERT in HEK-293 cells, as a result of SCAMP2 overexpression, could arise from either an increase in the rate for endocytosis and/or a reduction in recycling and/or insertion of transporter into the plasma membrane. Preliminary studies were in fact carried out during this study to assess whether the rate of SERT exocytosis was influenced by overexpression of SCAMP2. The experiments were performed using cell surface biotinylation at temperatures allowing trafficking of the transporter to and from the plasma membrane. The amount of total biotinylated SERT (cell surface + endocytosed SERT) was assessed at different time points, however, after 15-30 minutes incubation, the amount of biotinylated SERT was less than the amount present at t_0. Since the total amount of SERT (non-biotinylated + biotinylated) was unchanged, it could be ruled out that the attachment of biotin increased the likelihood of SERT being targeted for degradation. Rather, the

biotin itself appeared to be unstable at the temperatures and conditions used in this experiment. Thus, no conclusion could be drawn from these studies and an alternative approach should be considered for future experiments.

While one isoform, SCAMP1, has been shown to function in endocytosis (Fernandez-Chacon et al., 2000), an increasing number of studies provide evidence for a crucial role of SCAMP proteins, and in particular SCAMP2, in regulated exocytosis (Guo et al., 2002; Liu et al., 2002; Liu et al., 2005). SCAMP2 has been proposed as a candidate protein for linking SNARE complexes and secretory vesicles and to function in exocytic fusion pore formation through direct interaction with Arf6 and phospholipase D1 (Liu et al., 2005). In particular the E peptide appears to have an essential function in a late step in exocytosis (Guo et al., 2002; Liu et al., 2002). Interestingly, this peptide binds to plasma membrane lipids, and possibly sequesters phosphatidylinositol 4,5-biphosphate (Hubbard et al., 2000; Ellena et al., 2004). Although the E peptide has been implicated in exocytosis, it is interesting to note the presence of two tyrosine-based endocytic motifs within the E peptide of SCAMP2. The second tyrosine motif in particular is conserved throughout the animal kingdom indicating a role for the E peptide, and hence SCAMP2, in endocytosis.

Previous studies have shown that two residues, C201 and W202 within the E peptide are critical for regulated exocytosis (Guo et al., 2002; Liu et al., 2002). When studied as a free peptide, the E peptide was found to inhibit induced exocytosis in mast cells expressing endogenous SCAMP2. The E peptide was proposed to compete with endogenous SCAMP2 for an interaction partner involved in the final stage of exocytosis (Guo et al., 2002). In PC12 cells, the full-length SCAMP2 mutants, C201A and W202A, have been shown to inhibit induced exocytosis when compared to wild-type SCAMP2 (Liu et al., 2002). This might be explained by a model where vesicles containing mutant SCAMP2 are less likely to undergo exocytosis perhaps due to impaired interaction with an endogenous factor.

In the present study, a point mutation in C201 was found to abolish the SCAMP2-mediated decrease in 5-HT uptake and cell surface biotinylation of SERT. Mutation of C201 did not influence the interaction with SERT, demonstrating that the mere binding of SCAMP2 to SERT is not sufficient to down-regulate SERT. Interestingly, the

mutation of W202, a residue that was also found to be crucial for the regulation of exocytosis (Liu et al., 2002), did not alter the SCAMP2 effects on SERT activity. However, the effects of SCAMP2 mutants were studied in a non-secretory cell line, while the role of the E peptide residues on exocytosis was studied in neuroendocrine and mast cells, which possess well-studies regulated secretory pathways. The possibility that SCAMP2 also affects regulated exocytosis of SERT to the cell surface in neurons, for example under conditions where neurotransmitter is released and an increase in re-uptake capacities is required, cannot be excluded. However, the finding that C201, but not W202, is crucial for SERT regulation by SCAMP2, suggest that the role of SCAMP2 in regulating the cellular distribution of SERT is distinct from its role in regulating exocytosis in secretory cells.

The cysteine residue at position 201 in SCAMP2 is located in the border region between TMD2 and the cytoplasmic domain connecting TMD2 and TMD3. Palmitoylation of transmembrane proteins usually occurs at cysteine residues proximal to a transmembrane domain (Huang and El-Husseini, 2005). Thus, C201 might in fact represent a target for palmitoylation. Post-translational palmitoylation is a reversible modification with particular importance at synapses. Palmitoylation modulates protein-protein interactions and regulates localization of proteins to specific vesicular compartments and synaptic membranes (Huang and El-Husseini, 2005). Thus, although purely speculative, palmitoylation at C201 might be involved in SCAMP2-mediated SERT down-regulation.

Preliminary results presented in this study suggest that SCAMP2 prevents PKC-mediated SERT down-regulation. Since increasing amounts of SCAMP2 is able to further reduce 5-HT uptake, the mechanism underlying SCAMP2-mediated down-regulation of SERT does not appear to be saturated at the concentration used in these experiments. Activation of PKC appears unable to further reduce 5-HT uptake when SCAMP2 is present, thus, PKC seems to affect SERT via a different pathway than SCAMP2. However, if SCAMP2 instead renders SERT resistant or inaccessible to PKC-mediated down-regulation, PKC should still be able to affect SERT molecules not

bound to SCAMP2. Since these studies are only preliminary, it is too early to speculate on a model explaining this observation. However, considering this result it should be interesting to explore the relationship between the three transporter regulating factors SCAMP2, syntaxin 1A and PKC.

6. CONCLUDING REMARKS

For more than four decades, the monoamine hypothesis of depression has predominated. According to this hypothesis depression is a neurochemical disorder arising from dysfunctioning of brain monoamine systems. However, today monoaminergic dysregulation is viewed more as an associated factor rather than as a primary cause of depression. Serotonergic dysfunction, and in particular reduced serotonergic neurotransmission, has been discussed in connection with various psychiatric disorders. Since the serotonin transporter (SERT) controls the magnitude and duration of serotonergic neurotransmission, disturbances in serotonin signalling may be attributed to dysregulation of this transporter. Thus, determining the mechanisms regulating SERT availability and transport activity may contribute to a better understanding of some of the pathways underlying neuropsychiatric disorders. This particular idea constituted the basic rationale behind the present study.
Regulation of SERT in response to various protein kinases has been studied intensively for almost ten years. Although, phosphorylation is likely to play an essential role in SERT modulation there is still some controversy over whether SERT itself is actually phosphorylated. Instead, phosphorylation may affect SERT indirectly via phosphorylation of SERT-associating proteins. Also, constitutive and regulated SERT trafficking most likely require the participation of a broad range of proteins and thus, in recent years the focus has also been directed at identifying proteins interacting directly with SERT. However, only a few proteins have been found to interact with and influence SERT function and the cellular mechanisms involved are largely unknown.

The study of protein-protein interactions has advanced considerable in recent years with the introduction of new tools and technologies as well as computational approaches. Different experimental methods can generate different types of protein-protein interactions. Some methods can detect binary interactions while others can identify protein complexes. However, still nothing really compares with the original yeast two-hybrid system for screening thousands of potential interactions and the yeast two-hybrid system is still the most widely used method for detecting protein-protein

interactions. Initially, it was designed to confirm an interaction between two known proteins but was rapidly developed into a screening assay to identify interacting partners of a protein of interest in high-throughput mode. However, a general problem when performing yeast two-hybrid screens is the occurrence of a large number of false positives. This was also evident in the present study and efficient elimination of false positives proved to be an important step for successful isolation of genuine positive interactions.

Most of the proteins that have been reported to interact with membrane proteins such as transporters, ion channels and receptors were originally isolated using the yeast two-hybrid system. However, there are not many follow-up studies reporting additional proteins isolated from the same screen and thus, it appears that many two-hybrid screens result in isolation of only one single positive interacting partner or that additional positive yeast two-hybrid clones are not being investigated. An exception to this is the reported isolation of PICK1 and Hic-5, which were isolated from the same yeast two-hybrid screen using the C-terminus of DAT as bait (Torres et al., 2001; Carneiro et al., 2002). Thus, a systematic and extensive evaluation of all positive clones obtained in a yeast two-hybrid screen, regardless of the nature of the proteins, may lead to the identification of several more genuine interacting proteins and perhaps also the characterisation of intriguing interactions that otherwise would not have been identified.

One such protein is ESO3, a ubiquitously expressed protein that belongs to the NY-ESO-1 gene family. ESO3 inhibit SERT delivery to the cell surface by retaining the transporter in the ER compartment. There is very little information available regarding the ESO3 protein and since ESO3 only shares significant sequence similarity to other known proteins within relatively small regions, the interaction between SERT and ESO3 is difficult to relate to any known biological mechanism. The binding of ESO3 to SERT in the ER compartment rather supports the emerging concept of controlled regulation of neurotransmitter transporters in the early secretory pathway. Studies on neurotransmitter transporters have mainly focused on the dynamic regulation of transporter trafficking between the cell surface and endosomal compartment with little

emphasis on regulated transport from the ER to the Golgi apparatus. The ER provides a stringent quality control system to ensure that only correctly folded proteins are being transported to the Golgi and unfolded or misfolded proteins are retained and ultimately degraded. Only recently has oligomer formation of neurotransmitter transporters been hypothesised to be a prerequisite for transit from the ER to the Golgi apparatus and eventually the cell surface (Sitte et al., 2004). Thus, exit of properly assembled transporters from the ER appears to represent a key step in neurotransmitter transporter trafficking.

Transport of proteins from the ER is mediated by vesicles generated by the COPII coat complex. Cellular components of the COPII complex are known to discriminate between cargo molecules for selection into the COPII vesicles (Miller et al., 2003). Interestingly, the GABA transporter GAT1 has been shown to interact directly with Sec24D (Farhan et al., 2004), which function in a complex with Sec23 and constitute part of the COPII coat complex. Thus, transport of neurotransmitter transporters from the ER may be regulated via direct interaction with cytosolic components such as subunits of the COPII coat complex; interactions that may in fact be linked to the status of oligomeric assembly.

ESO3 might represent a regulatory protein of COPI- and/or COPII-dependent trafficking. The observation of fully glycosylated SERT argues against the transporter being permanently retained in the ER when co-expressed with ESO3. Rather, it suggests that SERT is retrieved from the Golgi after being modified by Golgi specific enzymes. Proteins that are retrieved from the Golgi are mostly ER-localized at steady-state but achieve this localization in a dynamic fashion through continues recycling between the ER and the Golgi (Duden, 2003). Membrane trafficking dynamically modulates neurotransmitter transporter surface expression to ensure fast and efficient regulation of neurotransmission (Melikian, 2004). Thus, continues recycling of transporters between the ER and Golgi might provide a latent pool of fully functional transporters that can be recruited to the cell surface under conditions where an increase in reuptake capacity is required. This mechanism was in fact recently suggested for the glutamate receptor (Fleck, 2006). A possible model of how ESO3 regulates SERT cell surface expression is shown in Figure 6.1.

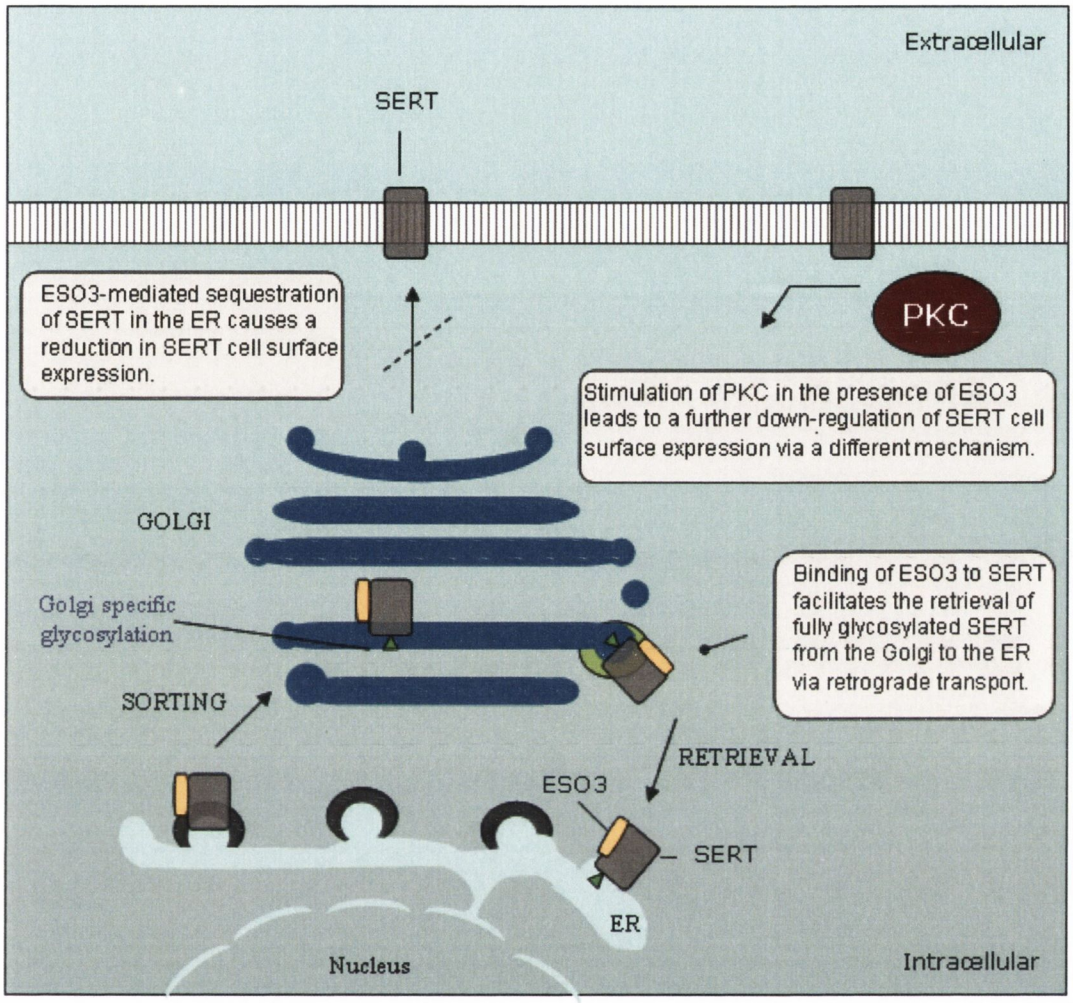


Figure 6.1 Possible mechanism for ESO3-mediated SERT regulation. The binding of ESO3 to SERT results in the retrieval of SERT from the Golgi complex after the transporter has been modified by Golgi specific enzymes. ESO3 affect SERT function via a mechanism distinct from PKC-mediated SERT down-regulation.

The secretory carrier membrane protein 2 (SCAMP2) was also described in the present study as an important regulator of SERT subcellular distribution. SCAMP2 regulates the subcellular distribution of SERT between the cell surface and intracellular compartments. The mere binding of SCAMP2 has no effect on SERT function and thus SCAMP2 does not appear to interfere with the 5-HT transport cycle. The SCAMP2-mediated mechanism is therefore clearly distinct from the proposed effect of syntaxin 1A on SERT and related transporters (Deken et al., 2000; Quick, 2003; Sung et al., 2003). Rather, the finding of SCAMP2 as a novel SERT interacting protein revealed a very specific regulatory mechanism dependent on a conserved cysteine residue within the E peptide of SCAMP2. A model of SCAMP2 mediated SERT regulation is shown in Figure 6.2.

It is interesting to note that the most promising SERT interacting proteins identified in this study were isolated with the two bait constructs containing a transmembrane domain. Thus, the decision to perform yeast two-hybrid screens using bait constructs containing a transmembrane domain turned out to be important for the success of this study. Whether the transmembrane domain present within the bait constructs is directly involved in the binding of associating proteins or whether the transmembrane domain merely serves as a structural segment stabilizing the folding of the remaining cytosolic terminus thus allowing isolation of proteins that would otherwise not be detected is not clear from these studies. For instance, both ESO3 and SCAMP2 were found to interact with the long N-terminal domain (containing TMD1) of both SERT and DAT. Whether residues within TMD1 of SERT and DAT are directly involved in the interaction with ESO3 and SCAMP2, respectively, is presently unknown but this question is currently being addressed using single amino acid mutagenesis of full-length SERT. It can also be questioned whether TMD1 is at all accessible to interacting proteins from the cytoplasmic or lateral side. As shown in Figure 1.4, the TMD1 of $LeuT_{Aa}$ is buried within the core of the protein and only the cytoplasmic half of TMD1 appears to be partially accessible.

It is interesting to note that SERT and related neurotransmitter transporters contain much longer N- and C-terminal domains than $LeuT_{Aa}$. These intracellular domains are likely to be important for regulation through interactions with modulatory proteins and

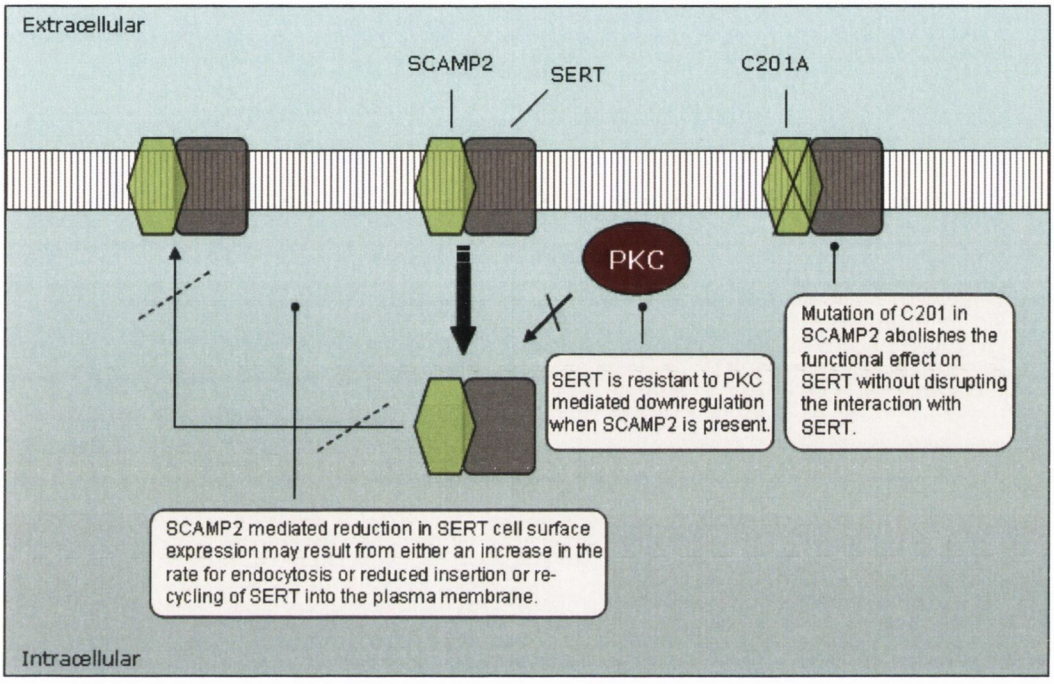


Figure 6.2 SCAMP2-mediated subcellular redistribution of SERT. Binding of SCAMP2 to the N-terminal domain of SERT results in the subcellular redistribution of SERT with a decrease in cell surface SERT. A single amino acid, cycteine-201, within the conserved cytoplasmic E peptide of SCAMP2 is critical for SCAMP2 mediated down-regulation of SERT cell surface expression. The presence of SCAMP2 renders SERT resistant or inaccessible to PKC-mediated down-regulation.

thus, it is likely that the termini evolved to meet specific demands for more complex regulatory mechanisms unique to eukaryotic members of the Na^+/Cl^- -dependent family of transporters.

The fact that an increasing number of transporter associating proteins are being identified suggests that neurotransmitter transporters exist in large dynamic protein complexes of which the composition is likely to change in response to various signals according to specific demands for the transporter at specialized sites.

Additional information regarding SERT subcellular localisation may provide important clues to the precise mechanisms of SERT regulation and thus, the proteins described in the present study will be explored in further detail.

References

Adayev T, Ranasinghe B, Banerjee P (2005) Transmembrane signaling in the brain by serotonin, a key regulator of physiology and emotion. Biosci Rep 25:363-385.

Adkins EM, Barker EL, Blakely RD (2001) Interactions of tryptamine derivatives with serotonin transporter species variants implicate transmembrane domain I in substrate recognition. Mol Pharmacol 59:514-523.

Alpen B, Gure AO, Scanlan MJ, Old LJ, Chen YT (2002) A new member of the NY-ESO-1 gene family is ubiquitously expressed in somatic tissues and evolutionarily conserved. Gene 297:141-149.

Anderson GM, Horne WC (1992) Activators of protein kinase C decrease serotonin transport in human platelets. Biochim Biophys Acta 1137:331-337.

Androutsellis-Theotokis A, Rudnick G (2002) Accessibility and conformational coupling in serotonin transporter predicted internal domains. J Neurosci 22:8370-8378.

Anguelova M, Benkelfat C, Turecki G (2003) A systematic review of association studies investigating genes coding for serotonin receptors and the serotonin transporter: II. Suicidal behavior. Mol Psychiatry 8:646-653.

Asberg M (1997) Neurotransmitters and suicidal behavior. The evidence from cerebrospinal fluid studies. Ann N Y Acad Sci 836:158-181.

Austin MC, Bradley CC, Mann JJ, Blakely RD (1994) Expression of serotonin transporter messenger RNA in the human brain. J Neurochem 62:2362-2367.

Barker EL, Blakely RD (1996) Identification of a single amino acid, phenylalanine 586, that is responsible for high affinity interactions of tricyclic antidepressants with the human serotonin transporter. Mol Pharmacol 50:957-965.

Barker EL, Kimmel HL, Blakely RD (1994) Chimeric human and rat serotonin transporters reveal domains involved in recognition of transporter ligands. Mol Pharmacol 46:799-807.

Bauman AL, Apparsundaram S, Ramamoorthy S, Wadzinski BE, Vaughan RA, Blakely RD (2000) Cocaine and antidepressant-sensitive biogenic amine transporters exist in regulated complexes with protein phosphatase 2A. J Neurosci 20:7571-7578.

Beckman ML, Bernstein EM, Quick MW (1998) Protein kinase C regulates the interaction between a GABA transporter and syntaxin 1A. J Neurosci 18:6103-6112.

Bell C, Abrams J, Nutt D (2001) Tryptophan depletion and its implications for psychiatry. Br J Psychiatry 178:399-405.

Bickel PE, Scherer PE, Schnitzer JE, Oh P, Lisanti MP, Lodish HF (1997) Flotillin and epidermal surface antigen define a new family of caveolae-associated integral membrane proteins. J Biol Chem 272:13793-13802.

Binda F, Lute BJ, Dipace C, Blakely RD, Galli A (2006) The N-terminus of the norepinephrine transporter regulates the magnitude and selectivity of the transporter-associated leak current. Neuropharmacology 50:354-361. Epub 2005 Nov 2014.

Blakely RD, Berson HE, Fremeau RT, Jr., Caron MG, Peek MM, Prince HK, Bradley CC (1991) Cloning and expression of a functional serotonin transporter from rat brain. Nature 354:66-70.

Blier P (2003) The pharmacology of putative early-onset antidepressant strategies. Eur Neuropsychopharmacol 13:57-66.

Boadle-Biber MC (1993) Regulation of serotonin synthesis. Prog Biophys Mol Biol 60:1-15.

Bonifacino JS, Traub LM (2003) Signals for sorting of transmembrane proteins to endosomes and lysosomes. Annu Rev Biochem 72:395-447.

Bradley CC, Blakely RD (1997) Alternative splicing of the human serotonin transporter gene. J Neurochem 69:1356-1367.

Brand SH, Castle JD (1993) SCAMP 37, a new marker within the general cell surface recycling system. Embo J 12:3753-3761.

Brand SH, Laurie SM, Mixon MB, Castle JD (1991) Secretory carrier membrane proteins 31-35 define a common protein composition among secretory carrier membranes. J Biol Chem 266:18949-18957.

Brent R, Ptashne M (1984) A bacterial repressor protein or a yeast transcriptional terminator can block upstream activation of a yeast gene. Nature 312:612-615.

Broer S (2006) The SLC6 orphans are forming a family of amino acid transporters. Neurochem Int 48:559-567. Epub 2006 Mar 2015.

Brownstein MJ, Hoffman BJ (1994) Neurotransmitter transporters. Recent Prog Horm Res 49:27-42.

Bruss M, Hammermann R, Brimijoin S, Bonisch H (1995) Antipeptide antibodies confirm the topology of the human norepinephrine transporter. J Biol Chem 270:9197-9201.

Burnet PW, Michelson D, Smith MA, Gold PW, Sternberg EM (1994) The effect of chronic imipramine administration on the densities of 5-HT1A and 5-HT2 receptors and the abundances of 5-HT receptor and transporter mRNA in the cortex, hippocampus and dorsal raphe of three strains of rat. Brain Res 638:311-324.

Butchbach ME, Tian G, Guo H, Lin CL (2004) Association of excitatory amino acid transporters, especially EAAT2, with cholesterol-rich lipid raft microdomains: importance for excitatory amino acid transporter localization and function. J Biol Chem 279:34388-34396. Epub 32004 Jun 34388.

Cai G, Salonikidis PS, Fei J, Schwarz W, Schulein R, Reutter W, Fan H (2005) The role of N-glycosylation in the stability, trafficking and GABA-uptake of GABA-transporter 1. Terminal N-glycans facilitate efficient GABA-uptake activity of the GABA transporter. Febs J 272:1625-1638.

Cao Y, Mager S, Lester HA (1997) H+ permeation and pH regulation at a mammalian serotonin transporter. J Neurosci 17:2257-2266.

Carneiro AM, Blakely RD (2006) Serotonin, protein kinase C and HIC-5 associated redistribution of the platelet serotonin transporter. J Biol Chem 27:27.

Carneiro AM, Ingram SL, Beaulieu JM, Sweeney A, Amara SG, Thomas SM, Caron MG, Torres GE (2002) The multiple LIM domain-containing adaptor protein Hic-5 synaptically colocalizes and interacts with the dopamine transporter. J Neurosci 22:7045-7054.

Castle A, Castle D (2005) Ubiquitously expressed secretory carrier membrane proteins (SCAMPs) 1-4 mark different pathways and exhibit limited constitutive trafficking to and from the cell surface. J Cell Sci 118:3769-3780.

Chamberlain LH, Gould GW (2002) The vesicle- and target-SNARE proteins that mediate Glut4 vesicle fusion are localized in detergent-insoluble lipid rafts present on distinct intracellular membranes. J Biol Chem 277:49750-49754. Epub 42002 Oct 49759.

Chang AS, Starnes DM, Chang SM (1998) Possible existence of quaternary structure in the high-affinity serotonin transport complex. Biochem Biophys Res Commun 249:416-421.

Chang AS, Chang SM, Starnes DM, Schroeter S, Bauman AL, Blakely RD (1996) Cloning and expression of the mouse serotonin transporter. Brain Res Mol Brain Res 43:185-192.

Chang MY, Lee SH, Kim JH, Lee KH, Kim YS, Son H, Lee YS (2001) Protein kinase C-mediated functional regulation of dopamine transporter is not achieved by direct phosphorylation of the dopamine transporter protein. J Neurochem 77:754-761.

Chen JG, Liu-Chen S, Rudnick G (1998a) Determination of external loop topology in the serotonin transporter by site-directed chemical labeling. J Biol Chem 273:12675-12681.

Chen JX, Pan H, Rothman TP, Wade PR, Gershon MD (1998b) Guinea pig 5-HT transporter: cloning, expression, distribution, and function in intestinal sensory reception. Am J Physiol 275:G433-448.

Cheng J, Randall AZ, Sweredoski MJ, Baldi P (2005) SCRATCH: a protein structure and structural feature prediction server. Nucleic Acids Res 33:W72-76.

Cool DR, Leibach FH, Bhalla VK, Mahesh VB, Ganapathy V (1991) Expression and cyclic AMP-dependent regulation of a high affinity serotonin transporter in the human placental choriocarcinoma cell line (JAR). J Biol Chem 266:15750-15757.

Corey JL, Quick MW, Davidson N, Lester HA, Guastella J (1994a) A cocaine-sensitive Drosophila serotonin transporter: cloning, expression, and electrophysiological characterization. Proc Natl Acad Sci U S A 91:1188-1192.

Corey JL, Davidson N, Lester HA, Brecha N, Quick MW (1994b) Protein kinase C modulates the activity of a cloned gamma-aminobutyric acid transporter expressed in Xenopus oocytes via regulated subcellular redistribution of the transporter. J Biol Chem 269:14759-14767.

Crane GE (1956) The psychiatric side-effects of iproniazid. Am J Psychiatry 112:494-501.

Cremona O, De Camilli P (2001) Phosphoinositides in membrane traffic at the synapse. J Cell Sci 114:1041-1052.

Dahlström A, Fuxe K (1964) Evidence for the Existence of Monoamine-Containing Neurons in the Central Nervous System. I. Demonstration of Monoamines in the Cell Bodies of Brain Stem Neurons. Acta Physiol Scand 62:SUPPL:1-55.

Dahm T, White J, Grill S, Fullekrug J, Stelzer EH (2001) Quantitative ER <--> Golgi transport kinetics and protein separation upon Golgi exit revealed by vesicular integral membrane protein 36 dynamics in live cells. Mol Biol Cell 12:1481-1498.

Daniels GM, Amara SG (1999) Regulated trafficking of the human dopamine transporter. Clathrin-mediated internalization and lysosomal degradation in response to phorbol esters. J Biol Chem 274:35794-35801.

Deken SL, Wang D, Quick MW (2003) Plasma membrane GABA transporters reside on distinct vesicles and undergo rapid regulated recycling. J Neurosci 23:1563-1568.

Deken SL, Beckman ML, Boos L, Quick MW (2000) Transport rates of GABA transporters: regulation by the N-terminal domain and syntaxin 1A. Nat Neurosci 3:998-1003.

Demchyshyn LL, Pristupa ZB, Sugamori KS, Barker EL, Blakely RD, Wolfgang WJ, Forte MA, Niznik HB (1994) Cloning, expression, and localization of a chloride-facilitated, cocaine-sensitive serotonin transporter from Drosophila melanogaster. Proc Natl Acad Sci U S A 91:5158-5162.

Di Bella D, Catalano M, Balling U, Smeraldi E, Lesch KP (1996) Systematic screening for mutations in the coding region of the human serotonin transporter (5-HTT) gene using PCR and DGGE. Am J Med Genet 67:541-545.

Duden R (2003) ER-to-Golgi transport: COP I and COP II function (Review). Mol Membr Biol 20:197-207.

Dugani CB, Klip A (2005) Glucose transporter 4: cycling, compartments and controversies. EMBO Rep 6:1137-1142.

Duman JG, Forte JG (2003) What is the role of SNARE proteins in membrane fusion? Am J Physiol Cell Physiol 285:C237-249.

Ellena JF, Moulthrop J, Wu J, Rauch M, Jaysinghne S, Castle JD, Cafiso DS (2004) Membrane position of a basic aromatic peptide that sequesters phosphatidylinositol 4,5 bisphosphate determined by site-directed spin labeling and high-resolution NMR. Biophys J 87:3221-3233.

Estojak J, Brent R, Golemis EA (1995) Correlation of two-hybrid affinity data with in vitro measurements. Mol Cell Biol 15:5820-5829.

Farhan H, Korkhov VM, Paulitschke V, Dorostkar MM, Scholze P, Kudlacek O, Freissmuth M, Sitte HH (2004) Two discontinuous segments in the carboxyl terminus are required for membrane targeting of the rat gamma-aminobutyric acid transporter-1 (GAT1). J Biol Chem 279:28553-28563. Epub 22004 Apr 28558.

Fernandez-Chacon R, Südhof TC (2000) Novel SCAMPs lacking NPF repeats: ubiquitous and synaptic vesicle-specific forms implicate SCAMPs in multiple membrane-trafficking functions. J Neurosci 20:7941-7950.

Fernandez-Chacon R, Achiriloaie M, Janz R, Albanesi JP, Südhof TC (2000) SCAMP1 function in endocytosis. J Biol Chem 275:12752-12756.

Fields S, Song O (1989) A novel genetic system to detect protein-protein interactions. Nature 340:245-246.

Flattem NL, Blakely RD (2000) Modified structure of the human serotonin transporter promoter. Mol Psychiatry 5:110-115.

Fleck MW (2006) Glutamate receptors and endoplasmic reticulum quality control: looking beneath the surface. Neuroscientist 12:232-244.

Foguet M, Hartikka JA, Schmuck K, Lubbert H (1993) Long-term regulation of serotonergic activity in the rat brain via activation of protein kinase A. Embo J 12:903-910.

Fremeau RT, Jr., Caron MG, Blakely RD (1992) Molecular cloning and expression of a high affinity L-proline transporter expressed in putative glutamatergic pathways of rat brain. Neuron 8:915-926.

Gagescu R, Demaurex N, Parton RG, Hunziker W, Huber LA, Gruenberg J (2000) The recycling endosome of Madin-Darby canine kidney cells is a mildly acidic compartment rich in raft components. Mol Biol Cell 11:2775-2791.

Galli A, Petersen CI, deBlaquiere M, Blakely RD, DeFelice LJ (1997) Drosophila serotonin transporters have voltage-dependent uptake coupled to a serotonin-gated ion channel. J Neurosci 17:3401-3411.

Gaspar P, Cases O, Maroteaux L (2003) The developmental role of serotonin: news from mouse molecular genetics. Nat Rev Neurosci 4:1002-1012.

Gassmann M, Haller C, Stoll Y, Aziz SA, Biermann B, Mosbacher J, Kaupmann K, Bettler B (2005) The RXR-type endoplasmic reticulum-retention/retrieval signal of GABAB1 requires distant spacing from the membrane to function. Mol Pharmacol 68:137-144.

Gasteiger E, Gattiker A, Hoogland C, Ivanyi I, Appel RD, Bairoch A (2003) ExPASy: The proteomics server for in-depth protein knowledge and analysis. Nucleic Acids Res 31:3784-3788.

Geerlings A, Lopez-Corcuera B, Aragon C (2000) Characterization of the interactions between the glycine transporters GLYT1 and GLYT2 and the SNARE protein syntaxin 1A. FEBS Lett 470:51-54.

Geerlings A, Nunez E, Lopez-Corcuera B, Aragon C (2001) Calcium- and syntaxin 1-mediated trafficking of the neuronal glycine transporter GLYT2. J Biol Chem 276:17584-17590. Epub 12001 Feb 17523.

Gerst JE (2003) SNARE regulators: matchmakers and matchbreakers. Biochim Biophys Acta 1641:99-110.

Gil C, Soler-Jover A, Blasi J, Aguilera J (2005) Synaptic proteins and SNARE complexes are localized in lipid rafts from rat brain synaptosomes. Biochem Biophys Res Commun 329:117-124.

Girod A, Storrie B, Simpson JC, Johannes L, Goud B, Roberts LM, Lord JM, Nilsson T, Pepperkok R (1999) Evidence for a COP-I-independent transport route from the Golgi complex to the endoplasmic reticulum. Nat Cell Biol 1:423-430.

Giros B, el Mestikawy S, Bertrand L, Caron MG (1991) Cloning and functional characterization of a cocaine-sensitive dopamine transporter. FEBS Lett 295:149-154.

Glatt CE, DeYoung JA, Delgado S, Service SK, Giacomini KM, Edwards RH, Risch N, Freimer NB (2001) Screening a large reference sample to identify very low frequency sequence variants: comparisons between two genes. Nat Genet 27:435-438.

Glebov OO, Bright NA, Nichols BJ (2006) Flotillin-1 defines a clathrin-independent endocytic pathway in mammalian cells. Nat Cell Biol 8:46-54. Epub 2005 Dec 2011.

Granas C, Ferrer J, Loland CJ, Javitch JA, Gether U (2003) N-terminal truncation of the dopamine transporter abolishes phorbol ester- and substance P receptor-stimulated phosphorylation without impairing transporter internalization. J Biol Chem 278:4990-5000. Epub 2002 Dec 4992.

Greenberg BD, Tolliver TJ, Huang SJ, Li Q, Bengel D, Murphy DL (1999) Genetic variation in the serotonin transporter promoter region affects serotonin uptake in human blood platelets. Am J Med Genet 88:83-87.

Gu HH, Wu X, Han DD (2006) Conserved serine residues in serotonin transporter contribute to high-affinity cocaine binding. Biochem Biophys Res Commun 343:1179-1185. Epub 2006 Mar 1127.

Gu HH, Wu X, Giros B, Caron MG, Caplan MJ, Rudnick G (2001) The NH(2)-terminus of norepinephrine transporter contains a basolateral localization signal for epithelial cells. Mol Biol Cell 12:3797-3807.

Guastella J, Brecha N, Weigmann C, Lester HA, Davidson N (1992) Cloning, expression, and localization of a rat brain high-affinity glycine transporter. Proc Natl Acad Sci U S A 89:7189-7193.

Guastella J, Nelson N, Nelson H, Czyzyk L, Keynan S, Miedel MC, Davidson N, Lester HA, Kanner BI (1990) Cloning and expression of a rat brain GABA transporter. Science 249:1303-1306.

Guimbal C, Kilimann MW (1993) A Na(+)-dependent creatine transporter in rabbit brain, muscle, heart, and kidney. cDNA cloning and functional expression. J Biol Chem 268:8418-8421.

Guo Z, Liu L, Cafiso D, Castle D (2002) Perturbation of a very late step of regulated exocytosis by a secretory carrier membrane protein (SCAMP2)-derived peptide. J Biol Chem 277:35357-35363.

Haase J, Killian AM, Magnani F, Williams C (2001) Regulation of the serotonin transporter by interacting proteins. Biochem Soc Trans 29:722-728.

Hahn MK, Blakely RD (2002) Monoamine transporter gene structure and polymorphisms in relation to psychiatric and other complex disorders. Pharmacogenomics J 2:217-235.

Hastrup H, Karlin A, Javitch JA (2001) Symmetrical dimer of the human dopamine transporter revealed by cross-linking Cys-306 at the extracellular end of the sixth transmembrane segment. Proc Natl Acad Sci U S A 98:10055-10060.

Hastrup H, Sen N, Javitch JA (2003) The human dopamine transporter forms a tetramer in the plasma membrane: cross-linking of a cysteine in the fourth transmembrane segment is sensitive to cocaine analogs. J Biol Chem 278:45045-45048. Epub 42003 Sep 45030.

Heils A, Teufel A, Petri S, Stober G, Riederer P, Bengel D, Lesch KP (1996) Allelic variation of human serotonin transporter gene expression. J Neurochem 66:2621-2624.

Heils A, Teufel A, Petri S, Seemann M, Bengel D, Balling U, Riederer P, Lesch KP (1995) Functional promoter and polyadenylation site mapping of the human serotonin (5-HT) transporter gene. J Neural Transm Gen Sect 102:247-254.

Heinz A, Mann K, Weinberger DR, Goldman D (2001) Serotonergic dysfunction, negative mood states, and response to alcohol. Alcohol Clin Exp Res 25:487-495.

Hicke L, Dunn R (2003) Regulation of membrane protein transport by ubiquitin and ubiquitin-binding proteins. Annu Rev Cell Dev Biol 19:141-172.

Hirschberg K, Miller CM, Ellenberg J, Presley JF, Siggia ED, Phair RD, Lippincott-Schwartz J (1998) Kinetic analysis of secretory protein traffic and

characterization of golgi to plasma membrane transport intermediates in living cells. J Cell Biol 143:1485-1503.
Hirschfeld RM (2000) History and evolution of the monoamine hypothesis of depression. J Clin Psychiatry 61:4-6.
Hoffman BJ, Mezey E, Brownstein MJ (1991) Cloning of a serotonin transporter affected by antidepressants. Science 254:579-580.
Hoffman BJ, Hansson SR, Mezey E, Palkovits M (1998) Localization and dynamic regulation of biogenic amine transporters in the mammalian central nervous system. Front Neuroendocrinol 19:187-231.
Holmes DS, Quigley M (1981) A rapid boiling method for the preparation of bacterial plasmids. Anal Biochem 114:193-197.
Holton KL, Loder MK, Melikian HE (2005) Nonclassical, distinct endocytic signals dictate constitutive and PKC-regulated neurotransmitter transporter internalization. Nat Neurosci 8:881-888.
Hommelgaard AM, Roepstorff K, Vilhardt F, Torgersen ML, Sandvig K, van Deurs B (2005) Caveolae: stable membrane domains with a potential for internalization. Traffic 6:720-724.
Horiuchi M, Nicke A, Gomeza J, Aschrafi A, Schmalzing G, Betz H (2001) Surface-localized glycine transporters 1 and 2 function as monomeric proteins in Xenopus oocytes. Proc Natl Acad Sci U S A 98:1448-1453. Epub 2001 Feb 1446.
Horton N, Quick MW (2001) Syntaxin 1A up-regulates GABA transporter expression by subcellular redistribution. Mol Membr Biol 18:39-44.
Huang K, El-Husseini A (2005) Modulation of neuronal protein trafficking and function by palmitoylation. Curr Opin Neurobiol 15:527-535.
Hubbard C, Singleton D, Rauch M, Jayasinghe S, Cafiso D, Castle D (2000) The secretory carrier membrane protein family: structure and membrane topology. Mol Biol Cell 11:2933-2947.
Hubner K, Windoffer R, Hutter H, Leube RE (2002) Tetraspan vesicle membrane proteins: synthesis, subcellular localization, and functional properties. Int Rev Cytol 214:103-159.
Ives JH, Fung S, Tiwari P, Payne HL, Thompson CL (2004) Microtubule-associated protein light chain 2 is a stargazin-AMPA receptor complex-interacting protein in vivo. J Biol Chem 279:31002-31009. Epub 32004 May 31010.
Jayanthi LD, Samuvel DJ, Ramamoorthy S (2004) Regulated internalization and phosphorylation of the native norepinephrine transporter in response to phorbol esters. Evidence for localization in lipid rafts and lipid raft-mediated internalization. J Biol Chem 279:19315-19326. Epub 12004 Feb 19319.
Jayanthi LD, Samuvel DJ, Blakely RD, Ramamoorthy S (2005) Evidence for biphasic effects of protein kinase C on serotonin transporter function, endocytosis, and phosphorylation. Mol Pharmacol 67:2077-2087. Epub 2005 Mar 2017.
Jess U, Betz H, Schloss P (1996) The membrane-bound rat serotonin transporter, SERT1, is an oligomeric protein. FEBS Lett 394:44-46.
Jess U, El Far O, Kirsch J, Betz H (2002) Interaction of the C-terminal region of the rat serotonin transporter with MacMARCKS modulates 5-HT uptake regulation by protein kinase C. Biochem Biophys Res Commun 294:272-279.

Just H, Sitte HH, Schmid JA, Freissmuth M, Kudlacek O (2004) Identification of an additional interaction domain in transmembrane domains 11 and 12 that supports oligomer formation in the human serotonin transporter. J Biol Chem 279:6650-6657.

Karhinen L, Makarow M (2004) Activity of recycling Golgi mannosyltransferases in the yeast endoplasmic reticulum. J Cell Sci 117:351-358.

Kekuda R, Torres-Zamorano V, Leibach FH, Ganapathy V (1997) Human serotonin transporter: regulation by the neuroprotective agent aurintricarboxylic acid and by epidermal growth factor. J Neurochem 68:1443-1450.

Kekuda R, Leibach FH, Furesz TC, Smith CH, Ganapathy V (2000) Polarized distribution of interleukin-1 receptors and their role in regulation of serotonin transporter in placenta. J Pharmacol Exp Ther 292:1032-1041.

Kilic F, Rudnick G (2000) Oligomerization of serotonin transporter and its functional consequences. Proc Natl Acad Sci U S A 97:3106-3111.

Kilic F, Murphy DL, Rudnick G (2003) A human serotonin transporter mutation causes constitutive activation of transport activity. Mol Pharmacol 64:440-446.

Kilty JE, Lorang D, Amara SG (1991) Cloning and expression of a cocaine-sensitive rat dopamine transporter. Science 254:578-579.

Kubota N, Kiuchi Y, Nemoto M, Oyamada H, Ohno M, Funahashi H, Shioda S, Oguchi K (2001) Regulation of serotonin transporter gene expression in human glial cells by growth factors. Eur J Pharmacol 417:69-76.

Kuhn R (1958) The treatment of depressive states with G 22355 (imipramine hydrochloride). Am J Psychiatry 115:459-464.

Kuroda Y, Watanabe Y, McEwen BS (1994) Tianeptine decreases both serotonin transporter mRNA and binding sites in rat brain. Eur J Pharmacol 268:R3-5.

Kyte J, Doolittle RF (1982) A simple method for displaying the hydropathic character of a protein. J Mol Biol 157:105-132.

Larsen MB, Elfving B, Wiborg O (2004) The chicken serotonin transporter discriminates between serotonin-selective reuptake inhibitors. A species-scanning mutagenesis study. J Biol Chem 279:42147-42156. Epub 42004 Jul 42122.

Larsen MB, Fjorback AW, Wiborg O (2006) The C-terminus is critical for the functional expression of the human serotonin transporter. Biochemistry 45:1331-1337.

Laurie SM, Cain CC, Lienhard GE, Castle JD (1993) The glucose transporter GluT4 and secretory carrier membrane proteins (SCAMPs) colocalize in rat adipocytes and partially segregate during insulin stimulation. J Biol Chem 268:19110-19117.

Lee KH, Kim MY, Kim DH, Lee YS (2004) Syntaxin 1A and receptor for activated C kinase interact with the N-terminal region of human dopamine transporter. Neurochem Res 29:1405-1409.

Lesch KP, Gutknecht L (2005) Pharmacogenetics of the serotonin transporter. Prog Neuropsychopharmacol Biol Psychiatry 29:1062-1073.

Lesch KP, Wolozin BL, Murphy DL, Reiderer P (1993a) Primary structure of the human platelet serotonin uptake site: identity with the brain serotonin transporter. J Neurochem 60:2319-2322.

Lesch KP, Wolozin BL, Estler HC, Murphy DL, Riederer P (1993b) Isolation of a cDNA encoding the human brain serotonin transporter. J Neural Transm Gen Sect 91:67-72.

Lesch KP, Aulakh CS, Wolozin BL, Tolliver TJ, Hill JL, Murphy DL (1993c) Regional brain expression of serotonin transporter mRNA and its regulation by reuptake inhibiting antidepressants. Brain Res Mol Brain Res 17:31-35.

Lesch KP, Balling U, Gross J, Strauss K, Wolozin BL, Murphy DL, Riederer P (1994) Organization of the human serotonin transporter gene. J Neural Transm Gen Sect 95:157-162.

Lesch KP, Bengel D, Heils A, Sabol SZ, Greenberg BD, Petri S, Benjamin J, Muller CR, Hamer DH, Murphy DL (1996) Association of anxiety-related traits with a polymorphism in the serotonin transporter gene regulatory region. Science 274:1527-1531.

Lewis MJ, Pelham HR (1992) Ligand-induced redistribution of a human KDEL receptor from the Golgi complex to the endoplasmic reticulum. Cell 68:353-364.

Li L, Chin LS (2003) The molecular machinery of synaptic vesicle exocytosis. Cell Mol Life Sci 60:942-960.

Li LB, Chen N, Ramamoorthy S, Chi L, Cui XN, Wang LC, Reith ME (2004) The role of N-glycosylation in function and surface trafficking of the human dopamine transporter. J Biol Chem 279:21012-21020. Epub 22004 Mar 21015.

Lin F, Lester HA, Mager S (1996) Single-channel currents produced by the serotonin transporter and analysis of a mutation affecting ion permeation. Biophys J 71:3126-3135.

Linnet K, Koed K, Wiborg O, Gregersen N (1995) Serotonin depletion decreases serotonin transporter mRNA levels in rat brain. Brain Res 697:251-253.

Liu L, Guo Z, Tieu Q, Castle A, Castle D (2002) Role of secretory carrier membrane protein SCAMP2 in granule exocytosis. Mol Biol Cell 13:4266-4278.

Liu L, Liao H, Castle A, Zhang J, Casanova J, Szabo G, Castle D (2005) SCAMP2 interacts with Arf6 and phospholipase D1 and links their function to exocytotic fusion pore formation in PC12 cells. Mol Biol Cell 16:4463-4472.

Liu QR, Lopez-Corcuera B, Nelson H, Mandiyan S, Nelson N (1992) Cloning and expression of a cDNA encoding the transporter of taurine and beta-alanine in mouse brain. Proc Natl Acad Sci U S A 89:12145-12149.

Loder MK, Melikian HE (2003) The dopamine transporter constitutively internalizes and recycles in a protein kinase C-regulated manner in stably transfected PC12 cell lines. J Biol Chem 278:22168-22174. Epub 22003 Apr 22167.

Lopez JF, Chalmers DT, Vazquez DM, Watson SJ, Akil H (1994) Serotonin transporter mRNA in rat brain is regulated by classical antidepressants. Biol Psychiatry 35:287-290.

MacKenzie A, Quinn J (1999) A serotonin transporter gene intron 2 polymorphic region, correlated with affective disorders, has allele-dependent differential enhancer-like properties in the mouse embryo. Proc Natl Acad Sci U S A 96:15251-15255.

Mager S, Min C, Henry DJ, Chavkin C, Hoffman BJ, Davidson N, Lester HA (1994) Conducting states of a mammalian serotonin transporter. Neuron 12:845-859.

Magnani F (2004) Thesis: Trafficking and Regulation of the serotonin transporter. In: Department of Biochemistry: Trinity College Dublin.
Magnani F, Tate CG, Wynne S, Williams C, Haase J (2004) Partitioning of the serotonin transporter into lipid microdomains modulates transport of serotonin. J Biol Chem 279:38770-38778.
Margeta-Mitrovic M, Jan YN, Jan LY (2000) A trafficking checkpoint controls GABA(B) receptor heterodimerization. Neuron 27:97-106.
Marone M, Mozzetti S, De Ritis D, Pierelli L, Scambia G (2001) Semiquantitative RT-PCR analysis to assess the expression levels of multiple transcripts from the same sample. Biol Proced Online 3:19-25.
McMahon HT, Mills IG (2004) COP and clathrin-coated vesicle budding: different pathways, common approaches. Curr Opin Cell Biol 16:379-391.
Melikian HE (2004) Neurotransmitter transporter trafficking: endocytosis, recycling, and regulation. Pharmacol Ther 104:17-27.
Melikian HE, Buckley KM (1999) Membrane trafficking regulates the activity of the human dopamine transporter. J Neurosci 19:7699-7710.
Melikian HE, Ramamoorthy S, Tate CG, Blakely RD (1996) Inability to N-glycosylate the human norepinephrine transporter reduces protein stability, surface trafficking, and transport activity but not ligand recognition. Mol Pharmacol 50:266-276.
Miller EA, Beilharz TH, Malkus PN, Lee MC, Hamamoto S, Orci L, Schekman R (2003) Multiple cargo binding sites on the COPII subunit Sec24p ensure capture of diverse membrane proteins into transport vesicles. Cell 114:497-509.
Miller GM, Yatin SM, De La Garza R, 2nd, Goulet M, Madras BK (2001) Cloning of dopamine, norepinephrine and serotonin transporters from monkey brain: relevance to cocaine sensitivity. Brain Res Mol Brain Res 87:124-143.
Miller KJ, Hoffman BJ (1994) Adenosine A3 receptors regulate serotonin transport via nitric oxide and cGMP. J Biol Chem 269:27351-27356.
Miranda M, Dionne KR, Sorkina T, Sorkin A (2006) Three Ubiquitin Conjugation Sites in the Amino Terminus of the Dopamine Transporter Mediate Protein Kinase C-dependent Endocytosis of the Transporter. Mol Biol Cell 1:1.
Miranda M, Wu CC, Sorkina T, Korstjens DR, Sorkin A (2005) Enhanced ubiquitylation and accelerated degradation of the dopamine transporter mediated by protein kinase C. J Biol Chem 280:35617-35624. Epub 32005 Aug 35618.
Mitchell SJ, Ryan TA (2004) Syntaxin-1A is excluded from recycling synaptic vesicles at nerve terminals. J Neurosci 24:4884-4888.
Mochizuki H, Amano T, Seki T, Matsubayashi H, Mitsuhata C, Morita K, Kitayama S, Dohi T, Mishima HK, Sakai N (2005) Role of C-terminal region in the functional regulation of rat serotonin transporter (SERT). Neurochem Int 46:93-105. Epub 2004 Nov 2026.
Montesinos ML, Castellano-Munoz M, Garcia-Junco-Clemente P, Fernandez-Chacon R (2005) Recycling and EH domain proteins at the synapse. Brain Res Brain Res Rev 49:416-428.
Morikawa O, Sakai N, Obara H, Saito N (1998) Effects of interferon-alpha, interferon-gamma and cAMP on the transcriptional regulation of the serotonin transporter. Eur J Pharmacol 349:317-324.

Mortensen OV, Kristensen AS, Wiborg O (2001) Species-scanning mutagenesis of the serotonin transporter reveals residues essential in selective, high-affinity recognition of antidepressants. J Neurochem 79:237-247.
Mortensen OV, Kristensen AS, Rudnick G, Wiborg O (1999a) Molecular cloning, expression and characterization of a bovine serotonin transporter. Brain Res Mol Brain Res 71:120-126.
Mortensen OV, Thomassen M, Larsen MB, Whittemore SR, Wiborg O (1999b) Functional analysis of a novel human serotonin transporter gene promoter in immortalized raphe cells. Brain Res Mol Brain Res 68:141-148.
Mossner R, Daniel S, Schmitt A, Albert D, Lesch KP (2001) Modulation of serotonin transporter function by interleukin-4. Life Sci 68:873-880.
Mossner R, Heils A, Stober G, Okladnova O, Daniel S, Lesch KP (1998) Enhancement of serotonin transporter function by tumor necrosis factor alpha but not by interleukin-6. Neurochem Int 33:251-254.
Murphy DL, Lerner A, Rudnick G, Lesch KP (2004) Serotonin transporter: gene, genetic disorders, and pharmacogenetics. Mol Interv 4:109-123.
Myers CL, Lazo JS, Pitt BR (1989) Translocation of protein kinase C is associated with inhibition of 5-HT uptake by cultured endothelial cells. Am J Physiol 257:L253-258.
Nelson H, Mandiyan S, Nelson N (1990) Cloning of the human brain GABA transporter. FEBS Lett 269:181-184.
Neumaier JF, Root DC, Hamblin MW (1996) Chronic fluoxetine reduces serotonin transporter mRNA and 5-HT1B mRNA in a sequential manner in the rat dorsal raphe nucleus. Neuropsychopharmacology 15:515-522.
Nguyen TT, Amara SG (1996) N-linked oligosaccharides are required for cell surface expression of the norepinephrine transporter but do not influence substrate or inhibitor recognition. J Neurochem 67:645-655.
Nishitani H, Hirose E, Uchimura Y, Nakamura M, Umeda M, Nishii K, Mori N, Nishimoto T (2001) Full-sized RanBPM cDNA encodes a protein possessing a long stretch of proline and glutamine within the N-terminal region, comprising a large protein complex. Gene 272:25-33.
Nordgard O, Dahle O, Andersen TO, Gabrielsen OS (2001) JAB1/CSN5 interacts with the GAL4 DNA binding domain: a note of caution about two-hybrid interactions. Biochimie 83:969-971.
Olivares L, Aragon C, Gimenez C, Zafra F (1995) The role of N-glycosylation in the targeting and activity of the GLYT1 glycine transporter. J Biol Chem 270:9437-9442.
Orban-Nemeth Z, Simader H, Badurek S, Trancikova A, Propst F (2005) Microtubule-associated protein 1S, a short and ubiquitously expressed member of the microtubule-associated protein 1 family. J Biol Chem 280:2257-2265. Epub 2004 Nov 2254.
Ozaki N, Goldman D, Kaye WH, Plotnicov K, Greenberg BD, Lappalainen J, Rudnick G, Murphy DL (2003) Serotonin transporter missense mutation associated with a complex neuropsychiatric phenotype. Mol Psychiatry 8:895, 933-896.
Ozaslan D, Wang S, Ahmed BA, Kocabas AM, McCastlain JC, Bene A, Kilic F (2003) Glycosyl modification facilitates homo- and hetero-oligomerization of the

serotonin transporter. A specific role for sialic acid residues. J Biol Chem 278:43991-44000. Epub 42003 Aug 43927.
Ozsarac N, Santha E, Hoffman BJ (2002) Alternative non-coding exons support serotonin transporter mRNA expression in the brain and gut. J Neurochem 82:336-344.
Pacholczyk T, Blakely RD, Amara SG (1991) Expression cloning of a cocaine- and antidepressant-sensitive human noradrenaline transporter. Nature 350:350-354.
Padbury JF, Tseng YT, McGonnigal B, Penado K, Stephan M, Rudnick G (1997) Placental biogenic amine transporters: cloning and expression. Brain Res Mol Brain Res 45:163-168.
Pandey GN (1997) Altered serotonin function in suicide. Evidence from platelet and neuroendocrine studies. Ann N Y Acad Sci 836:182-200.
Parkkinen JJ, Lammi MJ, Agren U, Tammi M, Keinanen TA, Hyvonen T, Eloranta TO (1997) Polyamine-dependent alterations in the structure of microfilaments, Golgi apparatus, endoplasmic reticulum, and proteoglycan synthesis in BHK cells. J Cell Biochem 66:165-174.
Pelham HR (1988) Evidence that luminal ER proteins are sorted from secreted proteins in a post-ER compartment. Embo J 7:913-918.
Pelham HR (1991) Recycling of proteins between the endoplasmic reticulum and Golgi complex. Curr Opin Cell Biol 3:585-591.
Piatigorsky J (2001) Dual use of the transcriptional repressor (CtBP2)/ribbon synapse (RIBEYE) gene: how prevalent are multifunctional genes? Trends Neurosci 24:555-557.
Plein H, Berk M (2001) The platelet as a peripheral marker in psychiatric illness. Hum Psychopharmacol 16:229-236.
Prasad HC, Zhu CB, McCauley JL, Samuvel DJ, Ramamoorthy S, Shelton RC, Hewlett WA, Sutcliffe JS, Blakely RD (2005) Human serotonin transporter variants display altered sensitivity to protein kinase G and p38 mitogen-activated protein kinase. Proc Natl Acad Sci U S A 102:11545-11550. Epub 12005 Jul 11529.
Prasad PD, Torres-Zamorano V, Kekuda R, Leibach FH, Ganapathy V (1997) Functional link between tyrosine phosphorylation and human serotonin transporter gene expression. Eur J Pharmacol 325:85-92.
Provoda CJ, Waring MT, Buckley KM (2000) Evidence for a primary endocytic vesicle involved in synaptic vesicle biogenesis. J Biol Chem 275:7004-7012.
Purselle DC, Nemeroff CB (2003) Serotonin transporter: a potential substrate in the biology of suicide. Neuropsychopharmacology 28:613-619. Epub 2002 Oct 2017.
Qian Y, Melikian HE, Rye DB, Levey AI, Blakely RD (1995) Identification and characterization of antidepressant-sensitive serotonin transporter proteins using site-specific antibodies. J Neurosci 15:1261-1274.
Qian Y, Galli A, Ramamoorthy S, Risso S, DeFelice LJ, Blakely RD (1997) Protein kinase C activation regulates human serotonin transporters in HEK-293 cells via altered cell surface expression. J Neurosci 17:45-57.
Quick MW (2002) Role of syntaxin 1A on serotonin transporter expression in developing thalamocortical neurons. Int J Dev Neurosci 20:219-224.
Quick MW (2003) Regulating the conducting states of a mammalian serotonin transporter. Neuron 40:537-549.

Radian R, Bendahan A, Kanner BI (1986) Purification and identification of the functional sodium- and chloride-coupled gamma-aminobutyric acid transport glycoprotein from rat brain. J Biol Chem 261:15437-15441.

Ramamoorthy JD, Ramamoorthy S, Papapetropoulos A, Catravas JD, Leibach FH, Ganapathy V (1995a) Cyclic AMP-independent up-regulation of the human serotonin transporter by staurosporine in choriocarcinoma cells. J Biol Chem 270:17189-17195.

Ramamoorthy S, Blakely RD (1999) Phosphorylation and sequestration of serotonin transporters differentially modulated by psychostimulants. Science 285:763-766.

Ramamoorthy S, Giovanetti E, Qian Y, Blakely RD (1998) Phosphorylation and regulation of antidepressant-sensitive serotonin transporters. J Biol Chem 273:2458-2466.

Ramamoorthy S, Cool DR, Mahesh VB, Leibach FH, Melikian HE, Blakely RD, Ganapathy V (1993a) Regulation of the human serotonin transporter. Cholera toxin-induced stimulation of serotonin uptake in human placental choriocarcinoma cells is accompanied by increased serotonin transporter mRNA levels and serotonin transporter-specific ligand binding. J Biol Chem 268:21626-21631.

Ramamoorthy S, Ramamoorthy JD, Prasad PD, Bhat GK, Mahesh VB, Leibach FH, Ganapathy V (1995b) Regulation of the human serotonin transporter by interleukin-1 beta. Biochem Biophys Res Commun 216:560-567.

Ramamoorthy S, Bauman AL, Moore KR, Han H, Yang-Feng T, Chang AS, Ganapathy V, Blakely RD (1993b) Antidepressant- and cocaine-sensitive human serotonin transporter: molecular cloning, expression, and chromosomal localization. Proc Natl Acad Sci U S A 90:2542-2546.

Ranganathan R, Sawin ER, Trent C, Horvitz HR (2001) Mutations in the Caenorhabditis elegans serotonin reuptake transporter MOD-5 reveal serotonin-dependent and -independent activities of fluoxetine. J Neurosci 21:5871-5884.

Rao MA, Cheng H, Quayle AN, Nishitani H, Nelson CC, Rennie PS (2002) RanBPM, a nuclear protein that interacts with and regulates transcriptional activity of androgen receptor and glucocorticoid receptor. J Biol Chem 277:48020-48027. Epub 42002 Oct 48021.

Rapport MM (1949) "Serum vasoconstrictor (serotonin) V. The presence of creatinine in the complex. A proposed structure of the vasoconstrictor principle,". J Biol Chem 180:961-969.

Rapport MM, Green AA, Page IH (1948) "Serum vasoconstrictor (serotonin) IV. Isolation and characterization,". J Biol Chem 176:1243-1251.

Reiter RJ (1991) Pineal melatonin: cell biology of its synthesis and of its physiological interactions. Endocr Rev 12:151-180.

Reith MEA (1998) Neurotransmitter Transporters: structure, function, and regulation: Humana Press.

Ribeiro FM, Black SA, Cregan SP, Prado VF, Prado MA, Rylett RJ, Ferguson SS (2005) Constitutive high-affinity choline transporter endocytosis is determined by a carboxyl-terminal tail dileucine motif. J Neurochem 94:86-96.

Rodriguez GJ, Roman DL, White KJ, Nichols DE, Barker EL (2003) Distinct recognition of substrates by the human and Drosophila serotonin transporters. J Pharmacol Exp Ther 306:338-346. Epub 2003 Apr 2007.

Roman DL, Walline CC, Rodriguez GJ, Barker EL (2003) Interactions of antidepressants with the serotonin transporter: a contemporary molecular analysis. Eur J Pharmacol 479:53-63.

Rost B, Yachdav G, Liu J (2004) The PredictProtein server. Nucleic Acids Res 32:W321-326.

Rudnick G (1998) Bioenergetics of neurotransmitter transport. J Bioenerg Biomembr 30:173-185.

Rudnick G, Wall SC (1993) Non-neurotoxic amphetamine derivatives release serotonin through serotonin transporters. Mol Pharmacol 43:271-276.

Sakai N, Kodama N, Ohmori S, Sasaki K, Saito N (2000) Involvement of the actin cytoskeleton in the regulation of serotonin transporter (SET) activity: possible mechanism underlying SET regulation by protein kinase C. Neurochem Int 36:567-579.

Sakai N, Sasaki K, Nakashita M, Honda S, Ikegaki N, Saito N (1997) Modulation of serotonin transporter activity by a protein kinase C activator and an inhibitor of type 1 and 2A serine/threonine phosphatases. J Neurochem 68:2618-2624.

Salaun C, Gould GW, Chamberlain LH (2005) Lipid raft association of SNARE proteins regulates exocytosis in PC12 cells. J Biol Chem 280:19449-19453. Epub 12005 Mar 19415.

Sambrook J, Russel DW (2001) Molecular Cloning: A Laboratory Manual, 3rd edition (January 15) Edition.

Samuvel DJ, Jayanthi LD, Bhat NR, Ramamoorthy S (2005) A role for p38 mitogen-activated protein kinase in the regulation of the serotonin transporter: evidence for distinct cellular mechanisms involved in transporter surface expression. J Neurosci 25:29-41.

Schildkraut JJ (1965) The catecholamine hypothesis of affective disorders: a review of supporting evidence. Am J Psychiatry 122:509-522.

Schmid JA, Scholze P, Kudlacek O, Freissmuth M, Singer EA, Sitte HH (2001) Oligomerization of the human serotonin transporter and of the rat GABA transporter 1 visualized by fluorescence resonance energy transfer microscopy in living cells. J Biol Chem 276:3805-3810. Epub 2000 Nov 3808.

Schmitz F, Konigstorfer A, Sudhof TC (2000) RIBEYE, a component of synaptic ribbons: a protein's journey through evolution provides insight into synaptic ribbon function. Neuron 28:857-872.

Schoenfeld TA, McKerracher L, Obar R, Vallee RB (1989) MAP 1A and MAP 1B are structurally related microtubule associated proteins with distinct developmental patterns in the CNS. J Neurosci 9:1712-1730.

Scott DB, Blanpied TA, Ehlers MD (2003) Coordinated PKA and PKC phosphorylation suppresses RXR-mediated ER retention and regulates the surface delivery of NMDA receptors. Neuropharmacology 45:755-767.

Scott DB, Blanpied TA, Swanson GT, Zhang C, Ehlers MD (2001) An NMDA receptor ER retention signal regulated by phosphorylation and alternative splicing. J Neurosci 21:3063-3072.

Shibanuma M, Kim-Kaneyama JR, Ishino K, Sakamoto N, Hishiki T, Yamaguchi K, Mori K, Mashimo J, Nose K (2003) Hic-5 communicates between focal adhesions and the nucleus through oxidant-sensitive nuclear export signal. Mol Biol Cell 14:1158-1171.

Shikano S, Li M (2003) Membrane receptor trafficking: evidence of proximal and distal zones conferred by two independent endoplasmic reticulum localization signals. Proc Natl Acad Sci U S A 100:5783-5788.

Shimada S, Kitayama S, Lin CL, Patel A, Nanthakumar E, Gregor P, Kuhar M, Uhl G (1991) Cloning and expression of a cocaine-sensitive dopamine transporter complementary DNA. Science 254:576-578.

Sitte HH, Farhan H, Javitch JA (2004) Sodium-Dependent Neurotransmitter TRANSPORTERS: OLIGOMERIZATION as a Determinant of Transporter Function and Trafficking. Mol Interv 4:38-47.

Smith KE, Borden LA, Hartig PR, Branchek T, Weinshank RL (1992a) Cloning and expression of a glycine transporter reveal colocalization with NMDA receptors. Neuron 8:927-935.

Smith KE, Borden LA, Wang CH, Hartig PR, Branchek TA, Weinshank RL (1992b) Cloning and expression of a high affinity taurine transporter from rat brain. Mol Pharmacol 42:563-569.

Sorkina T, Hoover BR, Zahniser NR, Sorkin A (2005) Constitutive and protein kinase C-induced internalization of the dopamine transporter is mediated by a clathrin-dependent mechanism. Traffic 6:157-170.

Sorkina T, Doolen S, Galperin E, Zahniser NR, Sorkin A (2003) Oligomerization of dopamine transporters visualized in living cells by fluorescence resonance energy transfer microscopy. J Biol Chem 278:28274-28283. Epub 22003 May 28213.

Spurlock G, Buckland P, O'Donovan M, McGuffin P (1994) Lack of effect of antidepressant drugs on the levels of mRNAs encoding serotonergic receptors, synthetic enzymes and 5HT transporter. Neuropharmacology 33:433-440.

Standley S, Roche KW, McCallum J, Sans N, Wenthold RJ (2000) PDZ domain suppression of an ER retention signal in NMDA receptor NR1 splice variants. Neuron 28:887-898.

Stanley M, Stanley B (1990) Postmortem evidence for serotonin's role in suicide. J Clin Psychiatry 51 Suppl:22-28; discussion 29-30.

Storrie B, White J, Rottger S, Stelzer EH, Suganuma T, Nilsson T (1998) Recycling of golgi-resident glycosyltransferases through the ER reveals a novel pathway and provides an explanation for nocodazole-induced Golgi scattering. J Cell Biol 143:1505-1521.

Strausberg RL, Feingold EA, Grouse LH, Derge JG, Klausner RD, Collins FS, Wagner L, Shenmen CM, Schuler GD, Altschul SF, Zeeberg B, Buetow KH, Schaefer CF, Bhat NK, Hopkins RF, Jordan H, Moore T, Max SI, Wang J, Hsieh F, Diatchenko L, Marusina K, Farmer AA, Rubin GM, Hong L, Stapleton M, Soares MB, Bonaldo MF, Casavant TL, Scheetz TE, Brownstein MJ, Usdin TB, Toshiyuki S, Carninci P, Prange C, Raha SS, Loquellano NA, Peters GJ, Abramson RD, Mullahy SJ, Bosak SA, McEwan PJ, McKernan KJ, Malek JA, Gunaratne PH, Richards S, Worley KC, Hale S, Garcia AM, Gay LJ, Hulyk SW, Villalon DK, Muzny DM, Sodergren EJ, Lu X, Gibbs RA, Fahey J, Helton

E, Ketteman M, Madan A, Rodrigues S, Sanchez A, Whiting M, Young AC, Shevchenko Y, Bouffard GG, Blakesley RW, Touchman JW, Green ED, Dickson MC, Rodriguez AC, Grimwood J, Schmutz J, Myers RM, Butterfield YS, Krzywinski MI, Skalska U, Smailus DE, Schnerch A, Schein JE, Jones SJ, Marra MA (2002) Generation and initial analysis of more than 15,000 full-length human and mouse cDNA sequences. Proc Natl Acad Sci U S A 99:16899-16903. Epub 12002 Dec 16811.

Sung U, Jennings JL, Link AJ, Blakely RD (2005) Proteomic analysis of human norepinephrine transporter complexes reveals associations with protein phosphatase 2A anchoring subunit and 14-3-3 proteins. Biochem Biophys Res Commun 333:671-678.

Sung U, Apparsundaram S, Galli A, Kahlig KM, Savchenko V, Schroeter S, Quick MW, Blakely RD (2003) A regulated interaction of syntaxin 1A with the antidepressant-sensitive norepinephrine transporter establishes catecholamine clearance capacity. J Neurosci 23:1697-1709.

Südhof TC (1995) The synaptic vesicle cycle: a cascade of protein-protein interactions. Nature 375:645-653.

Tanahashi H, Tabira T (1999) X11L2, a new member of the X11 protein family, interacts with Alzheimer's beta-amyloid precursor protein. Biochem Biophys Res Commun 255:663-667.

Tao-Cheng JH, Zhou FC (1999) Differential polarization of serotonin transporters in axons versus soma-dendrites: an immunogold electron microscopy study. Neuroscience 94:821-830.

Tate CG, Blakely RD (1994) The effect of N-linked glycosylation on activity of the Na(+)- and Cl(-)-dependent serotonin transporter expressed using recombinant baculovirus in insect cells. J Biol Chem 269:26303-26310.

Thaminy S, Miller J, Stagljar I (2004) The split-ubiquitin membrane-based yeast two-hybrid system. Methods Mol Biol 261:297-312.

Thoidis G, Chen P, Pushkin AV, Vallega G, Leeman SE, Fine RE, Kandror KV (1998) Two distinct populations of synaptic-like vesicles from rat brain. Proc Natl Acad Sci U S A 95:183-188.

Tork I (1990) Anatomy of the serotonergic system. Ann N Y Acad Sci 600:9-34.

Torres GE, Caron MG (2003) Center stage for the serotonin transporter: a gain-of-function polymorphism in persons with obsessive-compulsive disorder. Mol Pharmacol 64:196-198.

Torres GE, Yao WD, Mohn AR, Quan H, Kim KM, Levey AI, Staudinger J, Caron MG (2001) Functional interaction between monoamine plasma membrane transporters and the synaptic PDZ domain-containing protein PICK1. Neuron 30:121-134.

Traub LM, Kornfeld S (1997) The trans-Golgi network: a late secretory sorting station. Curr Opin Cell Biol 9:527-533.

Trojanowski JQ, Lee VM (2000) "Fatal attractions" of proteins. A comprehensive hypothetical mechanism underlying Alzheimer's disease and other neurodegenerative disorders. Ann N Y Acad Sci 924:62-67.

Twarog BM, Page IH (1953) Serotonin content of some mammalian tissues and urine and a method for its determination. Am J Physiol 175:157-161.

Uchida S, Kwon HM, Yamauchi A, Preston AS, Marumo F, Handler JS (1992) Molecular cloning of the cDNA for an MDCK cell Na(+)- and Cl(-)-dependent taurine transporter that is regulated by hypertonicity. Proc Natl Acad Sci U S A 89:8230-8234.

Urade Y, Hayaishi O (2000) Biochemical, structural, genetic, physiological, and pathophysiological features of lipocalin-type prostaglandin D synthase. Biochim Biophys Acta 1482:259-271.

Usdin TB, Mezey E, Chen C, Brownstein MJ, Hoffman BJ (1991) Cloning of the cocaine-sensitive bovine dopamine transporter. Proc Natl Acad Sci U S A 88:11168-11171.

Van Criekinge W, Beyaert R (1999) Yeast Two-Hybrid: State of the Art. Biol Proced Online 2:1-38.

Virtanen I, Ekblom P, Laurila P (1980) Subcellular compartmentalization of saccharide moieties in cultured normal and malignant cells. J Cell Biol 85:429-434.

Walch-Solimena C, Blasi J, Edelmann L, Chapman ER, von Mollard GF, Jahn R (1995) The t-SNAREs syntaxin 1 and SNAP-25 are present on organelles that participate in synaptic vesicle recycling. J Cell Biol 128:637-645.

Wall SC, Gu H, Rudnick G (1995) Biogenic amine flux mediated by cloned transporters stably expressed in cultured cell lines: amphetamine specificity for inhibition and efflux. Mol Pharmacol 47:544-550.

Walther DJ, Peter JU, Bashammakh S, Hortnagl H, Voits M, Fink H, Bader M (2003) Synthesis of serotonin by a second tryptophan hydroxylase isoform. Science 299:76.

Wang D, Quick MW (2005) Trafficking of the plasma membrane gamma-aminobutyric acid transporter GAT1. Size and rates of an acutely recycling pool. J Biol Chem 280:18703-18709. Epub 12005 Mar 18718.

Wang D, Li Z, Messing EM, Wu G (2002) Activation of Ras/Erk pathway by a novel MET-interacting protein RanBPM. J Biol Chem 277:36216-36222. Epub 32002 Jul 36229.

Wang Y, Takai R, Yoshioka H, Shirabe K (2006) Characterization and expression of serotonin transporter genes in zebrafish. Tohoku J Exp Med 208:267-274.

White LA, Eaton MJ, Castro MC, Klose KJ, Globus MY, Shaw G, Whittemore SR (1994) Distinct regulatory pathways control neurofilament expression and neurotransmitter synthesis in immortalized serotonergic neurons. J Neurosci 14:6744-6753.

Wiche G, Oberkanins C, Himmler A (1991) Molecular structure and function of microtubule-associated proteins. Int Rev Cytol 124:217-273.

Wong EY, Tse JY, Yao KM, Tam PC, Yeung WS (2002) VCY2 protein interacts with the HECT domain of ubiquitin-protein ligase E3A. Biochem Biophys Res Commun 296:1104-1111.

Wu TT, Castle JD (1998) Tyrosine phosphorylation of selected secretory carrier membrane proteins, SCAMP1 and SCAMP3, and association with the EGF receptor. Mol Biol Cell 9:1661-1674.

Yamashita A, Singh SK, Kawate T, Jin Y, Gouaux E (2005) Crystal structure of a bacterial homologue of Na+/Cl--dependent neurotransmitter transporters. Nature 437:215-223. Epub 2005 Jul 2024.

Yamauchi A, Uchida S, Kwon HM, Preston AS, Robey RB, Garcia-Perez A, Burg MB, Handler JS (1992) Cloning of a Na(+)- and Cl(-)-dependent betaine transporter that is regulated by hypertonicity. J Biol Chem 267:649-652.

Yuan H, Michelsen K, Schwappach B (2003) 14-3-3 dimers probe the assembly status of multimeric membrane proteins. Curr Biol 13:638-646.

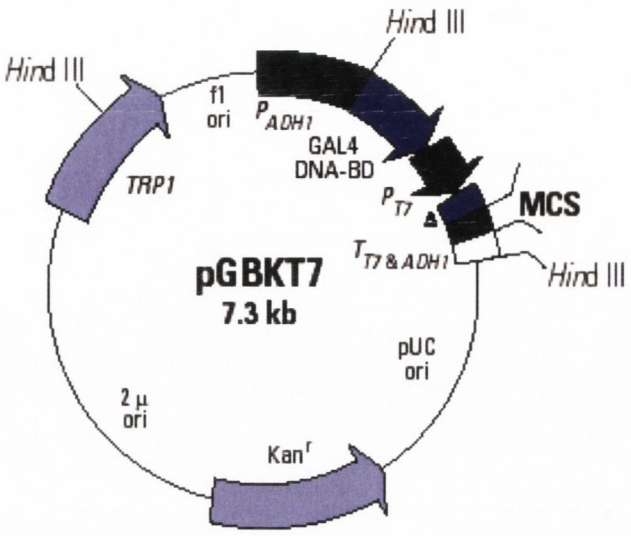
Zerangue N, Schwappach B, Jan YN, Jan LY (1999) A new ER trafficking signal regulates the subunit stoichiometry of plasma membrane K(ATP) channels. Neuron 22:537-548.

Zerial M, McBride H (2001) Rab proteins as membrane organizers. Nat Rev Mol Cell Biol 2:107-117.

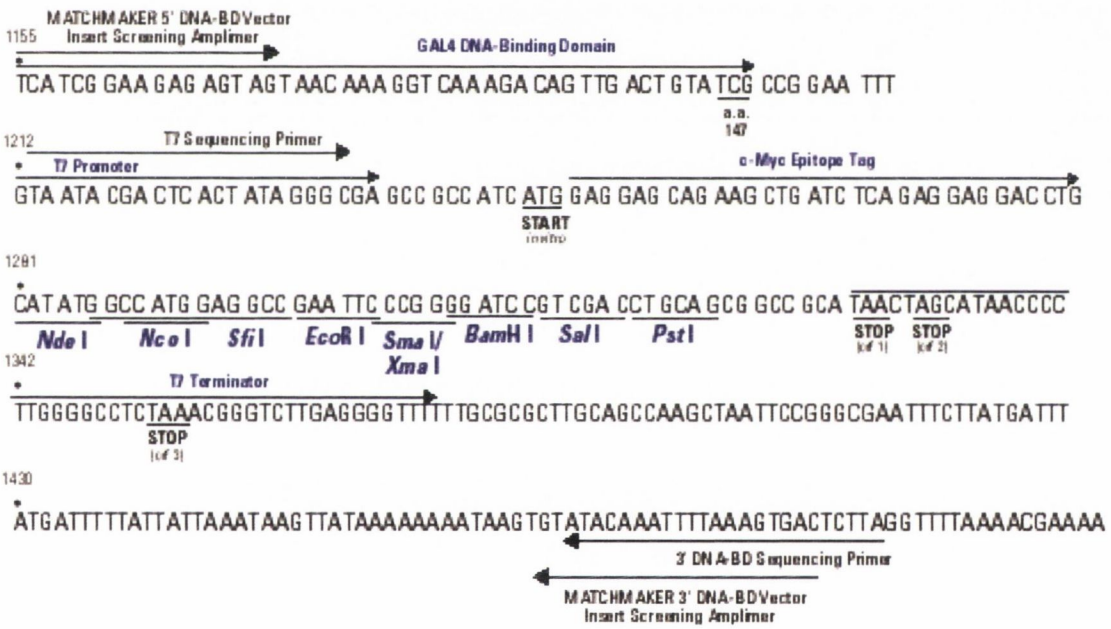
Zhang W, Crocker E, McLaughlin S, Smith SO (2003) Binding of peptides with basic and aromatic residues to bilayer membranes: phenylalanine in the myristoylated alanine-rich C kinase substrate effector domain penetrates into the hydrophobic core of the bilayer. J Biol Chem 278:21459-21466.

Zhu CB, Hewlett WA, Feoktistov I, Biaggioni I, Blakely RD (2004) Adenosine receptor, protein kinase G, and p38 mitogen-activated protein kinase-dependent up-regulation of serotonin transporters involves both transporter trafficking and activation. Mol Pharmacol 65:1462-1474.

Zhu CB, Carneiro AM, Dostmann WR, Hewlett WA, Blakely RD (2005) p38 MAPK activation elevates serotonin transport activity via a trafficking-independent, protein phosphatase 2A-dependent process. J Biol Chem 280:15649-15658. Epub 12005 Feb 15622.

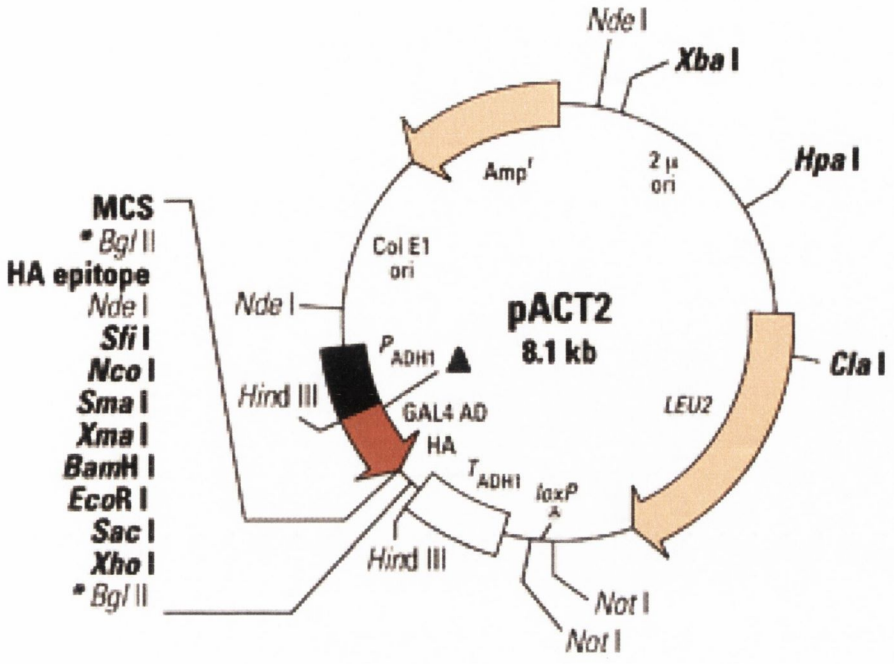


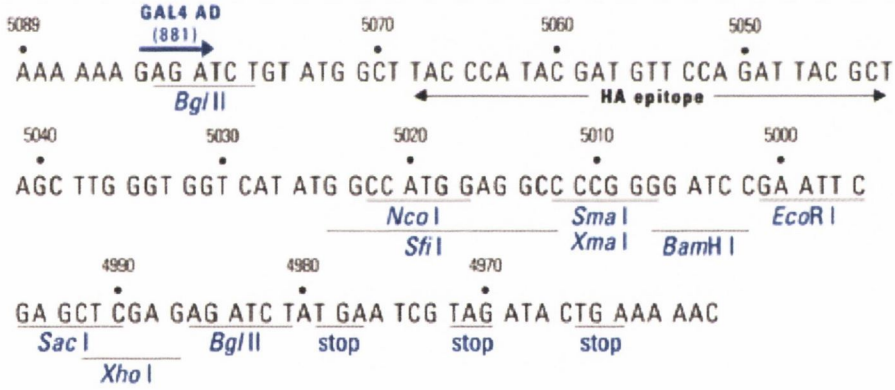
▲ c-Myc epitope tag



---

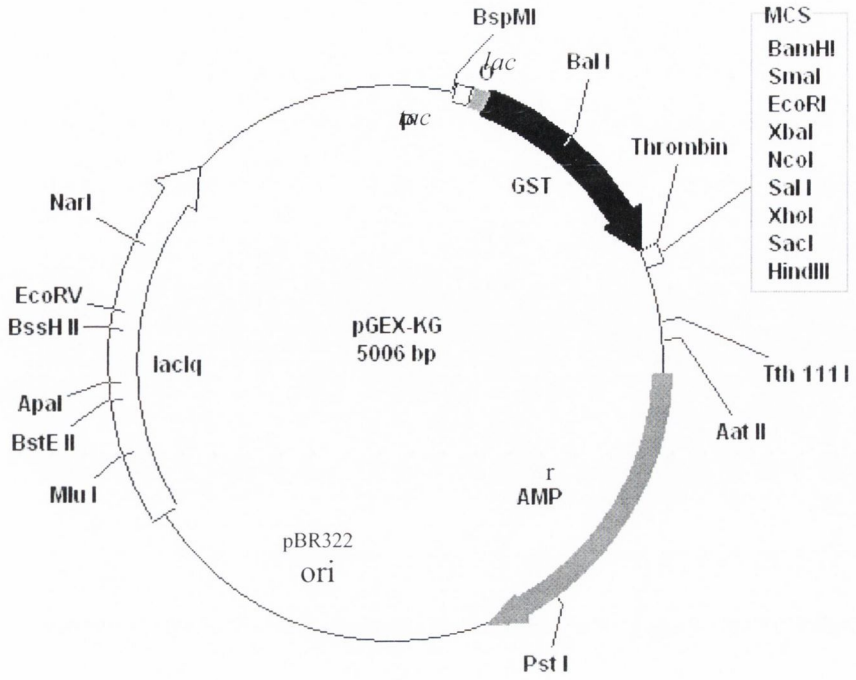
pGBKT7 generates a fusion of the GAL4 DNA-BD, a c-Myc epitope tag, and a protein of interest. In yeast, the hybrid protein is expressed at high levels from the constitutive ADH1 promoter and transcription is terminated by the T7 and ADH1 transcription termination signals. pGBKT7 also contains a T7 promoter which can be used for in vitro transcription and translation of the c-Myc tagged protein. pGBKT7 is a shuttle vector that replicates autonomously in both *E. coli* and *S. cerevisiae*. It carries Kan^r which confers kanamycin resistance in *E. coli* and the *TRP1* nutritional marker that allows yeast to be selected on medium lacking tryptone





---

pACT2 generates a fusion of the GAL4 AD, an HA epitope tag, and a protein of interest or a protein encoded by a cDNA in a fusion library. In yeast, the hybrid protein is expressed at high levels from the constitutive ADH1 promoter and transcription is terminated at the ADH1 transcription termination signal. The fusion protein is targeted to the yeast nucleus by the nuclear localization signal (NLS) from SV40 T-antigen. pACT2 is a shuttle vector that replicates autonomously in both *E. coli* and *S. cerevisiae*. It carries AMP^r which confers ampicillin resistance in *E. coli* and the *LEU2* nutritional marker that allows yeast to be selected on medium lacking leucine.



Thrombin

L V P R G S P G I S G G G G G I L D

CTG GTT CCG CGT GGA TCC CCG GGA ATT TCC GGT GGT GGT GGT GGA ATT CTA GAC

BamHI *SmaI* *EcoRI* *XbaI*

S M G R L E L K L N S S

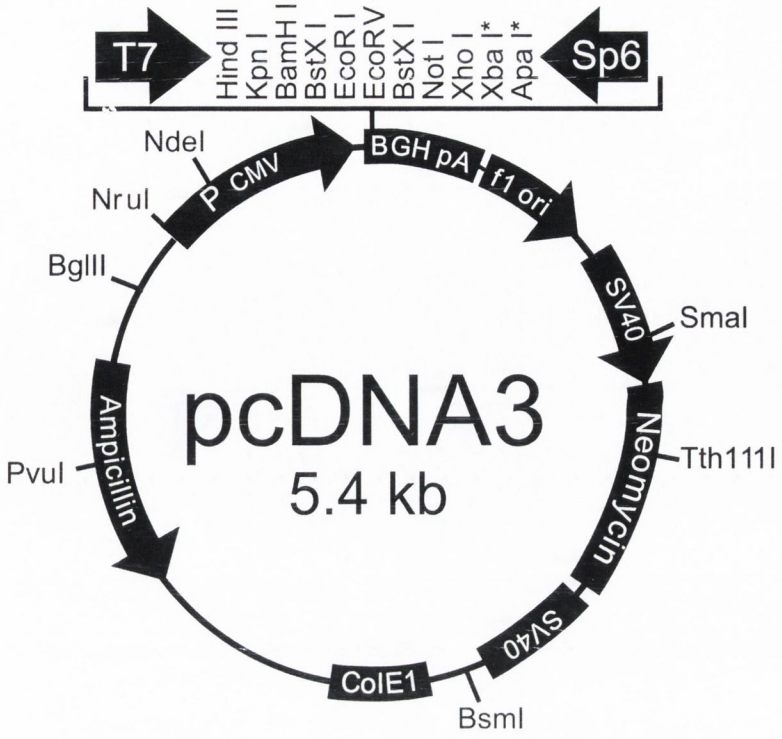
TCC ATG GGT CGA CTC GAG CTC AAG CTT AAT TCA TCG TGACTGACTGAC

NcoI *XhoI* *HindIII* STOP Orf 1 STOP Orf 2 STOP Orf 3

Sal I *SacI*

---

pGEX-KG is a derivative of pGEX-2T (Amersham Biosciences); a linker has been introduced in order to expand the multiple cloning site with additional six restriction sites. pGEX-KG generates a fusion of the 26 kDa glutathione S-transferase (GST) and a protein of interest. The GST can be removed from the fusion protein by enzymatic cleavage with thrombin. The GST fusion gene is under control of the *tac* promoter which is inducible with IPTG. A translation terminator is provided in each reading frame. pGEX-KG carries AMP^r which confers ampicillin resistance in *E. coli.*



enhancer region (3' end)

704 GAGTTTGTTT TGGCACCAAA ATCAACGGGA CTTTCCAAAA TGTCGTAACA ACTCCGCCCC

CAAT TATA 3' end of hCMV

764 ATTGACGCAA ATGGGCGGTA GGCGTGTACG GTGGGAGGTC TATATAAGCA GAGCTCTCTG

putative transcriptional start T7 promoter

824 GCTAACTAGA GAACCCACTG CTTACTGGCT TATCGAAATT AATACGACTC ACTATAGGGA

Hind III Kpn I BamH I BstXI EcoRI

884 GACCCAAGCT TGGTACCGAG CTCGGATCCA CTAGTAACGG CCGCCAGTGT GCTGGAATTC

EcoR V BstX I Not I XhoI XbaI ApaI

944 TGCAGATATC CATCACACTG GCGGCCGCTC GAGCATGCAT CTAGAGGGCC CTATTCTATA

Sp6 promoter

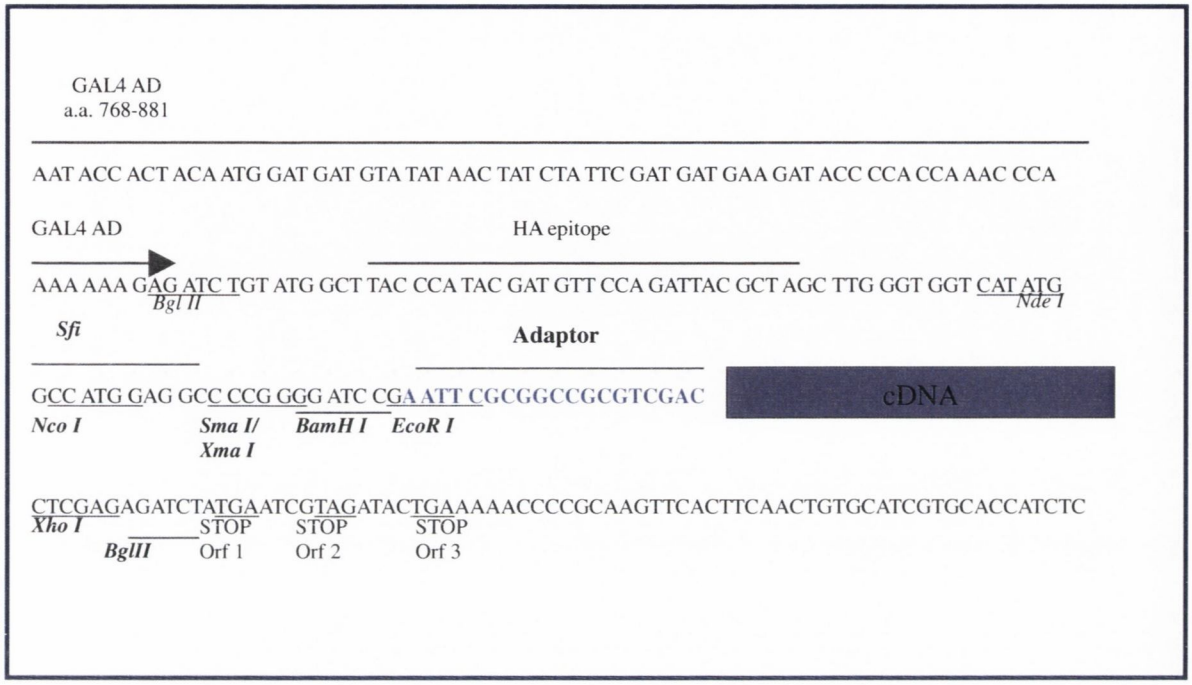
1004 GTGTCACCTA AATGCTAGAG CTCGCTGATC AGCCTCGACT GTGCCTTCTA GTTGCCAGCC

1064 ATCTGTTGTT TGCCCCTCCC CCGTGCCTTC CTTGACCCTG GAAGGTGCCA CTCCCACTGT

BGH polyA

1124 CCTTTCCTAA TAAAATGAGG AAATTGCAT

Pretransformed Human Brain cDNA Library



The human brain cDNA library was directional cloned into the EcoR I / Xho I cloning site in the pACT2 vector using Xho I-$(dT)_{15}$ + Xho I-random priming and an adaptor sequence in the 5' end of the cDNA :

5' AATTCGCGGCCGCGTCGAC 3'
3' GCGCCGGCGCAGCTG 5'

The source of mRNA was a whole brain from a 37 year old Caucasian male who died from trauma.

The cDNAs ranged in size from 0.5 to 4.5 kb with an average size of 1.5 kb and the number of independent clones was determined to 5 x 10^6.

Construct or PCR Product	Primers
pGBKT7-hSERT (1-87) (NdeI)	Forward: 5'- GCGTCAAGCATATGATGGAGACGACGCCCTTG Revers: 5'- CCAGCTTACATATGATCCACCTTCTTGCCCCA
pGBKT7-hSERT (1-108) (NcoI)	Forward: 5'- GCGTCCATGGAGATGGAGACGACGCCCTTG Revers: 5' - GCGTCCATGGCTATGTAGGGGAAGCGCCA
pGBKT7-hSERT (596-630) (NdeI)	Forward: 5'- GCGTCAAGCATATGCGGTTGATCATCACTCCAG Revers: 5'- CCAGCTTACATATGTTACACAGCATTCAAGCGG
pGBKT7-hSERT (577-630) (NdeI)	Forward: 5'- GCGTCAAGCATATGTTGGGTTACTGCATAGGAAC Revers: 5'- CCAGCTTACATATGTTACACAGCATTCAAGCGG
pGBKT7-hSERT (577-629) (NcoI/SalI)	Forward: 5'- GCGTCCATGGCATTGGGTTACTGCATAGGAAC Revers: 5'- GCGTGTCGACTTAAGCATTCAAGCGGATGTCCC
pGBKT7-hSERT (577-627) (NcoI/SalI)	Forward: 5'- GCGTCCATGGCATTGGGTTACTGCATAGGAAC Revers: 5'- GCGTGTCGACTTACAAGCGGATGTCCCCACAAG
pGBKT7-hDAT (560-620) (EcoRI/SalI)	Forward: 5'- GCGTGAATTCCTGGGCTGGGTCATCGCC Revers: 5'- GCGTGTCGACCTACACCTTGAGCCAGTGGCG
pGBKT7-hNET (557-617) (EcoRI/SalI)	Forward: 5'- GCGTGAATTCGTGGGGTGGGGCATCGC Revers: 5'- GCGTGTCGACTCAGATGGCCAGCCAGTG
pGBKT7-hSERT (41-108) (NcoI/BamHI)	Forward: 5'- GCGTCCATGGAGGGGCAAATATCCAATGGGTAC Revers: 5'- GCGTGGATCCCTATGTAGGGGAAGCGCCAGA
pGBKT7-hSERT (61-108) (NcoI/BamHI)	Forward: 5'- GCGTCCATGGAGCACTCTATCCCAGCGACC Revers: 5'- GCGTGGATCCCTATGTAGGGGAAGCGCCAGA
pGBKT7-hSERT (78-108) (NcoI/BamHI)	Forward: 5'- GCGTCCATGGAGCGGGAGACCTGGGGCAAG Revers: 5'- GCGTGGATCCCTATGTAGGGGAAGCGCCAGA

pGBKT7-hSERT (1-100) (NcoI/BamHI)	Forward: 5'- GCGTCCATGGAGATGGAGACGACGCCCTTG Revers: 5'- GCGTGGATCCCGCCCAGGTCCACAGCATAG
pACT2-hESO3 (1-60) (EcoRI/XhoI)	Forward: 5'- GCGTGAATTCTAATGCGGGACGCGGATGCA Revers: 5'- GCGTCTCGAGCGGCCGCATTCGTGACC
pACT2-hESO3 (1-101) (EcoRI/XhoI)	Forward: 5'- GCGTGAATTCTAATGCGGGACGCGGATGCA Revers: 5'- GCGTCTCGAGGCCACTCACTGTGAGATCC
pACT2-hESO3 (61-143) (EcoRI/XhoI)	Forward: 5'- GCGTGAATTCTGCACATATTCACCCTCAGCG Revers: 5'- GCGTCTCGAGCTTAGCGGGAAACGGGG
pGEX-KG-hSERT (1-87) (BamHI/SalI)	Forward: 5'- GCGTGGATCCATGGAGACGACGCCCTTG Revers: 5'- GCGTGTCGACTTAATCCACCTTCTTGCCCCA
pGEX-KG-hSERT (1-108) (BamHI/SalI)	Forward: 5'- GCGTGGATCCATGGAGACGACGCCCTTG Revers: 5'- GCGTGTCGACTTATATGTAGGGGAAGCGCCA
pGEX-KG-hSERT (596-630) (NcoI/SalI)	Forward: 5'- GCGTCCATGGCACGGTTGATCATCACTCCAG Revers: 5'- GCGTGTCGACTTACACAGCATTCAAGCGG
pGEX-KG-hSERT (577-630) (NcoI/SalI)	Forward: 5'- GCGTCCATGGCATTGGGTTACTGCATAGGAAC Revers: 5'- GCGTGTCGACTTACACAGCATTCAAGCGG
pGEX-KG-hSERT (577-629) (NcoI/SalI)	Forward: 5'- GCGTCCATGGCATTGGGTTACTGCATAGGAAC Revers: 5'- GCGTGTCGACTTAAGCATTCAAGCGGATGTCCC
pGEX-KG-hSERT (577-627) (NcoI/SalI)	Forward: 5'- GCGTCCATGGCATTGGGTTACTGCATAGGAAC Revers: 5'- GCGTGTCGACTTACAAGCGGATGTCCCCACAAG
pGEX-KG-hNET (1-85) (BamHI/NcoI)	Forward: 5'- GCGTGGATCCGCGATGCTTCTGGCGCGGATGAA Revers: 5'- GCGTCCATGGTTAGAGGTAGGGGAAGCGCCA
pGEX-KG-hDAT (1-89) (BamHI/NcoI)	Forward: 5'- GCGTGGATCCGCGATGAGTAAGAGCAAATGCTCCG Revers: 5'- GCGTCCATGGTTACAGGTAGGGGAACCGCCA

pGEX-KG-hNET (557-617) (EcoRI/SalI)	Forward: 5'- GCGTGAATTCTAGTGGGGTGGGGCATCGC Revers: 5'- GCGTGTCGACTCAGATGGCCAGCCAGTG
pGEX-KG-hDAT (560-620) (EcoRI/SalI)	Forward: 5'- GCGTGAATTCTACTGGGCTGGGTCATCGCC Revers: 5'- GCGTGTCGACCTACACCTTGAGCCAGTGGCG
pcDNA3-SCAMP2 (HindIII/NotI)	Forward: 5'- GCGTAAGCTTGATGTCGGCTTTCGACACCAAC Revers: 5'- GCGTGCGGCCGCCTAATTCCCCTGGAAGGCTC
pcDNA3-SCAMP2 C201A	Forward: 5'- CTCCCTGTGCCTTCCTTGCTTGGTACCGACCCATCTAT Revers: 5'- ATAGATGGGTCGGTACCAAGCAAGGAAGGCACAGGGAG
pcDNA3-SCAMP2 W202A	Forward: 5'- CCCTGTGCCTTCCTTTGTGCGTACCGACCCATCTATAAG Revers: 5'- CTTATAGATGGGTCGGTACGCACAAAGGAAGGCACAGGG
pcDNA3-hESO3 (EcoRI/XhoI)	Forward: 5'- GCGTGAATTCATGCGGGACGCGGATGC Revers: 5'- GCGTCTCGAGCCAGGCTTAGCGGGAAACG
pcDNA3-HA-hESO3 (EcoRI/XhoI)	Forward: 5'- GCGTGAATTCATGCGGGACGCGGATGC Revers: 5'- GCGTCTCGAGCCAGGCTTAGCGGGAAACG
pcDNA3-hESO3 (1-101) (EcoRI/XhoI)	Forward: 5'- GCGTGAATTCATGCGGGACGCGGATGC Revers: 5'- GCGTCTCGAGGCCACTCACTGTGAGATCC
pcDNA3-rESO3 (EcoRI/XhoI)	Forward: 5'- GCGTGAATTCATGCAGACGGCACACGCAG Revers: 5'- GCGTCTCGAGACCAGGCTTAACAGGAAATCG
pcDNA3-HA-rESO3 (EcoRI/XhoI)	Forward: 5'- GCGTGAATTCATGCAGACGGCACACGCAG Revers: 5'- GCGTCTCGAGACCAGGCTTAACAGGAAATCG
RT-PCR Human ESO3	Forward: 5'- CCTTGGAGGCGGAAATCGC Revers: 5'- GCCCAGGCCAGGCTTAGC
RT-PCR Rat ESO3	Forward: 5'- CGAGACGGCACACGCAG Revers: 5'- AGAGCTGAATGGTGTTCACC

RT-PCR GAPDH	Forward: 5'- ACCCAGAAGACTGTGGATGG Revers: 5'- TGCTGTAGCCAAATTCGTTG
RT-PCR SERT	Forward: 5'- CAGCCGCTCAGATCTTCTTC Revers: 5'- GCGTGGTACCCACAGCATTCAAGCGGATGTC
RT-PCR Human SCAMP1	Forward: 5'- GCGTGGTACCATGTCGGATTTCGACAGTAACC Revers: 5'- GCGTGCGGCCGCTTAAATCTGGTTACCCTTGAAAG
RT-PCR Human SCAMP2	Forward: 5'- GCGTAAGCTTGATGTCGGCTTTCGACACCAAC Revers: 5'- GCGTGCGGCCGCCTAATTCCCCTGGAAGGCTC
RT-PCR Human SCAMP3	Forward: 5'- GCGTAAGCTTGATGGCTCAGAGCAGAGACGG Revers: 5'- GCGTGCGGCCGCTCACGGGGCCCGGAAGGC
RT-PCR Rat SCAMP1	Forward: 5'- GTCAGTTTGCTGTACATGTGC Revers: 5'- CTGAGGAGGCTCGCTACATC
RT-PCR Rat SCAMP2	Forward: 5'- GTCAAATAGGAATCTACTTCATC Revers: 5'- GGAGAGTCAGGAAGACTAATTC
RT-PCR Rat SCAMP3	Forward: 5'- CAGGATGTGTTCTTTGTCCTC Revers: 5'- CTGCAGGGTTGGAGAAGACA

Clone No.[1,2]		Selection for diploids (SD/-Trp/-Leu)						Selection for interactions by activation of nutritional reporter genes (SD/-Trp/-Leu/-His/-Ade)						Selection for interactions by activation of LacZ reporter gene (SD/-Trp/-Leu/ + X-β-gal)					
		pGBKT7	pGBKT7-p53	N-SERT 1-87	N-SERT 1-108	C-SERT 596-630	C-SERT 577-630	pGBKT7	pGBKT7-p53	N-SERT 1-87	N-SERT 1-108	C-SERT 596-630	C-SERT 577-630	pGBKT7	pGBKT7-p53	N-SERT 1-87	N-SERT 1-108	C-SERT 596-630	C-SERT 577-630
pACT2		+++	+++	+++	+++	+++	+++												
pTD1-1		+++	+++	+++	+++	+++	+++		+++						+++				
A: 12		+++	+++	+++	+++	+++	+++	++	++	++	++	++	++	+	+	+	+	+	+
A: 73		+++	+++	+++	+++	+++	+++	++	++	++	++	++	++	+	+	+	+	+	+
A: 144		+++	+++	+++	+++	+++	+++	++	+	+	++	+		+		+	+	+	
A: 191		+++	+++	+++	+++	+++	+++	+		+	++			+		+	+		
A: 283		+++	+++	+++	+++	+++	+++	++	+	+	+	+		+		+	+		
A: 349		-	-	-	-	-	-	-	-	-	-	-	-	-	-	-	-	-	-
A: 361		+++	+++	+++	+++	+++	+++	+		++	++			+		+	+		
A: 388		-	-	-	-	-	-	-	-	-	-	-	-	-	-	-	-	-	-
A: 431		-	-	-	-	-	-	-	-	-	-	-	-	-	-	-	-	-	-
A: 497		+++	+++	+++	+++	+++	+++	++	+	++		+		+	+	+	+	+	
A: 528		+++	+++	+++	+++	+++	+++	++				++		++				++	
A: 529		+++	+++	+++	+++	+++	+++	+	+	++	++			+	+	+	+		
A: 542		+++	+++	+++	+++	+++	+++	++	+	+		++		+	+	+		++	+

A: 677	-	-	-	-	-	-	-	-	-	-	-	-	-	-	-	-	-	-	
A: 854	+++	+++	+++	+++	+++	+++	++	++	++	++	++	++	++	++	++	++	++	++	
A: 859	+++	+++	+++	+++	+++	+++	+	+			+		+	+	+		++		
A: 880	-	-	-	-	-	-	-	-	-	-	-	-	-	-	-	-	-	-	
A: 884	-	-	-	-	-	-	-	-	-	-	-	-	-	-	-	-	-	-	
A: 891	-	-	-	-	-	-	-	-	-	-	-	-	-	-	-	-	-	-	
A: 908	+++	+++	+++	+++	+++	+++	++				++		++				++		
B: 15	+++	+++	+++	+++	+++	+++	++	++	++	++	++	++	++	++	++	++	++	++	
B: 20	+++	+++	+++	+++	+++	+++				+++						+++			
B: 45	+++	+++	+++	+++	+++	+++	+			+	+		+			+	+		
B: 120	+++	+++	+++	+++	+++	+++					+	+					+	+	
B: 123	+++	+++	+++	+++	+++	+++			++	++					++	++			
B: 283	+++	+++	+++	+++	+++	+++				+++						+++			
B: 344	+++	+++	+++	+++	+++	+++	+			++						++			
B: 362	+++	+++	+++	+++	+++	+++	++			++			++			++			
B: 401	+++	+++	+++	+++	+++	+++	++	++					++	++					
B: 417	-	-	-	-	-	-	-	-	-	-	-	-	-	-	-	-	-	-	
B: 421	-	-	-	-	-	-	-	-	-	-	-	-	-	-	-	-	-	-	
B: 447	+++	+++	+++	+++	+++	+++				+						+++			
B: 459	+++	+++	+++	+++	+++	+++	++	++	++	++	++	++	++	++	++	++	++	++	
B: 472	-	-	-	-	-	-	-	-	-	-	-	-	-	-	-	-	-	-	
B: 489	+++	+++	+++	+++	+++	+++				+++						+++			
B: 511	+++	+++	+++	+++	+++	+++	+			+			+			+			
B: 516	+++	+++	+++	+++	+++	+++	+			+++			+			++			

B: 528	+++	+++	+++	+++	+++	+++	++	++	++	++	++	++	++	++	++	++	++	++
B: 693	+++	+++	+++	+++	+++	+++	+	+	++	++			+	+	++	++		
B: 790	+++	+++	+++	+++	+++	+++				+++						+++		
B: 891	+++	+++	+++	+++	+++	+++				+++		+				+++		+
B: 1013	+++	+++	+++	+++	+++	+++	++	++	++	++	++	++	++	++	++	++	++	++
C: 14	+++	+++	+++	+++	+++	+++	+				+		+				+	
C: 15	+++	+++	+++	+++	+++	+++	+				++		+				+++	
C: 30	+++	+++	+++	+++	+++	+++	+++						++					
C: 42	+++	+++	+++	+++	+++	+++	++	+	+	+	+	+	+	+	+	+	+	+
C: 76	+++	+++	+++	+++	+++	+++							+					
C: 154	+++	+++	+++	+++	+++	+++	+	+					+	+				
C: 251	-	-	-	-	-	-	-	-	-	-	-	-	-	-	-	-	-	-
C: 295	+++	+++	+++	+++	+++	+++												
C: 319	-	-	-	-	-	-	-	-	-	-	-	-	-	-	-	-	-	-
C: 331	+++	+++	+++	+++	+++	+++	+	+	+		++		+		+		++	
C: 352	-	-	-	-	-	-	-	-	-	-	-	-	-	-	-	-	-	-
C: 355	+++	+++	+++	+++	+++	+++	+				+		+				+	
C: 402	-	-	-	-	-	-	-	-	-	-	-	-	-	-	-	-	-	-
C: 419	+++	+++	+++	+++	+++	+++												
C: 478	+++	+++	+++	+++	+++	+++	+		+		++		+		+		+	
C: 590	+++	+++	+++	+++	+++	+++					+						+	
C: 670	+++	+++	+++	+++	+++	+++	++	+	+	+	++	+	+	+	+	+	+	+
C: 690	+++	+++	+++	+++	+++	+++	+				++		+				+	
C: 694	-	-	-	-	-	-	-	-	-	-	-	-	-	-	-	-	-	-

C: 813	+++	+++	+++	+++	+++	+++												
C: 856	-	-	-	-	-	-	-	-	-	-	-	-	-	-	-	-	-	-
C: 1110	+++	+++	+++	+++	+++	+++	+				+		+				+	
C: 1168	-	-	-	-	-	-	-	-	-	-	-	-	-	-	-	-	-	-
C: 1194	+++	+++	+++	+++	+++	+++	+	+	+	+	+		+	+	+	+	++	
C: 1211	+++	+++	+++	+++	+++	+++					+++	+++					+++	+++
C: 1279	-	-	-	-	-	-	-	-	-	-	-	-	-	-	-	-	-	-
C: 1398	+++	+++	+++	+++	+++	+++	+		+		+++		+		+		+++	
C: 1437	-	-	-	-	-	-	-	-	-	-	-	-	-	-	-	-	-	-
C: 1595	+++	+++	+++	+++	+++	+++												
D: 105	+++	+++	+++	+++	+++	+++	+					+	+					+
D: 110	-	-	-	-	-	-	-	-	-	-	-	-	-	-	-	-	-	-
D: 115	+++	+++	+++	+++	+++	+++												
D: 186	+++	+++	+++	+++	+++	+++	+					+	+					+
D: 258	+++	+++	+++	+++	+++	+++						+++						++
D: 285	+++	+++	+++	+++	+++	+++						++						++
D: 295	+++	+++	+++	+++	+++	+++					+++	+++					+++	+++
D: 303	-	-	-	-	-	-	-	-	-	-	-	-	-	-	-	-	-	-
D: 320	+++	+++	+++	+++	+++	+++						+++						++
D: 384	+++	+++	+++	+++	+++	+++	+				+	+	+				+	+
D: 399	+++	+++	+++	+++	+++	+++					+++	+++					+++	+++
D: 458	+++	+++	+++	+++	+++	+++					++	++					++	++
D: 463	+++	+++	+++	+++	+++	+++												
D: 507	+++	+++	+++	+++	+++	+++						++						++

D: 508	+++	+++	+++	+++	+++	+++	+	+	+	+	+	+	+	+	+	+	+	+
D: 515	+++	+++	+++	+++	+++	+++	+					+	+					+
D: 522	+++	+++	+++	+++	+++	+++												
E: 1H	+++	+++	+++	+++	+++	+++						+++						+++
E: 7A	+++	+++	+++	+++	+++	+++						+++						+++
E: 7B	+++	+++	+++	+++	+++	+++						+++						++
E: 7E	+++	+++	+++	+++	+++	+++				++		+++				++		+++
E: 11D	+++	+++	+++	+++	+++	+++	+			+		+++	+			+		++
E: 30A	+++	+++	+++	+++	+++	+++				+		++				+		++
E: 42D	+++	+++	+++	+++	+++	+++	+++	+++	+++	+++	+++	+++	+++	+++	+++	+++	+++	+++
E: 47E	+++	+++	+++	+++	+++	+++				+		+++						+++
E: 49H	+++	+++	+++	+++	+++	+++	+			+	+++	+++				+	+++	+++
E: 50H	+++	+++	+++	+++	+++	+++				+	+++	+++				+	+++	+++
E: 58E	+++	+++	+++	+++	+++	+++	+					+	+					+
E: 58H	+++	+++	+++	+++	+++	+++						+++						+++
E: 59A	+++	+++	+++	+++	+++	+++				+		++				+		++
E: 60L	+++	+++	+++	+++	+++	+++				+		++				+		++
E: 61F	+++	+++	+++	+++	+++	+++	+			+	+	++	+			+	+	++
E: 61J	+++	+++	+++	+++	+++	+++				+		++				+		++
E: 66F	+++	+++	+++	+++	+++	+++	++			++		++	+			++		++
E: 66A	-	-	-	-	-	-	-	-	-	-	-	-	-	-	-	-	-	-
E: 66E	+++	+++	+++	+++	+++	+++	+	+	+	+	+	+	+	+	+	+	+	+
E: 66I	+++	+++	+++	+++	+++	+++						+						+
E: 80I	+++	+++	+++	+++	+++	+++	+			++		++	+			+		++

E: 84K	+++	+++	+++	+++	+++	+++						++						+
E: 89F	+++	+++	+++	+++	+++	+++				+++		+++	+			++		+
E: 93I	+++	+++	+++	+++	+++	+++	+			+		+++				+		++
E: 93L	-	-	-	-	-	-	-	-	-	-	-	-	-	-	-	-	-	-
E: 95F	+++	+++	+++	+++	+++	+++						+++						++
E: 129F	+++	+++	+++	+++	+++	+++						+++				+		+++
E: 147A	+++	+++	+++	+++	+++	+++				++		++				++		+

[1] Screens; A: hSERT(1-87), B: hSERT(1-108), C: hSERT(596-630), D: hSERT(577-630), E: hSERT(577-630)

[2] +++/+++, major growth/intense dark blue; ++/++, moderate growth/aquamarine blue; +/+ little growth/faint blue; -/- not determined

ALIGNMENT OF THE N-TERMINAL DOMAIN OF SERT, DAT AND NET

